AUGMENTATION OF NERVE ALLOGRAFTS WITH ANGIOGENESIS AND STEM CELLS

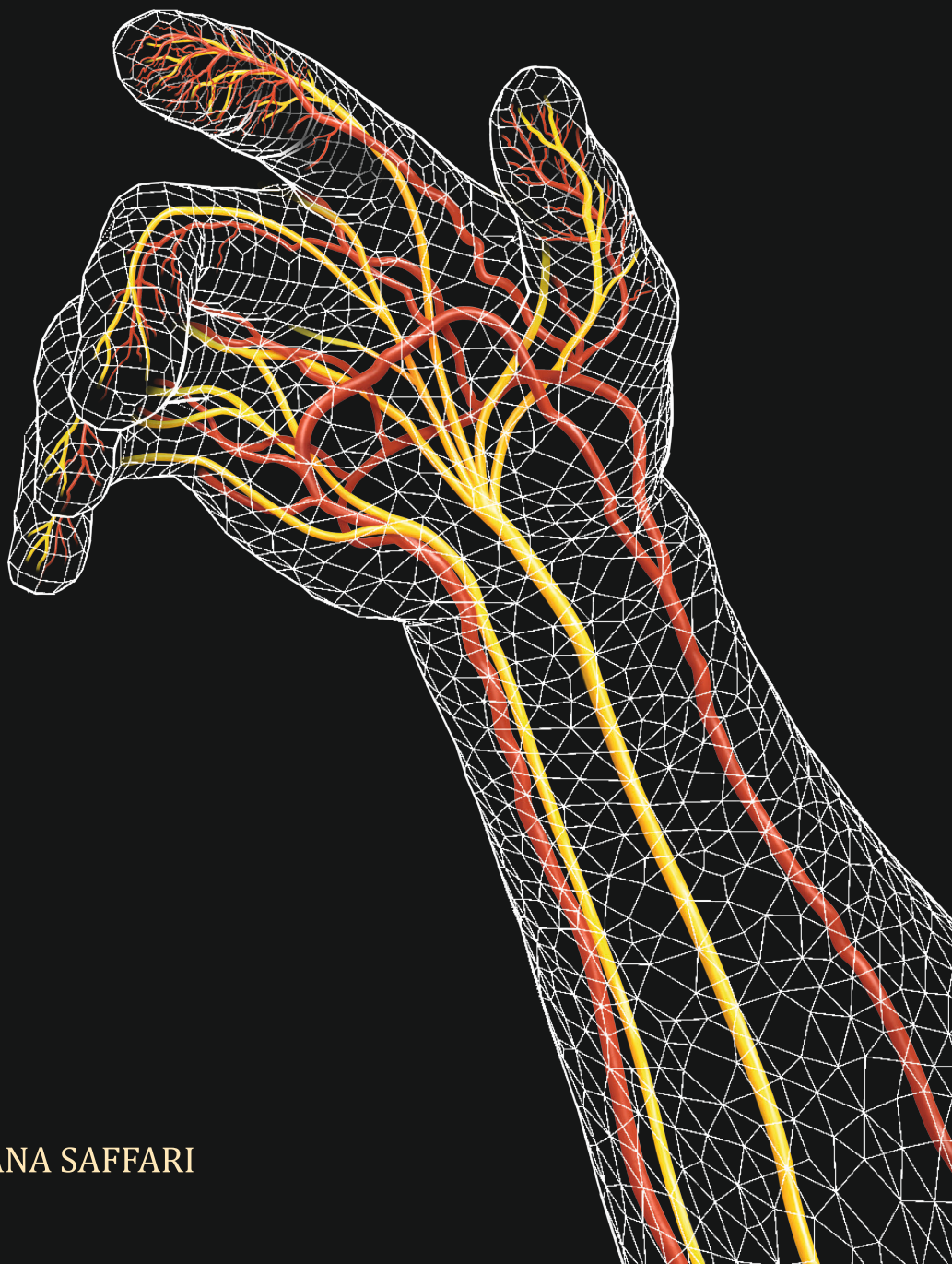

TIAM MANA SAFFARI

AUGMENTATION OF NERVE ALLOGRAFTS WITH ANGIOGENESIS AND STEM CELLS

Tiam Mana Saffari

Scan the QR code to view the digital version of this thesis

Augmentation of Nerve Allografts with Angiogenesis and Stem Cells

ISBN: 978-94-6416-704-7
Cover design: Jim Postier (Mayo Clinic, Rochester, USA)
Layout: Marilou Maes, persoonlijkproefschrift.nl
Printing: Ridderprint | www.ridderprint.nl

Printing of this thesis was kindly supported by the Radboud University Medical Center, and further financial support was kindly provided by Nederlandse Vereniging voor Plastische Chirurgie (NVPC) and ChipSoft BV.

The author would like to acknowledge the National Institutes of Health (Grant R01 NS102360) for providing funding for this work.

The work presented in this thesis was carried out in collaboration with the Mayo Clinic and the Radboud Institute for Health Sciences.

Augmentation of Nerve Allografts with Angiogenesis and Stem Cells

Doctoral Thesis

to obtain the degree of doctor

from Radboud University Nijmegen

on the authority of the Rector Magnificus prof. dr. J.H.J.M. van Krieken,

according to the decision of the Council of Deans

to be defended in public on Friday, September 10, 2021

at 14.30 hours

by

Tiam Mana Saffari

born on May 3, 1992

in Capelle aan den IJssel (the Netherlands)

SUPERVISORS

Prof. dr. D.J.O. Ulrich

Prof. dr. S.E.R. Hovius Erasmus Medical Center

DOCTORAL THESIS COMMITTEE

Prof. dr. R.H.M.A. Bartels

Prof. dr. M.J.A. Malessy Leiden University Medical Center

Dr. T.J. H. Ruigrok Erasmus Medical Center

PARANYMPHS

Drs. Bahar Golyardi

Drs. Tara Saffari

Augmentation of Nerve Allografts with Angiogenesis and Stem Cells

PROEFSCHRIFT

ter verkrijging van de graad van doctor

aan de Radboud Universiteit Nijmegen

op gezag van de rector magnificus prof. dr. J.H.J.M. van Krieken,

volgens besluit van het college van decanen

in het openbaar te verdedigen op

vrijdag 10 september 2021

om 14:30 uur precies

door

Tiam Mana Saffari

geboren op 3 mei 1992

te Capelle aan den IJssel

PROMOTOREN

Prof. dr. D.J.O. Ulrich

Prof. dr. S.E.R. Hovius Erasmus Medisch Centrum

MANUSCRIPTCOMMISSIE

Prof. dr. R. H.M.A. Bartels

Prof. dr. M. J.A. Malessy Leiden Universiteit Medisch Centrum

Dr. T. J. H. Ruigrok Erasmus Medisch Centrum

PARANYMFEN

Drs. Bahar Golyardi

Drs. Tara Saffari

To my entire family

TABLE OF CONTENTS

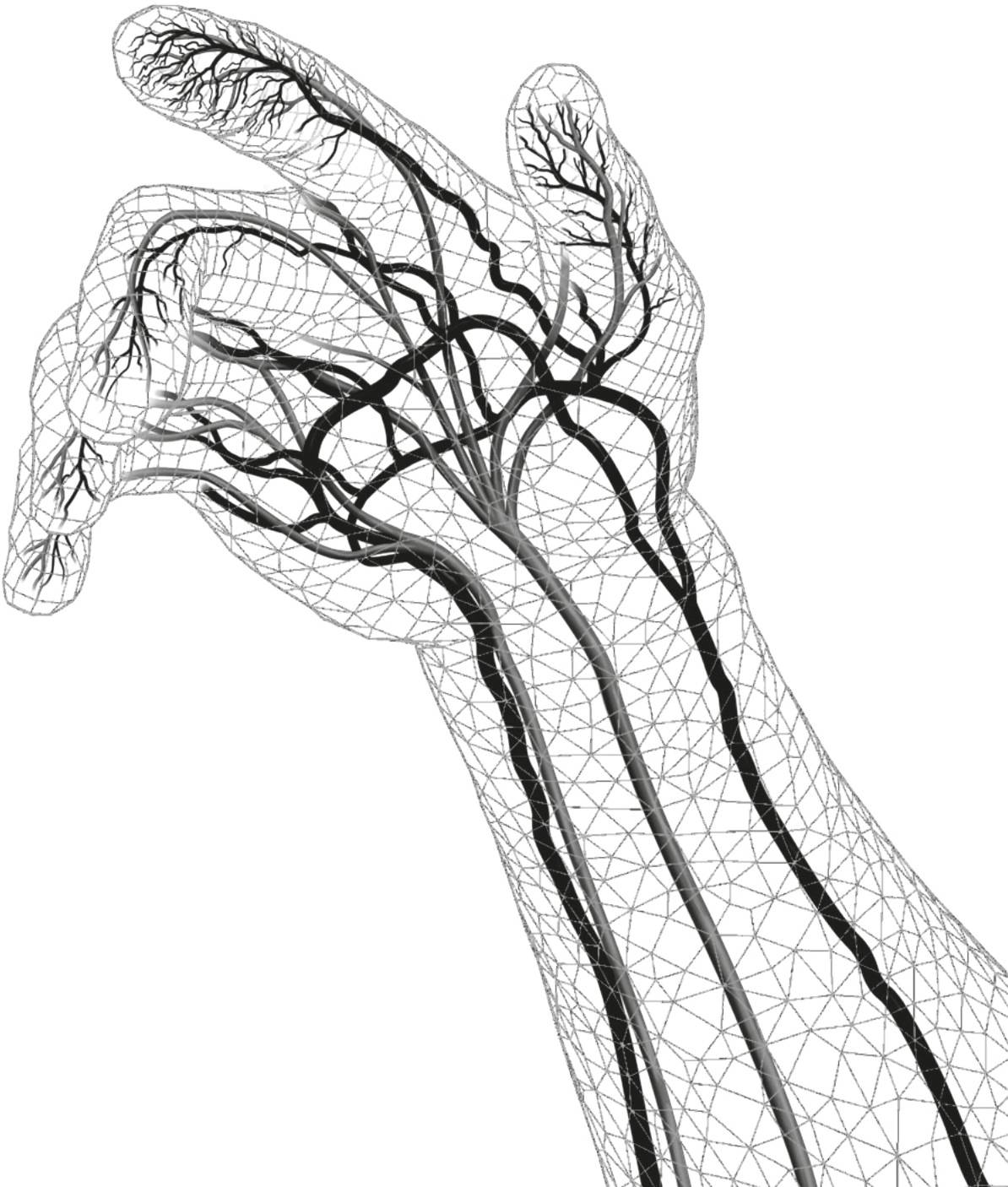

CHAPTER

ONE

General Introduction

BACKGROUND

Peripheral nerve injuries occur in approximately 5% of all trauma cases. The majority of these cases rarely recover completely and can cause lifelong physiological and functional disabilities leading to a diminished quality of life [1-3]. The most common nerve injuries are caused by high energy traumas, such as motor vehicle accidents. In addition, penetrating wounds and lacerations caused by tumor excision result in injuries to the peripheral nervous system [4,5]. The peripheral nervous system is one of two components that make up the nervous system, with the other subdivision being the central nervous system. The central nervous system, comprising the brain and spinal cord, integrates data and conducts impulses via a network of peripheral nerves consisting of bundles of nerve fibers or axons [6].

ANATOMY OF THE PERIPHERAL NERVOUS SYSTEM

The peripheral nervous system consists of the somatic and autonomic division. The somatic division is associated with voluntary movement and sensibility, controlled by motor and sensory neurons, respectively. The autonomic division mediates visceral functions, such as heart rate and digestion [7]. This thesis will solely focus on the somatic subdivision of the peripheral nervous system. Each peripheral nerve trunk consists of many axons, supported by an outer surrounding layer of fibrous connective tissue called the epineurium, and longitudinal blood vessels that supply the nerve with nutrients (Figure 1). Within the nerve, axons are bundled into fascicles (depicted with the square), each surrounded by their own perineurium. The epineurium and perineurium consist of layers of fibroblasts and collagen to provide tensile strength. Finally, the endoneurium surrounds each individual axon within the fascicles [8]. Myelinating Schwann cells insulate the axon with a myelin sheath, consisting of many regular layers of plasma membrane, that aids in conduction of nerve impulses. The nodes of Ranvier facilitate saltatory conduction by allowing action potentials to jump from node to node, resulting in increased velocity of conduction [9].

The blood supply source to peripheral nerves is called the vasa nervorum, consisting of small vessels that are adjacent to the nerve and torturous to allow for freedom of translational movement of peripheral nerves, particularly in the vicinity of joints. The vascular tree and the nervous branching networks are often patterned similarly in

peripheral tissues and share several anatomical and functional characteristics [10]. The embryologic formation of vessels is called angiogenesis and describes endothelial cells to migrate toward and align with peripheral nerves in response to vascular endothelial growth factor-A (VEGF-A) [10]. VEGF is a potent multifunctional cytokine that stimulates angiogenesis and plays a large role in revascularization after injury to the nerve [11].

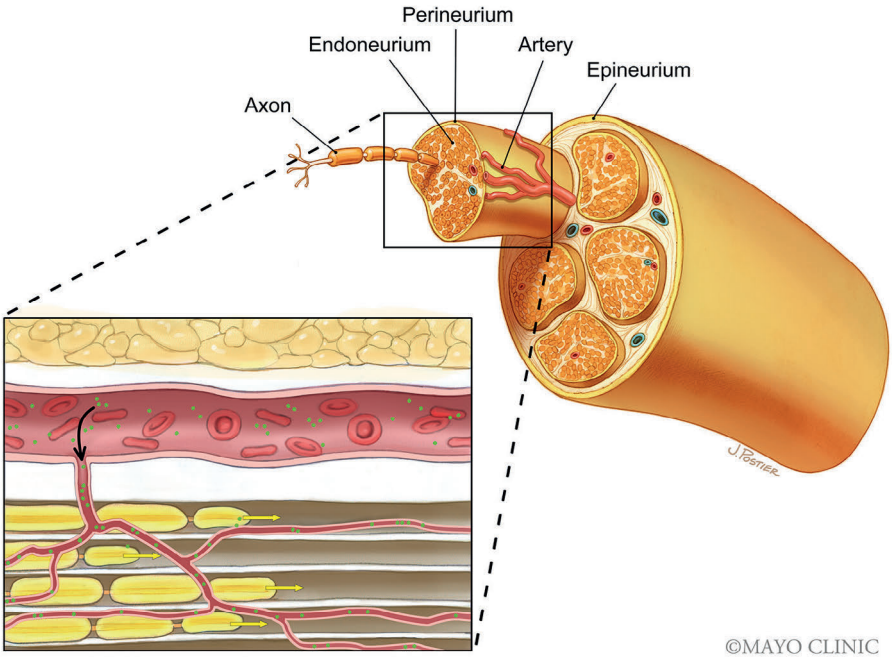

Figure 1. Schematic illustration of a peripheral nerve. The peripheral nerve is depicted with groups of fascicles that are surrounded by the epineurium. Each fascicle of endoneurium contains up to several thousands of axons. The nerve fascicle (depicted with the square) is enveloped by the perineurium. Blood is supplied by a network of capillary-like micro vessels derived from arterioles and venules, which are branches of major limb vessels. The zoomed image depicts the close relationship of vessels and axons. When the nerve is injured, vascular endothelial cells guide the regeneration of peripheral nerve axons by producing vascular endothelial growth factor (VEGF, green dots) to induce angiogenesis. *With permission of the Mayo Foundation, Copyright Mayo Foundation. All rights reserved.*

PERIPHERAL NERVE REGENERATION AFTER INJURY

Following traumatic peripheral nerve injury, the nerve undergoes a number of processes. At the proximal stump, the neuronal cell body undergoes chromatolysis. This is characterized by swelling within 48 hours, causing displacement of the nucleus to one side of the cytoplasm (an eccentric nucleus) and fragmentation of the Nissl granule (Figure 2) [12]. The distal nerve segment undergoes a process known as Wallerian degeneration to create a microenvironment conducive for axonal reinnervation [13]. Schwann cells clear cell debris through phagocytosis and by recruiting macrophages, and release important neurotrophic factors and cytokines crucial for successful nerve regeneration [12,14]. Within two-three weeks, the axons and myelin degenerate along the entire length of the nerve distal to the lesion, creating an empty tube for axons. Schwann cells in the nerve segment proliferate by aligning longitudinally and form bands of Bünger to guide the regenerating axons from the proximal nerve stump, thus establishing reinnervation of the target muscle [15-17]. Axonal regeneration proceeds at a rate of approximately 1 mm per day [18].

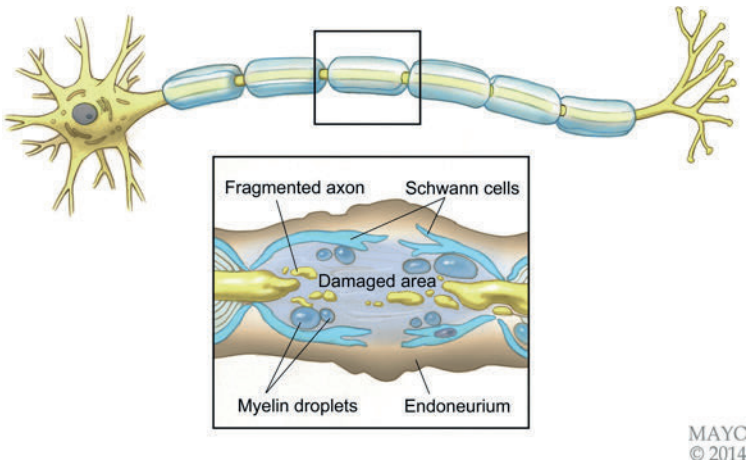

Figure 2. Schematic illustration of Wallerian degeneration. A typical motor neuron with its axon surrounded by myelin sheath, formed by Schwann cells, is depicted. Traumatic injury (e.g. axotomy) results in immediate tissue damage at the lesion site (marked by square). The proximal nerve segment undergoes chromatolysis and swelling of the nucleus. Schwann cells that surround the distal portion of the axon shed their myelinated lipids (droplets). Phagocytic activity is stimulated by Schwann cells and macrophages to remove debris and subsequently release trophic factors in the preparation of nerve regeneration. *With permission of the Mayo Foundation, Copyright Mayo Foundation. All rights reserved.*

Peripheral nerve recovery elicits a fine balance of axonal sprouting and scar formation, following the principles of wound healing. In severe injuries, fibroblasts secrete large amounts of collagen, resulting in the formation of dense scarring. Nerve scarring, or fibrosis, can alter perineural microvasculature and impair nerve regeneration [19].

CURRENT APPROACHES FOR NERVE RECONSTRUCTION

The prevailing wisdom regarding the surgical management of the peripheral nerve gap has changed over the past century. The current surgical intervention for peripheral nerve reconstruction consists of microsurgical epineural suture of aligned proximal and distal stumps, performed when a tension-free coaptation can be achieved [20,21]. Tension into the nerve cable is deleterious to nerve regeneration and has been demonstrated to result in scar formation in the 1970s by Millesi and colleagues [22]. Following severe nerve trauma with excessive tension between nerve ends, primary (end-to-end) repair is therefore is not possible, and nerve interposition is needed to reconstruct the nerve defect. Although nerve interposition was thought to yield inferior outcomes prior to the 1970s, the novel insights introduced interfascicular tension-free nerve grafting with fascicles matching in size, as a new option for repair of peripheral nerves [23]. The speed at which nerves regenerate through the graft to reach the motor endplate is time dependent, which can significantly affect motor outcome and restoration of function [24,25]. Currently, there are several options for nerve reconstruction, each associated with its own advantages and disadvantages.

Nerve autograft

For the reconstruction of segmental nerve defects, the gold standard remains the use of an autologous nerve graft (autograft): the use of the patient's healthy nerve, as donor, to bridge the nerve gap [22]. The autograft provides a scaffold for nerve regeneration, while including preserved nervous architecture and biology, e.g. viable Schwann cells and vasculature. Furthermore, the autograft is non-immunogenic and the preferred option for reconstruction of motor and mixed nerves [26]. The disadvantages include the associated donor site morbidity and limited availability [27]. The sural nerve, which is purely sensory and easily harvested, is the most common nerve graft donor and provides a graft length up to 40 cm in adults (Figure 3). Donor nerve selection is based on size match to the injured nerve, ease of harvest and minimizing postoperative

deficit [28]. Autografts could be used in various techniques, including cable grafts which comprise multiple lengths of a smaller diameter donor nerve to meet the caliber of the recipient nerve (Figure 3), and for vascularized grafts [26].

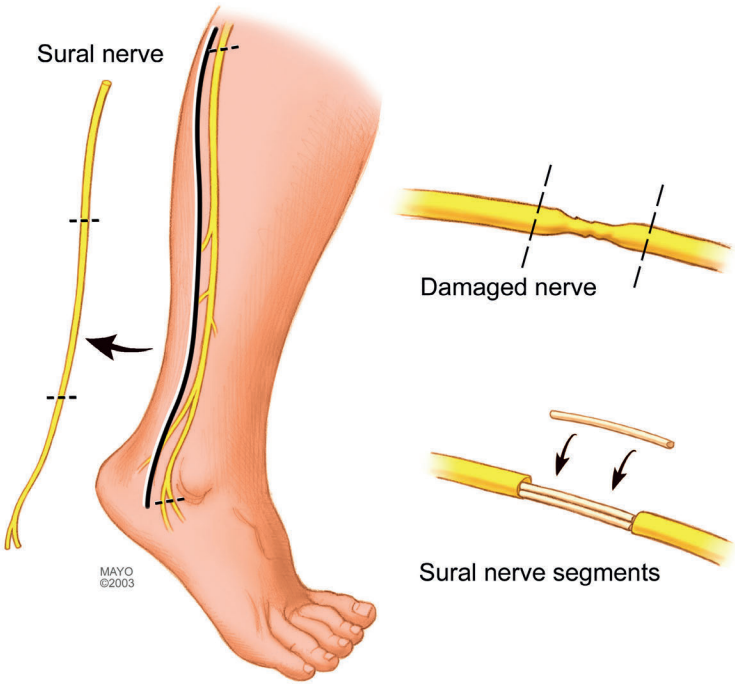

Figure 3. Schematic illustration of the sural nerve harvest. The sural nerve could be used as cable grafts, by comprising multiple lengths of smaller diameter nerve aligned in parallel to meet the caliber of the recipient nerve. *With permission of the Mayo Foundation, Copyright Mayo Foundation. All rights reserved.*

Nerve allograft

The history of nerve allografts exceeds that of autografts, however, the need of systemic immunosuppressive therapy and risk of disease transmission precluded widespread use of this treatment modality [29,30]. Many experimental and clinical efforts have been directed towards diminishing the antigenicity of the allograft by pretreatment with irradiation, enzymatic treatment, detergent processing and cryopreservation. While the internal nerve architecture and the basal lamina remain intact, these techniques process the allografts to become acellular, thus reducing graft immunogenicity [29,31,32].

The downside of processing is that it modifies the nerve, by removing Schwann cells, destroying neurotrophic factors and vascularity, resulting in an altered extracellular matrix with reduced regenerative potency [31,32]. Introduced in 2007, the Avance® nerve graft was the first commercially available nerve allograft and combined pretreatments including chemical decellularization and gamma irradiation [33]. Their outcomes have demonstrated sufficient nerve regeneration over small distances not exceeding 3 cm, however, remain inferior to fresh autografts in large nerve defects [34-37]. Therefore, ongoing research has focused on augmentation of nerve allografts to enhance nerve regeneration.

HISTORICAL BACKGROUND OF PERIPHERAL NERVE REGENERATION RESEARCH LINE

Understanding of peripheral nerve injury and providing patient individualized nerve substitute to improve nerve regeneration in large nerve defects is an ongoing challenge for surgeons and nerve scientists. The goal is to enhance a decellularized nerve allograft to equal autograft performances in large nerve defects. Augmenting the nerve injury site of allografts to meet environmental advances of the autograft holds promise for enhancing nerve regeneration. This thesis is part of an ongoing research line with the Neural Regeneration Research Laboratory at Mayo Clinic, under supervision of Prof. Shin and Prof. Bishop, and builds on the results of previously conducted research that has focused on optimizing decellularized nerve allografts and seeding these allograft with stem cells.

Optimizing nerve allograft decellularization

Previously established pretreatment techniques of nerve allografts provided suboptimal results, especially with increasing gap distances [38]. Therefore, the primary approach in this research line focused on advancing decellularization techniques to better support nerve regeneration. Decellularization of a nerve allograft was successfully optimized by modifying previous processing protocols and adding elastase, an enzyme that significantly reduces the amount of axonal debris and immunogenicity, while maintaining ultrastructural properties. Furthermore, a comparison was performed between preservation conditions at 4 °C and -80 °C. Freeze-storage at -80 °C was found to damage the basal lamina structure, leading to impaired

functional recovery of 20-mm nerve gaps reconstructed with decellularized nerve allografts in a rabbit peroneal nerve defect model [39,40]. Decellularization including elastase and cold storage at 4 °C were identified as the optimal conditions and used in subsequent experiments (Figure 4A, rectangle 1).

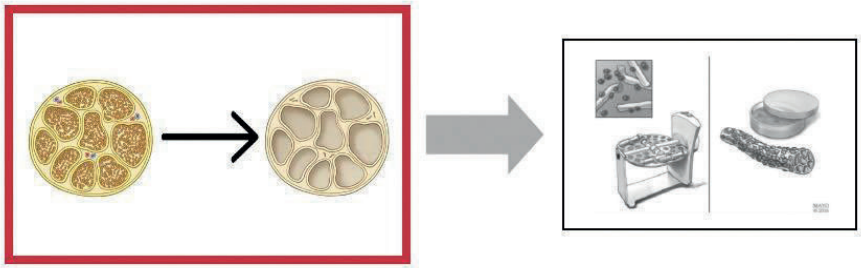

Figure 4A. Flowchart of historical background of this thesis. This thesis is part of an ongoing research line and builds on the results of previously conducted research that has focused on optimizing a decellularized nerve allograft (rectangle 1) and seeding these allografts with stem cells. *With permission of the Mayo Foundation, Copyright Mayo Foundation. All rights reserved.*

Augmenting decellularized allograft with stem cells

Schwann cells are essential within the context of peripheral nerve regeneration after trauma and are crucial during Wallerian degeneration, however, difficult to transplant. The acquisition of autologous Schwann cells requires harvest of large segments of healthy nerve tissue, resulting in donor site morbidities [41,42]. As a result of these limitations, research has been directed towards the use of mesenchymal stem cells (MSC), which are easily accessible, and can be differentiated into Schwann cell-like cells [42]. The importance of MSCs in peripheral nerve regeneration relies on their ability to enhance neurotrophic factors, promote myelin formation and their capacity to be influenced by the microenvironment to differentiate into Schwann cell-like cells [43]. Despite progress in pre-clinical studies, translation to clinical practice is currently limited by many unanswered questions on the application of MSCs in peripheral nerve repair and their interaction with vascularity.

Previous research conducted in our research line has focused on individualizing nerve allograft repair by addition of adipose-derived MSCs to the nerve allograft. A new method was described and validated to dynamically seed MSCs on nerve

allografts *in vitro* and evaluate their survivability in the rat. Rotation of tubes in which decellularized nerve allografts were combined with MSCs, allowed for adherence of MSCs to the nerve, without inducing trauma to the nerve or MSCs. After 12 to 24 hours of dynamic seeding, seeding efficiency was found to be approximately 80% and cells were distributed homogeneously over the surface of the grafts [44]. When placed *in vivo*, labeled MSCs could be detected up to 29 days, without any migration of cells to surrounding tissues [45]. Differentiation of MSCs into Schwann cell-like cells, to induce Schwann cell neuroregenerative properties, was successfully validated and found to enhance secretion of various angiogenic factors and neurotrophic factors (Figure 4B, rectangle 2) [46,47].

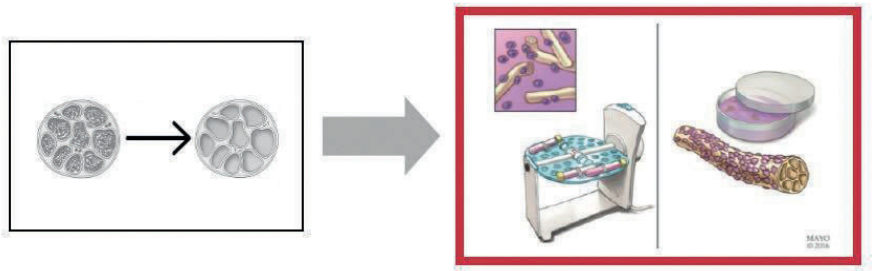

Figure 4B. Flowchart of historical background of this thesis. This thesis is part of an ongoing research line and builds on the results of previously conducted research that has focused on seeding the decellularized nerve allografts with stem cells. Moreover, stem cells were differentiated into Schwann cell-like cells to resemble Schwann cell properties (rectangle 2). *With permission of the Mayo Foundation, Copyright Mayo Foundation. All rights reserved.*

Augmenting decellularized allograft with angiogenesis

Vascularization is one of the great challenges faced in nerve reconstruction, especially in nerve autograft substitutes such as nerve allografts that have been processed and do not contain living cells [48]. In nerve allografts, revascularization needs to be achieved to ensure cellular survival and avoid central necrosis. This has been a longstanding challenge in nerve grafts with large diameters and in long defects [48,49]. The first free vascularized nerve graft (VNG) was reported in 1976 and indicated in cases lacking well-vascularized beds. VNGs have the advantage of overcoming a period of ischemia and ensure continuous nutrition of the graft, which is suggested to prevent intraneural fibrosis. However, evidence for their clinical superiority has remained inconclusive [50].

Over the past decade, it has been suggested that vascular endothelial cells guide the regeneration of peripheral nerve axons by producing VEGF, and subsequently VEGF became the focus of numerous investigations. Clinical attempts to enhance nerve allografts using VEGF led to conflicting results, suggesting that the specific molecular regulations of angiogenesis following peripheral nerve injury are more complex [51-55]. Prior to implementation of nerve allografts augmented with angiogenesis in the clinical setting, understanding of processes that are necessary for new vessel formation after nerve injury needs to be provided.

Augmenting decellularized allograft with stem cells and angiogenesis combined

Stem cell-based therapy may offer a suitable treatment with several regenerative benefits to restore neuronal function, including supporting remyelination and revascularization of the affected organ [43]. Blood vessels, on the other hand, have been postulated to be a systemic source of stem cells in regenerating tissues secondary to their vascular origin [56]. Studies that investigate the potential synergistic effects of blood supply and stem cell delivery are lacking. To this end, the experimental approach in this thesis has been to augment decellularized nerve allografts with angiogenesis and stem cells combined.

PROJECT OBJECTIVE AND HYPOTHESIS

The objective of this thesis is to enhance peripheral nerve regeneration in nerve allografts to meet outcomes of nerve autografts by augmenting the nerve injury site with angiogenesis and stem cells (Figure 4C). This thesis' hypothesis is that augmentation of nerve allograft environment with angiogenesis and stem cells improves nerve regeneration and revascularization.

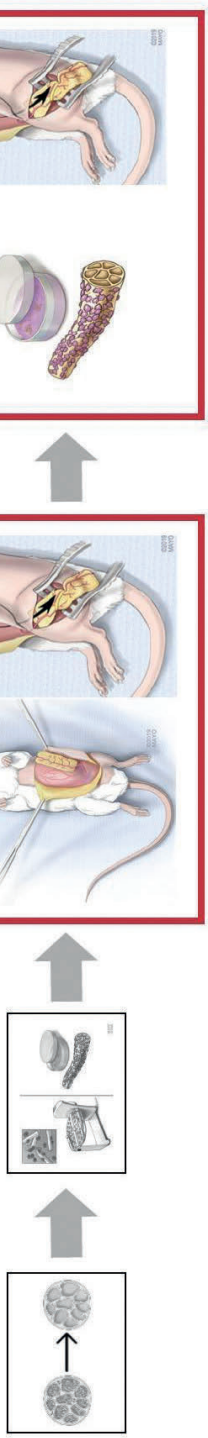

Figure 4C. Flowchart of objectives of this thesis. In this thesis, the research line is advanced towards the augmentation of decellularized nerve allografts with angiogenesis (rectangle 3) and the combination of stem cell delivery and angiogenesis to the decellularized nerve allograft (rectangle 4). *With permission of the Mayo Foundation, Copyright Mayo Foundation. All rights reserved.*

SPECIFIC AIMS AND OUTLINE OF THIS THESIS

In part I, the role of angiogenesis in revascularization and nerve regeneration will be discussed.

In **Chapter 2**, the role of angiogenesis in nerve regeneration will be discussed and the key regulation molecules that are suggested to mediate this process will be introduced. Available literature on the mechanisms of angiogenesis and its effect in basic science as well as clinical applications will be summarized.

How can we provide vascularity to the sciatic nerve area to investigate its role in nerve regeneration and revascularization?
In **Chapter 3**, a surgical technique for a pedicled adipofascial flap in the rat will be described to provide vascularity to the sciatic nerve area. This technique will be used in following experiments in this thesis.

What are objective strategies to evaluate blood vessels in nerve samples?
New methods to objectively measure angiogenesis in nerve samples will be investigated in **Chapter 4.** Using these techniques, we will investigate in **Chapter 5,** *how augmentation of nerve allografts with angiogenesis affects revascularization patterns* in a rat sciatic nerve defect model over time**.**

What effect does angiogenesis have on nerve allografts at a cellular level?
In **Chapter 6**, the effect of augmentation of nerve allografts with angiogenesis will be studied at a cellular level to investigate its effect on nerve fibrosis. *In vivo* gene expression profiles will be evaluated and combined with immune cell evaluation in a rat sciatic nerve defect model.

In **Chapter 7**, *the impact of angiogenesis on functional motor recovery will be investigated*. Functional, electrophysiological, histological and immunofluorescence analyses will be assessed to understand how augmentation of nerve allografts with angiogenesis affects nerve regeneration.

In part II, the contribution of angiogenesis and stem cells in nerve regeneration will be discussed.

In **Chapter 8**, the interaction of stem cells and angiogenesis in nerve regeneration will be investigated. Current available literature on stem cell-based therapy applications in peripheral nerve injuries will be presented and its interaction with angiogenesis in peripheral nerve regeneration will be discussed.

To understand the role of stem cells in nerve regeneration, the *effect of augmentation of nerve allografts with stem cells on functional motor recovery will be investigated* in **Chapter 9**. Both undifferentiated stem cells and stem cells differentiated into Schwann cell-like cells will be seeded onto nerve allografts to understand their long-term effect on nerve regeneration.

How does augmentation of nerve allografts with angiogenesis and stem cells combined affect revascularization?
In **Chapter 10**, *the microvascular architecture of nerve allografts after combined stem cell delivery and angiogenesis* in a rat sciatic nerve defect model will be evaluated. Both undifferentiated stem cells and stem cells differentiated into Schwann cell-like cells will be combined with angiogenesis and vascular distributions will be objectively measured.

In the general discussion, described in **Chapter 11**, we will present the results of this thesis in a broader perspective. The relevance of the results will be explained and the significance of the findings will be described in light of the current literature to discuss how this thesis advances the understanding of a still existing challenge: *Could we augment off-the-shelf decellularized nerve allografts to meet outcomes of autografts in segmental nerve defects?*

Future perspectives and research needed to translate these findings from bench to bedside will also be described.

In **Chapter 12**, a summary in English and Dutch will be presented.

REFERENCES

1. Noble J, Munro CA, Prasad VS, Midha R. Analysis of upper and lower extremity peripheral nerve injuries in a population of patients with multiple injuries. *J Trauma.* 1998;45(1):116-122.
2. Kemp SW, Cederna PS, Midha R. Comparative outcome measures in peripheral regeneration studies. *Exp Neurol.* 2017;287(Pt 3):348-357.
3. Ashley WW, Jr., Baty JD, Hollander T, Noetzel MJ, Park TS. Long-term motor outcome analysis using a motor score composite following surgical brachial plexus repair. *J Neurosurg.* 2007;106(4 Suppl):276-281.
4. Kline DG. Surgical repair of peripheral nerve injury. *Muscle Nerve.* 1990;13(9):843-852.
5. Robinson LR. Traumatic injury to peripheral nerves. *Muscle Nerve.* 2000;23(6):863-873.
6. Horner PJ, Gage FH. Regenerating the damaged central nervous system. *Nature.* 2000;407(6807):963-970.
7. Catala M, Kubis N. Gross anatomy and development of the peripheral nervous system. *Handb Clin Neurol.* 2013;115:29-41.
8. Fox IK, Mackinnon SE. Adult peripheral nerve disorders: nerve entrapment, repair, transfer, and brachial plexus disorders. *Plast Reconstr Surg.* 2011;127(5):105e-118e.
9. Poliak S, Peles E. The local differentiation of myelinated axons at nodes of Ranvier. *Nat Rev Neurosci.* 2003;4(12):968-980.
10. James JM, Mukouyama YS. Neuronal action on the developing blood vessel pattern. *Semin Cell Dev Biol.* 2011;22(9):1019-1027.
11. Cattin AL, Burden JJ, Van Emmenis L, et al. Macrophage-Induced Blood Vessels Guide Schwann Cell-Mediated Regeneration of Peripheral Nerves. *Cell.* 2015;162(5):1127-1139.
12. Menorca RM, Fussell TS, Elfar JC. Nerve physiology: mechanisms of injury and recovery. *Hand Clin.* 2013;29(3):317-330.
13. Waller A. Experiments on the Section of the Glosso-Pharyngeal and Hypoglossal Nerves of the Frog, and Observations of the Alterations Produced Thereby in the Structure of Their Primitive Fibres. *Edinb Med Surg J.* 1851;76(189):369-376.
14. Reichert F, Saada A, Rotshenker S. Peripheral nerve injury induces Schwann cells to express two macrophage phenotypes: phagocytosis and the galactose-specific lectin MAC-2. *J Neurosci.* 1994;14(5 Pt 2):3231-3245.
15. Gaudet AD, Popovich PG, Ramer MS. Wallerian degeneration: gaining perspective on inflammatory events after peripheral nerve injury. *J Neuroinflammation.* 2011;8:110.
16. Stoll G, Muller HW. Nerve injury, axonal degeneration and neural regeneration: basic insights. *Brain Pathol.* 1999;9(2):313-325.
17. Jessen KR, Mirsky R. The repair Schwann cell and its function in regenerating nerves. *J Physiol.* 2016;594(13):3521-3531.
18. Jacobson S, Guth L. An electrophysiological study of the early stages of peripheral nerve regeneration. *Experimental Neurology.* 1965;11(1):48-60.

19. Dvali L, Mackinnon S. The role of microsurgery in nerve repair and nerve grafting. *Hand Clin.* 2007;23(1):73-81.
20. Millesi H. Forty-two years of peripheral nerve surgery. *Microsurgery.* 1993;14(4):228-233.
21. Terzis J, Faibisoff B, Williams B. The nerve gap: suture under tension vs. graft. *Plast Reconstr Surg.* 1975;56(2):166-170.
22. Millesi H, Meissl G, Berger A. The interfascicular nerve-grafting of the median and ulnar nerves. *J Bone Joint Surg Am.* 1972;54(4):727-750.
23. Berger A, Millesi H. Nerve grafting. *Clin Orthop Relat Res.* 1978(133):49-55.
24. Noland SS, Bishop AT, Spinner RJ, Shin AY. Adult Traumatic Brachial Plexus Injuries. *J Am Acad Orthop Surg.* 2019;27(19):705-716.
25. Pulos N, Shin EH, Spinner RJ, Shin AY. Management of Iatrogenic Nerve Injuries. *J Am Acad Orthop Surg.* 2019;27(18):e838-e848.
26. Moore AM, Mackinnon SE. *Nerve Repair and Transfers from Hand to Shoulder, An issue of Hand Clinics, E-Book.* Vol 32: Elsevier Health Sciences; 2016.
27. Sunderland S. Factors influencing the course of regeneration and the quality of the recovery after nerve suture. *Brain.* 1952;75(1):19-54.
28. Slutsky DJ. A practical approach to nerve grafting in the upper extremity. *Atlas Hand Clin.* 2005;10(73):e92.
29. Rinker B, Vyas KS. Clinical applications of autografts, conduits, and allografts in repair of nerve defects in the hand: current guidelines. *Clin Plast Surg.* 2014;41(3):533-550.
30. Fox IK, Mackinnon SE. Experience with nerve allograft transplantation. *Semin Plast Surg.* 2007;21(4):242-249.
31. Hudson TW, Liu SY, Schmidt CE. Engineering an improved acellular nerve graft via optimized chemical processing. *Tissue Eng.* 2004;10(9-10):1346-1358.
32. Hudson TW, Zawko S, Deister C, et al. Optimized acellular nerve graft is immunologically tolerated and supports regeneration. *Tissue Eng.* 2004;10(11-12):1641-1651.
33. Moore AM, MacEwan M, Santosa KB, et al. Acellular nerve allografts in peripheral nerve regeneration: a comparative study. *Muscle Nerve.* 2011;44(2):221-234.
34. Griffin JW, Hogan MV, Chhabra AB, Deal DN. Peripheral nerve repair and reconstruction. *J Bone Joint Surg Am.* 2013;95(23):2144-2151.
35. Safa B, Shores JT, Ingari JV, et al. Recovery of Motor Function after Mixed and Motor Nerve Repair with Processed Nerve Allograft. *Plast Reconstr Surg Glob Open.* 2019;7(3):e2163.
36. Brooks DN, Weber RV, Chao JD, et al. Processed nerve allografts for peripheral nerve reconstruction: a multicenter study of utilization and outcomes in sensory, mixed, and motor nerve reconstructions. *Microsurgery.* 2012;32(1):1-14.
37. Shin AY. Peripheral nerve injuries: advancing the field through research, collaboration, and education. *J Hand Surg Am.* 2014;39(10):2052-2058.
38. Szynkaruk M, Kemp SW, Wood MD, Gordon T, Borschel GH. Experimental and clinical evidence for use of decellularized nerve allografts in peripheral nerve gap reconstruction. *Tissue Eng Part B Rev.* 2013;19(1):83-96.

39. Hundepool CA, Nijhuis TH, Kotsougiani D, Friedrich PF, Bishop AT, Shin AY. Optimizing decellularization techniques to create a new nerve allograft: an in vitro study using rodent nerve segments. *Neurosurg Focus.* 2017;42(3):E4.
40. Bulstra LF, Hundepool CA, Friedrich PF, Bishop AT, Hovius SER, Shin AY. Functional Outcome after Reconstruction of a Long Nerve Gap in Rabbits Using Optimized Decellularized Nerve Allografts. *Plast Reconstr Surg.* 2020;145(6):1442-1450.
41. Salzer JL, Bunge RP. Studies of Schwann cell proliferation. I. An analysis in tissue culture of proliferation during development, Wallerian degeneration, and direct injury. *J Cell Biol.* 1980;84(3):739-752.
42. De la Rosa MB, Kozik EM, Sakaguchi DS. Adult Stem Cell-Based Strategies for Peripheral Nerve Regeneration. *Adv Exp Med Biol.* 2018;1119:41-71.
43. Jiang L, Jones S, Jia X. Stem Cell Transplantation for Peripheral Nerve Regeneration: Current Options and Opportunities. *Int J Mol Sci.* 2017;18(1).
44. Rbia N, Bulstra LF, Bishop AT, van Wijnen AJ, Shin AY. A Simple Dynamic Strategy to Deliver Stem Cells to Decellularized Nerve Allografts. *Plast Reconstr Surg.* 2018;142(2):402-413.
45. Rbia N, Bulstra LF, Thaler R, Hovius SER, van Wijnen AJ, Shin AY. In Vivo Survival of Mesenchymal Stromal Cell-Enhanced Decellularized Nerve Grafts for Segmental Peripheral Nerve Reconstruction. *J Hand Surg Am.* 2019;44(6):514 e511-514 e511.
46. Mathot F, Rbia N, Bishop AT, Hovius SER, Van Wijnen AJ, Shin AY. Adhesion, distribution, and migration of differentiated and undifferentiated mesenchymal stem cells (MSCs) seeded on nerve allografts. *J Plast Reconstr Aesthet Surg.* 2020;73(1):81-89.
47. Mathot F, Rbia N, Thaler R, Bishop AT, Van Wijnen AJ, Shin AY. Gene expression profiles of differentiated and undifferentiated adipose derived mesenchymal stem cells dynamically seeded onto a processed nerve allograft. *Gene.* 2020;724:144151.
48. Muangsanit P, Shipley RJ, Phillips JB. Vascularization Strategies for Peripheral Nerve Tissue Engineering. *Anat Rec (Hoboken).* 2018;301(10):1657-1667.
49. Auger FA, Gibot L, Lacroix D. The pivotal role of vascularization in tissue engineering. *Annu Rev Biomed Eng.* 2013;15:177-200.
50. Terzis JK, Kostopoulos VK. Vascularized nerve grafts and vascularized fascia for upper extremity nerve reconstruction. *Hand (N Y).* 2010;5(1):19-30.
51. Hobson MI, Green CJ, Terenghi G. VEGF enhances intraneural angiogenesis and improves nerve regeneration after axotomy. *J Anat.* 2000;197 Pt 4:591-605.
52. Lee JY, Giusti G, Friedrich PF, Bishop AT, Shin AY. Effect of Vascular Endothelial Growth Factor Administration on Nerve Regeneration after Autologous Nerve Grafting. *J Reconstr Microsurg.* 2016;32(3):183-188.
53. Mohammadi R, Ahsan S, Masoumi M, Amini K. Vascular endothelial growth factor promotes peripheral nerve regeneration after sciatic nerve transection in rat. *Chin J Traumatol.* 2013;16(6):323-329.
54. Li Y, Zhang F, Nagai N, et al. VEGF-B inhibits apoptosis via VEGFR-1-mediated suppression of the expression of BH3-only protein genes in mice and rats. *J Clin Invest.* 2008;118(3):913-923.

55. Storkebaum E, Carmeliet P. VEGF: a critical player in neurodegeneration. *J Clin Invest.* 2004;113(1):14-18.
56. Chen CW, Corselli M, Peault B, Huard J. Human blood-vessel-derived stem cells for tissue repair and regeneration. *J Biomed Biotechnol.* 2012;2012:597439.

PART I

The Role of Angiogenesis in Nerve Regeneration

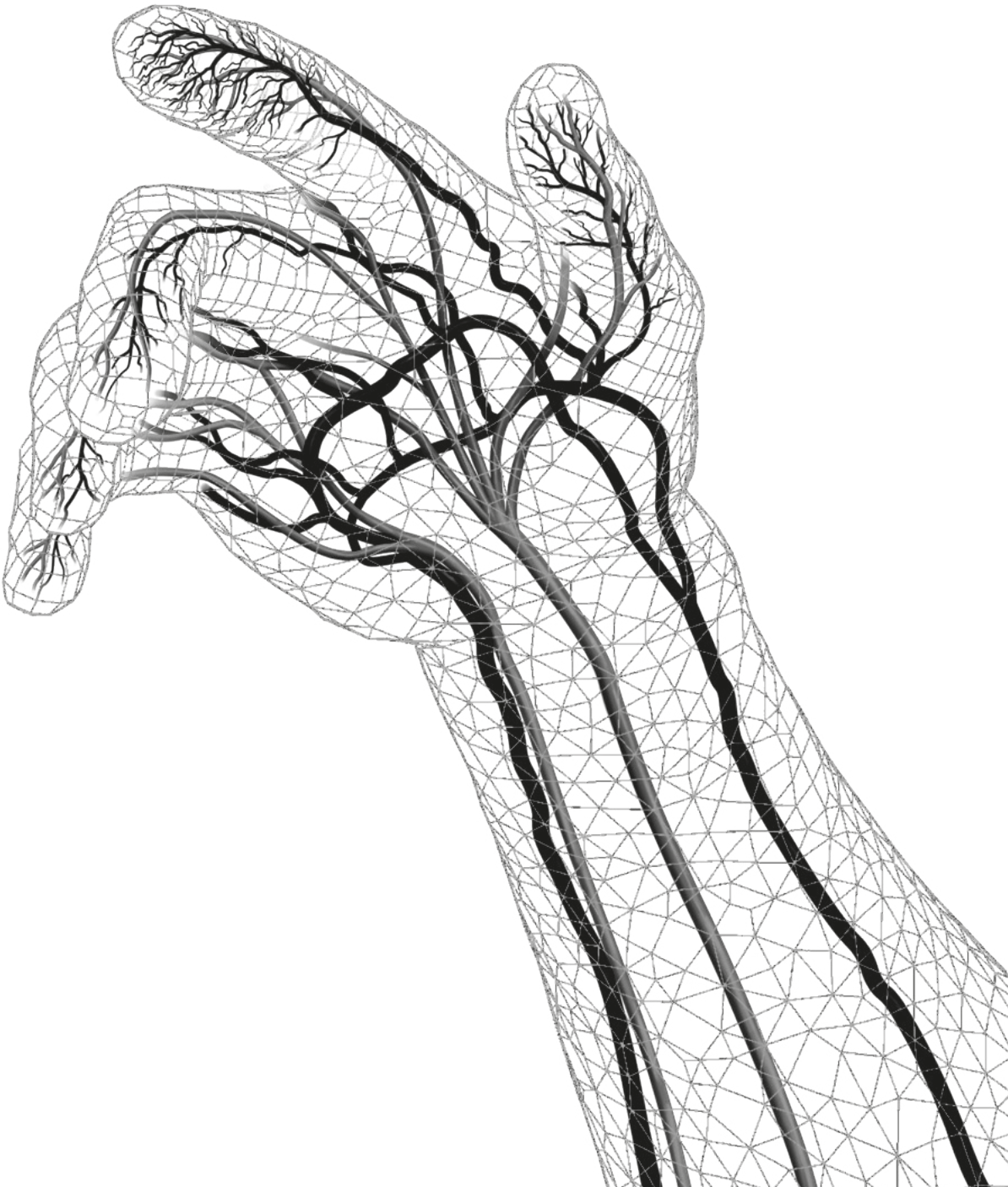

CHAPTER **TWO**

The Role of Vascularization in Nerve Regeneration of Nerve Graft: A Review of Literature

Tiam M. Saffari[1,2]
Meiwand Bedar[1,2]
Caroline A. Hundepool[2]
Allen T. Bishop[1]
Alexander Y. Shin[1]

Affiliations

[1]Department of Orthopedic Surgery, Mayo Clinic, Rochester, MN, USA

[2]Department of Plastic-, Reconstructive- and Hand Surgery, Erasmus Medical Center, Rotterdam, the Netherlands

Neural Regeneration Research. 2020;15(9):1573-1579

ABSTRACT

Vascularization is an important factor in nerve graft survival and function. The specific molecular regulations and patterns of angiogenesis following peripheral nerve injury are in a broad complex of pathways. This review aims to summarize current knowledge on the role of vascularization in nerve regeneration, including the key regulation molecules, and mechanisms and patterns of revascularization after nerve injury. Angiogenesis, the maturation of pre-existing vessels into new areas, is stimulated through angiogenic factors such as vascular endothelial growth factor (VEGF) and precedes the repair of damaged nerves. VEGF administration to nerves has demonstrated to increase revascularization after injury; however, it remained insufficient in improving functional recovery on the long term in basic science research. In the clinical setting, vascularized nerve grafts (VNG) could be used in the reconstruction of large segmental peripheral nerve injuries. VNGs are postulated to accelerate revascularization and enhance nerve regeneration by providing an optimal nutritional environment, especially in scarred beds, and decrease fibroblast infiltration. This could improve functional recovery after nerve grafting, however, conclusive evidence of the superiority of VNGs is lacking in human studies. A well-designed randomized controlled trial comparing VNGs to NVNGs involving patients with similar injuries, nerve graft repair and follow-up times is necessary to demonstrate the efficacy of VNGs. Due to technical challenges, composite transfer of a nerve graft along with its adipose tissue has been proposed to provide a healthy tissue bed. Basic science research has shown that a vascularized fascial flap containing adipose tissue and a vascular bundle improves revascularization through excreted angiogenic factors, provided by the stem cells in the adipose tissue as well as by the blood supply and environmental support. While it was previously believed that revascularization occurred from both nerve ends, recent studies propose that revascularization occurs primarily from the proximal nerve coaptation. Fascial flaps or VNGs have limited applicability and future directions could lead towards off-the-shelf alternatives to autografting, such as biodegradable nerve scaffolds which include capillary-like networks to enable vascularization and avoid graft necrosis and ischemia.

INTRODUCTION

Vascularization is one of the great challenges faced in nerve reconstruction, especially in nerve autograft substitutes such as nerve allografts or conduits that do not contain living cells [1]. In these substitutes, vascularization needs to be achieved to ensure cellular survival and avoid central necrosis, which is observed in nerve grafts with large diameters and long defects [1,2]. The diffusion limit of oxygen to meet the demands of cellular metabolism is around 100-200 µm, which is an essential to recognize when evaluating the role of vascularity in neural regeneration [3,4]. There is an increased understanding of nerve regeneration and cell biology with compelling evidence for the association of arterial blood vessels and nerves, in particular the alignment of peripheral nerves with blood vessels. The nervous system forms intricate branching networks reaching every organ in the body and relies on the vascular tree to supply oxygen and nutrients to meet substantial metabolic demands supporting organ development [5].

It has been suggested that vascular endothelial cells guide the regeneration of peripheral nerve axons by producing vascular endothelial growth factor (VEGF) to induce angiogenesis preceding the repair of damaged nerves [6] (Figure 1). VEGF is a potent multifunctional cytokine that stimulates the outgrowth of Schwann cells and blood vessels, while enhancing axonal outgrowth from the dorsal root ganglia [7-10]. As a result, VEGF has become the focus of numerous investigations with regards to its effects on the peripheral nerves [7,11-14]. Clinical attempts to augment vascularization and improve nerve graft outcomes using VEGF have led to conflicting results [15,16], suggesting that the specific molecular regulations and patterns of angiogenesis following peripheral nerve injury are broader and more complex.

In this review, the role of vascularization in nerve regeneration will be discussed, including the key regulation molecules in vascularization, the vascular system of the nerve, the mechanisms of vascularization and the application of vascularized nerve grafts (VNG) in peripheral nerve reconstruction.

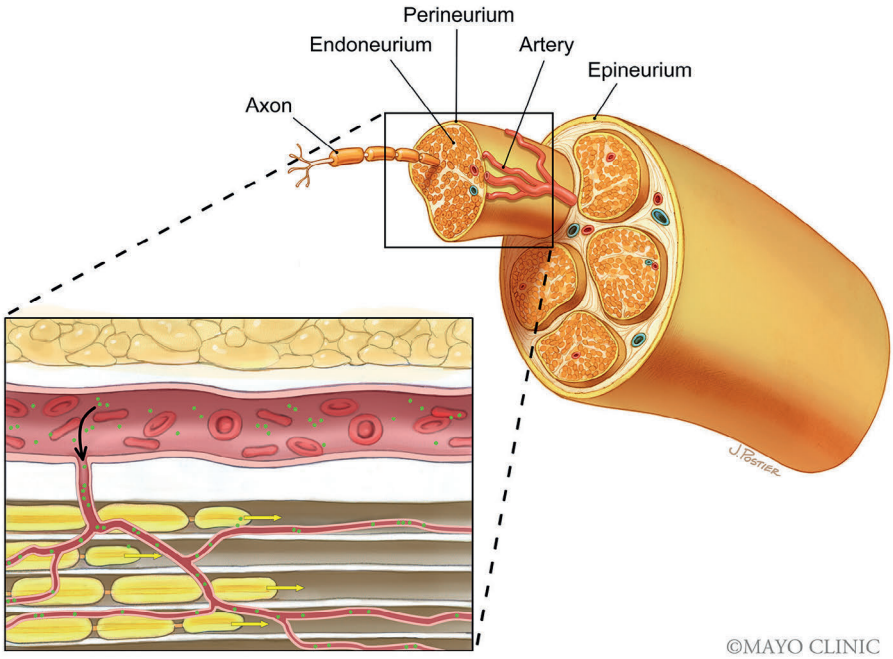

Figure 1. Schematic illustration of the components of a peripheral nerve. The peripheral nerve is depicted, demonstrating the axon protected by the endoneurium. The nerve fascicle is enveloped by the perineurium. Groups of fascicles are surrounded by the epineurium. Each fascicle of endoneurium contains up to several thousands of axons. Blood is supplied by a network of capillary-like microvessels derived from arterioles and venules, which are branches of major limb vessels. The zoomed image depicts the close relationship of vessels and axons. When the nerve is injured, vascular endothelial cells guide the regeneration of peripheral nerve axons by producing vascular endothelial growth factor (VEGF, green dots) to induce angiogenesis preceding the repair of damaged nerves. *With permission of the Mayo Foundation, Copyright Mayo Foundation 2019. All rights reserved.*

SEARCH STRATEGY

Literature research was performed using PubMed, Medline, Cochrane, Web of Science and Google Scholar databases using the following combination of keywords: “angiogenesis” OR “vascularization” OR “blood perfusion” AND “nerve regeneration” OR “nerve graft” OR “nerve transplantation” until August 2019. The results were further screened by title and abstract to only present studies in peripheral nerve injuries in both animals and humans. Other inclusion criteria were articles (i) written in English, (ii) published in the last 35 years and (iii) that had available abstracts. Articles describing nerve studies in spinal cord surgery, facial and eye surgery were

excluded. Six exceptionally valuable articles published prior to 1985 were included based on snowballing.

MECHANISMS OF VASCULARIZATION

Formation of a vascular network of peripheral nerves

The processes underlying the formation of blood vessels are vasculogenesis and angiogenesis [17]. Vasculogenesis describes the formation of the primitive vasculature in the embryo. After development of this primary vascular system, remodeling of pre-existing vessels into new areas forms mature vasculature as a result of angiogenesis. Central to the control of angiogenesis is VEGF, which is also critical to the maturation and stabilization of vessels in this process [17]. VEGF-induced effects are mediated through receptor tyrosine kinases, predominantly expressed on endothelial cells [18].

A cadaver study identified five different patterns of blood supply to the nerves varying from no dominant arterial pedicle to multiple dominant arterial pedicles forming a continuous artery that accompanies the nerve [19]. While identifying vascular supply to peripheral nerve contributes to our knowledge, this does not clarify the mechanisms of peripheral nerve revascularization.

Revascularization of the nerve

The vascular tree and the nervous system branching networks are often patterned similarly in peripheral tissues and share several anatomical and functional characteristics [5]. This parallel pattern has raised questions regarding their interactions to explain whether both networks are independent of one another. In the embryonic limb skin, endothelial cells migrate toward and align with peripheral nerves in response to nerve and Schwann cell-derived VEGF-A; this is called angiogenesis [5]. Subsequently, the pattern of axons provides a spatial template for the pattern of arterial vessel branching resulting in congruence of these two networks.

Transplanted nerves have no vascular supply and need to undergo revascularization in the recipient bed [20]. Experimental models have investigated the pattern of endoneurial perfusion. These models provided evidence that the primary mechanism of

revascularization in a conventional autograft is longitudinal inosculation (host vessels grow into the graft from both ends and anastomose with donor vessels) [21-23]. The evidence of peripheral neovascularization or dependence on the graft bed as a source of revascularization had not evolved until later when centripetal revascularization, growth from the surrounding tissue bed, was described [24]. Inosculation results in endothelial-lined formed vessels at the nerve graft coaptation site. When the nerve graft metabolic requirements exceed the ability of the inosculated vessels to provide adequate blood flow, centripetal revascularization occurs from the surrounding bed [25]. Previously, it was believed that inosculation occurs equally from both nerve graft ends, but recent research using novel micro CT visualization techniques has shown that inosculation occurs primarily from proximal to distal [26,27]. This supports the fact that success of the grafted nerve is partly affected by the length of the graft, as a longer graft is subject to higher risk of necrosis in the mid-section [25,27]. Prolonged denervation time leads to intraneural fibrosis and core necrosis negatively affecting the nerve regeneration process [20]. Moreover, it was realized that multiple thin diameter cable grafts instead of single large diameter grafts could overcome central necrosis secondary to faster revascularization in smaller diameter cables [28].

To appreciate the potential benefits and limitations of our understanding of vascularization, it is important to comprehend the basic physiology of its effect on nerve regeneration in basic science and clinical applications as discussed below.

EFFECT OF VASCULARIZATION ON NERVE REGENERATION

Basic science applications

Since 1976, studies have suggested the superiority of VNGs. The major reason for the lack of evidence in peripheral nerve injuries is the fact that studies include the use of different animal species, reconstructive strategies, follow-up times and outcome measures to assess nerve regeneration. These methodological differences make translation from animal models to humans challenging and nearly impossible. An overview of the available studies is provided.

It is postulated that vascularity improves results of nerve grafts by increasing the number of Schwann cells, while minimizing intraneural fibrosis and enhancing axonal

regeneration [29]. Thus, vascularity would accelerate revascularization compared to non-vascularized nerve grafts (NVNG) [30,31]. A well vascularized bed does not only decrease fibroblast infiltration, but also provides an optimal nutritional environment [30]. In a scarred, non-vascularized wound bed model, increase in myelination has been found when providing vascularization [32,33]. However, no differences were found in nerve conduction velocity [34]. When intraneural blood supply is limited, the fibroblasts replace the Schwann cells, causing a fibrotic distal nerve and scarred endoneurial tube [28]. In normal, vascularized beds, reported results have been conflicting. Some studies found no differences between VNGs and NVNGs [35-37] in rat models, while in rabbit models increased remyelination and enhanced contraction force have been reported in VNGs [38,39]. These results may be explained by the length of the gap and regeneration process in these animal models. The rat model could be used as a bioassay to evaluate treatments but translation to larger animals may be complicated as differences may occur due to the small gap (<11 mm) and superlative regeneration rate in rats [40].

Other studies have focused on VEGF administration to the nerve site to enhance vessel formation and thus nerve regeneration and subsequently motor recovery [7,8]. It has been demonstrated that VEGF increases revascularization [7,8], however, the application of VEGF did not improve functional motor nerve recovery in the long term [7]. It is assumed that producing a supportive microenvironment after nerve injury including stable blood supply may have more effect than the application of VEGF alone. A vascularized fascial flap containing adipose tissue and a vascular bundle has been suggested to improve revascularization through the excreted angiogenic factors, provided by the stem cells in the adipose tissue as well as the blood supply and environmental support. The application of the superficial inferior epigastric artery fascial (SIEF) flap to provide vascularization to the nerve graft site in an experimental model has been described [41] and found to increase revascularization of transplanted nerve allografts [27] (Figure 2). However, further animal studies are required to determine its role in nerve reconstruction.

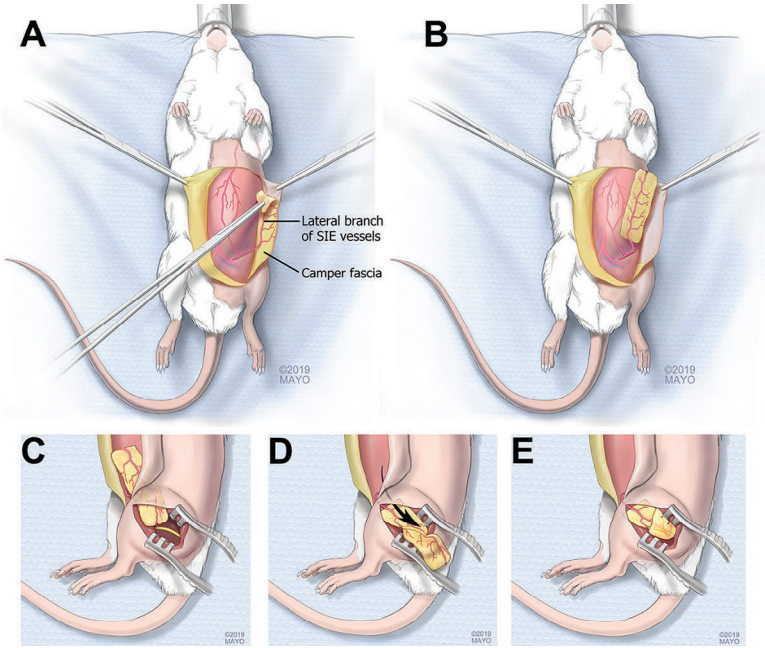

Figure 2. Schematic drawing of the superficial inferior epigastric fascia (SIEF) flap harvest. Depicted is the elevation of the flap from distal to proximal (A), providing a 4 x 3 cm adipofascial flap (B) with lateral branch of the superficial inferior (SIE) vessels. The SIEF flap was tunneled subcutaneously toward the nerve without vascular twisting of the epigastric trunk (C) and wrapped around the nerve graft reaching both anastomoses (D). The flap edges were trimmed if needed and two 10-0 nylon sutures were placed to secure the position of the SIEF flap (E). *With permission of the Mayo Foundation, Copyright Mayo Foundation 2019. All rights reserved.*

Clinical applications

In 1870, Phillipeaux and Vulpian performed the first successful nerve autograft [27,42] in cases in which direct tensionless nerve repair could not be achieved. In the years after, the increased application of cable grafting instead of trunk grafts, improved clinical outcomes [24,42,43]. To further overcome the problem of ischemia in conventional nerve grafts and optimize nutrient delivery, St. Clair Strange introduced the first pedicled VNG in 1945 by using a pedicled ulnar nerve graft for the reconstruction of the median nerve [44]. It was not until 1976, when the use of a free VNG was described; a 24 cm superficial radial nerve graft based on the radial artery to reconstruct a median nerve in a 26-year-old woman [45]. Postoperative angiography at six weeks confirmed successful transfer of the radial artery and positive Tinel's sign progressed to the distal border of the flexor retinaculum at six months, which indicated that at least a

portion of the axons had recovered [45]. Although this result was encouraging, technical difficulties were recognized and the procedure was suggested to be only performed in young patients, based on a case report and opinion of the authors.

In the 1980's, several experimental and clinical studies investigated the effectiveness of adding vascularization to a nerve graft [37,38,46-50]. Some of these studies demonstrated superior results of VNGs compared to NVNGs, while others suggested that the sensory- and motor functional recovery after VNGs were not significantly enhanced. The risk of thrombosis of the anastomosis in a VNG with subsequent necrosis of the nerve graft was considered by some authors as concerning and they advised against use of VNGs [51]. Conclusive findings on the superiority of VNGs in a clinical setting remain lacking due to multiple confounders, different duration of outcomes and the studies being mostly case reports or small case series [52-57]. There is no clear consensus on the clinical indications for VNGs. The application of VNGs should be considered in the following cases: large length of nerve gap of more than 6-7 cm, large diameter of the injured nerve, scarred recipient bed that could not support a NVNG and substantial pre-operative delay of more than 24 months [16,38,46,47,57,58]. It is imperative to understand that this recommendation is based on case reports, small case series and the anecdote of expert opinions.

Doi and colleagues compared 27 cases of free vascularized sural nerve grafts in the upper extremity to 22 non-vascularized sural nerve grafts. These grafts were used to repair axillary, median, ulnar, radial and digital nerves, with a mean nerve gap of 6.0 cm in the VNG group versus 4.7 cm in the NVNGs. Two years postoperatively, the VNGs performed better in terms of rate of axonal regeneration, rate of EMG return and motor- and sensory outcome [59]. Significant changes were found evaluating (i) the abductor pollicis brevis muscle (M2.5, S3 and M1, S2.3) for the median nerve, (ii) the abductor digiti minimi muscle (M3.3, S3 and M2, S2) for the ulnar nerve and (iii) extensor digiti communis muscle (M3.5 and M1) for the radial nerve, comparing the successful VNGs to conventional grafts using the Medical Research Council (MRC) scale, respectively. The authors concluded that VNGs are technically difficult and equally good to conventional grafts. The variability in use e.g. different motor nerves, mixed motor and sensory nerves, or sensory nerves, and difficulties in consistent measures of outcome, combined with the small numbers, make a definite conclusion

difficult. Nevertheless, others have endeavored describing techniques to repair defects of larger than 12 cm [60,61].

Similarly, Terzis and Kostopoulos found good to excellent sensory return, depending on the injury, after VNG reconstruction of 21 cases with upper extremity nerve injuries in which NVNGs had failed. [57]. In their lower extremity cases with injuries at the level of the knee or thigh, these same techniques were applied to regain muscle strength when denervation time was less than six months in patients reconstructed with large nerve grafts and regained remarkable muscle strength of at least M4, mostly in traction avulsion injuries [56]. Unfortunately, these results have yet to be duplicated.

VNGs are also often used in the reconstruction of proximal nerve lesions, such as traumatic brachial plexus injuries (BPI) [16]. In the largest BPI case series to date, 151 reconstructions for posttraumatic BPI were described [55]. Free and pedicled vascularized ulnar grafts were used for reconstruction and concluded that patients with long denervation times (>12 months) yielded inferior results compared with those that were operated earlier (<6 months) [55]. A similar study found unsatisfying recovery of elbow flexion and wrist extension after BPI when repaired around 4.6 months after trauma [52]. While there was no direct comparison to NVNGs in these studies, the importance of denervation time was well-stated and described as less receptivity of the neuromuscular junction when nerve repair is delayed for a long period of time [62]. It is accepted that outcomes are correlated with both the time course and the degree of denervation, however, an exact cut off point has not been defined, which may be worthwhile to evaluate. With no direct comparison to NVNGs, conclusions on the superiority of VNGs is only speculated and not proven.

To summarize, the above mentioned studies have used VNGs to repair large nerve defects to improve outcomes in complex and unique cases. Ideally, clinical studies comparing VNGs to NVNGs should be randomized and involve patients with similar injuries, nerve graft repair and follow-up times. Due to diversity in cases, critical analysis has not been feasible to date, recognizing a still existing clinical problem. Moreover, reconstructions are evaluated mostly by investigating axonal regeneration via Tinel's sign, EMG return and functional motor recovery. While these outcome measurements are clinically relevant, they are not a direct reflection of the applied vascularization. Very recent research investigated the use of ultrasound to describe

intraneural hypervascularization proximal to the site of nerve injury [63]. Although the increased blood flow does not directly implicate for patient management, it may reflect neovascularization and provide insight into pathophysiological processes after nerve injury treatments or serve as a potential prognostic tool, as it is known that the number of endoneurial capillaries significantly increases after nerve injury [64]. Implementing ultrasound as prognostic tool in future clinical trials would allow for direct measurement of the vascularization.

Technical challenges

The most frequently used VNGs are the saphenous and sural nerve graft, due to their dominant arterial pedicles and the acceptable donor site morbidity [19]. Several other VNGs, as described above, are associated with higher donor site morbidity or are mainly used in free flap reconstructions and not solely as nerve grafts. In very specific patients with brachial plexus avulsions of C8 and T1, the ulnar nerve can be used as a VNG based on the superior collateral artery [65] (Figure 3).

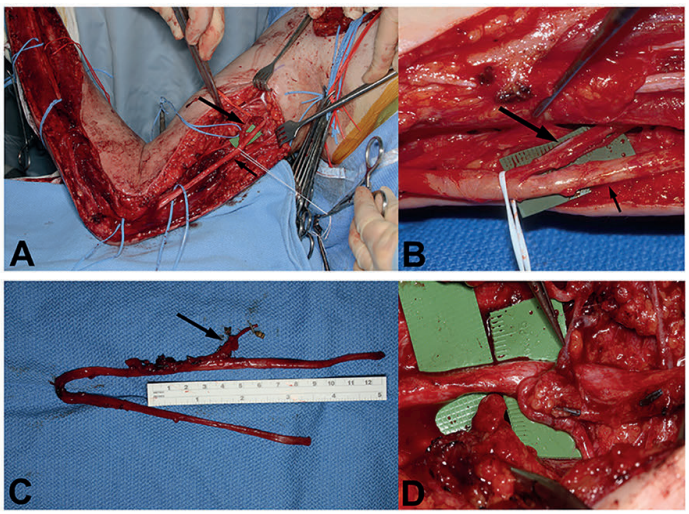

Figure 3. Vascularized ulnar nerve graft (VUNG) harvest. Depicted is the harvest of the ulnar nerve (small arrow), based on the superior ulnar collateral artery (SUCA, denoted with large arrow, A) in a patient with a C8-T1 brachial plexus root avulsion. B denoted a close-up view of the SUCA joining the ulnar nerve (ulnar nerve denoted with small arrow, SUCA denoted with large arrow). The completion of the harvest of the entire length of the ulnar nerve based on the SUCA measured approximately 30 cm (C, SUCA denoted with arrow). The VUNG was used to graft the C6 root to the lateral cord. In D the vascular anastomosis of the SUCA to the thoracoacromial trunk was depicted.

Vascularization of a long nerve segment can be achieved by using a VNG alone, placed together or enveloped with a NVNG, or a vascularized adipose flap can be placed around a NVNG to induce angiogenesis [57]. When using a sural nerve graft, blood supply will be based on the sural artery or the saphenous vein can be arterialized [66]. In cases of a larger nerve defect, grafts up to 60 cm could be harvested from the saphenous nerve, depending on the height of the patient [67]. Other options are the superficial peroneal nerve with its vascular pedicle, to reconstruct multiple nerves ranging from 14 to 30 cm [66], or the superficial radial nerve which could be harvested with the radial artery [68]. To use this VNG, however, it is advocated that the radial artery should be reconstructed with a vein graft, in order to minimize donor site morbidity.

Although VNGs have the potential to improve nerve reconstruction after injury, the surgeries are demanding and require microvascular experience. Technical challenges in matching diameter by cabling, while preserving blood supply, and finding recipient vessels if done as a free tissue transfer may prevent widespread adoption. In addition, considerations in the clinical application include location of obtaining sufficient peripheral nervous tissue and the associated donor site morbidity. Not only is the choice of donor site of importance, the injury site limits graft options as well, especially when the injury is situated near joint creases. In these cases, the environment of the nerve graft could be optimized by using a vascularized adipose-nerve composite transfer. Foo and colleagues described a novel technique of transferring a posterior interosseous nerve graft along with vascularized synovial and adipose tissue based on a branch of the posterior interosseous artery for neuromas of digital nerves, to provide a healthy tissue bed [69]. In large nerve defects with concomitant vascular trauma, immediate revascularization of a damaged artery has priority, limiting options for VNG harvest. In these cases, vascularized allografts could be applied [70], potentially vascularized with the use of a flap.

FUTURE DIRECTIONS

Although several studies have discussed the surgical techniques of VNGs [19,68,71,72], the clinical use has been sparse. Limited availability of VNGs in patients with nerve injuries stimulates the need for alternative methods for introducing vascularity to nerve reconstructions. The number of biomedical companies involved in regenerative medicine and tissue engineering has been steadily increasing, representing future interest in off-the-shelf suitable alternatives to autografting, such as biodegradable scaffolds which maintain mechanical properties and ultrastructure. Both biomaterials and decellularized nerve grafts have been combined with growth factors or stem cells to provide options to reconstruct nerve defects [73,74]. Moreover, exosomes, extracellular vesicles carrying microRNA, derived from Schwann cells, macrophages or stem cells provide exciting prospects for future treatment as the exosomes overcome the obstacles associated with cell therapy [75,76]. Other promising techniques include the generation of capillary-like networks in scaffolds to support the growth and viability of tissue substitutes that require blood supply, mainly when nutrient demand cannot be covered by diffusion processes in the center of these three-dimensional (3D) constructs [77,78].

Future 3D printing may be able to precisely recreate the structure of the scaffold to mimic a native nerve. Apart from the design and ultrastructure of the scaffold, several different factors are important and currently studied, such as biodegradation. The slow pace of nerve regeneration necessitates the scaffold to not be a fast degrading polymer, especially when reconstructing large defects. Moreover, the acetic environment created by the degradation of biocompatible polymers needs to be addressed in order to maintain a healthy bed for nerve regeneration [79]. Other considerations may be the thickness of the outer scaffold, which should not exceed 100-200 μm which is the diffusion limit of oxygen, aforementioned [4]. The application of 3D printed nerves with or without vessels will evolve over the next decade and may be implemented and improve outcomes in peripheral nerve injuries, especially to successfully repair large segmental defects.

CONCLUSIONS

Peripheral nerves are living dynamic tissues that thrive on nutritive blood supply. The interaction of vessels and nerves after a nerve injury is complex. Although the relationship between angiogenesis and neuroregeneration was originally thought to be related to nutritional factors, recently more evidence advocates for the Schwann cells to guide neuronal precursors via a complex pathway of factor secretion, among which VEGF, to enhance nerve regeneration. Revascularization of nerve grafts after injury relies mostly on environment and primarily on inosculation from host vessels. Clinical studies comparing VNGs to NVNGs remain lacking and existing studies are inconclusive. Future studies should be randomized and involve patients with similar injuries, nerve graft repair and follow-up times to be able to critically elucidate differences between VNGs and NVNGs. The technical obstacles could be overcome by provision of vascularized fascial flaps that enhance revascularization. The field of tissue engineering is evolving and predicted to take a larger part in treatment options for peripheral nerve injuries using biodegradable scaffolds.

Acknowledgements

The authors would like to thank Jim Postier (Rochester, MN) for the artwork of Figure 1 and 2.

Disclosure statement

No competing financial interests exist.

REFERENCES

1. Muangsanit P, Shipley RJ, Phillips JB. Vascularization Strategies for Peripheral Nerve Tissue Engineering. *Anat Rec (Hoboken).* 2018;301(10):1657-1667.
2. Auger FA, Gibot L, Lacroix D. The pivotal role of vascularization in tissue engineering. *Annu Rev Biomed Eng.* 2013;15:177-200.
3. Rouwkema J, Koopman B, Blitterswijk C, Dhert W, Malda J. Supply of nutrients to cells in engineered tissues. *Biotechnol Genet Eng Rev.* 2010;26:163-178.
4. Jain RK, Au P, Tam J, Duda DG, Fukumura D. Engineering vascularized tissue. *Nat Biotechnol.* 2005;23(7):821-823.
5. James JM, Mukouyama YS. Neuronal action on the developing blood vessel pattern. *Semin Cell Dev Biol.* 2011;22(9):1019-1027.
6. Cattin AL, Burden JJ, Van Emmenis L, et al. Macrophage-Induced Blood Vessels Guide Schwann Cell-Mediated Regeneration of Peripheral Nerves. *Cell.* 2015;162(5):1127-1139.
7. Lee JY, Giusti G, Friedrich PF, Bishop AT, Shin AY. Effect of Vascular Endothelial Growth Factor Administration on Nerve Regeneration after Autologous Nerve Grafting. *J Reconstr Microsurg.* 2016;32(3):183-188.
8. Wongtrakul S, Bishop AT, Friedrich PF. Vascular endothelial growth factor promotion of neoangiogenesis in conventional nerve grafts. *J Hand Surg Am.* 2002;27(2):277-285.
9. Sondell M, Lundborg G, Kanje M. Vascular endothelial growth factor stimulates Schwann cell invasion and neovascularization of acellular nerve grafts. *Brain Res.* 1999;846(2):219-228.
10. Dumpich M, Theiss C. VEGF in the nervous system: an important target for research in neurodevelopmental and regenerative medicine. *Neural Regen Res.* 2015;10(11):1725-1726.
11. Li Y, Zhang F, Nagai N, et al. VEGF-B inhibits apoptosis via VEGFR-1-mediated suppression of the expression of BH3-only protein genes in mice and rats. *J Clin Invest.* 2008;118(3):913-923.
12. Hobson MI, Green CJ, Terenghi G. VEGF enhances intraneural angiogenesis and improves nerve regeneration after axotomy. *J Anat.* 2000;197 Pt 4:591-605.
13. Mohammadi R, Ahsan S, Masoumi M, Amini K. Vascular endothelial growth factor promotes peripheral nerve regeneration after sciatic nerve transection in rat. *Chin J Traumatol.* 2013;16(6):323-329.
14. Storkebaum E, Carmeliet P. VEGF: a critical player in neurodegeneration. *J Clin Invest.* 2004;113(1):14-18.
15. Best TJ, Mackinnon SE. Peripheral nerve revascularization: a current literature review. *J Reconstr Microsurg.* 1994;10(3):193-204.
16. D'Arpa S. Vascularized nerve "grafts": just a graft or a worthwhile procedure? *Plast Aesthet Res.* 2016;2(4):183-192.
17. Akhavani MA, Sivakumar B, Paleolog EM, Kang N. Angiogenesis and plastic surgery. *J Plast Reconstr Aesthetic Surg.* 2008;61(12):1425-1437.
18. Neufeld G, Cohen T, Gengrinovitch S, Poltorak Z. Vascular endothelial growth factor (VEGF) and its receptors. *FASEB J.* 1999;13(1):9-22.

19. El-Barrany WG, Marei AG, Vallée B. Anatomic basis of vascularised nerve grafts: The blood supply of peripheral nerves. *Surg Radiol Anat.* 1999;21(2):95-102.
20. Bassilios Habre S, Bond G, Jing XL, Kostopoulos E, Wallace RD, Konofaos P. The Surgical Management of Nerve Gaps: Present and Future. *Ann Plast Surg.* 2018;80(3):252-261.
21. Best TJ, Mackinnon SE, Midha R, Hunter DA, Evans PJ. Revascularization of peripheral nerve autografts and allografts. *Plast Reconstr Surg.* 1999;104(1):152-160.
22. Lind R, Wood MB. Comparison of the pattern of early revascularization of conventional versus vascularized nerve grafts in the canine. *J Reconstr Microsurg.* 1986;2(4):229-234.
23. Penkert G, Bini W, Samii M. Revascularization of nerve grafts: an experimental study. *J Reconstr Microsurg.* 1988;4(4):319-325.
24. Tarlov I. The importance of an adequate blood supply. *J Neurosurg* 1945;2:49-71.
25. Terzis JK, Skoulis TG, Soucacos PN. Vascularized nerve grafts. A review. *Int Angiol.* 1995;14(3):264-277.
26. Chalfoun C, Scholz T, Cole MD, Steward E, Vanderkam V, Evans GRD. Primary nerve grafting: A study of revascularization. *Microsurgery.* 2003;23(1):60-65.
27. Saffari TM, Mathot, F. , Friedrich, P.F. , Bishop, A.T., Shin, A.Y. Revascularization patterns of nerve allografts in a rat sciatic nerve defect model. *Journal of Plastic, Reconstructive & Aesthetic Surgery.* 2019.
28. Breidenbach WC, Terzis JK. Vascularized nerve grafts: An experimental and clinical review. *ANN PLAST SURG.* 1987;18(2):137-146.
29. Oudega M, Gautier SE, Chapon P, et al. Axonal regeneration into Schwann cell grafts within resorbable poly(alpha-hydroxyacid) guidance channels in the adult rat spinal cord. *Biomaterials.* 2001;22(10):1125-1136.
30. Donzelli R, Capone C, Sgulò FG, Mariniello G, Maiuri F. Vascularized nerve grafts: an experimental study. *Neurol Res.* 2016;38(8):669-677.
31. Bertelli JA, Taleb M, Mira JC, Calixto JB. Muscle fiber type reorganization and behavioral functional recovery of rat median nerve repair with vascularized or conventional nerve grafts. *RESTOR NEUROL NEUROSCI.* 1996;10(1):5-12.
32. Koshima I, Harii K. Experimental study of vascularized nerve grafts: multifactorial analyses of axonal regeneration of nerves transplanted into an acute burn wound. *J Hand Surg Am.* 1985;10(1):64-72.
33. Ozcan G, Shenaq S, Mirabi B, Spira M. Nerve regeneration in a bony bed: Vascularized versus nonvascularized nerve grafts. *PLAST RECONSTR SURG.* 1993;91(7):1322-1331.
34. Mani GV, Shurey C, Green CJ. Is early vascularization of nerve grafts necessary ? *J HAND SURG.* 1992;17 B(5):536-543.
35. McCullough CJ, Gagey O, Higginson DW, Sandin BM, Crow JC, Sebille A. Axon regeneration and vascularisation of nerve grafts. An experimental study. *J Hand Surg [Br].* 1984;9(3):323-327.
36. Seckel BR, Ryan SE, Simons JE. Vascularized versus nonvascularized nerve grafts: An experimental structural comparison. *PLAST RECONSTR SURG.* 1986;78(2):211-220.
37. Pho RW, Lee YS, Rujiwetpongstorn V, Pang M. Histological studies of vascularised nerve graft and conventional nerve graft. *J Hand Surg [Br].* 1985;10(1):45-48.

38. Shibata M, Tsai TM, Firrell J, Breidenbach WC. Experimental comparison of vascularized and nonvascularized nerve grafting. *J HAND SURG.* 1988;13(3):358-365.
39. Kanaya F, Firrell J, Tsai TM, Breidenbach WC. Functional results of vascularized versus nonvascularized nerve grafting. *Plast Reconstr Surg.* 1992;89(5):924-930.
40. Saffari S, Saffari TM, Moore AM, Shin AY. Peripheral Nerve Basic Science Research-What Is Important for Hand Surgeons to Know? *J Hand Surg Am.* 2021.
41. Saffari TM, Bishop AT, Shin AY. The Superficial Inferior Epigastric Artery Fascia Flap in Rats. *Journal of Reconstructive Microsurgery Open* 2020; 05(01): e7-e14
42. Dellon ES, Dellon AL. The first nerve graft, Vulpian, and the nineteenth century neural regeneration controversy. *J Hand Surg Am.* 1993;18(2):369-372.
43. Seddon HJ. The use of autogenous grafts for the repair of large gaps in peripheral nerves. *Br J Surg.* 1947;35(138):151-167.
44. Strange FG. An operation for nerve pedicle grafting; preliminary communication. *Br J Surg.* 1947;34(136):423-425.
45. Taylor GI, Ham FJ. Free Vascularized Nerve Graft - Further Experimental and Clinical Application of Microvascular Techniques. *Plast Reconstr Surg.* 1976;57(4):413-426.
46. Koshima I, Harii K. Experimental study of vascularized nerve grafts: Multifactorial analyses of axonal regeneration of nerves transplanted into an acute burn wound. *J HAND SURG.* 1985;10(1):64-72.
47. Restrepo Y, Merle M, Michon J. Free vascularized nerve grafts: An experimental study in the rabbit. *MICROSURGERY.* 1985;6(2):78-84.
48. Daly PJ, Wood MB. Endoneural and epineural blood flow evaluation with free vascularized and conventional nerve grafts in the canine. *J RECONSTR MICROSURG.* 1985;2(1):45-49.
49. Doi K, Kuwata N, Sakai K, Tamaru K, Kawai S. A reliable technique of free vascularized sural nerve grafting and preliminary results of clinical applications. *J Hand Surg [Am].* 1987;12(5 Pt 1):677-684.
50. Rose EH, Kowalski TA, Norris MS. The reversed venous arterialized nerve graft in digital nerve reconstruction across scarred beds. *Plast Reconstr Surg.* 1989;83(4):593-604.
51. Merle M, Dautel G. Vascularised nerve grafts. *J HAND SURG.* 1991;16 B(5):483-488.
52. Bertelli JA, Ghizoni MF. Results of C5 Root Grafting to the Musculocutaneous Nerve Using Pedicled, Vascularized Ulnar Nerve Grafts. *J Hand Surg (USA).* 2009;34(10):1821-1826.
53. del Piñal F, García-Bernal FJ, Regalado J, Studer A, Cagigal L, Ayala H. The Tibial Second Toe Vascularized Neurocutaneous Free Flap for Major Digital Nerve Defects. *J Hand Surg (USA).* 2007;32(2):209-217.
54. Farzan M, Mortazavi SMJ, Asadollahi S. Cubital tunnel syndrome: Review of 14 anterior subcutaneous transpositions of the vascularized ulnar nerve. *Acta Med Iran.* 2005;43(3):197-203.
55. Terzis JK, Kostopoulos VK. Vascularized ulnar nerve graft: 151 reconstructions for posttraumatic brachial plexus palsy. *Plast Reconstr Surg.* 2009;123(4):1276-1291.
56. Terzis JK, Kostopoulos VK. Vascularized nerve grafts for lower extremity nerve reconstruction. *Ann Plast Surg.* 2010;64(2):169-176.
57. Terzis JK, Kostopoulos VK. Vascularized nerve grafts and vascularized fascia for upper extremity nerve reconstruction. *Hand.* 2010;5(1):19-30.

58. Kallio PK, Vastamaki M. An analysis of the results of late reconstruction of 132 median nerves. *J Hand Surg Br.* 1993;18(1):97-105.
59. Doi K, Tamaru K, Sakai K, Kuwata N, Kurafuji Y, Kawai S. A comparison of vascularized and conventional sural nerve grafts. *J HAND SURG.* 1992;17(4):670-676.
60. Hasegawa T, Nakamura S, Manabe T, Mikawa Y. Vascularized nerve grafts for the treatment of large nerve gap after severe trauma to an upper extremity. *Arch Orthop Trauma Surg.* 2004;124(3):209-213.
61. Koshima I, Nanba Y, Tsutsui T, Takahashi Y, Kawai A. Vascularized femoral nerve graft with anterolateral thigh true perforator flap for massive defects after cancer ablation in the upper arm. *J Reconstr Microsurg.* 2003;19(5):299-302.
62. Wu P, Chawla A, Spinner RJ, et al. Key changes in denervated muscles and their impact on regeneration and reinnervation. *Neural Regen Res.* 2014;9(20):1796-1809.
63. Arányi Z, Csillik A, Dévay K, Rosero M. Ultrasonographic demonstration of intraneural neovascularization after penetrating nerve injury. *Muscle Nerve.* 2018;57(6):994-999.
64. Nukada H. Post-traumatic endoneurial neovascularization and nerve regeneration: A morphometric study. *BRAIN RES.* 1988;449(1-2):89-96.
65. Hattori Y, Doi K, Ikeda K, Pagsaligan JM. Vascularized ulnar nerve graft for reconstruction of a large defect of the median or radial nerves after severe trauma of the upper extremity. *J Hand Surg (USA).* 2005;30(5):986-989.
66. Breidenbach W, Terzis JK. The anatomy of free vascularized nerve grafts. *CLIN PLAST SURG.* 1984;11(1):65-71.
67. Terzis JK, Kostopoulos VK. Vascularized nerve grafts: A review. *Atlas Hand Clin.* 2005;10(1 SPEC. ISS.):101-124.
68. Shafi M, Hattori Y, Doi K. Surgical Technique of Harvesting Vascularized Superficial Radial Nerve Graft. *J Hand Surg (USA).* 2010;35(2):312-315.
69. Foo A, Martin-Playa P, Sebastin Muttath SJ. Arterialized Posterior Interosseous Nerve Graft for Digital Neuroma. *Tech Hand Up Extrem Surg.* 2019.
70. Bain JR. Peripheral nerve and neuromuscular allotransplantation: current status. *Microsurgery.* 2000;20(8):384-388.
71. Giesen T, Acland RD, Thirkannad S, Elliot D. The vascularization of the median nerve in the distal forearm and its potential clinical importance. *J Hand Surg (USA).* 2012;37(6):1200-1207.
72. Mozaffarian K, Zemoodeh HR, Zarenezhad M, Owji M. "In Situ Vascular Nerve Graft" for Restoration of Intrinsic Hand Function: An Anatomical Study. *J Hand Surg Asian Pac Vol.* 2018;23(2):248-254.
73. Mathot F, Rbia N, Thaler R, Bishop AT, van Wijnen AJ, Shin AY. Introducing human adipose-derived mesenchymal stem cells to Avance nerve grafts and NeuraGen nerve guides. *J Plast Reconstr Aesthet Surg.* 2020;73(8):1473-1481.
74. Patel NP, Lyon KA, Huang JH. An update-tissue engineered nerve grafts for the repair of peripheral nerve injuries. *Neural Regen Res.* 2018;13(5):764-774.
75. Ching RC, Kingham PJ. The role of exosomes in peripheral nerve regeneration. *Neural Regen Res.* 2015;10(5):743-747.

76. Qing L, Chen H, Tang J, Jia X. Exosomes and Their MicroRNA Cargo: New Players in Peripheral Nerve Regeneration. *Neurorehabil Neural Repair.* 2018;32(9):765-776.
77. Laschke MW, Menger MD. Vascularization in tissue engineering: angiogenesis versus inosculation. *Eur Surg Res.* 2012;48(2):85-92.
78. Auger FA, Gibot L, Lacroix D. The pivotal role of vascularization in tissue engineering. *Annual review of biomedical eng.* 2013.
79. Sung HJ, Meredith C, Johnson C, Galis ZS. The effect of scaffold degradation rate on three-dimensional cell growth and angiogenesis. *Biomaterials.* 2004;25(26):5735-5742.

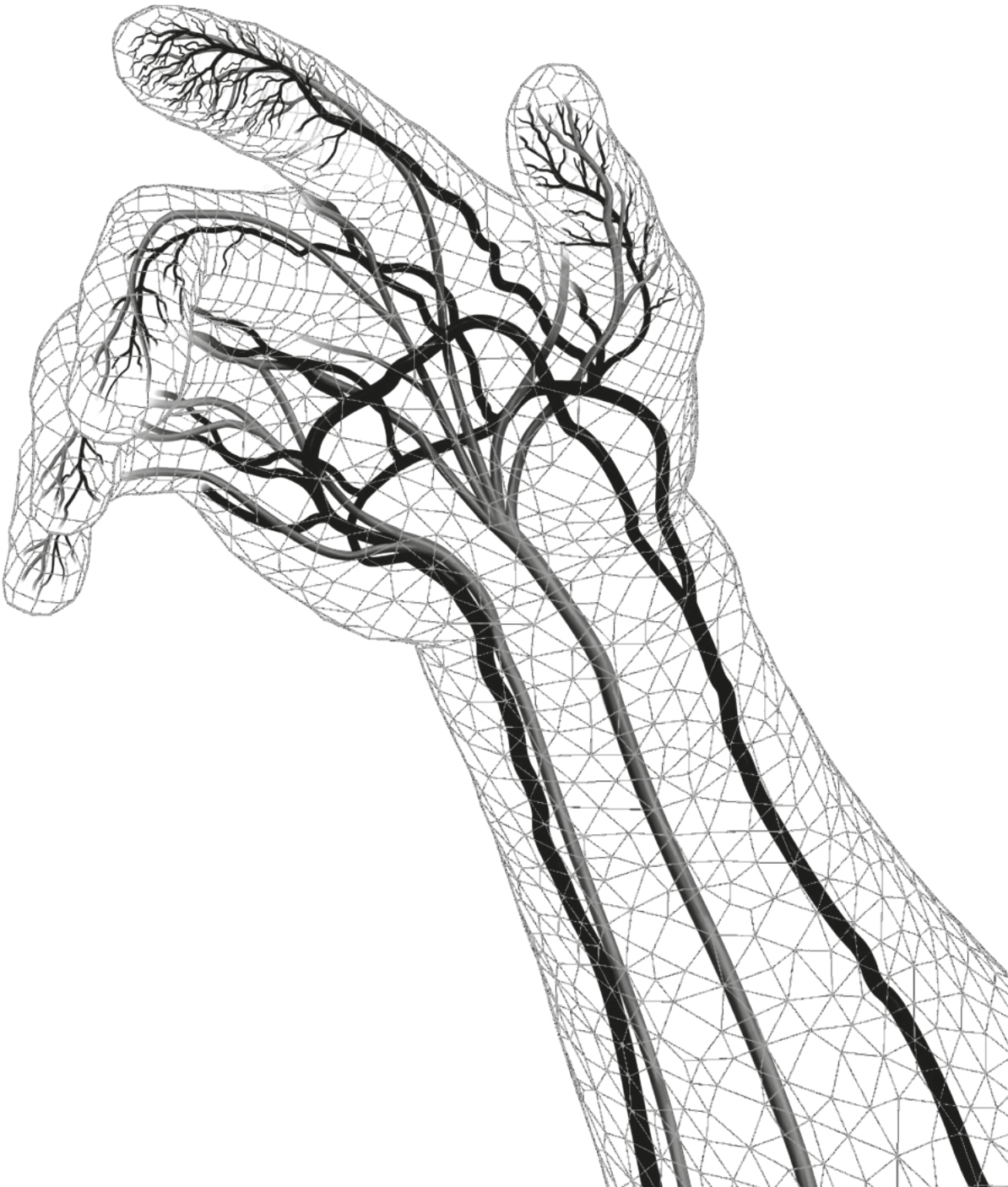

CHAPTER

THREE

The Superficial Inferior Epigastric Artery Fascia Flap in Rats

Tiam M. Saffari[1, 2]
Allen T. Bishop[1]
Alexander Y. Shin[1]

Affiliations

[1]Department of Orthopedic Surgery, Mayo Clinic, Rochester, MN, USA

[2]Department of Plastic-, Reconstructive- and Hand Surgery, Erasmus Medical Center, Rotterdam, the Netherlands

Journal of Reconstructive Microsurgery Open. 2020:e7–e14

ABSTRACT

Background

An adipofascial flap in the rat may provide new options for adding vascularization to scarred or nonvascularized beds for a variety of research studies. Current literature lacks sufficient description for a simple reproducible flap model for a vascularized pedicled flap in rats, in particular for neovascularization of allograft nerves for reconstruction of sciatic nerve defects. The purpose of this study was to describe a surgical technique and determine long-term survivability for the pedicled superficial inferior epigastric artery fascial (SIEF) flap in the rat to meet requirement for a tunneled adipofascial flap to add vascularization to the sciatic nerve area.

Materials and Methods

The technique and use of a 4 x 3 cm SIEF flap are described. Twenty Lewis rats underwent the technique to determine feasibility. The flap was wrapped around processed allograft nerve reconstructions and viability of the flap was evaluated after 12 and 16 weeks. To visualize vessels, nerve grafts were harvested at 12 weeks and stained with hematoxylin-eosin and an antibody against microvessels (CD-34).

Results

All flaps remained viable after survival of 12 and 16 weeks. Complications included one hematoma formation and two lymphocele formations which did not have any impact on the flap. Immunohistochemistry confirmed an increase in microvessels and Schwann cell nuclei in the SIEF group compared to nerve samples from the unoperated, contralateral side.

Conclusions

A pedicled adipofascial flap model in the rat to provide a vascular bed for sciatic nerve reconstruction is detailed with long-term survivability evaluation of the flap. This flap is technically simple to be harvested and is suitable for revascularization procedures of various tissues in the lower abdomen, genital area, thigh or upper limb of the rat.

INTRODUCTION

It has been postulated that the application of either vascularized nerve grafts or a vascularized flap wrapped around the nerve graft will improve outcomes of nerve grafts in severely scarred tissue beds [1-6]. A well vascularized bed becomes more critical as length and caliber of a nerve graft increase [6]. The literature regarding pedicled fascial flaps in animals is scarce. The free superficial inferior epigastric artery (SIEA) flap in rats was first described in 1967 by Strauch and Murray [7]. This free tissue transfer could be designed in various sizes and has been applied in different investigational and training models (e.g. distal flap necrosis [8-12], ischemia reperfusion injury [13-16], and microvascular training [17]). In the rat, no previously described facial flaps have been described or used to wrap around the sciatic nerve [18,19]. One study had been performed elevating a SIEA flap and evaluated for short term viability after seven days [19]. While this pedicled flap was demonstrated to be safe and avoids the potential risk of free flap failure (microvascular anastomosis complications), long-term viability was never assessed [19,20]. Another study described pedicled flaps to vascularize nerve grafts in an intratemporal facial nerve defect model and focused on histological outcomes [18]. The sciatic nerve defect model is a well-established model to investigate multiple outcomes varying from functional motor outcomes to histology [21-23]. A pedicled flap model in rats to provide vascularization to the nerve wound bed has not been described and requires validation prior to measurement of other outcomes. Therefore, the purpose of this study was to describe a reproducible surgical technique and determine long-term survivability for the pedicled superficial inferior epigastric artery fascial (SIEF) flap in the rat to meet requirement for a tunneled adipofascial flap to add vascularization to the sciatic nerve bed.

METHODS

Animals

The study was approved by our Institutional Animal Care and Use Committee (IACUC A3348-18). Twenty male adult Lewis rats, weighing 250-300 grams (Envigo, USA) had a unilateral 10 mm sciatic nerve gap repaired with an decellularized processed nerve allograft [24]. Ten Sprague-Dawley rats (Envigo, Madison, WI, USA) weighing 250-300 grams served as major histocompatibility mismatch donors [25,26]. A 15-mm segment of

the sciatic nerve was harvested bilaterally. The nerves were cleaned from external debris and decellularized using a five-day previously described decellularization protocol [24]. The nerves were sterilized using γ-irradiation and stored in a Sodium Phosphate Buffer (PBS) at 4°C until surgery. During the survival period, the Lewis rats were housed individually with a twelve-hour light-dark cycle and *ad libitum* access to food and water. Flap viability was evaluated after 12 (N=10) and 16 weeks (N=10).

Anesthesia

Rats were anesthetized in an isoflurane chamber, shaved, prepped and positioned in the nosecone to maintain anesthesia throughout the procedure. Body temperature was maintained at 37°C with a heating pad. Preoperatively, the following were administered subcutaneously; 5 mL of NaCl 0.9% to prevent dehydration, buprenorphine SR (Buprenorphine SR-LAB, ZooPharm pharmacy, 0.6mg/kg) for pain control and Enrofloxacin (Baytril, Bayer, Germany, 10mg/kg) providing infection prophylaxis. Postoperatively, the rats were kept warm in towels. The rats were observed daily until completion of the experiment. During sacrifice, rats were euthanized with 1 mL intraperitoneal injection of Pentobarbital Sodium (Fatal Plus, 390 mg/mL, Vortech, Dearborn, MI, USA).

Surgical procedure

The SIEF flap is a pedicled flap supplied by superficial inferior epigastric (SIE) vessels including both the arteries and the accompanying veins. These vessels arise from femoral vessels close to branches of the popliteal and saphenous vessels and are direct branches of the cutaneous arteries and veins. The main trunk of the SIE vessels divides into two branches. The main, lateral trunk branches from the femoral vessels in the groin and enters the abdominal wall skin. The smaller medial branch extends toward the medical abdominal skin to collateralize with a branch in the internal mammary vessel [27] (Figure 1).

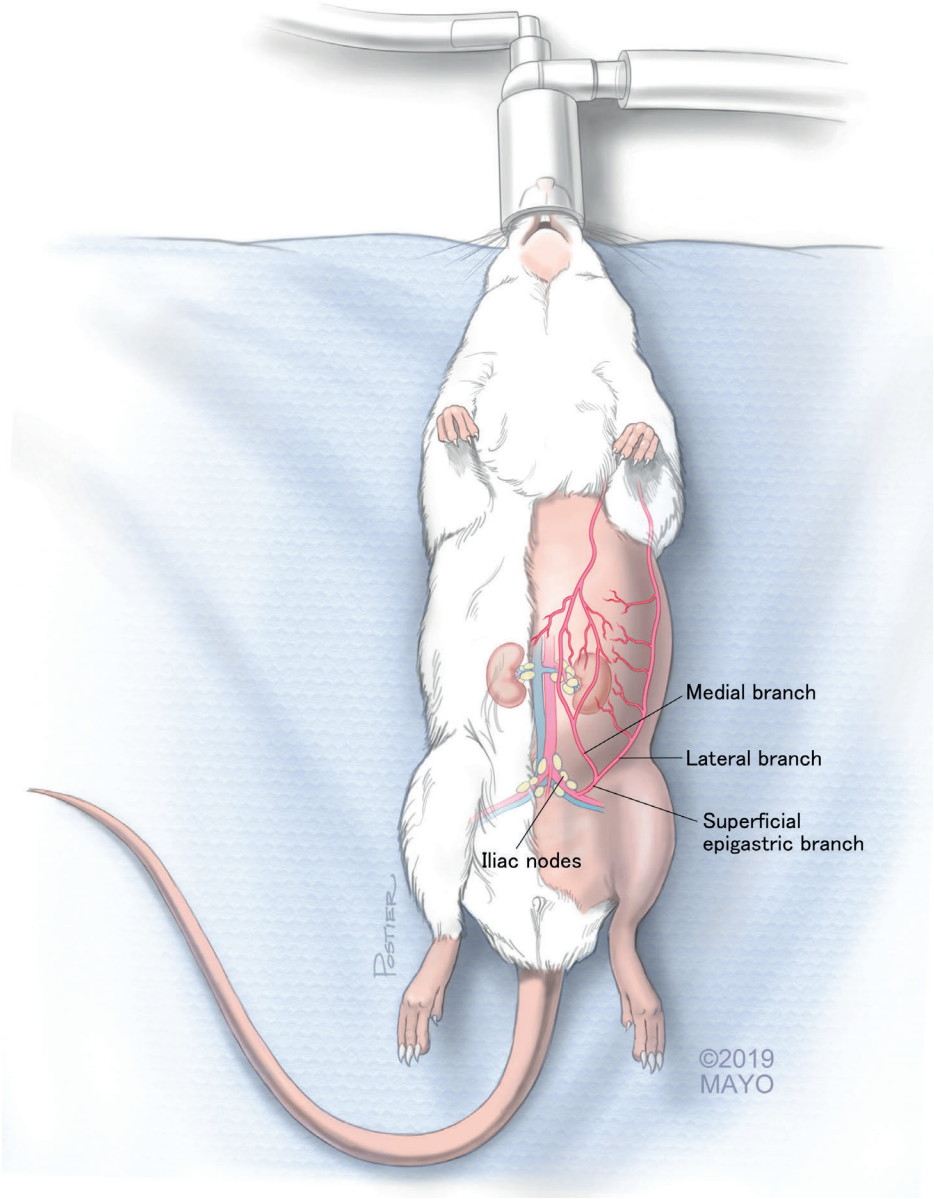

Figure 1. Schematic drawing of the rat superficial vascular abdominal anatomy. The superficial epigastric artery originates from the femoral artery and divides into two branches to supply the abdominal fascia: the lateral and the medial branch. Close to the bifurcation lie the iliac nodes. *With permission of the Mayo Foundation, Copyright Mayo Foundation 2019.*

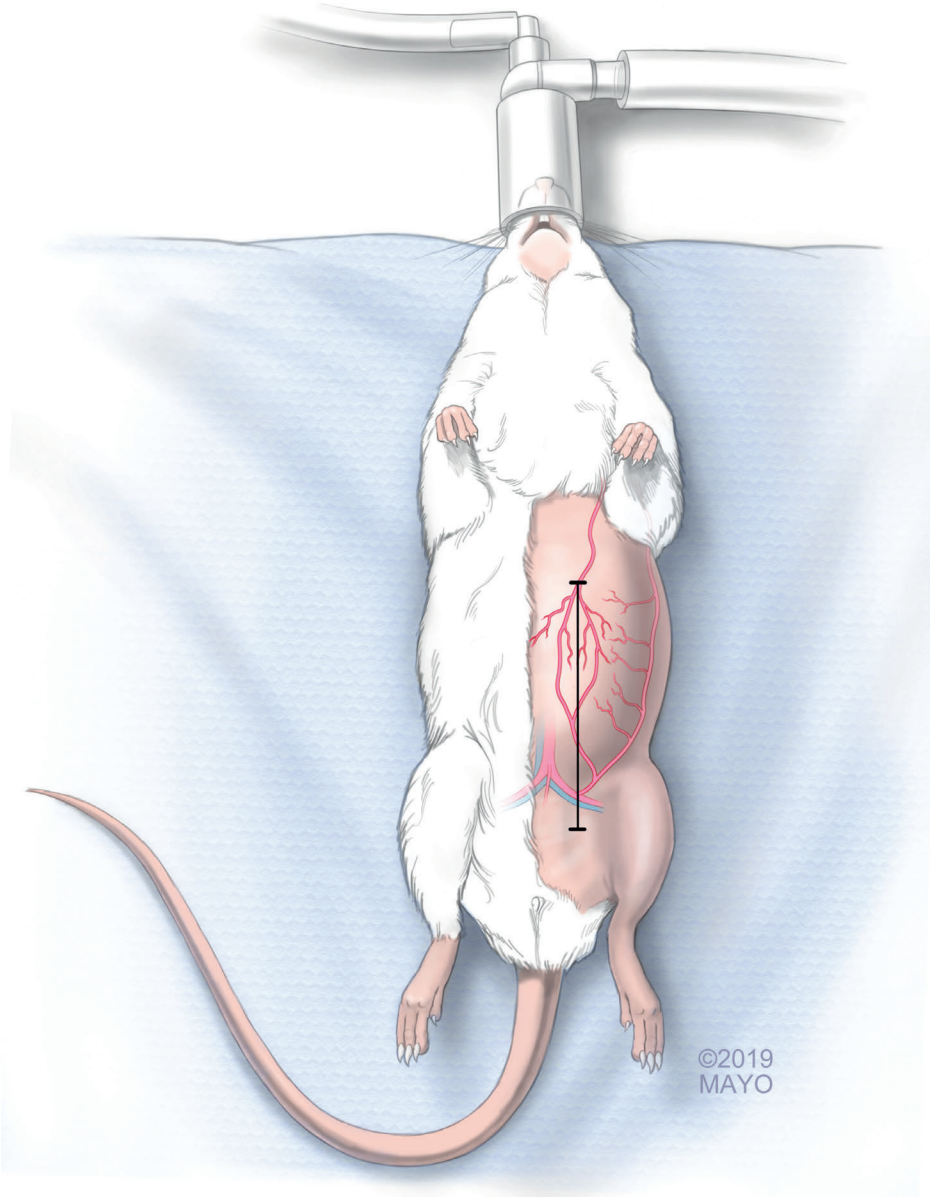

Figure 2. Schematic drawing of the 4 cm paramedian incision. This incision allows for harvesting the flap without damaging the superficial inferior epigastric (SIE) vessels or other vessels supplying the abdominal skin. *With permission of the Mayo Foundation, Copyright Mayo Foundation 2019.*

The SIEF flap measured 4 x 3 cm and was designed in the ventral abdomen. After a 4 cm paramedian incision, on the ipsilateral side of the nerve reconstruction, the femoral artery was identified in the groin (Figure 2).

The SIE lateral vessels were exposed proximally and protected with a vessel loop. The flap was dissected distally, starting on the medial side. The superficial- and deep membranous layers of subcutaneous tissue (Camper fascia and Scarpa fascia) were separated from the abdominal muscles, leaving the fascia intact. Using microsurgical scissors, the flap was raised toward the proximal branch of the SIE vessels (Figure 3).

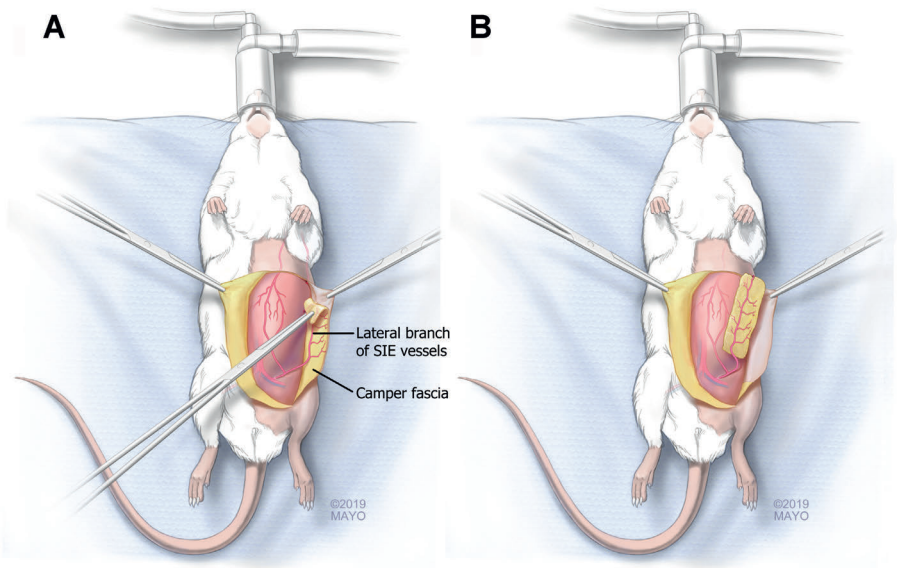

Figure 3. Schematic drawing of superficial inferior epigastric fascia (SIEF) flap harvest. Depicted is elevating the flap from distal to proximal (A), providing a 4 x 3 cm adipofascial flap (B) with lateral branch of the superficial inferior (SIE) vessels. *With permission of the Mayo Foundation, Copyright Mayo Foundation 2019.*

This dissection was performed under surgical loupe magnification to avoid damage to the SIE vessels. While dissecting, lymph nodes in the inguinal area were seen and preserved. Small vessel branches were anticoagulated using a bipolar as needed to prevent postoperative hematomas. The epigastric nerve was consistently encountered running in conjunction with the SIE vessels and transected in all cases. The flap was

raised to the level of the bifurcation of the femoral artery and then kept moist in gauze until the nerve reconstruction was finished.

The sciatic nerve was fully exposed proximally from the inferior margin of the piriformis muscle to approximately 5 mm distal to the bifurcation, under an operating microscope (Zeiss OpMi 6, Carl Zeiss Surgica, Oberkochen, Germany). A 10-mm segment of the sciatic nerve was excised by sharp transection with microsurgical scissors and bridged with a 10-mm nerve allograft with six 10-0 nylon (10-0 Ethilon, Ethicon Inc., Sommerville, NJ, USA), epineural interrupted sutures on either side of anastomosis.

A 2 cm linear incision was made from the patella toward the pelvis to develop a wide subcutaneous tunnel from the distal aspect of the nerve reconstruction toward the femoral artery. A hemostat was passed through the distal incision into the inguinal region, and the flap was delivered through the tunnel, with approximate 100° rotation clockwise about its original axis (Figure 4). Caution was taken to prevent vascular twisting. The 4 x 3 cm SIEF flap contained subcutaneous fat, inguinal fat, femoral vasculature and SIE vessels and was tunneled subcutaneously toward the nerve reconstruction without torsion of the pedicle (Figure 5A).

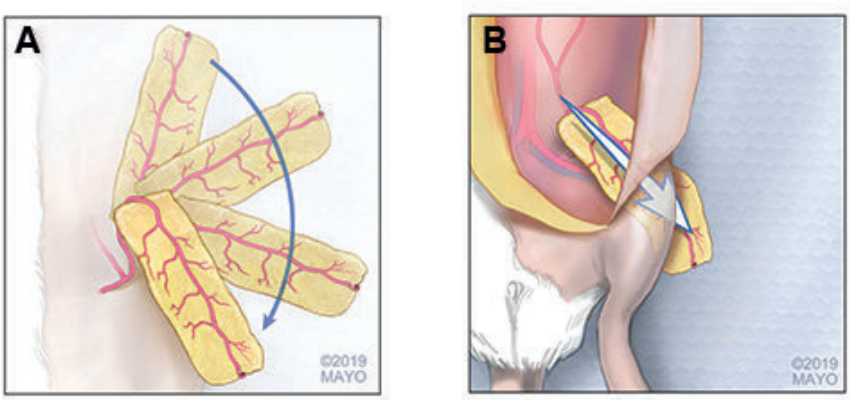

Figure 4. Schematic drawing of flap rotation (A) and tunneling (B). The vessels were kept ventrally and the flap was tunneled without vascular twisting of the epigastric trunk. *With permission of the Mayo Foundation, Copyright Mayo Foundation 2019.*

The flap was wrapped around the nerve allograft with the SIE vessels in line with the nerve and reaching both the proximal and distal anastomoses, as shown in Figure

5B. The flap edges were trimmed to fit the defect (Figure 5C). Care was taken to ensure that there was no tension on the nerve anastomoses while positioning the flap under the reconstructed nerve. After ensuring that there was no pedicle compression in the subcutaneous tunnel, the vascular pedicle remained freely mobile with full ranging of the leg and that the nerve anastomoses were without tension, two loosely tied 10-0 nylon-sutures (10-0 Ethilon, Ethicon Inc., Sommerville, NJ, USA) were placed through the SIEF flap (Figure 5D). Wounds were closed in layers, with muscle approximated with 5-0 absorbable sutures (5-0 Vicryl Rapide, Ethicon Inc., Sommerville, NJ, USA), and the skin of the leg and the abdomen was closed subcutaneously using the same suture.

Evaluation SIEF flap

The viability of the SIEF flap was evaluated at sacrifice by 12 and 16 weeks. This was performed using the milking patency test [28]. The SIEA was found and the vessel was occluded with forceps distal to the flap. The other forceps was placed just distally to the first. The vessel would be milked a few millimeters away from the flap. Thereafter the proximal forceps would be released. Rapid filling from proximal to distal would indicate that the artery was not occluded (1), if no filling occurred, the test would be scored a (0). Viability of the flap was also characterized by color of the flap and active bleeding at the edges of the flap.

Immunohistochemistry

At 12 weeks, immunohistochemical staining of the nerves was obtained to confirm revascularization of the nerve. After sacrifice, the nerve grafts were harvested and fixed in 10% formalin (Fisher Scientific, NH, USA) for 48 hours and then transferred to 70% Ethanol and stored at 4°C. After embedding in paraffin, serial sections (5µm) were obtained from distal parts of the nerve grafts. These sections were stained with hematoxylin and eosin (H&E) and primary antibody rabbit anti-rat CD34 (1:4000, Abcam, Cambridge, MA, USA) to visualize vascularization and fibrosis in the nerve graft. CD34 is a transmembrane phosphoglycoprotein and established as a marker of hematopoietic cell types, including vascular endothelial progenitors and extensively expressed on blood vessels [29]. Contralateral nerve samples were stained as control. Immunohistochemical digital photographs were taken at 40x magnification with a microscope (Nikon Eclipse 50i) equipped with a digital camera. Images were qualitatively assessed.

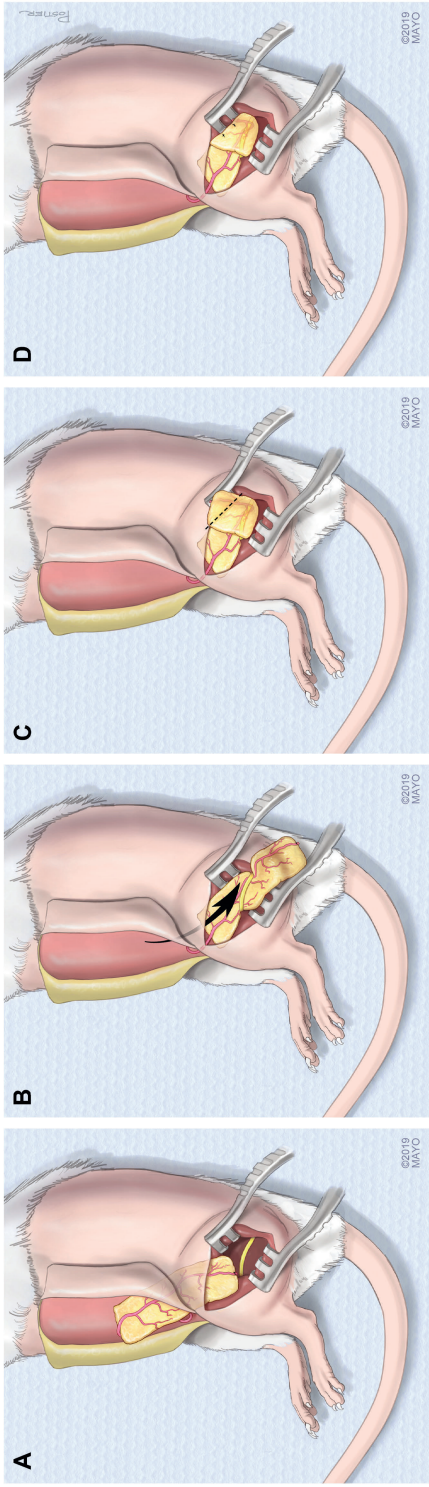

Figure 5. Schematic drawings of superficial inferior epigastric fascia (SIEF) flap positioning. The SIEF flap was tunneled subcutaneously toward the nerve reconstruction (5A) without torsion of the pedicle and wrapped around the nerve graft reaching both anastomoses (5B) without tension on the reconstructed nerve. The flap edges were trimmed (5C) and two 10-0 nylon sutures were placed to secure the position of the SIEF flap (5D). *With permission of the Mayo Foundation, Copyright Mayo Foundation 2019.*

RESULTS

Evaluation SIEF flap

Successful flap transfer was accomplished in all rats. After 12 and 16 weeks rats were sacrificed and flap viability was investigated. The patency of the artery was checked with the milking patency test at sacrifice and all arteries were patent after 12 and 16 weeks survival. The flap was well vascularized and demonstrated active bleeding at its margins. The vessels were in line with the nerve graft (Figure 6).

No flap necrosis occurred and no infections were seen. Of the 12 week survival rats, lymphedema occurred in two, which did not infect or complicate recovery and resolved by itself. In one rat, a small subcutaneous hematoma was seen on the abdominal side at four weeks, which did not increase size during follow up and did not have any impact on the SIEF flap. The 16 week survival rats did not show any complications. The SIEF flap had an acceptable and aesthetic donor site scar without any observable loss of function.

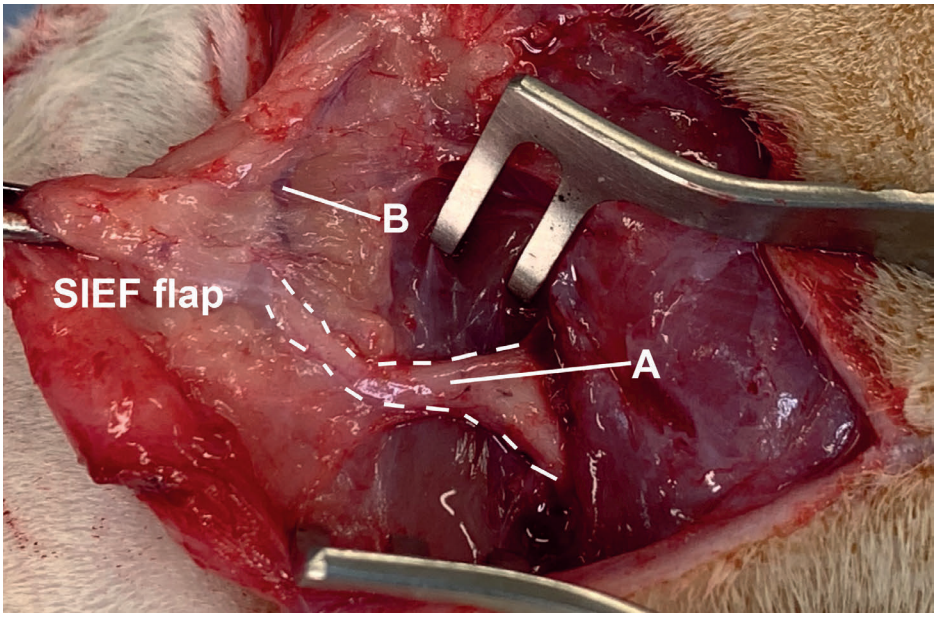

Figure 6. Relation superficial inferior epigastric (SIE) vessels and nerve after 16 weeks. The white dashed line surrounds the nerve allograft (A). Depicted is the close relationship between the nerve allograft (A) and the SIE vessels (B) after 16 weeks of survival. Also, flap viability could clearly be seen.

Immunohistochemistry

To assess the effect of the SIEF flap on nerve allograft samples, nerve samples were stained for H&E and anti-CD34. Results of H&E staining in cross-sections of the nerve showed no infiltration of inflammatory cells in either group at 12 weeks. As can be concluded from the H&E staining, no fibrosis was seen. In the SIEF group, an increase in vessels and Schwann cell nuclei was evident in the H&E stained samples. This increase in vessels was consistent with the notable increase of CD34-positive microvessels in nerve grafts that were surgically revascularized at 12 weeks compared to unoperated nerve samples (Figure 7).

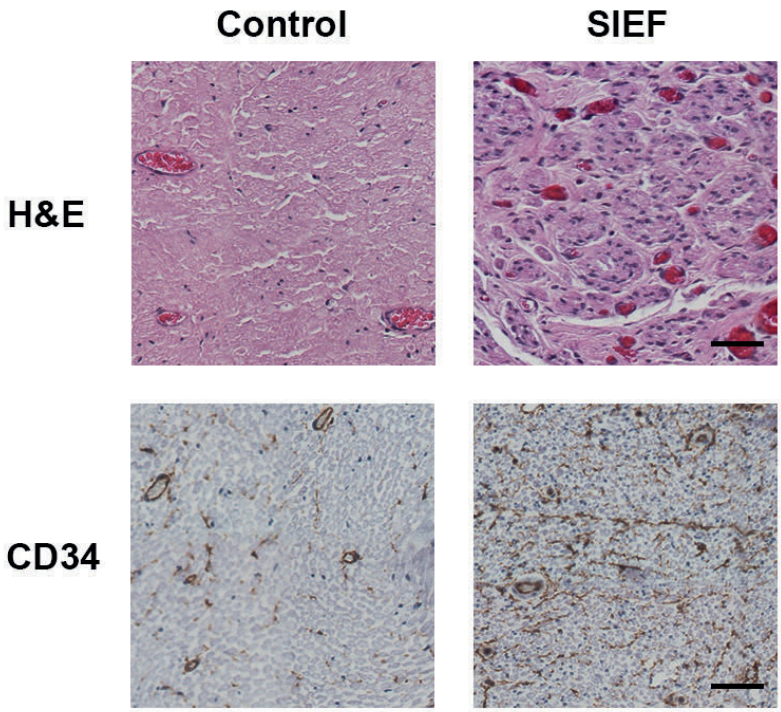

Figure 7. Immunohistochemical digital photographs of nerve samples. Representative images of H&E staining in control (contralateral unoperated nerve) and SIEF (vascularized flap wrapped around the processed nerve allograft) samples at 12 weeks. Purple nuclei denote the Schwann cell nuclei. Digital photographs were taken at 40x magnification. Scale bars, 200 μm.

DISCUSSION

The surgical technique for the rat SIEF flap harvest was described and evaluated. While this flap has been reported previously in a few animal studies [17,19,20], long-term viability has not been adequately assessed or determined. Additionally, a succinct and detailed description of this technique in rats has not been illustrated or reported.

The main findings of this study were that the SIEF flap is an easy flap to raise and remains viable in all rats after either a 12 or 16 weeks survival period. Complications included two lymphoceles and one hematoma acutely, but no long term consequences at 12 and 16 weeks.

The flap demonstrated to have 100 percent success rates after elevation without flap failure or necrosis at the donor site. One major advantage is that the SIE vessels of the rat are approximately 0.5 mm in diameter [30], which categorizes it as relatively large and makes them to be easily dissected under loupe magnification. By only including the lateral branch, necrosis at the donor site is prevented. This flap design can be applied to other rat strains as well as rats of different sizes as the anatomical branches are easily recognized. The pedicled flap eliminates the need for microvascular anastomosis and minimizes flap failures secondary to surgical techniques. This pedicled flap allows for a technically simple elevation without intramuscular dissection and a relatively short operation time. An additional benefit is that the transplanted adipofascial tissue can improve blood flow in adjacent tissues such as bone, nerve and muscles and be a readily applied pedicle flap for studies on vascularization [20,31]. The inclusion of adipofascial tissue in the flap decreases intravascular resistance of the bundle, resulting in improved blood flow in the flap which decreases the risk of thrombosis [20,31].

Immunohistochemical qualitative analysis of the nerve samples confirms the increase in vascularity in the SIEF group (vascularized flap wrapped around the processed nerve allograft) in both H&E and anti CD-34 sections at 12 weeks. Vasculature is known to play a crucial role in supporting nerve regeneration following injury [32]. A lack of blood supply could lead to nerve hypoxia and damage, leading to nerve fibrosis [33,34]. At time of a nerve injury, Wallerian degeneration is activated causing Schwann cell proliferation distal to the nerve injury [35,36]. This process causes blood vessels to precede Schwann cell migration and to stimulate axonal extension, describing

an important interaction between Schwann cells and blood vessels [34,37]. Schwann cells are known to produce neurotrophic factors to support neurite outgrowth [38]. After nerve injury, these cells and their secreted neuro-supportive factors enhance axonal growth [39]. Although comparison of nerve allograft in a well vascularized bed to the contralateral unoperated nerve is not an adequate comparison of nerve tissue, the increase of vessels and Schwann cell nuclei in the nerve allografts confirm the relationship between blood supply and nerve regeneration and suggest that addition of a well vascularized bed to the nerve area may enhance nerve regeneration. This study describes a pedicled adipofascial flap model in rats and validates its use in future investigations in the rat sciatic nerve model.

CONCLUSIONS

This study demonstrated a total success rate of SIEF flap viability without necrosis at 12 and 16 weeks, providing evidence that this flap is durable and can be used for future studies in a rat model. We recommend this simple technique to add vascularization to various tissues in the lower abdomen, genital area, thigh and upper limb of the rat.

Acknowledgments

Artwork of Figure 1-5 was created by Jim Postier, Rochester, MN.

Disclosure statement

No competing financial interests exist.

REFERENCES

1. Taylor GI, Ham FJ. The free vascularized nerve graft. A further experimental and clinical application of microvascular techniques. *Plast Reconstr Surg.* 1976;57(4):413-426.
2. Townsend PL, Taylor GI. Vascularised nerve grafts using composite arterialised neuro-venous systems. *Br J Plast Surg.* 1984;37(1):1-17.
3. Rose EH, Kowalski TA, Norris MS. The reversed venous arterialized nerve graft in digital nerve reconstruction across scarred beds. *Plast Reconstr Surg.* 1989;83(4):593-604.
4. Doi K, Kuwata N, Kawakami F, Tamaru K, Kawai S. The free vascularized sural nerve graft. *Microsurgery.* 1984;5(4):175-184.
5. Doi K, Kuwata N, Sakai K, Tamaru K, Kawai S. A reliable technique of free vascularized sural nerve grafting and preliminary results of clinical applications. *J Hand Surg Am.* 1987;12(5 Pt 1):677-684.
6. D'Arpa S. Vascularized nerve "grafts": just a graft or a worthwhile procedure? *Plast Aesthet Res.* 2016;2(4):183-192.
7. Strauch B, Murray DE. Transfer of composite graft with immediate suture anastomosis of its vascular pedicle measuring less than 1 mm. in external diameter using microsurgical techniques. *Plast Reconstr Surg.* 1967;40(4):325-329.
8. Padubidri AN, Browne E, Jr. Modification in flap design of the epigastric artery flap in rats--a new experimental flap model. *Ann Plast Surg.* 1997;39(5):500-504.
9. Freeman TJ, Cohen JI. The ventral 'L' island flap. A refined model for skin flap research. *Arch Otolaryngol Head Neck Surg.* 1990;116(2):189-190.
10. Tsuzuki K, Yanai A, Tange I, Bandoh Y. The influence of congestion and ischemia on survival of an experimental vascular pedicle island flap. *Plast Reconstr Surg.* 1989;84(5):789-793.
11. Takayanagi S, Ota C, Kusumoto K, Hosomi Y. Experimental evaluation of vascular pedicle in island flaps. *Br J Plast Surg.* 1986;39(3):352-355.
12. Zuker RM, Harii K. A random pattern flap borne on an axial pattern flap: experimental study in rats. *Br J Plast Surg.* 1978;31(4):286-289.
13. Hsu CE, Shyu VB, Wen CJ, Wei FC, Huang XT, Cheng HY. The rat groin flap model redesigned for evaluating treatment effects on ischemia-reperfusion injury. *J Surg Res.* 2018;222:160-166.
14. Ylmaz KB, Gurunluoglu R, Bayramicli M. Flap survival after previous vascular pedicle division and preexisting scar formation at the pedicle site: an experimental study. *Ann Plast Surg.* 2014;73(4):434-440.
15. Demirseren ME, Yenidunya MO, Yenidunya S. Island rat groin flaps with twisted pedicles. *Plast Reconstr Surg.* 2004;114(5):1190-1194.
16. Tark KC, Khouri RK, Shin KS, Shaw WW. The fasciovascular pedicle for revascularization of other tissues. *Ann Plast Surg.* 1991;26(2):149-155.
17. Dunn RM, Mancoll J. Flap models in the rat: a review and reappraisal. *Plast Reconstr Surg.* 1992;90(2):319-328.

18. O'Sullivan KL, Pap SA, Megerian CA, et al. Improved axon diameter and myelin sheath thickness in facial nerve cable grafts wrapped in temporoparietal fascial flaps. *Ann Plast Surg.* 1998;40(5):478-485.
19. Valdatta L, Reguzzoni M, Buoro M, et al. Neurovenous superficial inferior epigastric flaps in rats. *Minerva Chir.* 2003;58(3):361-368.
20. Giessler GA, Friedrich PF, Shin RH, Bishop AT. The superficial inferior epigastric artery fascia flap in the rabbit. *Microsurgery.* 2007;27(6):560-564.
21. Giusti G, Willems WF, Kremer T, Friedrich PF, Bishop AT, Shin AY. Return of motor function after segmental nerve loss in a rat model: comparison of autogenous nerve graft, collagen conduit, and processed allograft (AxoGen). *J Bone Joint Surg Am.* 2012;94(5):410-417.
22. Shin RH, Vathana T, Giessler GA, Friedrich PF, Bishop AT, Shin AY. Isometric tetanic force measurement method of the tibialis anterior in the rat. *Microsurgery.* 2008;28(6):452-457.
23. Hundepool CA, Nijhuis TH, Rbia N, Bulstra LF, Selles RW, Hovius SE. Noninvasive Ultrasound of the Tibial Muscle for Longitudinal Analysis of Nerve Regeneration in Rats. *Plast Reconstr Surg.* 2015;136(5):633e-639e.
24. Hundepool CA, Nijhuis TH, Kotsougiani D, Friedrich PF, Bishop AT, Shin AY. Optimizing decellularization techniques to create a new nerve allograft: an in vitro study using rodent nerve segments. *Neurosurg Focus.* 2017;42(3):E4.
25. Hudson TW, Zawko S, Deister C, et al. Optimized acellular nerve graft is immunologically tolerated and supports regeneration. *Tissue Eng.* 2004;10(11-12):1641-1651.
26. Kumta S, Yip K, Roy N, Lee SK, Leung PC. Revascularisation of bone allografts following vascular bundle implantation: an experimental study in rats. *Arch Orthop Trauma Surg.* 1996;115(3-4):206-210.
27. Petry JJ, Wortham KA. The anatomy of the epigastric flap in the experimental rat. *Plast Reconstr Surg.* 1984;74(3):410-413.
28. Hayhurst JW, O'Brien BM. An experimental study of microvascular technique, patency rates and related factors. *Br J Plast Surg.* 1975;28(2):128-132.
29. Fina L, Molgaard HV, Robertson D, et al. Expression of the CD34 gene in vascular endothelial cells. *Blood.* 1990;75(12):2417-2426.
30. Cubitt J, Pennington T, Wang C, Allen R, Bishop A, Sharland A. Reliable and reproducible murine models for commonly used abdominal plastic surgical flaps. *J Reconstr Microsurg.* 2012;28(3):161-166.
31. Sasmor MT, Reus WF, Straker DJ, Colen LB. Vascular resistance considerations in free-tissue transfer. *J Reconstr Microsurg.* 1992;8(3):195-200.
32. Terzis JK, Skoulis TG, Soucacos PN. Vascularized nerve grafts. A review. *Int Angiol.* 1995;14(3):264-277.
33. Muangsanit P, Shipley RJ, Phillips JB. Vascularization Strategies for Peripheral Nerve Tissue Engineering. *Anat Rec (Hoboken).* 2018;301(10):1657-1667.
34. Hobson MI, Brown R, Green CJ, Terenghi G. Inter-relationships between angiogenesis and nerve regeneration: a histochemical study. *Br J Plast Surg.* 1997;50(2):125-131.

35. Stoll G, Muller HW. Nerve injury, axonal degeneration and neural regeneration: basic insights. *Brain Pathol.* 1999;9(2):313-325.
36. Jessen KR, Mirsky R. The repair Schwann cell and its function in regenerating nerves. *J Physiol.* 2016;594(13):3521-3531.
37. Hobson MI, Green CJ, Terenghi G. VEGF enhances intraneural angiogenesis and improves nerve regeneration after axotomy. *J Anat.* 2000;197 Pt 4:591-605.
38. Bunge RP. The role of the Schwann cell in trophic support and regeneration. *J Neurol.* 1994;242(1 Suppl 1):S19-21.
39. Koppes AN, Nordberg AL, Paolillo GM, et al. Electrical stimulation of schwann cells promotes sustained increases in neurite outgrowth. *Tissue Eng Part A.* 2014;20(3-4):494-506.

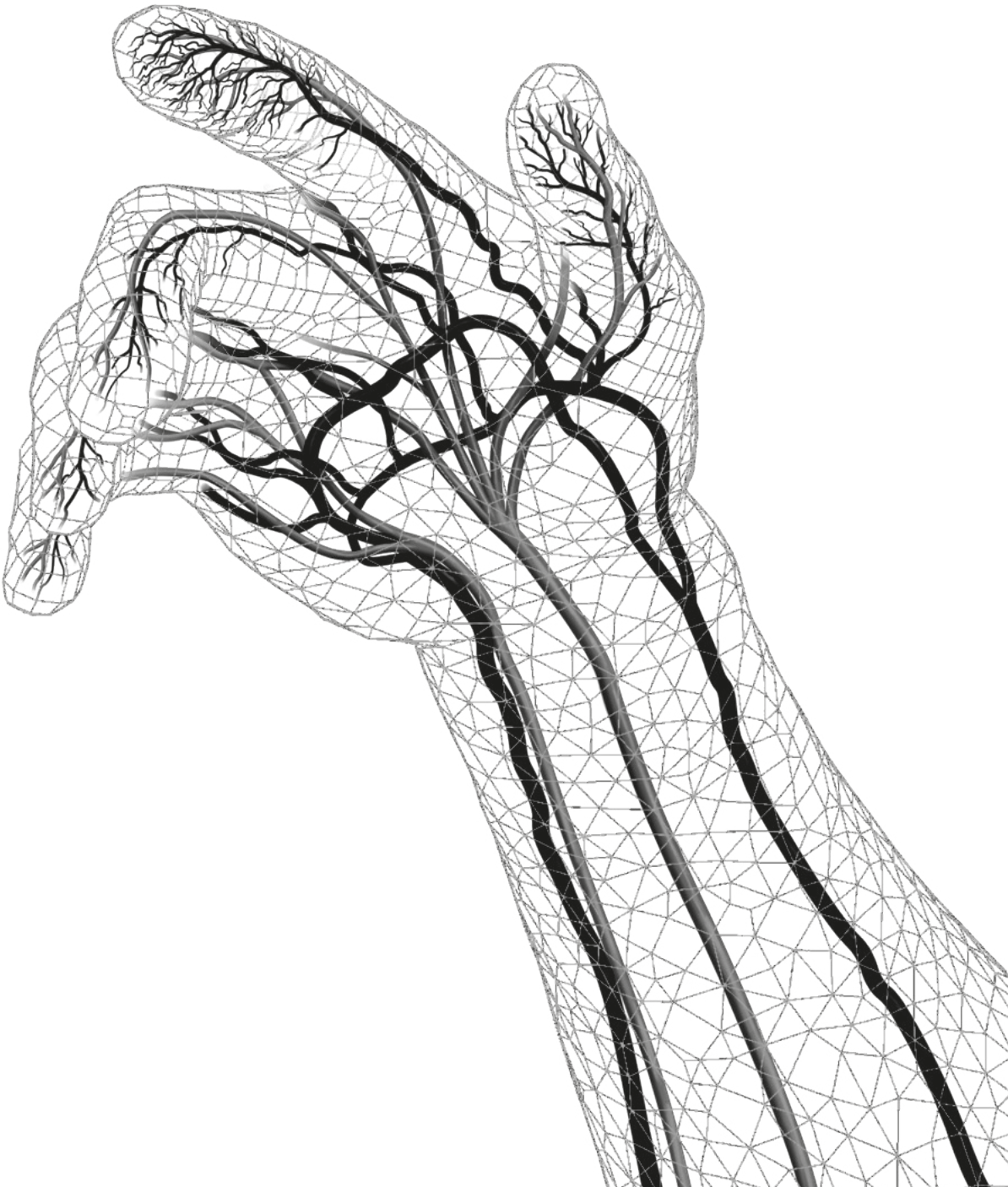

CHAPTER

FOUR

New Methods for Objective Angiogenesis Evaluation of Rat Nerves using Microcomputed Tomography Scanning and Conventional Photography

Tiam M. Saffari[1,2]
Femke Mathot[1,3]
Allen T. Bishop[1]
Alexander Y. Shin[1]

Affiliations

[1]Department of Orthopedic Surgery, Mayo Clinic, Rochester, MN, USA

[2]Department of Plastic-, Reconstructive- and Hand Surgery, Erasmus Medical Center, Rotterdam, the Netherlands

[3]Department of Plastic Surgery, Radboud University, Nijmegen, the Netherlands

Microsurgery. 2020;40(3):370-376

ABSTRACT

Introduction

Nerve regeneration involves multiple processes which enhance blood supply that can be promoted by growth factors. Currently, tools are lacking to visualize the vascularization patterns in transplanted nerves *in vivo*.

Materials and Methods

A protocol to visualize the vasculature of the sciatic nerves has been developed with two available techniques. In this study, we describe a step-by-step procedure for preservation of the vasculature of sciatic nerve autografts (N=12) and contralateral non-operated control nerves (N=12) in the Lewis rat at 12 and 16 weeks postoperatively. After sacrifice of the rats, Microfil® contrast compound was injected and the nerves were cleared while preserving the vasculature. The amount of vascularization was measured by quantifying the vascular surface area using conventional photography (two dimensional) and the vascular volume was calculated with micro-computed tomography (micro CT, three dimensional).

Results

Successful preservation of vasculature was achieved in all nerve samples. Using micro CT, the vascular volume was significantly increased from 12 to 16 weeks in both groups. The same trend was seen in the vascular surface area, but this was not significant. The correlation between both methods was statistically significant.

Conclusions

Both methods are considered to successfully reflect the degree of vascularization. Application of this technique could be used to visualize and objectively quantify angiogenesis of the transplanted nerve graft. Moreover, this simple method is easily reproducible and could be extrapolated to any other desired target organ *ex vivo* in small animals to investigate the vascular network.

INTRODUCTION

It has been postulated that blood supply affects nerve regeneration [1-7], as it is reported that vascular endothelial cells directly guide the regeneration of peripheral nerve axons [7]. Vascularization (angiogenesis) can be enhanced through growth factors [8], in particular angiopoietin-1 (Ang-1) an important angiogenic factor that promotes vascular stabilization [9] and vascular endothelial growth factor (VEGF) which enhances intraneural angiogenesis [2]. To quantify blood vessels in nerve grafts or conduits, previous studies have focused on immunohistochemical staining [10-12]. Unfortunately, the amount of (neo)angiogenesis was not evaluated in these studies.

Histomorphometric analyses are used to describe angiogenesis, but are limited in the ability to identify the three-dimensional interconnectivity of the vasculature in serial histological sections [13,14] and focuses on representing superficial blood flow [15]. Connectivity defines the maximal number of branches that may be cut without separating the structure [15]. Insight in the connectivity of the vascular tree may contribute to crucial description of neovascularization patterns. Therefore, two-dimensional measures of vasculature deliver incomplete information [13]. Three-dimensional reconstruction of blood vessels in sciatic nerves of the rat has been technically difficult because the average diameter of the small endoneurial vessels in the rat is 8.8 mm [16].

Micro-computed tomography (micro CT) facilitates the visualization of contrast enhanced microvessels and could separate vessels from surrounding tissues, such as bone, fat tissue or nerve [17]. It provides three-dimensional volume imaging with spatial resolution at the micrometer scale and is applied in many fields, for instance in tumor visualization, cardiovascular plaque imaging [15,17] and evaluation of surgical angiogenesis in a bone allotransplantation models [18-20].

As technology continues evolving, modern micro CT systems are more commonly available and are capable of generating very small voxels with short scan acquisition times allowing both *ex vivo* and *in vivo* scanning [15]. Moreover, due to voxels as small as 1μm, the vascular system in rat and even mice could now be visualized [13,14,21,22]. As perfusion with a radiopaque contrast agent is the only requirement to delineate the

vascular tree, a closer-meshed network of smaller vessels, contrast enhanced micro CT can become a powerful tool in quantifying angiogenesis [13].

Information collected from conventional photography may complement the micro CT. Photographs could be analyzed by measuring the ratio of vessel area and total nerve area digitally [23]. More conventional methods such as manual vessel counts per sub-segment of the nerve, providing a vessel density per mm^2, have also been described [24]. These techniques have never been verified and are questionably representative for the entire quantification of the nerve vasculature when used solely. However, with evolving technology, the quality of conventional photography has improved and there are numerous photo editing software available providing a cost-effective way to measure vessel and nerve surface areas.

The purpose of this study was to describe three-dimensional visualization of the vascular system in the rat sciatic nerve and to quantify angiogenesis of nerve reconstruction. The micro CT and conventional photography were used to objectively quantify vascular volume and vascular surface area, respectively, as measurements of angiogenesis in rat nerve. These methods will allow us to advance angiogenesis related research by improving the tools for studying and understanding vascular development and the mechanisms of neoangiogenesis.

MATERIALS AND METHODS

Animals

Animal experiments were approved by our Institutional Animal Care and Use Committee (IACUC A3348-18). For this study, a total of 12 male Lewis rats (Envigo, USA) were used, weighing between 250 – 300 grams, in which 10 mm unilateral sciatic nerve gaps were repaired with a reverse autologous graft. All animals were housed with *ad libitum* access to food and water, with a 12-hour light-dark cycle after surgery.

Experimental design

A unilateral 10 mm sciatic nerve gap was repaired with an ipsilateral reversed autologous nerve graft to create a mismatch in the alignment of the nerve gap [25,26].

This group was considered the gold standard for nerve repair. Rats survived for either 12 or 16 weeks. At the time of the sacrifice, the nerve vasculature was preserved to obtain the vascular volume and vascular surface area measurements.

Surgical procedure

After anesthesia in an isoflurane chamber, rats were shaved, prepped and positioned in the nosecone to maintain anesthesia throughout the procedure. Preoperatively the following were administrated subcutaneously; infection prophylaxis provided by Enrofloxacin (Baytril, Bayer, Germany, 10mg/kg), 5 ml of NaCl 0.9% solution to prevent dehydration and Buprenorphine SR (Buprenorphine SR-LAB, ZooPharm pharmacy, 0.6mg/kg) for pain control. During surgery, body temperature was maintained at 37°C with a heating pad.

The sciatic nerve was fully exposed proximally from the inferior margin of the piriformis muscle to approximately 5 mm distal to the bifurcation, under an operating microscope (Zeiss OpMi 6, Carl Zeiss Surgica, Oberkochen, Germany). A 10 mm segment of the sciatic nerve was excised by sharp transection with microsurgical scissors. The nerve graft was reversed and reconstructed with six 10-0 nylon (Ethilon, Ethicon Inc., Sommerville, NJ, USA), epineural interrupted sutures on either side of the anastomosis. Wounds were closed in layers, approximating muscle with two 5-0 absorbable interrupted sutures (5-0 Vicryl Rapide, Ethicon Inc., Sommerville, NJ, USA). The skin was closed subcutaneously, using the same suture. Postoperatively, the rats were kept warm with towels. The rats were observed weekly until completion of the experiment.

Perfusion of contrast

Twelve and 16 weeks postoperatively, rats were sacrificed. Access for aortic infusion catheter placement was achieved via the abdomen. A large midline incision was made in the abdomen to expose the aorta and vena cava. A small retractor was used to retract the digestive organs providing stable exposure of the aorta and vena cava throughout the experiment. The fat surrounding the thoracic aorta and vena cava was cleaned using cotton tip applicators taking care not to harm the vascular structures. The thoracic aorta and vena cava were ligated proximally with a 5-0 Vicryl suture (5-0 Vicryl Rapide, Ethicon Inc., Sommerville, NJ, USA) which was kept long to act as grip

sutures. The ligation was placed as proximal as possible and distal to any large hepatic bifurcations, depending on the anatomic variation. The aorta was dissected from the vena cava distally using cotton tip applicators. This was performed approximately 1 cm proximal to the iliac bifurcation. A loose 5-0 Vicryl suture was placed under the aorta. To facilitate the passage of contrast, a 24 Gauge catheter (Jelco IV Catheter Radiopaque, Smiths Medical International, UK) connected to an IV tubing system, was introduced in the aorta just distally to the proximally placed grip sutures, while keeping the aorta on tension by slightly pulling the grip sutures (Figure 1). After the catheter was fixated with the previously placed suture around the aorta distally, 2-3 ml of saline (NaCl 0.9%) was infused through the tubing system to evaluate the patency of the aorta. The needle was removed off the cannula, while maintaining the cannula in the artery. Care was taken that the tip of the cannula would still be proximal to the iliac bifurcation, so that the contrast would reach both limbs. A yellow-colored (MV-122) Microfil® compound (MV 8ml, diluent 15 ml, and curing agent 1.2 ml, Flow Tech, Inc., Carver, MA, USA) in a 50 cc syringe was connected to the tubing system to be infused in the aorta. While putting pressure on the insertion site using gauze, the perfusion was performed with constant perfusion of approximately 100 mmHg. The perfusion was continued until the syringe was empty and yellow nailbeds on either paw were observed. After the perfusion was completed, a clamp was placed on the cannula to prevent leakage of the infused contrast. The rat was kept at room temperature while the agents cured for at least 90 minutes.

Collection and clearing of samples

After the vascular bed was perfused and the contrast cured, the sciatic nerve was exposed and harvested extending to approximately 3 mm on either side of the anastomoses. The contralateral nerve samples were harvested as non-operated, control samples (N=12). The nerve samples were collected in phosphate buffered saline (PBS) and cleared for five days by immersion in graded series of ethyl alcohol as follows: the samples were first placed in 25% ethyl alcohol and at successive 24-48 hour intervals the concentration was raised to 50%, 75%, 95% and 100%. As the final step, the samples were immersed in methyl salicylate. If tissue had not cleared, a second clearing starting from 95% ethyl alcohol stage was performed to repeat the final steps of the clearing procedure. This procedure allowed clearing of all structures, with exception of the opacified microvascular structures that were filled with contrast.

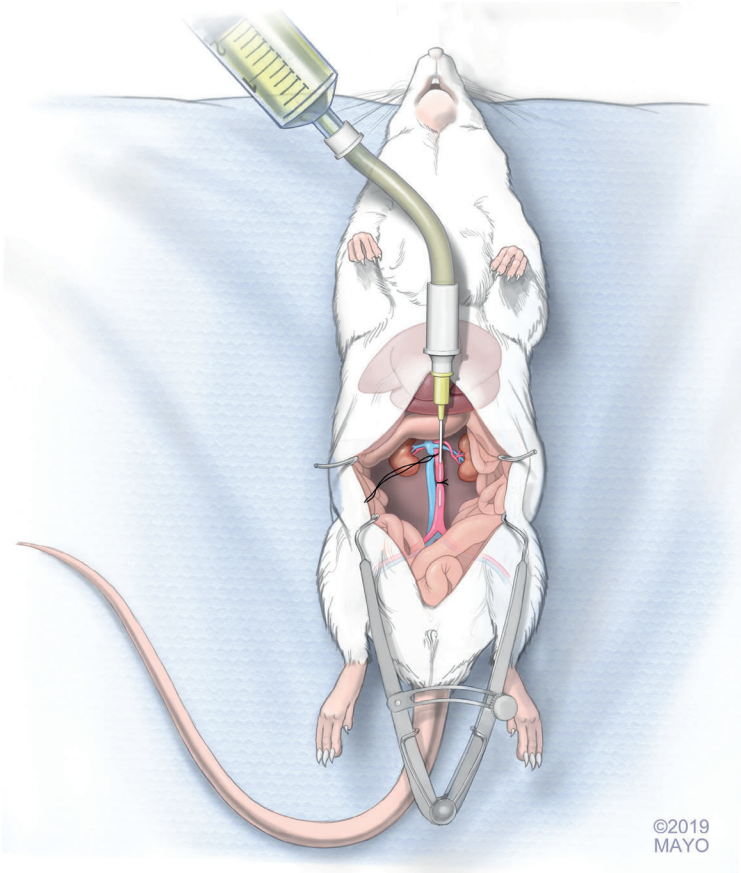

Figure 1. Schematic drawing of the insertion of the catheter into the rat aorta. Long sutures indicate the grip sutures that have ligated the aorta and vena cava proximally. Short cut suture serves to hold catheter in place while injecting the Microfil® contrast compound into both common iliac arteries of the rat. *With permission of the Mayo Foundation, Copyright Mayo Foundation 2019.*

Outcome measurements

Micro CT for calculating the vascular volume

After clearing had taken place, the samples were scanned in a SkyScan 1276 micro CT (Bruker Corporation, Billerica, MA, USA) at 40 kV voltage, 200 µA current and 10 µm resolution to calculate vascular volume. Three samples were scanned at a time, taking approximately 26 minutes per scan with frame averaging set at three in order to reduce noise. Three-dimensional images of the samples were reconstructed using Hierarchical InstaRecon software (NRecon, 1.7.4.2., InstaRecon, 2.0.4.0. InstaRecon). This software

was used to adjust the following parameters while reconstructing the images; Beam Hardening Correction (%) was set at 51, Ring Artifact Correction at 9, Smoothing at 1, Post alignment compensation and Histogram windows were manually adjusted for each scan. After obtaining reconstruction of the images, AnalyzePro software (AnalyzeDirect, Inc., Overland Park, KS, USA) was used to measure the volume of the vasculature and the volume of the total nerve. A vessel/nerve area ratio was calculated and expressed in percentages (vessel%).

Photography for calculating the vascular surface area

After micro CT scanning was completed, the nerve samples were stretched by suturing both nerve ends onto a solid holder. Detailed pictures of the samples were obtained using a Canon 5D Mark IV camera, (Manual Mode, ISO 200, 1/200th of a sec, f/16), a Canon MP-E 65mm Macro lens and a Canon MT-26-RT Twin Lite Macro strobe light source. During photography, samples were placed in a petri dish with methyl salicylate in order to obtain clean photographs allowing for the specimen to be separated from the background for better measurement. The petri dish was placed on a black background to achieve maximum contrast with the yellow vessels in the nerve samples. Polarized light was used to reduce reflections and a 1:1 magnification was used to ensure consistency of the pictures. To correct for the surface area that altered depending on the angle of the image, two pictures of each nerve sample were obtained; one of the front whereafter the holder was flipped and the picture of the other side was obtained. With NIS-Elements software (NIS-Elements BR 4.51.01), the total vessel area and the total vessel area in the graft were measured in a blinded fashion. For each image, a vessel/nerve area ratio was calculated. The ratios of the two images (front and back) were averaged per sample.

Statistical analysis

The vascular volume and the vascular surface area were analyzed and compared to the non-operated side (control). A nonpaired student t-test for comparisons between time points and between the two groups was used for statistical investigation. Correlations were analyzed using Pearson's correlation test. Results were reported as the mean and standard error or the mean (SEM), and the level of significance was set at $\alpha \leq 0.05$.

RESULTS

Macroscopic appearance of the vessels in nerve samples

Successful preservation of vasculature was achieved in all nerve samples (N=24). After the clearing process, the nerve samples were transparent and vessels were filled with Microfil®. For 3D imaging, the micro CT was used and allowed visualization of the vessels in space (Figure 2). The size and position of the vessels were visualized. Figure 3 shows the macroscopic images of the nerve autografts at 12 and 16 weeks and a control sample at 12 weeks obtained with a conventional digital camera. Sutures are clearly visible and were used to set the borders of the analysis frame. As demonstrated, the microvasculature was clearly visualized. The smallest diameter of blood vessels detected was 9.3 µm using micro CT and 7.4 µm using conventional photography.

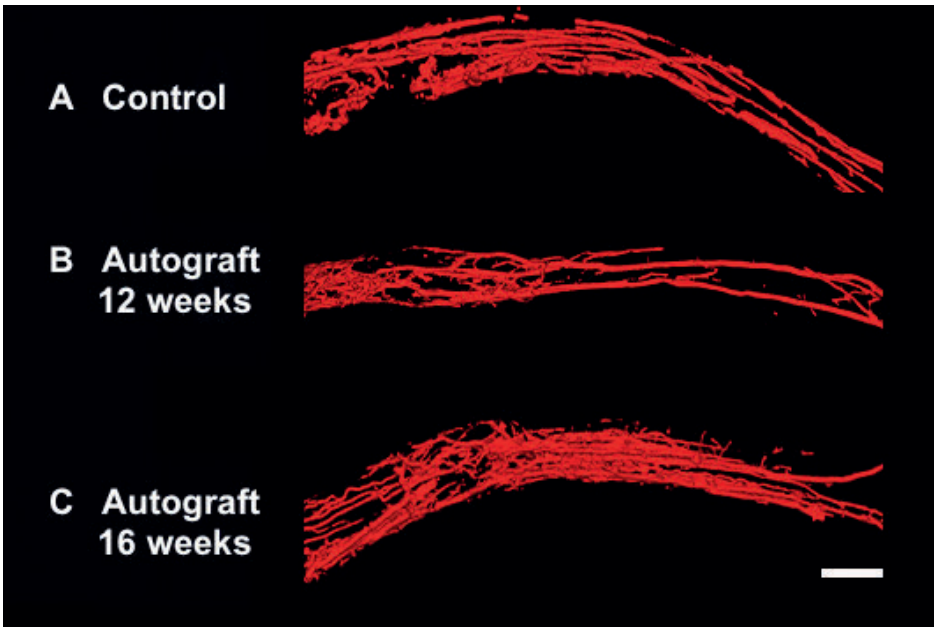

Figure 2. Micro computed tomography (micro CT) images of nerve samples. Micro CT images of control nerve at 12 weeks (A), nerve autograft at 12 weeks (B) and nerve autograft at 16 weeks (C). Nerve samples are positioned from proximal to distal (left to right, respectively). Scale bar is set a 1 millimeters (mm).

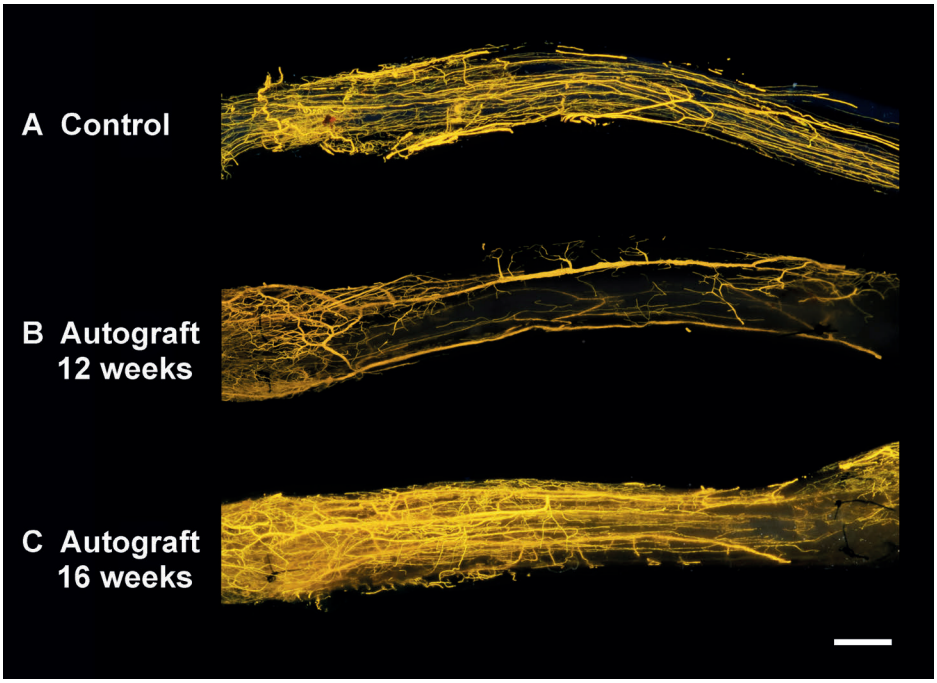

Figure 3. Macroscopic images of nerve samples obtained with conventional digital photography. Photography images of same samples visualized in Figure 2. Microvessels could be clearly seen in the control nerve at 12 weeks (A), nerve autograft at 12 weeks (B) and nerve autograft at 16 weeks (C). Sutures that are used to repair the graft are visible in nerve autograft groups (B+C) and depict the border of the analyzed frame. Nerve samples are positioned from proximal to distal (left to right, respectively). Scale bar is set at 1 millimeters (mm).

Vascular volume measured with micro CT

The vascular volume was successfully measured using the micro CT. At 12 weeks, the control nerve samples measured 4.83% vessel ± 0.45 (mean ± SEM) and this had increased to 6.19% ± 0.29 at 16 weeks. This increase between time points was significant (P=0.045). The nerve autografts showed similar results in vascularity between time points when compared to control nerve samples. The 16 week nerve autograft samples (4.95% ± 0.44) were superior to autografts at 12 weeks (3.53% ± 0.43), P=0.043. These outcomes are depicted in Figure 4.

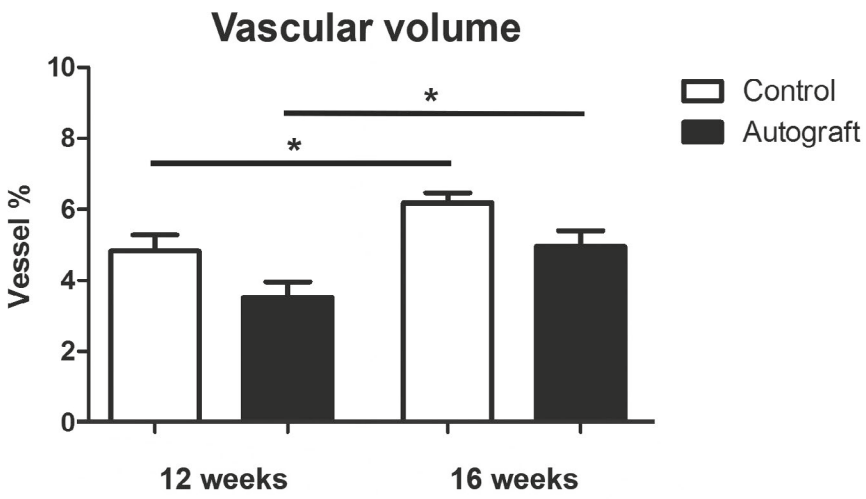

Figure 4. Vascular volume of control and nerve autograft samples at 12 and 16 weeks using micro CT. Results are expressed as a percentage (vessel %) of the total nerve area and are given as the mean ±SEM. *Indicates significance at P<0.05. SEM: Standard error of the mean.

Vascular surface area measured with conventional photography

After 12 weeks, the vascular surface area was 26.87% ± 2.13 (mean ± SEM) for the non-operated control nerve samples, compared to 25.04% vessel ± 2.77 for the nerve autograft sample. After 16 weeks the control samples measured a vascular surface area of 33.71% ± 2.60 and 28.11% ± 3.47 for the autograft nerves. No significant differences were found between the groups or time points (Figure 5).

Correlations

The vascular volume and vascular surface area were significantly correlated with both time points and groups (r=0.951, P=0.049).

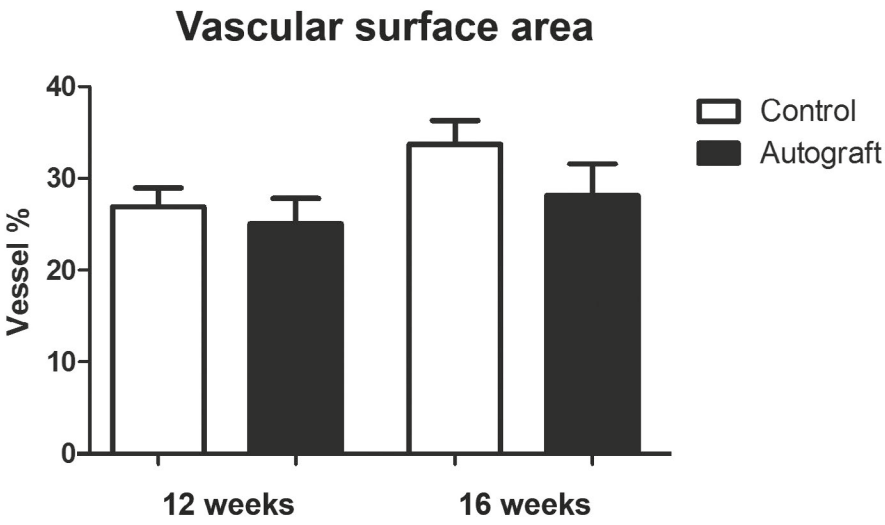

Figure 5. Vascular surface area of control and nerve autograft samples at 12 and 16 weeks using digital photography. Results are expressed as a percentage (vessel %) of the total nerve area and are given as the mean ±SEM. SEM: Standard error of the mean.

DISCUSSION

In this study, the authors successfully preserved the vasculature of the sciatic nerve in rats to provide more insight in the amount of angiogenesis and the patterns of neoangiogenesis occurring in nerve regeneration. Due to the limited options available to visualize the small vessels of the rat had previously impeded the understanding of the underlying neoangiogenesis patterns after nerve graft reconstruction.

The utility of the method described in the current study is two-fold. First, it provides an objective quantification of the amount of angiogenesis, independently from the size of the vessels, in relation to the size of the nerve. Second, it eminently demonstrates the patterns of angiogenesis in (transplanted) nerves. Nerve revascularization is postulated to be composed of angiogenesis and neoangiogenesis; vessels that sprout into the existing vascular tree and vessels that create new pathways [27]. However, this theory has yet to be objectively described. The vascularization of nerves and in particular, the alignment of vessels in nerves is attributed to a directional role for regenerating axons [28,29]. Applying the described techniques at several time points after

nerve graft implementation may provide insight to the ratio between revascularization components. These techniques may demonstrate the relationship between vessel alignment and the level of nerve regeneration. Thus, allowing us to improve our understanding of the process and the importance of vascular development in nerve grafts.

As blood vessels provide little inherent contrast, viscosity is one of the most important properties of the implemented vehicle [15]. With viscosity levels around 20-30, Microfil® is the best available compound that injects both the arterial and venous system and reaches even the smallest angiogenic vessels to allow complete study of the vascular network [15]. The injected Microfil® does not directly interact with the histology but could influence the proportion of axon and nerve areas during the analysis. Therefore, we would suggest harvesting other tissue prior to Microfil® injection to secure reliable histologic analysis.

There are a few considerations associated with this technique. Although micro CT systems become more commonly available with improving quality [15], it is still conceivable that micro CT devices with small effective voxel size are not available for all researchers. In this case, solely the described conventional photography strategy could be used, as it is cost-effective, simple to perform and correlates with micro volume measurements. However, conventional photography does not describe vascularization in space and lacks detailed information. As only two sides of the nerve sample are measured and the surface area could not be corrected for the thickness of the nerve (i.e. depth of the obtained photo), representation of the amount of angiogenesis using vascular surface area may be questionable. The difference between various groups of nerve samples, however, could be described with conventional photography. The micro CT has the advantage of precisely measuring vessel volume in relation to total measured nerve volume. Also, clearing of samples is not necessary as the lead pigments in Microfil® provide high contrast compared to background tissue to acquire complete high resolution 3D images of the vessels [17].

Our results indicate the significant correlation between the vascular volume and the vascular surface area measurements demonstrating that the methods could be used either complementary or separately, depending on the goals of the study. These methods will allow us to advance angiogenesis related research by improving the

tools for studying and understanding vascular development and the mechanisms of neoangiogenesis.

CONCLUSIONS

This study provides accurate objective analysis of the newly formed vascular network of the sciatic nerve. The use of the micro CT and conventional photography provides many modalities for vascular exploration, allowing the exploration of the structure and organization of blood vessels. These imaging methods are easily reproducible and could be extrapolated to any other desired target organ *ex vivo* in small animals to investigate the vascular network.

Acknowledgments

Artwork of Figure 1 was created by Jim Postier, Rochester, MN.

Disclosure statement

No competing financial interests exist.

REFERENCES

1. Weddell G. Axonal regeneration in cutaneous nerve plexuses. *J Anat.* 1942;77(Pt 1):49-62 43.
2. Hobson MI, Green CJ, Terenghi G. VEGF enhances intraneural angiogenesis and improves nerve regeneration after axotomy. *J Anat.* 2000;197 Pt 4:591-605.
3. Best TJ, Mackinnon SE. Peripheral nerve revascularization: a current literature review. *J Reconstr Microsurg.* 1994;10(3):193-204.
4. Sondell M, Lundborg G, Kanje M. Vascular endothelial growth factor has neurotrophic activity and stimulates axonal outgrowth, enhancing cell survival and Schwann cell proliferation in the peripheral nervous system. *J Neurosci.* 1999;19(14):5731-5740.
5. Mompeo B, Engele J, Spanel-Borowski K. Endothelial cell influence on dorsal root ganglion cell formation. *J Neurocytol.* 2003;32(2):123-129.
6. Skold MK, Svensson M, Tsao J, et al. Karolinska institutet 200-year anniversary. Symposium on traumatic injuries in the nervous system: injuries to the spinal cord and peripheral nervous system - injuries and repair, pain problems, lesions to brachial plexus. *Front Neurol.* 2011;2:29.
7. Cattin AL, Burden JJ, Van Emmenis L, et al. Macrophage-Induced Blood Vessels Guide Schwann Cell-Mediated Regeneration of Peripheral Nerves. *Cell.* 2015;162(5):1127-1139.
8. Cui WL, Qiu LH, Lian JY, Li JC, Hu J, Liu XL. Cartilage oligomeric matrix protein enhances the vascularization of acellular nerves. *Neural Regen Res.* 2016;11(3):512-518.
9. Brindle NP, Saharinen P, Alitalo K. Signaling and functions of angiopoietin-1 in vascular protection. *Circ Res.* 2006;98(8):1014-1023.
10. Connolly DT, Heuvelman DM, Nelson R, et al. Tumor vascular permeability factor stimulates endothelial cell growth and angiogenesis. *J Clin Invest.* 1989;84(5):1470-1478.
11. Hu DE, Fan TP. Suppression of VEGF-induced angiogenesis by the protein tyrosine kinase inhibitor, lavendustin A. *Br J Pharmacol.* 1995;114(2):262-268.
12. Norrby K. Vascular endothelial growth factor and de novo mammalian angiogenesis. *Microvasc Res.* 1996;51(2):153-163.
13. Perrien DS, Saleh MA, Takahashi K, et al. Novel methods for microCT-based analyses of vasculature in the renal cortex reveal a loss of perfusable arterioles and glomeruli in eNOS-/- mice. *BMC Nephrol.* 2016;17:24.
14. Kline TL, Knudsen BE, Anderson JL, Vercnocke AJ, Jorgensen SM, Ritman EL. Anatomy of hepatic arteriolo-portal venular shunts evaluated by 3D micro-CT imaging. *J Anat.* 2014;224(6):724-731.
15. Zagorchev L, Oses P, Zhuang ZW, et al. Micro computed tomography for vascular exploration. *J Angiogenes Res.* 2010;2:7.
16. Bell MA, Weddell AG. A descriptive study of the blood vessels of the sciatic nerve in the rat, man and other mammals. *Brain.* 1984;107 (Pt 3):871-898.
17. Ghanavati S, Yu LX, Lerch JP, Sled JG. A perfusion procedure for imaging of the mouse cerebral vasculature by X-ray micro-CT. *J Neurosci Methods.* 2014;221:70-77.

18. Kotsougiani D, Hundepool CA, Bulstra LF, Friedrich PF, Shin AY, Bishop AT. Bone vascularized composite allotransplantation model in swine tibial defect: Evaluation of surgical angiogenesis and transplant viability. *Microsurgery.* 2019;39(2):160-166.
19. Willems WF, Kremer T, Friedrich P, Bishop AT. Surgical revascularization induces angiogenesis in orthotopic bone allograft. *Clin Orthop Relat Res.* 2012;470(9):2496-2502.
20. Willems WF, Kremer T, Friedrich P, Bishop AT. Surgical revascularization in structural orthotopic bone allograft increases bone remodeling. *Clin Orthop Relat Res.* 2014;472(9):2870-2877.
21. Lee S, Barbe MF, Scalia R, Goldfinger LE. Three-dimensional reconstruction of neovasculature in solid tumors and basement membrane matrix using ex vivo X-ray microcomputed tomography. *Microcirculation.* 2014;21(2):159-170.
22. Deshpande SS, Donneys A, Farberg AS, Tchanque-Fossuo CN, Felice PA, Buchman SR. Quantification and characterization of radiation-induced changes to mandibular vascularity using micro-computed tomography. *Ann Plast Surg.* 2014;72(1):100-103.
23. Giusti G, Lee JY, Kremer T, Friedrich P, Bishop AT, Shin AY. The influence of vascularization of transplanted processed allograft nerve on return of motor function in rats. *Microsurgery.* 2014.
24. Wongtrakul S, Friedrich PF, Bishop AT. Vascular endothelial growth factor promotion of neoangiogenesis in conventional nerve grafts. *J Hand Surg [Am].* 2002;27(2):277-285.
25. Kumta S, Yip K, Roy N, Lee SK, Leung PC. Revascularisation of bone allografts following vascular bundle implantation: an experimental study in rats. *Arch Orthop Trauma Surg.* 1996;115(3-4):206-210.
26. Hudson TW, Zawko S, Deister C, et al. Optimized acellular nerve graft is immunologically tolerated and supports regeneration. *Tissue Eng.* 2004;10(11-12):1641-1651.
27. Best TJ, Mackinnon SE, Midha R, Hunter DA, Evans PJ. Revascularization of peripheral nerve autografts and allografts. *Plastic and reconstructive surgery.* 1999;104(1):152-160.
28. Cutting CB, McCarthy JG. Comparison of residual osseous mass between vascularized and nonvascularized onlay bone transfers. *Plastic & Reconstructive Surgery.* 1983;72(5):672-675.
29. Parrinello S, Napoli I, Ribeiro S, et al. EphB signaling directs peripheral nerve regeneration through Sox2-dependent Schwann cell sorting. *Cell.* 2010;143(1):145-155.

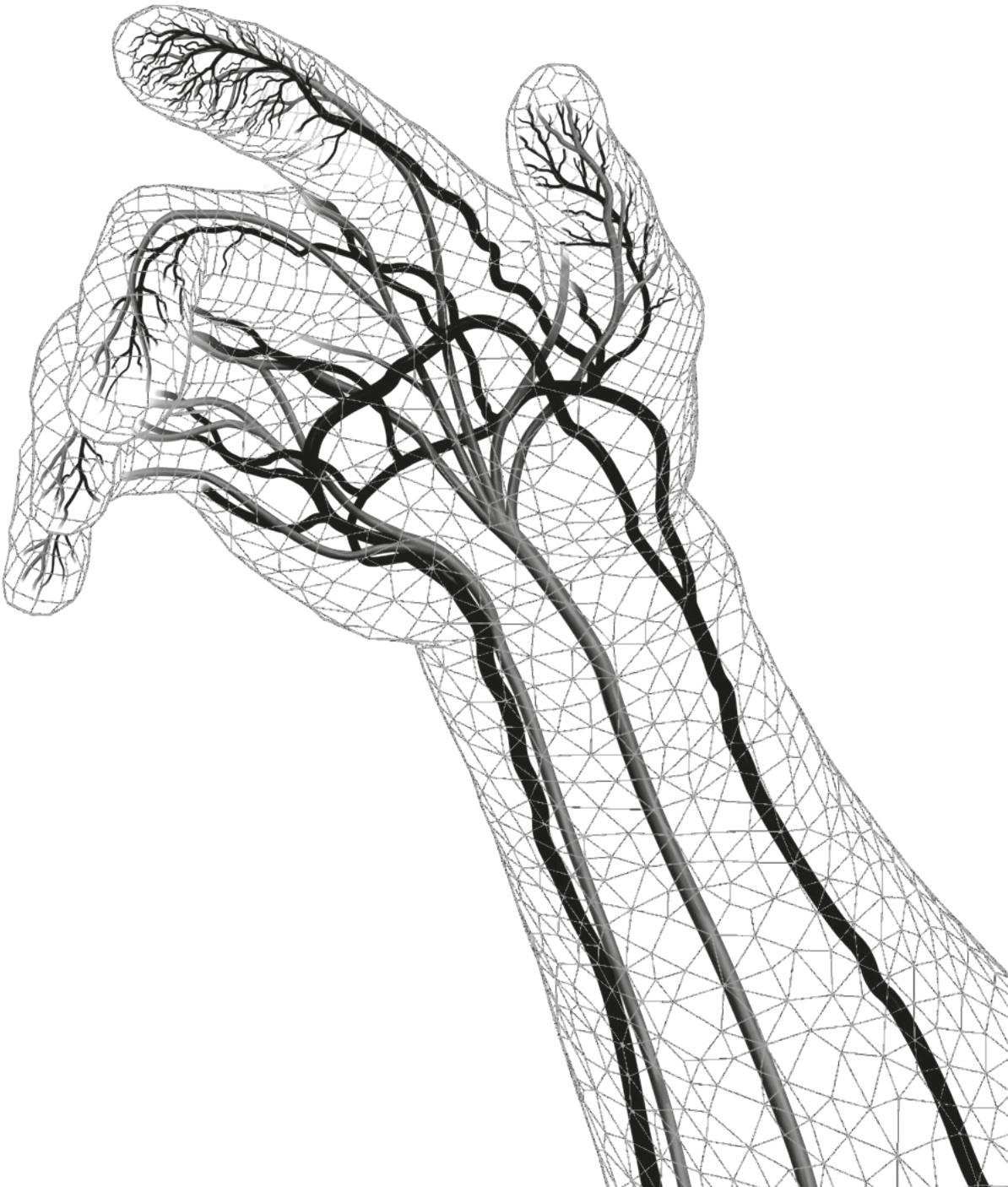

CHAPTER **FIVE**

Revascularization Patterns of Nerve Allografts in a Rat Sciatic Nerve Defect Model

Tiam M. Saffari[1,2]
Femke Mathot[1,3]
Patricia F. Friedrich[1]
Allen T. Bishop[1]
Alexander Y. Shin[1]

Affiliations

[1]Department of Orthopedic Surgery, Mayo Clinic, Rochester, MN, USA

[2]Department of Plastic-, Reconstructive- and Hand Surgery, Erasmus Medical Center, Rotterdam, the Netherlands

[3]Department of Plastic-, Reconstructive- and Hand Surgery, Radboud University, Nijmegen, the Netherlands

Journal of Plastic, Reconstructive & Aesthetic Surgery. **2020;73(3):460-468**

ABSTRACT

Introduction

The specific patterns of revascularization of allograft nerves after addition of vascularization remain unknown. The aim of this study was to determine the revascularization patterns of decellularized processed nerve allograft after surgically induced angiogenesis to the wound bed in a rat sciatic nerve model.

Materials and Methods

In 51 Lewis rats, sciatic nerve gaps were repaired with (i) autografts, (ii) nerve allograft and (iii) nerve allograft wrapped in a pedicled superficial inferior epigastric artery fascia flap (SIEF) to provide vascularization to the wound bed. At two, 12 and 16 weeks, the vascular volume and vascular surface area in nerve samples were measured using micro CT and photography. Cross-sectional images were obtained and the number of vessels was quantified in the proximal, mid and distal sections of the nerve samples.

Results

At two weeks, the vascular volume of SIEF nerves was comparable to control ($P=0.1$). The vascular surface area in SIEF nerves was superior to other groups ($P<0.05$). At 12 weeks, vascularity in SIEF nerves was significantly higher than allografts ($P<0.05$) and superior compared to all other groups ($P<0.0001$) at 16 weeks. SIEF nerves had a significantly increased number of vessels compared to allografts alone in the proximal ($P<0.05$) and mid-section of the graft ($P<0.05$).

Conclusions

Addition of surgical angiogenesis to the wound bed greatly improves revascularization. It was demonstrated that revascularization occurs primarily from proximal to distal (proximal inosculation) and not from both ends as previously believed and confirms the theory of centripetal revascularization.

INTRODUCTION

The outcome of tissue transplantation critically depends on the revascularization process and consequently regeneration of nerve is similarly dependent on this process [1-5]. Neovascularization precedes neural regeneration and stimulates injured axons and non-neuronal cells to produce a supportive microenvironment [6]. The nerve vascularization consists of both an extrinsic and intrinsic blood supply [7]. The intrinsic system is formed by an extensive microvascular network that maintains blood supply within a nerve (epineural, perineural and endoneural vessels) [7,8]. The extrinsic system consists of vessels that accompany a nerve outside of its epineurium. While it is known that both the intrinsic and extrinsic blood supply systems are interrupted during injury [7], little is known about the revascularization patterns after such an injury. In 1945, Tarlov and colleagues demonstrated by roentgenographic studies of transplanted sciatic nerves that an important source of blood supply for grafts is from the surrounding tissue [9]. Furthermore, they suggested that the vascular pattern between normal nerves and vascularized nerve autografts is similar and revascularization occurs along the preexistent vascular channels by ingrowth of blood vessels from the host stumps (proximal and distal) as well as from the surrounding tissues [9]. In order to improve clinical outcomes of free autologous nerve grafting, multiple nerve grafts (cable grafts) were applied to increase surface area as it was postulated that this would improve graft revascularization and avoid central necrosis which was observed in larger diameter nerve grafts [9,10]. To improve outcomes of nerve autografts in severely scarred tissue beds, the application of either vascularized nerve grafts or vascularized flaps around nerve grafts has been suggested [11-14]. These theories can not be extrapolated to the revascularization of nerve allografts, as in processed nerve allografts, preexistent vascular channels have been removed during the process. Little has been published regarding other strategies to revascularize processed nerve allografts or the patterns that revascularization follows, partly due to the lack of an appropriate model. Thus, there are remaining questions regarding the mechanism and pattern of peripheral nerve allograft revascularization. The purpose of this study was to explore the effect of surgical angiogenesis on processed nerve allografts and to compare the revascularization patterns in nerve autografts, allografts and allografts placed in a vascularized bed to provide insight into neovascularization of nerve grafts.

MATERIALS AND METHODS

Animal experiments were approved by the Mayo Clinic Institutional Animal Care and Use Committee (IACUC A3348-18). For this study, all animals were housed with ad libitum access to food and water, with a twelve-hour light-dark cycle after surgery.

Experimental design

In a total of 51 male Lewis rats, weighing between 250-300 grams (Envigo, USA), unilateral sciatic nerve gaps were repaired with three groups of nerve grafts. The experimental design of this study is depicted in Table 1. In group I (autograft), a unilateral 10-mm sciatic nerve gap was repaired with an ipsilateral reversed autologous graft to create a mismatch in the alignment of the nerve fibers (gold standard). For group II and III, decellularized processed nerve allografts were used to reconstruct the nerve gap. In group III, these nerve allografts were placed in a vascularized bed using a pedicled superficial inferior epigastric artery fascia (SIEF) flap [15]. Rats were sacrificed at two weeks (short-term), 12 and 16 weeks (long-term).

Table 1. Experimental design. SIEF flap: Superficial inferior epigastric artery fascial (SIEF) flap.

Groups	Surgery	Survival time 2 weeks (N)	Survival time 12 weeks (N)	Survival time 16 weeks (N)
I	Autograft	5	6	6
II	Allograft	5	6	6
III	Allograft + SIEF flap	5	6	6

Nerve allograft harvest and processing

Seventeen Sprague-Dawley rats (Envigo, Madison, WI, USA), weighing 250-300 grams, served as donors for harvesting a 15-mm segment of the sciatic nerve bilaterally. The sciatic nerves were cleaned from external debris and processed using a five-day decellularization protocol [16]. Sprague-Dawley rats were used to obtain a major histocompatibility complex mismatch with the recipient Lewis rats [17,18]. Briefly, rats were anesthetized in an isoflurane induction chamber and euthanized with an overdose of Pentobarbital Sodium (Fatal Plus, 390 mg/mL, Vortech, Dearborn, MI, USA). The nerves were harvested and collected in RPMI 1640 culture medium. After

processing, the nerves were sterilized using g-irradiation and stored in a Sodium Phosphate Buffer (PBS) at 4°C. All steps were carried out at room temperature with agitation under sterile conditions and in laminar flow hood.

Surgical procedure

Rats were anesthesized in an isoflurane chamber, shaved, prepped and positioned in the nosecone to maintain anesthesia throughout the procedure. Preoperatively, the following were administered subcutaneously: 5 mL of NaCl 0.9% solution (to prevent dehydration), Enrofloxacin (Baytril, Bayer, Germany, 10mg/kg, providing infection profylaxis) and Buprenorphine SR (Buprenorphine SR-LAB, ZooPharm pharmacy, 0.6mg/kg, pain control). During surgery, body temperature was maintained at 37°C with a heating pad.

The sciatic nerve on the left side of each rat was fully exposed proximally from the inferior margin of the piriformis muscle to approximately 5 mm distal to the bifurcation, under an operating microscope (Zeiss OpMi 6, Carl Zeiss Surgica, Oberkochen, Germany). A 10-mm segment of the sciatic nerve was excised by sharp transection with microsurgical scissors. In group I, the nerve segment was reversed and placed as an interposition autograft with six 10-0 nylon (10-0 Ethilon, Ethicon Inc., Sommerville, NJ, USA), epineural interrupted sutures on either side of anastomosis. In group II, the nerve gap was bridged with a 10-mm allograft with use of a similar surgical technique. In group III, the gap was also repaired with a 10-mm allograft, but consecutively a pedicled adipofascial flap was wrapped around the nerve allograft. The superficial inferior epigastric artery fascial (SIEF) flap was harvested as previously described [15]. Briefly, a 4-cm paramedian abdominal incision on the ipsilateral side of the nerve reconstruction was made. The femoral artery was identified in the groin, whereafter the superficial inferior epigastric (SIE) vessels were exposed. The 4 x 3 cm SIEF flap containing subcutaneous fat, inguinal fat, the femoral vasculature and SIE vessels, was tunneled subcutaneously toward the nerve reconstruction and wrapped around the nerve. Both the proximal and distal nerve anastomoses were covered with the flap.

In all groups, wounds were closed in layers, approximating muscle with two 5-0 absorbable interrupted sutures (5-0 Vicryl Rapide, Ethicon Inc., Sommerville, NJ,

USA). The skin was closed subcutaneously, using the same suture. Postoperatively, the rats were kept warm with towels. The rats were observed until completion of the experiment.

Nonsurvival procedure

After completion of the designated survival period, rats were sacrificed and neoangiogenesis was measured using two measures; the vascular surface area and the vascular volume.

Anesthesia
At survival time points (two, 12 and 16 weeks), rats were anesthetized and euthanized with 1 mL intraperitoneal injection of Pentobarbital Sodium.

Vascular preservation
Both thighs as well as the abdomen of the rat were shaved. On both sides, the sciatic nerve was exposed carefully. The vasculature of the lower extremity was preserved by aortic infusion [19]. A long longitudinal cut was made medially to expose the vena cava and aorta and these were cleaned from debris. These vessels were ligated as proximal as possible using a 5-0 Vicryl suture (Vicryl Rapide, Ethicon Inc., Sommerville, NJ, USA). Distal to the ligation, a catheter was inserted in the aorta. A yellow Microfil® compound (MV 8ml, diluent 15 ml, and curing agent 1.2 ml, Flow Tech, Inc., Carver, MA, USA) was infused into the aorta. After the contrast agents had cured, bilateral sciatic nerves were harvested. Nerves were temporarily stored in PBS and cleared in graded series of ethyl alcohol (25%, 50%, 75%, 95%, 100%) and placed in methyl salicylate. Clearing the nerve tissue while preserving the injected Microfil® allowed for measurement of the vascularity of the nerve segments.

Outcome measurements

Preserved vasculature in the nerve segments was quantified using a SkyScan 1276 micro computed tomography (micro CT, Bruker Corporation, Billerica, MA, USA) to calculate the vascular volume (three dimensional) and a Canon 5D Mark IV camera, (Manual Mode, ISO 200, 1/200th of a sec, f/16), a Canon MP-E 65mm Macro lens and

a Canon MT-26-RT Twin Lite Macro strobe light source for calculating the vascular surface area (two dimensional), according to protocol [19].

Statistical analysis

The vascular volume and the vascular surface area were analyzed and compared to the non-operated sciatic nerve (control). Analysis of variance (ANOVA) with Bonferroni post-hoc tests were used for comparisons between groups and time points. Results were reported as the mean and standard error or the mean (SEM), and the level of significance was set at $\alpha \leq 0.05$.

Cross sectional analysis

To describe the revascularization patterns in various parts of the nerve, cross sectional images from micro CT imaging were obtained for the 12 and 16 week survival periods. The length of the nerve between both anastomoses was divided into three equal sections: proximal (part I), mid (part II) and distal (part III). For each section, four cross sectional images were obtained. Cross-sectional images were divided into three equally concentric rings (central (A), middle (B) and outer (C)). The number of vessels was counted in each ring. Number of vessels in each part of the nerve (proximal, mid or distal) and ring (central, middle or outer) were averaged and compared to other groups of nerve grafts using multivariate analysis of variance (MANOVA) with Bonferroni post-hoc testing. Results were reported as the mean and SEM, and the level of significance was set at $\alpha \leq 0.05$.

RESULTS

Macroscopic appearance of the vessels in the nerve samples

All rats were sacrificed at their designated survival periods and successful preservation of vasculature was achieved in all nerve samples (N=51). After clearing had taken place, the nerves were imaged using the micro CT to allow 3D visualization of the vessels (Figure 1). Macroscopic photographs were obtained from these nerve samples for 2D visualization of vessels (Figure 2).

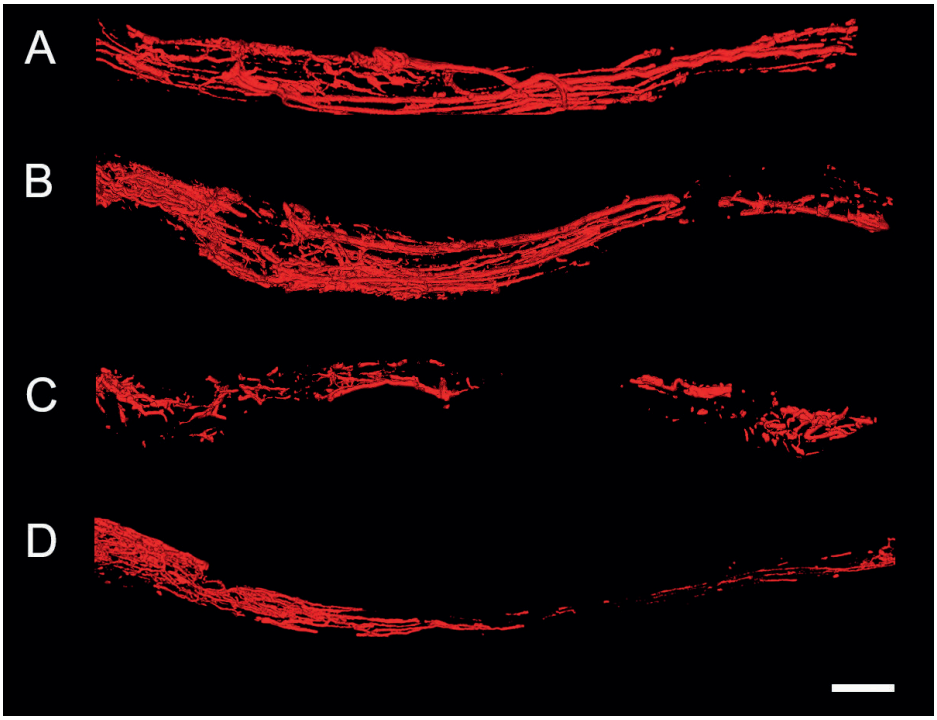

Figure 1. Micro computed tomography (micro CT) images of nerve samples. Micro CT images of control nerve (A), autograft (B), allograft (C) and allograft wrapped in a pedicled superficial inferior epigastric fascial (SIEF) flap (D). Images were obtained at 16 weeks. Nerve samples were positioned from proximal to distal (left to right respectively). Scale bar is set at 1 millimeter.
In the supplementary data videos of these nerve samples were provided to give a 3D representation of the micro CT.

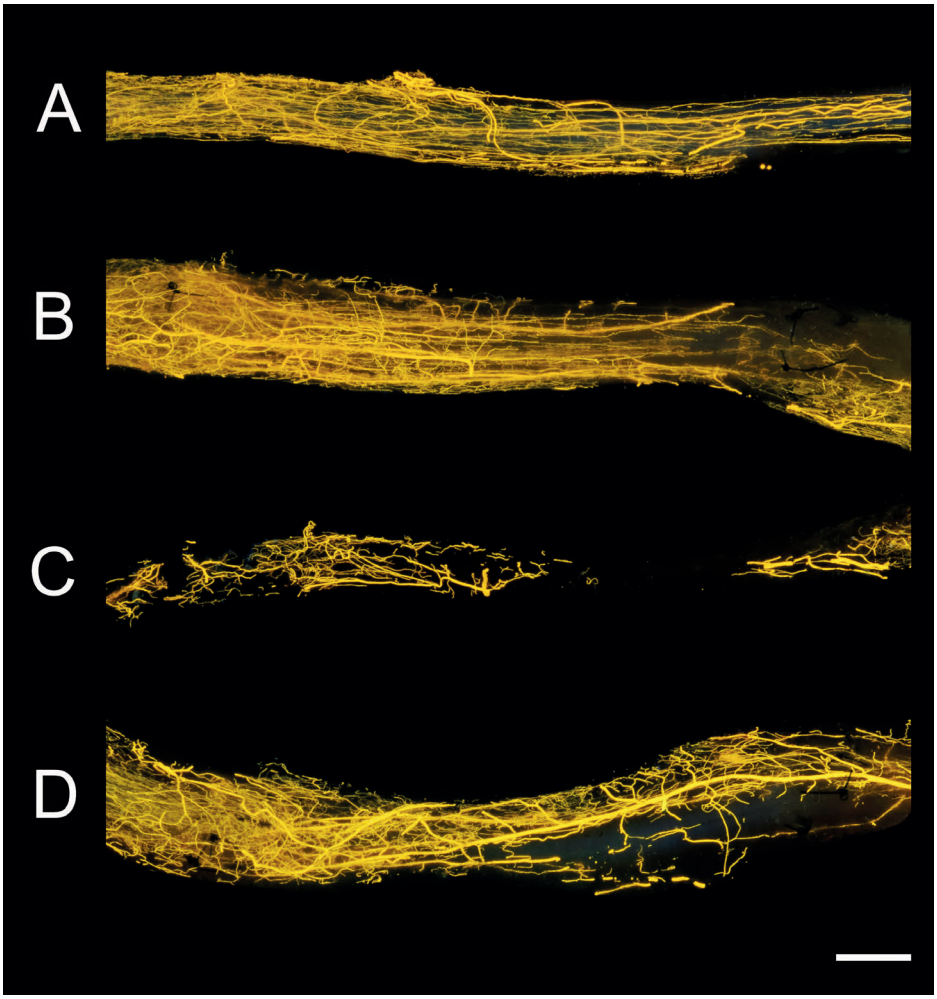

Figure 2. Macroscopic images of nerve samples obtained with conventional digital photography. Images of the same samples visualized in Figure 2. Microvessels were clearly seen in the control nerve (A), autograft (B), allograft (C) allograft wrapped in a pedicled superficial inferior epigastric fascial (SIEF) flap (D). These photographs depicted nerve groups at 16 weeks. Sutures that were used to repair the graft were visible in nerve graft groups (B,D) and depicted the border of the analyzed frame. Nerve samples were positioned from proximal to distal (left to right respectively). Scale bar is set at 1 millimeter.

Vascular volume and vascular surface area at two weeks

The vascular volume was successfully measured in the three experimental groups and compared to control. At two weeks, the control nerve samples measured 4.5 ± 0.3% vessel (mean ± SEM), compared to 2.5 ± 0.3% in nerve autografts, 1.4 ± 0.4% in nerve allografts and 3.4 ± 0.6% in the SIEF group. Control samples were superior to autograft (P<0.05) and allograft (P<0.0001), and comparable to the SIEF group (P=0.1, Figure 3A).

The vascular surface area measured 23.0 ± 0.6% vessel in control samples, 23.4 ± 0.9% in autografts, 13.8 ± 1.5% in allografts and 28.7 ± 1.1% in SIEF nerves. SIEF nerves were superior to all other groups and allografts were inferior to all other groups (P<0.01 compared to control, P<0.05 compared to autograft, P<0.0001 compared to allograft) as shown in Figure 3B.

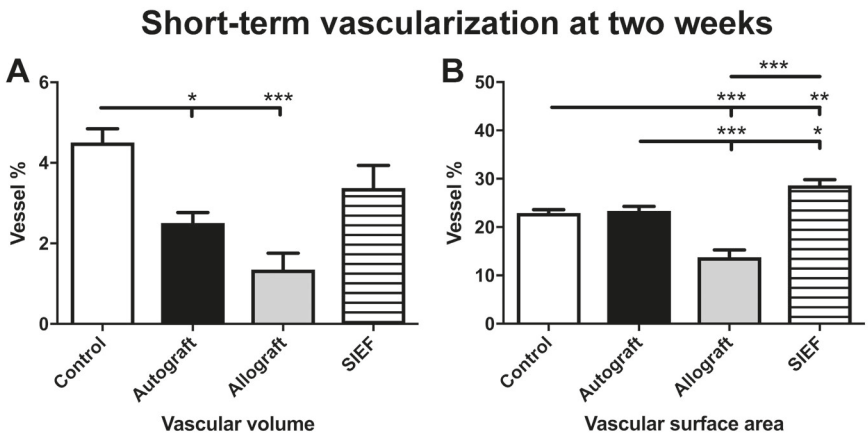

Figure 3. Short-term vascularization at two weeks measured by vascular volume (micro CT, 3A) and vascular surface area (conventional digital photography, 3B). Results of control, autograft, allograft and allograft wrapped in a pedicled superficial inferior epigastric fascial (SIEF) flap expressed as percentage (vessel %) of the total nerve area and were given as the mean ± SEM. Please note that the range of the Y-axes is different. * Indicates significance at P<0.05, ** P<0.01, *** P<0.0001. SEM = Standard error of the mean.

Long-term outcomes of vascular volume and vascular surface area

Vascularization outcomes obtained using vascular volume and vascular surface area are shown in Table 2 for control, autograft, allograft and SIEF nerve samples at 12 and 16 weeks. Significance is visualized in Figure 4 (vascular volume) and Figure 5 (vascular surface area).

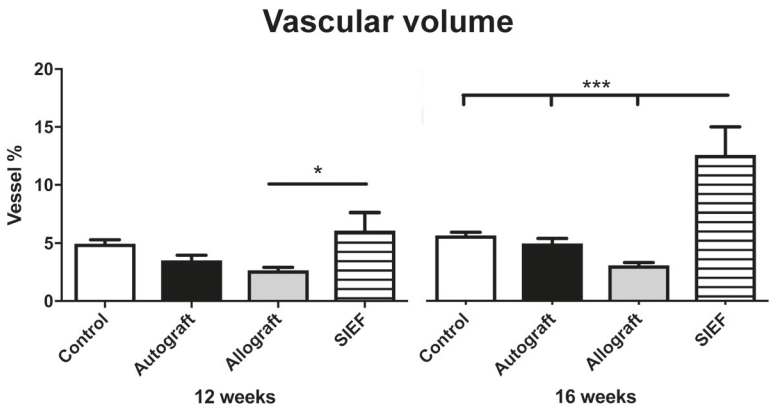

Figure 4. Vascular volume of nerve groups at 12 and 16 weeks using micro CT. Results of control, autograft, allograft and allograft wrapped in a pedicled superficial inferior epigastric fascial (SIEF) flap were expressed as a percentage (vessel %) of the total nerve area and were given as the mean ± SEM. *Indicates significance at P<0.05, *** P<0.0001. SEM = Standard error of the mean

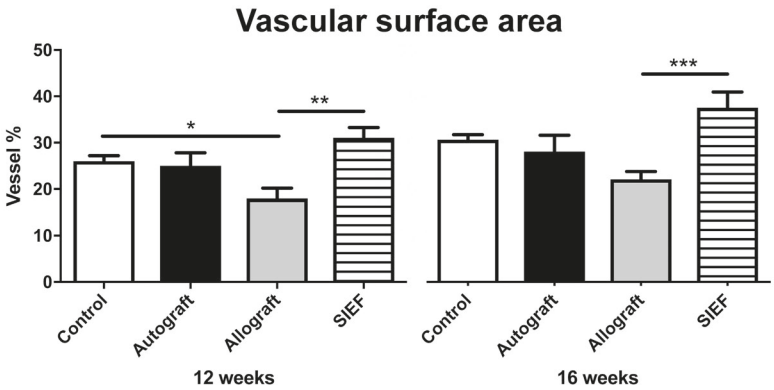

Figure 5. Vascular surface area of nerve groups at 12 and 16 weeks using digital photography. Results of control, autograft, allograft and allograft wrapped in a pedicled superficial inferior epigastric fascial (SIEF) flap were expressed as a percentage (vessel %) of the total nerve area and were given as the mean ± SEM. *Indicates significance at P<0.05, *** P<0.0001. SEM = Standard error of the mean

Table 2. Long-term outcomes of vascular volume and vascular surface area. Values were expressed as the mean ± standard error of the mean. SIEF: superficial inferior epigastric fascial (SIEF) flap.

	Vascular volume	Vascular surface area
Control		
12 wk	5.0 ± 0.3	26.0 ± 1.2
16 wk	5.7 ± 0.3	30.6 ± 1.1
Autograft		
12 wk	3.5 ± 0.4	25.0 ± 2.8
16 wk	5.0 ± 0.4	28.1 ± 3.5
Allograft		
12 wk	2.7 ± 0.2	18.0 ± 2.2
16 wk	3.1 ± 0.2	22.1 ± 1.7
SIEF		
12 wk	6.1 ± 1.5	31.1 ± 2.2
16 wk	12.6 ± 2.4	37.6 ± 3.4

Revascularization patterns over time

Starting at two weeks, vascularization consisting of a mesh-network occurred from both host stumps in nerve allograft and SIEF nerve samples, leaving the middle part avascularized. This invasion of microvessels was more evident from the proximal than from the distal end. Over time, these differences became more evident in the 12 and 16 week samples, as the sprouted vessels reached to the middle parts of the nerve. In nerve autografts, longitudinal running vessels were recognized that ran along the entire length of the nerve. These vessels appeared thicker compared to the newly formed vessels in the allograft and SIEF nerve samples.

At 12 weeks, the proximal sections of the nerve samples showed that the addition of vascularization to allograft nerves (SIEF group) resulted in the highest number of vessels in the outer ring of the nerve ($P<0.01$). The SIEF group had significantly more vessels in the middle and central ring as well, compared to the allograft alone ($P<0.05$). In the mid-section of the nerve, the number of vessels in the allograft was lowest compared to all other groups in the middle ring ($P<0.05$). In the central ring, the allograft also measured the least number of vessels and was significantly inferior to SIEF nerves and control nerves ($P<0.05$). The number of vessels in SIEF nerves and control nerves were similar in the central ring of the mid-section of the nerve. In the distal section of the nerve, a trend towards a higher number of vessels was seen in

SIEF nerves, however, this was not significant. Schematic visualization of the number of vessels in different parts of the nerve are depicted in Figure 6.

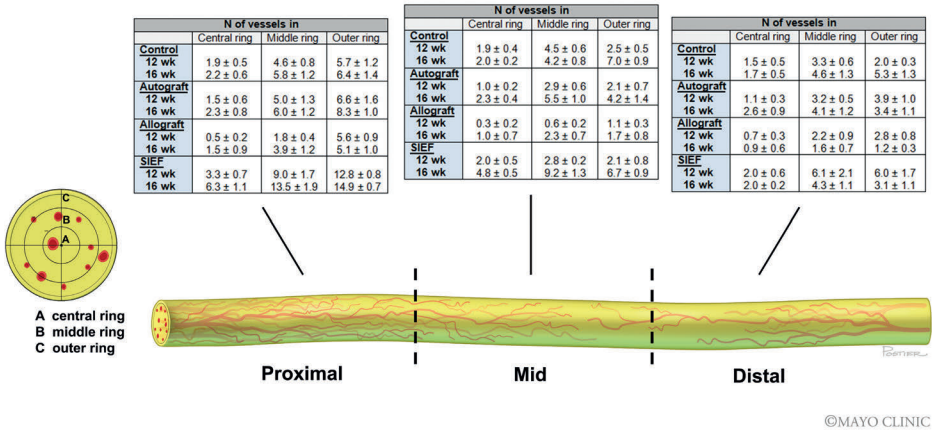

	N of vessels in		
	Central ring	Middle ring	Outer ring
Control			
12 wk	1.9 ± 0.5	4.6 ± 0.8	5.7 ± 1.2
16 wk	2.2 ± 0.6	5.8 ± 1.2	6.4 ± 1.4
Autograft			
12 wk	1.5 ± 0.6	5.0 ± 1.3	6.6 ± 1.6
16 wk	2.3 ± 0.8	6.0 ± 1.2	8.3 ± 1.0
Allograft			
12 wk	0.5 ± 0.2	1.8 ± 0.4	5.6 ± 0.9
16 wk	1.5 ± 0.9	3.9 ± 1.2	5.1 ± 1.0
SIEF			
12 wk	3.3 ± 0.7	9.0 ± 1.7	12.8 ± 0.8
16 wk	6.3 ± 1.1	13.5 ± 1.9	14.9 ± 0.7

	N of vessels in		
	Central ring	Middle ring	Outer ring
Control			
12 wk	1.9 ± 0.4	4.5 ± 0.6	2.5 ± 0.5
16 wk	2.0 ± 0.2	4.2 ± 0.8	7.0 ± 0.9
Autograft			
12 wk	1.0 ± 0.2	2.9 ± 0.6	2.1 ± 0.7
16 wk	2.3 ± 0.4	5.5 ± 1.0	4.2 ± 1.4
Allograft			
12 wk	0.3 ± 0.2	0.6 ± 0.2	1.1 ± 0.3
16 wk	1.0 ± 0.7	2.3 ± 0.7	1.7 ± 0.8
SIEF			
12 wk	2.0 ± 0.5	2.8 ± 0.2	2.1 ± 0.8
16 wk	4.8 ± 0.5	9.2 ± 1.3	6.7 ± 0.9

	N of vessels in		
	Central ring	Middle ring	Outer ring
Control			
12 wk	1.5 ± 0.5	3.3 ± 0.6	2.0 ± 0.3
16 wk	1.7 ± 0.5	4.6 ± 1.3	5.3 ± 1.3
Autograft			
12 wk	1.1 ± 0.3	3.2 ± 0.5	3.9 ± 1.0
16 wk	2.6 ± 0.9	4.1 ± 1.2	3.4 ± 1.1
Allograft			
12 wk	0.7 ± 0.3	2.2 ± 0.9	2.8 ± 0.8
16 wk	0.9 ± 0.6	1.6 ± 0.7	1.2 ± 0.3
SIEF			
12 wk	2.0 ± 0.6	6.1 ± 2.1	6.0 ± 1.7
16 wk	2.0 ± 0.2	4.3 ± 1.1	3.1 ± 1.1

Figure 6. Nerve vascularization patterns of nerve groups at 12 and 16 weeks. Micro CT cross-sectional images throughout the length of the nerve grafts were obtained. The length of the nerve was divided into three sections: (I) proximal, (II) mid and (III) distal. The cross-sectional images were divided into three rings: (A) central ring, (B) middle ring, (C) outer ring to count the number of vessels. Nerve tissue was depicted in yellow and the vessels were depicted in red. Tables describe the number of vessels in each of the rings per nerve section (proximal, mid and distal) for control, autograft, allograft and allograft wrapped in a superficial inferior epigastric artery fascia (SIEF) flap. The first row denotes the number of vessels (mean ± SEM) at 12 weeks and the second row at 16 weeks. SEM = Standard error of the mean.

At 16 weeks, the proximal section of the nerve showed superiority of the number of vessels in SIEF nerves in all three rings of the cross-sections compared to other groups ($P<0.0001$ in outer ring, $P<0.05$ in middle and central ring). In the mid-section of the nerve, the number of vessels in the outer ring was lowest in the allografts and inferior to the SIEF and control nerve samples ($P<0.05$). In the middle ring, the SIEF group was superior to allograft ($P<0.0001$) and control nerves ($P<0.05$) and in the central ring the SIEF group measured the highest number of vessels and was superior to all other groups ($P<0.0001$). In the distal section of the nerve, no significant differences were found when comparing the groups and different rings (Figure 6).

DISCUSSION

Revascularization of nerve is postulated to occur from (i) extraneural vascular contribution from surrounding beds (centripetal revascularization) and (ii) longitudinal bidirectional inosculation from the proximal and distal ends of the graft

[9,20,21]. Inosculation results in endothelial-lined newly formed blood vessels starting from day three, without formation of vessels in the middle segment of the graft [9,22,23]. It is believed that the vessels in the mid-section are formed by ingrowth of blood vessels from the surrounding bed, starting by day six to eight [22]. The larger the grafts, the longer it takes to be completely revascularized, with risk of fibrosis and central necrosis [22]. Neovascularization is a complex process of critical importance involving endothelial cells, sprouting from the parent vessel, and releasing of growth factors, such as vascular endothelial growth factor (VEGF), a potent angiogenic factor required during tissue repair [6,24]. The predominant mechanism (centripetal versus bidirectional inosculation) of revascularization remains unknown.

The findings in this study are in line with the theory that inosculation occurs prior to centripetal revascularization. At two weeks, early revascularization in nerve allografts occurred from both nerve stumps, but primarily from proximal to distal. In allografts wrapped in a pedicled flap, this amount of inosculation was greater, suggesting that an improved vascularized bed promotes longitudinal inosculation, in particular proximal inosculation. Favored proximal vascular advancement was also suggested by Chalfoun and colleagues using microvascular blood flow imaging [25]. This finding may support the fact that success of the nerve graft is partly affected by the length of the nerve graft [22] as a longer graft is subject to higher risk of necrosis in the mid to distal sections. Between autografts and control nerves a similar pattern of vascularization was seen, indicating that reestablishment of blood supply occurs along preexisting vascular channels [22,26].

In VNGs (vascularized nerve grafts), neovascularization is triggered in the first 72 hours as the blood flow is equal or greater than that in normal nerves suggesting to prevent early ischemia [22]. This is clearly seen in the increase in vascular volume of the revascularized allografts compared to the allografts at two weeks. The vascular volume represents the actual volume of vessels in the nerve, whereas the vascular surface area is more likely to be an estimation of vessels as a three dimensional structure is converted to a two dimensional structure. In small nerve samples, a high resolution of micro CT is crucial to identify the smallest vessels. When such a micro CT is not available, vascular surface areas can be used to clarify differences between experimental groups as similar trends between the vascular volume and vascular

surface areas are seen and these methods are correlated [19], however, based on the findings of this study, vascular volume is preferred.

The blood supply of the recipient bed affects the success of a nerve graft substantially, which is believed to be resulting in early revascularization of the graft and ultimately speed of axonal regeneration and degree of restored function of the target muscle [22]. Central necrosis of thick nerve grafts has been a confirmed problem and commonly described as necrosis of the central ring of the graft (core necrosis) [7,27-29]. Our data are consistent with previous studies in which not only the core but also the central section of the length of the allograft nerve has been shown to be predisposed to avascularity, with potentially higher risk of necrosis [30]. A VNG greatly affects vascularization, impeding both types of central necrosis. Due to a decrease in graft ischemic time, VNGs are suggested to lead to faster nerve regeneration than nonvascularized nerve grafts (NVNG) [30]. However, the rate of axonal regeneration has not found to be different between non-vascularized and conventional nerve grafts [30-32]. Functional recovery needs to be tested, as suggested to be positively affected by VNGs [11].

The theoretical advantages of a VNG or provision of a well-vascularized bed for the nerve graft are well accepted [7]. Maintaining vascularization after nerve injury may yield several advantages: not only may it restore extrinsic neural blood vessels that were damaged during nerve trauma, intraneural fibrosis secondary to ischemia will also be reduced. This may result in an increase of axonal regeneration particularly in thicker grafts [22,33], subsequently preventing target muscle atrophy [7]. In order to have these potential advantages, surgically provided vascularization to the nerve site needs to be applied accurately. The vascular pedicle should be of large enough diameter to support microvascular anastomoses in the case of free flaps. To overcome this problem a simple pedicled flap could be used. Another condition that influences the outcomes of the peripheral nerve is the fact that blood supply should emanate from a vascular pedicle that travels parallel with the nerve over an adequate distance [22,33]. The surgical technique that provides the pedicled adipofascial flap has been validated while taken these prerequisite conditions in account [15].

The limitation of this study is the large time gap between the short-term and long-term outcomes. To better describe revascularization patterns, time points at four or eight weeks may have provided additional information. Vascular response to nerve

injury is composed of two phases: after the early first phase, triggered by Wallerian degeneration in the first week, the second phase comprises from one to six weeks after injury. This phase is characterized by the increase in number of vessels and associated with nerve regeneration and axonal myelination [6,34,35]. However, differences between these phases, or newly developed vessels could not be distinguished from older vessels using these techniques.

CONCLUSIONS

The results of this study highlight the revascularization patterns after interposition nerve grafting in rats over time. The importance of adding a well-vascularized bed for nerve allografts, in means of a pedicled flap wrapped around a nerve, are objectively measured and visualized over the length of the nerve as well as in the various cross sectional rings of the nerve. Based on this study, we can conclude that the blood supply of the recipient bed determines the degree of early revascularization of the nerve graft. Furthermore, revascularization occurs primarily from proximal to distal (proximal inosculation) and not from both ends as previously believed and confirms the theory of centripetal revascularization.

Acknowledgments

The authors would like to thank Jim Postier (Rochester, MN) for the artwork of Figure 6.

Conflicts of interest

None declared.

Supplemental Video 1: Videos of the micro CT imaged nerves in Figure 1.

Scan the QR code to view the videos of Chapter 5.

REFERENCES

1. Ferretti A, Boschi E, Stefani A, et al. Angiogenesis and nerve regeneration in a model of human skin equivalent transplant. Life Sci 2003;73):1985-1994.
2. Gu XH, Terenghi G, Kangesu T, et al. Regeneration pattern of blood vessels and nerves in cultured keratinocyte grafts assessed by confocal laser scanning microscopy. Br J Dermatol 1995;132:376-383.
3. Manek S, Terenghi G, Shurey C, Nishikawa H, Green CJ, Polak JM. Neovascularisation precedes neural changes in the rat groin skin flap following denervation: an immunohistochemical study. Br J Plast Surg 1993;46:48-55.
4. Kangesu T, Manek S, Terenghi G, et al. Nerve and blood vessel growth in response to grafted dermis and cultured keratinocytes. Plast Reconstr Surg 1998;101:1029-1038.
5. Hobson MI, Brown R, Green CJ, Terenghi G. Inter-relationships between angiogenesis and nerve regeneration: a histochemical study. Br J Plast Surg 1997;50:125-131.
6. Caillaud M, Richard L, Vallat JM, Desmouliere A, Billet F. Peripheral nerve regeneration and intraneural revascularization. Neural Regen Res 2019;14:24-33.
7. D'Arpa S. Vascularized nerve "grafts": just a graft or a worthwhile procedure? Plast Aesthet Res 2016;2:183-192.
8. Krames ES. Possible malfunction of electronic medical devices caused by computed tomography scanning. Neuromoduolation 2009;12:5-7.
9. Tarlov IM EJ. Nerve grafts: The importance of an adequate blood supply. J Neurosurg 1945;2:49-71.
10. Seddon HJ. The use of autogenous grafts for the repair of large gaps in peripheral nerves. Br J Surg 1947;35:151-167.
11. Restrepo Y, Merle M, Michon J, Folliguet B, Barrat E. Free vascularized nerve grafts: an experimental study in the rabbit. Microsurg 1985;6:78-84.
12. Shibata M, Tsai TM, Firrell J, Breidenbach WC. Experimental comparison of vascularized and nonvascularized nerve grafting. J Hand Surg Am 1988;13:358-365.
13. Kanaya F, Firrell J, Tsai TM, Breidenbach WC. Functional results of vascularized versus nonvascularized nerve grafting. Plast Reconstr Surg 1992;89:924-930.
14. Karcher H, Kleinert R. Regeneration in vascularized and free nerve grafts. A comparative morphological study in rats. J Maxillofac Surg 1986;14:341-343.
15. Saffari TM, Bishop AT, Shin AY. The Superficial Inferior Epigastric Artery Fascia Flap in Rats. Journal of Reconstructive Microsurgery Open 2020; 05(01): e7-e14
16. Hundepool CA, Nijhuis TH, Kotsougiani D, Friedrich PF, Bishop AT, Shin AY. Optimizing decellularization techniques to create a new nerve allograft: an in vitro study using rodent nerve segments. Neurosurg Focus 2017;42:E4.
17. Hudson TW, Zawko S, Deister C, et al. Optimized acellular nerve graft is immunologically tolerated and supports regeneration. Tissue Eng 2004;10:1641-1651.

18. Kumta S, Yip K, Roy N, Lee SK, Leung PC. Revascularisation of bone allografts following vascular bundle implantation: an experimental study in rats. Arch Orthop Trauma Surg 1996;115:206-210.
19. Saffari TM, Bishop AT, Shin AY. New methods for objective angiogenesis evaluation of rat nerves using microcomputed tomography scanning and conventional photography. Microsurgery. 2020;40(3):370-376.
20. Lind R, Wood MB. Comparison of the pattern of early revascularization of conventional versus vascularized nerve grafts in the canine. J Reconstr Microsurg 1986;2:229-234.
21. Penkert G, Bini W, Samii M. Revascularization of nerve grafts: an experimental study. J Reconstr Microsurg 1988;4:319-325.
22. Terzis JK, Skoulis TG, Soucacos PN. Vascularized nerve grafts. A review. Int Angiol 1995;14:264-277.
23. Wongtrakul S, Bishop AT, Friedrich PF. Vascular endothelial growth factor promotion of neoangiogenesis in conventional nerve grafts. J Hand Surg Am 2002;27:277-285.
24. Pereira Lopes FR, Lisboa BC, Frattini F, et al. Enhancement of sciatic nerve regeneration after vascular endothelial growth factor (VEGF) gene therapy. Neuropathol Appl Neurobiol 2011;37:600-612.
25. Chalfoun C, Scholz T, Cole MD, Steward E, Vanderkam V, Evans GR. Primary nerve grafting: A study of revascularization. Microsurg. 2003;23:60-65.
26. Wong D, Dupree J, Terzis JK. Vascularized versus nonvascularized nerve grafts: the controversy persists. 1988.
27. Sunderland S. Nerves and Nerve Injuries. Vol 2nd edition Edinburgh: Churchill Livingstone; 1978.
28. Brooks D. The place of nerve-grafting in orthopaedic surgery. J Bone Joint Surg Am 1955;37:299-305.
29. Seddon HJ. Nerve Grafting. J Bone Joint Surg Br 1963;45:447-461.
30. McCullough CJ, Gagey O, Higginson DW, Sandin BM, Crow JC, Sebille A. Axon regeneration and vascularisation of nerve grafts. An experimental study. J Hand Surg Br 1984;9:323-327.
31. Seckel BR, Ryan SE, Simons JE, Gagne RG, Watkins E, Jr. Vascularized versus nonvascularized nerve grafts: an experimental structural comparison. Plast Reconstr Surg 1986;78:211-220.
32. Pho RW, Lee YS, Rujiwetpongstorn V, Pang M. Histological studies of vascularised nerve graft and conventional nerve graft. J Hand Surg Br 1985;10:45-48.
33. Taylor GI. Nerve grafting with simultaneous microvascular reconstruction. Clin Orthop Relat Res. 1978:56-70.
34. Podhajsky RJ, Myers RR. The vascular response to nerve crush: relationship to Wallerian degeneration and regeneration. Brain Res 1993;623:117-123.
35. Podhajsky RJ, Myers RR. The vascular response to nerve transection: neovascularization in the silicone nerve regeneration chamber. Brain Res 1994;662:88-94.

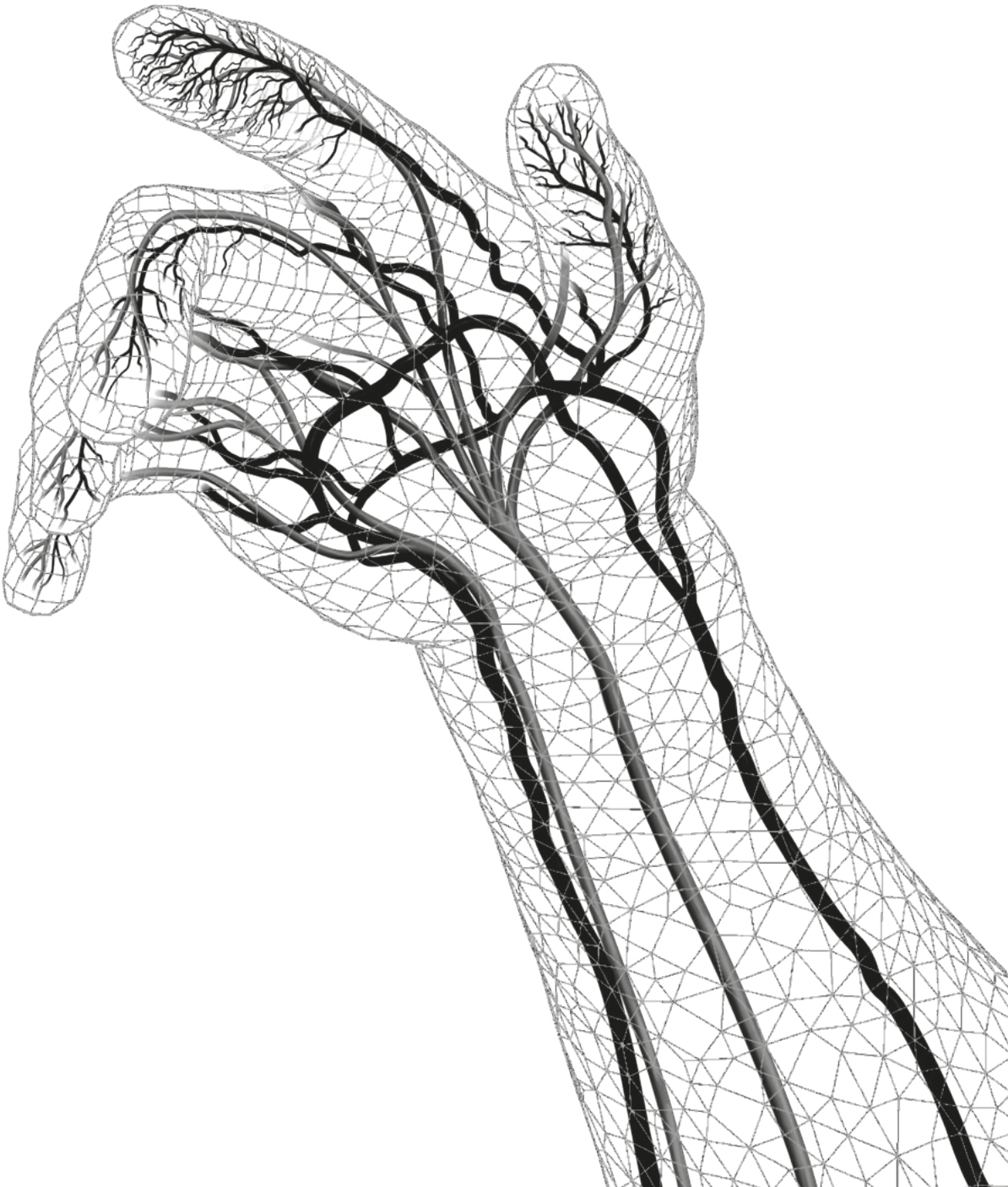

CHAPTER SIX

Surgical Angiogenesis Modifies the Cellular Environment of Nerve Allografts in a Rat Sciatic Nerve Defect Model

Tiam M. Saffari[1,2]
Amr Badreldin[1]
Femke Mathot[1,2]
Leila Bagheri[1]
Allen T. Bishop[1]
Andre J. van Wijnen[1,3]
Alexander Y. Shin[1]

Affiliations

[1]Department of Orthopedic Surgery, Mayo Clinic, Rochester, MN, USA
[2]Department of Plastic-, Reconstructive- and Hand Surgery, Radboud University, Nijmegen, the Netherlands
[3]Department of Biochemistry and Molecular Biology, Mayo Clinic, Rochester, MN, USA

Gene. 2020;751:144711

ABSTRACT

Background

A well-vascularized bed for nerve grafts may diminish nerve rejection by altering the microenvironment and intricate paracrine mechanisms that control local cellular pathways. The purpose of this study was to determine how surgical angiogenesis alters the cellular environment of processed nerve allografts in a rat sciatic nerve defect model.

Materials and Methods

Unilateral sciatic nerve defects of Lewis rats (N=39) were repaired with (i) autografts, (ii) decellularized processed nerve allografts, or (iii) allografts wrapped with a superficial inferior epigastric fascial (SIEF) flap to provide vascularization. Animals were evaluated at two weeks (N=5/group) for flow cytometry and gene expression profiles, and at 12 and 16 weeks (N=4/group/time point) for immunohistochemistry. Gene expression was quantified by quantitative polymerase chain reaction (qPCR) analysis of representative biomarkers, including angiogenic, neurotrophic, immunotrophic and extracellular matrix (ECM) genes.

Results

Flow cytometry revealed a significant increase in T helper population (CD4) in SIEF rats, compared to baseline, untreated rats ($P=0.02$) after one week. Expression of several angiogenic markers, including Cd34, Pecam1/Cd31, Vegfa and Mmp2 ($P<0.05$ compared to autograft), as well as extracellular matrix proteins such as collagen type I (Col1A1) and type III (Col3A1) ($P<0.01$, compared to allograft) was significantly increased in SIEF samples and confirmed by immunohistochemistry.

Conclusions

Surgical angiogenesis of processed nerve allografts alters the cellular environment confirmed with immune cells obtained from peripheral blood, gene expression profiles and immunohistochemical staining. These immunological and angiogenic changes may enhance short- and long-term outcomes of nerve regenerative strategies.

INTRODUCTION

Traumatic injury to the peripheral nerve results in Wallerian degeneration at the distal stump [1], causing discontinuation of the nerve and disturbance of blood supply, consequently preventing nutrition delivery [2]. Regeneration of nerve is achieved in a series of actions mediated by vascular endothelial growth factor (VEGF) and Schwann cell migration as a result of hypoxia during trauma [3]. VEGF, originally known as vascular permeability factor (VPF) is a signaling protein with vascular permeability activity that plays a role in regulating new blood vessel formation to provide nutrients to the injury site [4,5]. Vasculature also allows endothelial cells to secrete growth factors that can be beneficial for nerve regeneration by interacting with specific cell membrane surface receptors and stimulating signaling pathways that regulate proliferation, survival, migration and differentiation [6,7]. The importance of growth factors as regulators of post-injury tissue repair is well-established, however, direct delivery has not resulted in improved outcomes as postulated [8-10]. This apparent lack of efficacy at present could be due to the incredible complexity of multiple cellular responses during tissue healing, as well as technical obstacles related to management of the local delivery and pharmacokinetics of growth factors. Recipient gene expression is profoundly altered after nerve transplantation, however, these complex molecular events and cellular responses are neither fully understood nor easy to dissect. The biological functions of genes expressed in a paracrine environment influenced by angiogenic and neurotrophic factors, cytokines controlling immune signal transduction, as well as collagenous and non-collagenous extracellular matrix (ECM) proteins are important parameters that are frequently encountered during acute nerve allograft rejection. Combining gene expression profiles with flow cytometry data of immune cells obtained from blood and long-term immunohistochemical staining may provide mechanistic insights into the cellular effect of vascularization on nerve allografts. The purpose of this study was to evaluate the cellular responses that control the healing environment of processed nerve allografts in a rat sciatic nerve defect model after addition of surgical angiogenesis.

MATERIALS AND METHODS

Animal experiments were approved by the Institutional Animal Care and Use Committee (IACUC A3348-18). All animals were individually housed with *ad libitum* access to food and water, with a twelve-hour light-dark cycle until sacrifice.

Experimental design

Thirty-nine male Lewis rats, weighing between 200 to 300 grams (Envigo, Madison, WI, USA), were randomly divided into three groups. All rats underwent excision of a 10-mm portion of the sciatic nerve that was reconstructed with (i) autografts, (ii) decellularized processed nerve allografts, or (iii) allografts wrapped around with a superficial inferior epigastric fascial (SIEF) flap to provide vascularization to the wound bed (SIEF group). At one and two weeks, CD4 and CD8 levels were measured using flow cytometry. Four extra unoperated rats served for baseline control levels. Animals were sacrificed at two weeks (N=5/group) or 12 weeks and 16 weeks (N=4/group/time point) to evaluate gene expression profiles and immunohistochemistry staining in the nerve graft samples, respectively (Table 1).

Table 1. Experimental design. SIEF flap: Superficial inferior epigastric artery fascial (SIEF) flap, qPCR: quantitative polymerase chain reaction

	Groups	Outcome measurements	Time points and N
I	Autograft	• qPCR analysis • T cell measurement in blood samples	• At 2 weeks • 5 samples/group
II	Allograft		
III	Allograft + SIEF flap	• Immunohistochemistry analysis	• At 12 and 16 weeks • 4 samples/group

Nerve allograft harvest and processing

A total of thirteen male Sprague-Dawley rats, weighing 250-300 grams, (Envigo, Madison, WI, USA) served as donors for the bilateral harvest of 15-mm segments of the sciatic nerve. These rats were used to create a histocompatibility barrier [11,12]. The sciatic nerves were cleaned from external tissue debris and treated using a five-day decellularization protocol to generate acellular allografts as described previously [13]. Briefly, the nerves underwent multiple sequential washing steps, were incubated in

chondroitinase and elastase, sterilized using g-irradiation and stored in phosphate buffer saline (PBS) at 4°C until surgery.

Surgical procedure

Rats were anesthetized in an isoflurane chamber, shaved and positioned in the nosecone to maintain anesthesia throughout the procedure. Preoperatively the following were subcutaneously injected; Enrofloxacin (Infection profylaxis, Baytril, Bayer, Germany, 10mg/kg), 5 mL of NaCl 0.9% and buprenorphine SR (pain control, Buprenorphine SR-LAB, ZooPharm pharmacy, 0.6mg/kg). Body temperature was maintained at 37°C with a heating pad.

The sciatic nerve was fully exposed proximally from the inferior margin of the piriformis muscle to approximately 5 mm distal to the bifurcation, under an operating microscope (Zeiss OpMi 6, Carl Zeiss Surgica, Oberkochen, Germany). A 10-mm segment of the sciatic nerve was excised by sharp transection with microsurgical scissors. In group I, the nerve segment was reversed and placed as an interposition autograft with six 10-0 nylon (10-0 Ethilon, Ethicon Inc., Sommerville, NJ, USA), epineural interrupted sutures on either side. In group II, the nerve gap was bridged with a 10-mm nerve allograft using a similar surgical technique. In group III, a 10-mm nerve allograft was used to reconstruct the nerve defect and wrapped in a pedicled adipofascial flap harvested from the abdomen to provide vascularization to the nerve allograft. Preparation of the superficial inferior epigastric fascial (SIEF) flap was previously described [14]. Briefly, a 4-cm paramedian abdominal incision was made on the ipsilateral side of the nerve reconstruction. The femoral artery was identified in the groin and the superficial inferior epigastric (SIE) vessels were exposed. The 4 x 3 cm SIEF flap containing subcutaneous fat, inguinal fat, the femoral vasculature and SIE vessels, was tunneled subcutaneously toward the nerve reconstruction and wrapped around the nerve. Both the proximal and distal nerve anastomoses were covered with the flap. In all groups, wounds were closed in layers, approximating muscle with two 5-0 absorbable interrupted sutures. The skin was closed subcutaneously (5-0 Vicryl Rapide, Ethicon Inc., Sommerville, NJ, USA). Postoperatively, the rats were kept warm with towels.

Blood collection

At one and two weeks postoperatively, rats were anesthetized using isoflurane and blood was drawn from the tail vein to measure CD4 and CD8 levels. Rats were positioned on a heat pad to dilate the tail vein during this experiment.

Flowcytometry

Per sample, 2 ml of blood was collected in heparin tubes. Within an hour, blood was transferred to vials containing 1 ml of PBS. After decantation of Ficoll-Paque, vials were centrifuged at room temperature at 2000 RPM for 30 minutes to separate the buffy coat. The buffy coat of peripheral blood lymphocytes (PBL) was transferred to a vial containing 1 ml of FACS buffer. This suspension was centrifuged at 4°C at 1500 RPM for 5 minutes, the supernatant was discarded and the pellet was used for the next steps. For detection of CD4 and CD8 cells, PE-anti-CD4 monoclonal antibody (clone W3/25, 1:100, ThermoFisher, IL, USA) and FITC anti-CD8 alpha monoclonal antibody (clone OX-8, 1:100, ThermoFisher, IL, USA) was used, respectively. Samples were incubated on ice for 30 minutes, washed with FACS buffer and centrifuged at 4°C at 1500 RPM for 5 minutes. The supernatant was discarded and washing was performed three times. Cells were fixated with 500 ul of 1% PFA and analyzed using flow cytometry (FACScan, LSR II, BD™).

Messenger ribonucleic acid (mRNA) quantitative real time PCR (RT-qPCR)

All chemicals and primers for RNA extraction and analysis were purchased from Millipore Sigma (St. Louis, MO) unless stated otherwise. After sacrifice, nerve grafts within the sutures were collected in 1 mL Trizol (TRI Reagent, Sigma, USA), placed on ice immediately and stored at -80°C. Samples were mechanically homogenized (IKA Ultra Turrax T8 Homogenizer, NC, USA) and stored on ice for 15 minutes before manual extraction of RNA. To 1 mL of Trizol suspension, 200 µl of chloroform was added. Samples were vortexed, spun down at 4°C for 15 minutes at 12,000g and the aqueous phase was carefully transferred to a new tube. After adding 500 µl of isopropyl alcohol (2-propanol), samples were precipitated at -20°C for one hour and spun down at 4°C for 20 minutes at 12,000g. The supernatant was removed and the RNA pellet was washed with 75% Ethanol (EtOH). Samples were spun down for 20

minutes at 7,500g in 4°C, the supernatant was removed, the RNA was resuspended in 15 µl RNAse free water and RNA concentrations were measured using a NanoDropTM 2000/2000c Spectrophotometer (ThermoFisher Scientific, Waltham, MA, USA). Complementary DNA (cDNA) was generated using reverse transcriptase and obtained in a concentration of 10 ng/µl. cDNA was amplified with a CFX384 real time PCR system (Bio-Rad Laboratories, Inc., CA, USA) using SYBR Green detection.

Genes evaluated

Genes were selected based on their involvement in nerve regeneration and neovascularization, as well as other biological properties and functions [7,15-17] (Table 2). Results were normalized to the mRNA for the general cytoskeletal protein β-actin gene (*Actb*) because this reference gene remains relatively invariable among many tissues and cell types [18]. The differences in gene expression levels were quantified using the comparative delta crossover threshold ($2^{-\Delta\Delta CT}$) method [19,20]. Primer sequences per gene are provided in the Appendix.

Immunohistochemistry

To visualize nerve fibers and vascularization, nerve grafts obtained from four rats of each group were used for immunohistochemical staining at 12 and 16 weeks after reconstruction. Nerve grafts were harvested, fixed in 10% formalin under agitation for 48 hours, stored in 70% ETOH and embedded in paraffin. Cross-sectional sections (5 µm) from the mid-distal portion of the graft were cut and stained for protein gene product 9.5 (PGP9.5) a pan-neuronal marker (diluted 1:500, Agilent, USA), which stains both myelinated and unmyelinated nerve fibers [21], S100B, a common marker of neural tissue (diluted 1:5000, Agilent, USA) and CD34 (diluted 1:4000, Abcam, USA), staining vascular endothelial cells and extensively expressed on blood vessels [22]. A qualitative assessment of the number of blood vessels and nerve fibers in the nerve sections was performed by four blinded observers, using an established scoring system [23].

Statistical analysis

Results of qPCR measurements were analyzed for each gene using analysis of variance (ANOVA) corrected with Bonferroni post-hoc testing. Cytokine blood levels were

analyzed using an unpaired student t-test. Results were reported as the mean and standard error of the mean (SEM), and the level of significance was set at $\alpha \leq 0.05$.

Table 2. Investigated genes including their description and function.

Gene Symbol	Description	Function
Gapdh	Glyceraldehyde-3-phosphate dehydrogenase	Housekeeping gene
Actb	Cytoskeletal protein β-actin	Housekeeping gene
Neurotrophic markers		
Gdnf	Glial cell derived neurotrophic factor	Promotes survival of neurons by prevention of apoptosis
Ngf	Nerve growth factor	Guider of axonal growth and promotes Schwann cell activity
Pmp22	Peripheral myelin protein 22	Schwann cell growth, important component of myelin
Ptn	Pleiotrophin	Neuronal protection
Angiogenic markers		
Vegfa	Vascular endothelial growth factor a	Proliferation and migration of vascular endothelial cells
Pecam1/Cd31	Platelet endothelial cell adhesion molecule or Cd31	Maintains vascular permeability barrier
Mmp2	Matrix metallopeptidase 2	Expression is correlated with increased angiogenesis
Cd34	Cd34 molecule	Role in early hematopoiesis
Immunogenic markers		
Cd4	Cd4 molecule	Helper T cells
Cd8	Cd8 molecule	Cytotoxic T cells
Tnf	Tumor necrosis factor	Inflammation – type M1 macrophages
Extracellular matrix (ECM) markers		
Col1A1	Type I collagen	Interaction with ECM
Col3A1	Type III collagen	Interaction with ECM
Fbln1	Fibulin1	Perineurium of peripheral nerve
Lamb2	Laminin subunit beta 2	Regulates cell growth, motility and cell adhesion

RESULTS

Peripheral T cells

To understand systemic levels of inflammation, we examined classical T cell markers in blood samples. After one week, T helper population (CD4) was significantly increased in SIEF rats (59.7±1.0%), compared to baseline, untreated rats (47.4±4.3%, P=0.02). CD4 cells measured 58.6±3.0% in autografts and 54.8±3.5% in allografts at one week, respectively. At two weeks, CD4 decreased to 48.9±5.8% in autografts, 57.1±4.0% in allografts and 56.7±1.1% in SIEF rats, respectively (P=0.10). CD8 cells measured 23.2±1.2% and 21.7±3.0% in autografts, 22.2±1.0% and 22.8±1.2% in allografts and 22.7±0.2 and 23.7±0.9% in SIEF rats, at one and two weeks, respectively. No significant differences in proportions of T cytotoxic/suppressor populations (CD8) were seen, compared to baseline (26.2±1.9%, P>0.10), or between time points (P=0.20, Figure 1). These results indicate that CD4-positive T helper cells are selectively elevated in SIEF rats.

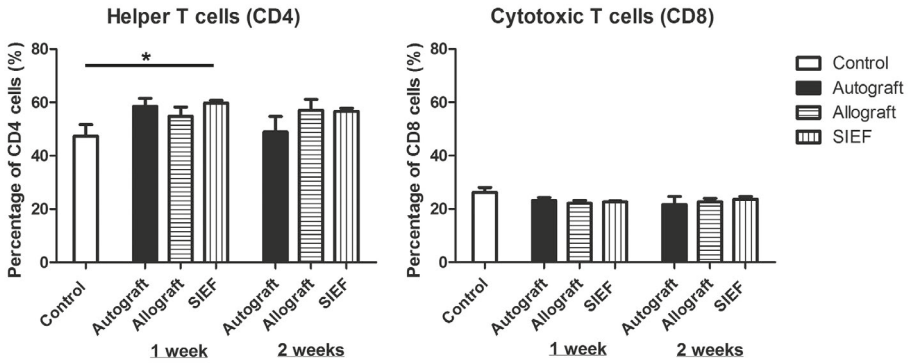

Figure 1. Helper T cells (CD4) and cytotoxic T cells (CD8) in peripheral blood. Percentage of live cells in control (baseline) rats and rats in which the 10- mm sciatic nerve gap has been repaired with autograft, allograft and allograft wrapped around with a superficial inferior epigastric artery fascial (SIEF) flap to provide vascularization, at one week and two weeks post-surgery. Bars denote mean ± SEM. *Indicates significance at P < 0.05. SEM: Standard error of the mean.

Quantitative PCR analysis

Paracrine environment

To understand the local cellular environment near the nerve repair site, we examined the relative expression of angiogenic and neurotrophic markers in rats in which the nerve defect was reconstructed with autograft, allograft or allograft wrapped around with a SIEF flap at two weeks (Figure 2). Expression of angiogenic markers including Cd34, Pecam1/Cd31, Vegfa and Mmp2 exhibited a significant increase in SIEF samples (0.050±0.011, 0.774±0.123 0.367±0.101 and 5.175±1.207 for these markers, respectively) compared to autograft nerve (0.012±0.005, 0.222±0.025, 0.075±0.007 and 1.365±0.065 for these markers, respectively, $P<0.05$). Expression values for allograft samples were 0.024±0.005 for Cd34, 0.681±0.167 for Pecam1, 0.152±0.020 for Vegfa and 2.628±0.437 for Mmp2. The relative expression of neurotrophic markers such as Gdnf, Ngf, Pmp22 and Ptn was also analyzed. Expression of Gdnf and Ngf, was below or near the level of detection (smaller than 0.02, data not shown). Pmp22 demonstrated significantly increased expression of allograft nerves (0.882±0.118) compared to autograft (0.446±0.099, $P<0.05$) and SIEF nerves (0.182±0.030, $P<0.05$) (Figure 2). Expression levels of Ptn revealed superiority of autograft (0.417±0.043, $P<0.01$) and allograft (0.312±0.036, $P<0.05$) compared to SIEF (0.105±0.012), but the expression levels that were detected are relatively low. These results indicate that the addition of an adipofascial flap to the nerve allograft repair modifies the paracrine environment.

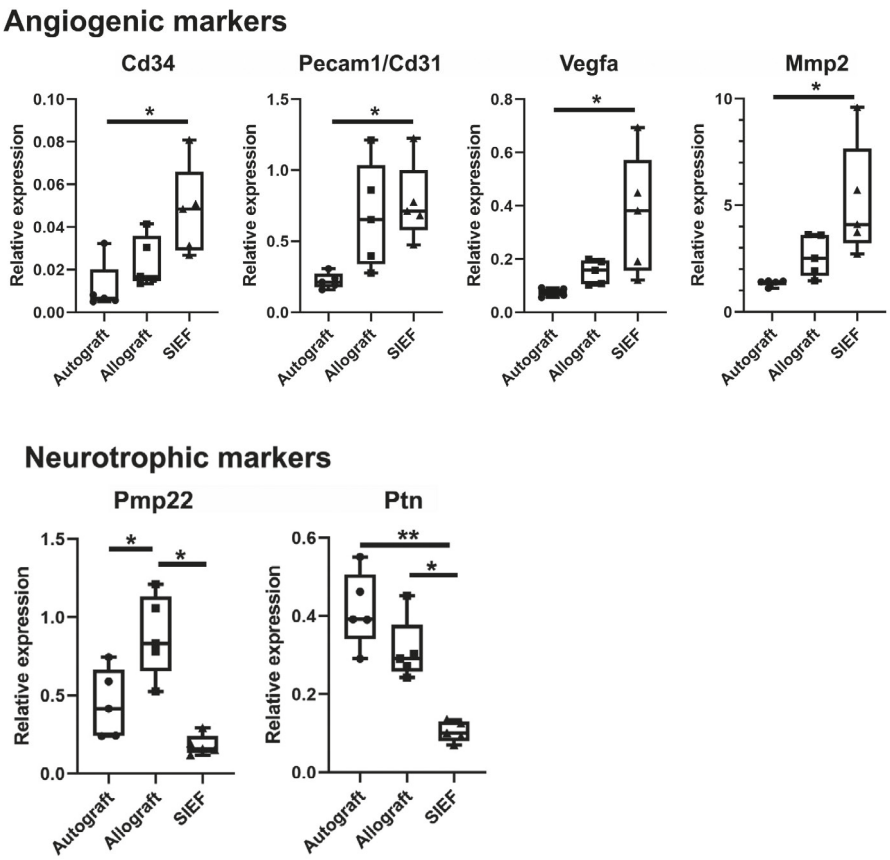

Figure 2. Gene expression profiles of paracrine environment including angiogenic and neurotrophic markers. Expression profiles for angiogenic markers included Cd34, Pecam1/Cd31, Vegfa and Mmp2. Neurotrophic markers included Pmp22 and Ptn. Expression levels for Gdnf and Ngf were < 0.02, thus considered non-detectable. Gene expression profiles are shown for autograft, allograft and allograft wrapped around with a superficial inferior epigastric artery fascial (SIEF) flap, and were normalized to Actb. *Indicates significance at P < 0.05, **P < 0.01.

Immunotrophic gene expression

Relative expression of immunotrophic genes was examined to assess the local inflammatory environment (Figure 3). Expression of Cd4 was significantly highest in allograft (0.913±0.058) compared to autograft (0.152±0.004, P<0.001) and SIEF (0.585±0.096, P<0.05). Cd8 expression was highest in SIEF samples (0.243±0.035), compared to autograft (0.069±0.010, P<0.001) and allograft (0.069±0.004, P<0.001). Expression values for Tnf revealed very low expression profiles in all three graft groups, with significantly highest expression in SIEF samples (P<0.05). These results indicate that distinct subtypes of T cells may be active near the grafts during nerve tissue repair.

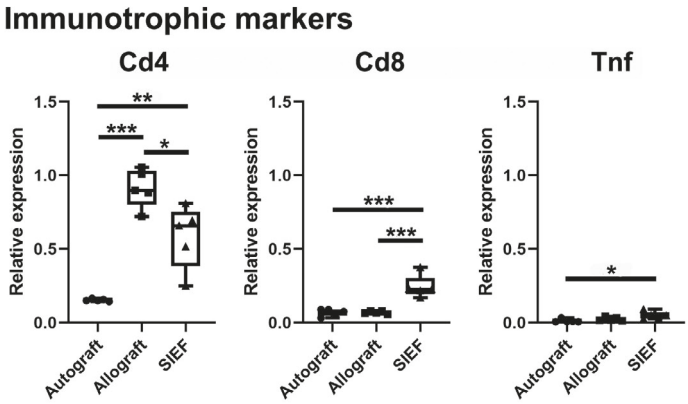

Figure 3. Gene expression profiles of immunotrophic markers including Cd4, Cd8 and Tnf. Gene expression profiles from autograft, allograft and allograft wrapped around with a superficial inferior epigastric artery fascial (SIEF) flap. Gene expression was normalized to Actb. *Indicates significance at P < 0.05, **P < 0.01, ***P < 0.001.

Extracellular matrix gene expression

The activity of fibroblastic cell types in nerve regenerative surgery was investigated by examining the expression of collagenous and non-collagenous extracellular matrix proteins (Figure 4). SIEF nerves measured a significantly higher expression values for Col1a1 (139.850±31.192) and Col3a1 (31.257±7.284) compared to allograft nerves (36.602±8.43 for Col1a1 and 4.395±1.856 for Col3a1, P<0.01), and superiority to autograft nerves for Col3a1 (0.749±0.235, P<0.01), but not for Col1a1 (69.211±5.028). Fibulin (Fbln1) expression was lower in SIEF nerves (0.155±0.022) compared allograft (0.401±0.093, P<0.05) and autograft (0.712±0.032, P<0.001). Laminin β2 (Lamb2) expression was very low in all samples and did not significantly differ between graft groups (0.138±0.009 for autograft, 0.092±0.029 for allograft and 0.094±0.011 for SIEF) (Figure 4). The active expression of different collagen proteins is consistent with the presence of fibroblastic cell types that generate fibrous repair tissues near nerve grafts.

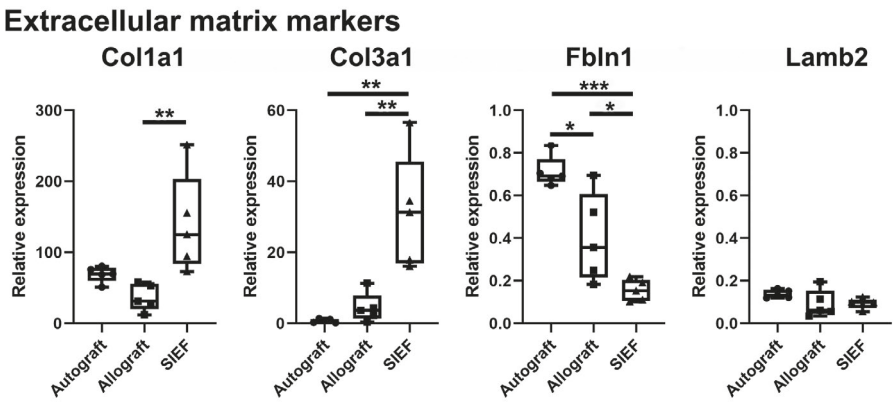

Figure 4. Gene expression profiles of extracellular markers including Col1a1, Col3a1, Fbln1 and Lamb2. Gene expression profiles from autograft, allograft and allograft wrapped around with a superficial inferior epigastric artery fascial (SIEF) flap. Gene expression was normalized to Actb. *Indicates significance at P < 0.05, **P < 0.01, ***P < 0.001.

Immunohistochemistry

The in situ inter-relationship between nerve tissues and blood vessels in the nerve graft tissue was assessed. Immunohistochemical signals were depicted using antibodies against PGP 9.5, S100, identifying neural tissue, and CD34 for staining blood vessels (Figure 5A). Established qualitative assessment showed a consistent distribution for PGP 9.5 and S100 throughout the nerve tissue in all groups at 12 and 16 weeks (Figure 5B). CD34 showed differences in expression between groups and time points. Allograft nerve tissue wrapped with the SIEF flap showed highest expression of CD34 at both time points. At 12 weeks, CD34 was occasionally present in allograft nerve tissue, while higher expressed in autograft and control nerve. At 16 weeks, CD34 expression had increased slightly in allografts, but still lowest expression compared to other groups. Representative mid-distal graft nerve sections of the four groups including non-operated control and Haemotoxylin and Eosin (H&E) marker at 12 weeks are depicted in Figure 5A. Collectively, these studies suggest that wrapping with the SIEF flap enhances vascularization in nerve graft tissue.

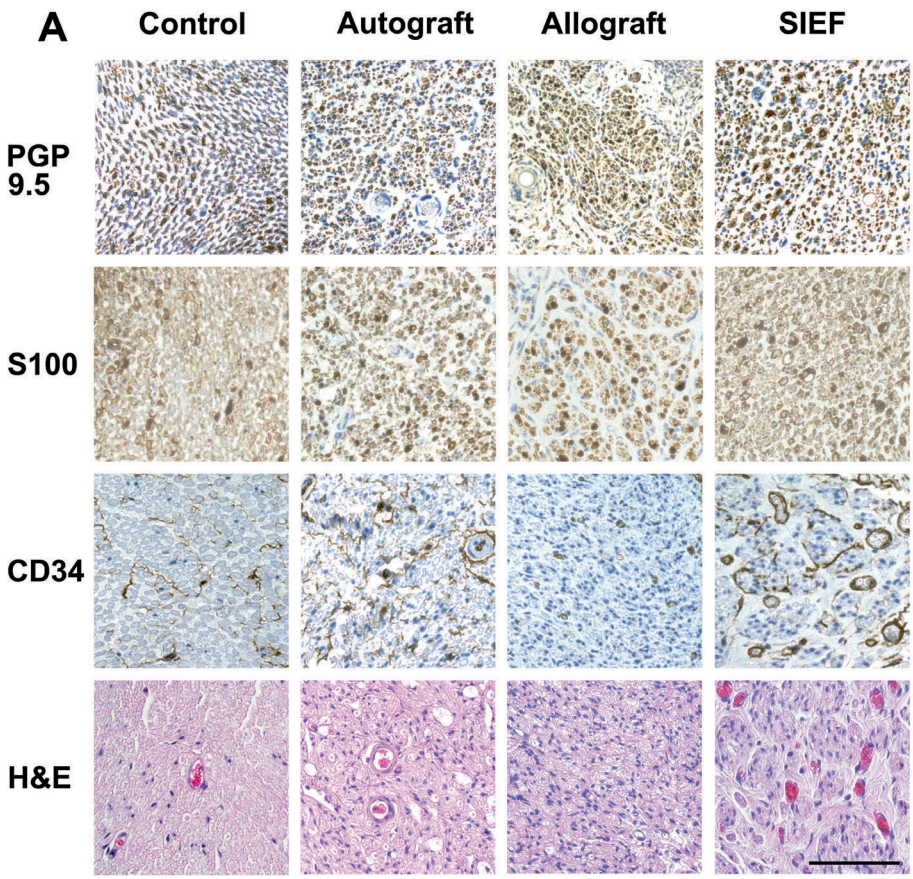

B

	Control	Autograft	Allograft	SIEF
PGP 9.5				
12 wk	++++	++++	++++	++++
16 wk	++++	++++	++++	++++
S100				
12 wk	++++	++++	++++	++++
16 wk	++++	++++	++++	++++
CD34				
12 wk	+	++	+/-	+++
16 wk	++	++	+	+++

Figure 5. Density of protein gene product 9.5 (PGP9.5), S100 and CD34 immunoreactivity. (A) Micrographs showing density in mid-distal graft sections from control nerve samples, autograft, allograft and allograft wrapped with a superficial inferior epigastric fascial (SIEF) flap at 12 weeks. Hematoxylin and Eosin (H&E) marker was used as principal stain. Scale bar is set at 100 µm. (B) Qualitative assessment of immunohistochemistry. Density: 0 none, +/- occasional, + sparse, ++ few, +++ moderate, ++++ abundant, assessment described by Ferretti et al. (2003)[23].

DISCUSSION

In this study, gene expression profiles combined with immunohistochemistry staining against neuronal and angiogenic markers in nerve gaps repaired with autograft, allograft and allograft wrapped around with a SIEF flap to provide vascularization, were analyzed. These studies were conducted to understand the regulatory mechanisms in the physiological microenvironment generated after nerve transplantation and how vascularization of the nerve bed could alter this healing niche. We examined the expression of the most prominent groups of genes that were predicted to play a role in the effect of vascularization on nerve regeneration and compared their expression in autograft, allograft and SIEF nerve samples, two weeks after nerve reconstruction.

After nerve trauma, a series of responses occur that involves Wallerian degeneration [24]. During Wallerian degeneration, the axons and myelin degenerate in the distal stump of the axotomized nerve, leading to phenotypic changes that promote axonal regeneration [1,25]. The molecular changes in the paracrine environment, described as the immediate extracellular environment, and the peripheral environment both contribute to form a favorable environment for axonal outgrowth [26].

Angiogenesis

Expression for all assessed angiogenic markers including Cd34, Pecam1/Cd31, Vegfa and Mmp2, was increased in allografts wrapped with the SIEF flap compared to autograft and allograft alone. The increase for these markers in SIEF group was shown to be statistically significant compared to autograft. Previous studies revealed that VEGF expression is significantly upregulated during the early phases after nerve trauma, while a strong downregulation was shown in degenerating nerve, suggesting its possible role during the regenerative process [27]. Our results corroborate these findings and could be explained by the fact that the decellularized nerve allograft is free from vascular cells and undergoes revascularization immediately following nerve reconstruction, whereas this is not necessary in autografts. The process of revascularization is upregulated when providing an adipofascial flap around the nerve allograft. Immunohistochemical staining against CD34 revealed that long-term vascularity is enhanced at 12 and 16 weeks in allografts wrapped with the SIEF flap.

This improved vascularization is predicted to facilitate nerve graft survival and neural tissue regeneration.

Neuronal expression

Neurotrophic factors play essential roles in axonal guidance, myelination and neuronal survival [28]. In this study, Gdnf and Ngf expression levels were shown to be near to non-detectable. Gdnf was shown to promote survival of neurons by prevention of apoptosis [15,29] and Ngf to promote Schwann cell activity [30-32]. Yet, these genes were only found to be upregulated in sensory nerves and not in motor nerves [17,33,34], providing a plausible explanation for these findings. Data on neurotrophic factors is limited and would require additional longitudinal studies with multiple time points to draw definitive conclusions regarding their modulation. Studies presented to date have shown that expression of Gdnf and Ngf is highly variable and clearly fluctuates over the course of the first 21 days *in vitro* [7]. Long-term results in this study, showed no differences in neuronal expression between groups using immunohistochemistry against PGP 9.5 and S100. Neurotrophic factors after nerve repair are highly variable and require additional studies prior to drawing definitive conclusions.

Immunology

Two classical subpopulations of T cells are involved in rejection of tissue allografts [35]. In our study, the fraction of CD4 positive T cells measured in peripheral blood were significantly increased in allografts wrapped with the SIEF flap at one week postoperatively. No differences between groups were found for CD8 positive T cell when compared to control baseline levels. A previous study has found a peak of cytotoxic CD8 T cells [35], but this finding did not replicate under our experimental conditions. Processed decellularized nerve grafts, used in this study, are acellular and are not expected to evoke immune rejection to any large extent that it would result in recruitment of CD8 positive cells to the graft site. Immunotrophic genes showed measurable differences in mRNA levels, but these levels were close to background levels thus precluding definitive interpretation. The alloimmune response involves many cytokines influencing the progression of the response leading to either allograft survival or rejection [36]. Based on these findings, it could be concluded that nerve defect

repaired with a nerve graft results in immunotrophic changes locally, and also in the peripheral environment.

Extracellular matrix (ECM)

Collagen is found in most connective tissues and plays a key role in each phase of healing after injury [37]. *In vitro*, high levels of ECM-related gene expression profiles demonstrate cell adhesion and cell-to-cell communication abilities [17]. In rat skin, type III collagen is associated with early increase in collagen synthesis and may function in supporting healing [37]. These studies are consistent with our observation that ECM related gene expression is increased in SIEF nerve tissue.

Strengths and limitations

Evaluation of gene expression profiles in a surgical nerve repair model in which a pedicled adipofascial flap supports vascularization of nerve allografts represents a new approach to understand how vascularization alters the local healing environment. Molecular results can support the assessment of functional outcomes and provide mechanistic answers to success or failure of nerve repair strategies by elucidating effects of surgical angiogenesis on nerve allografts. Unfortunately, the set-up of these experiments did not allow for functional recovery outcomes. Future animal studies will focus on combining molecular results with functional motor outcomes to describe the effect of surgical angiogenesis on nerve regeneration in more detail.

Another limitation of the current *in vivo* study is the lack of gene expression profiles evaluation over time. Gene expression may vary over time and following these profiles over a time course may provide more information. One obstacle remains the experimental logistics, the cost of surgery and animal maintenance to obtain longitudinal results that permit assessment of nerve vascularization over time. We also appreciate the limitation that gene expression profiles may be altered due to the trauma or inflammation caused at time of surgery, and that some growth factors and EMC proteins in the healing environment are triggered *in vivo* only and cannot be recapitulated *in vitro*.

CONCLUSIONS

This study demonstrates that addition of a pedicled adipofascial SIEF flap to the nerve allograft increases vascularity when compared to allografts only and alters immunotrophic factors locally and in peripheral blood. Results obtained from peripheral blood, gene expression profiles and immunohistochemistry at both short- and long-term suggest that surgical angiogenesis alters the cellular environment of processed nerve allografts to potentially enhance nerve regeneration.

Declaration of competing interest

The authors declare that they have neither known competing financial interests nor personal relationships that could have appeared to influence the reported work.

Acknowledgments

We would like to thank Michael J. Hansen for his technical assistance (flowcytometry) and the observers Roman Thaler, Farzaneh Khani and Meiwand Bedar, who together with Amr Badreldin scored the immunohistochemical sections. We also thank Patricia F. Friedrich for technical assistance during surgery, as well as other members of the van Wijnen laboratory for stimulating discussions and sharing ideas.

REFERENCES

1. Waller A. Experiments on the Section of the Glosso-Pharyngeal and Hypoglossal Nerves of the Frog, and Observations of the Alterations Produced Thereby in the Structure of Their Primitive Fibres. *Edinb Med Surg J.* 1851;76(189):369-376.
2. Gao Y, Weng C, Wang X. Changes in nerve microcirculation following peripheral nerve compression. *Neural Regen Res.* 2013;8(11):1041-1047.
3. Nishida Y, Yamada Y, Kanemaru H, Ohazama A, Maeda T, Seo K. Vascularization via activation of VEGF-VEGFR signaling is essential for peripheral nerve regeneration. *Biomed Res.* 2018;39(6):287-294.
4. Storkebaum E, Carmeliet P. VEGF: a critical player in neurodegeneration. *J Clin Invest.* 2004;113(1):14-18.
5. Zupanc HRH, Alexander PG, Tuan RS. Neurotrophic support by traumatized muscle-derived multipotent progenitor cells: Role of endothelial cells and Vascular Endothelial Growth Factor-A. *Stem Cell Res Ther.* 2017;8(1):226.
6. Muangsanit P, Shipley RJ, Phillips JB. Vascularization Strategies for Peripheral Nerve Tissue Engineering. *Anat Rec (Hoboken).* 2018;301(10):1657-1667.
7. Mathot F, Rbia N, Thaler R, Bishop AT, Van Wijnen AJ, Shin AY. Gene expression profiles of differentiated and undifferentiated adipose derived mesenchymal stem cells dynamically seeded onto a processed nerve allograft. *Gene.* 2020;724:144151.
8. Hoyng SA, De Winter F, Gnavi S, et al. A comparative morphological, electrophysiological and functional analysis of axon regeneration through peripheral nerve autografts genetically modified to overexpress BDNF, CNTF, GDNF, NGF, NT3 or VEGF. *Exp Neurol.* 2014;261:578-593.
9. Lee JY, Giusti G, Friedrich PF, Bishop AT, Shin AY. Effect of Vascular Endothelial Growth Factor Administration on Nerve Regeneration after Autologous Nerve Grafting. *J Reconstr Microsurg.* 2016;32(3):183-188.
10. Piquilloud G, Christen T, Pfister LA, Gander B, Papaloizos MY. Variations in glial cell line-derived neurotrophic factor release from biodegradable nerve conduits modify the rate of functional motor recovery after rat primary nerve repairs. *Eur J Neurosci.* 2007;26(5):1109-1117.
11. Kumta S, Yip K, Roy N, Lee SK, Leung PC. Revascularisation of bone allografts following vascular bundle implantation: an experimental study in rats. *Arch Orthop Trauma Surg.* 1996;115(3-4):206-210.
12. Hudson TW, Zawko S, Deister C, et al. Optimized acellular nerve graft is immunologically tolerated and supports regeneration. *Tissue Eng.* 2004;10(11-12):1641-1651.
13. Hundepool CA, Nijhuis TH, Kotsougiani D, Friedrich PF, Bishop AT, Shin AY. Optimizing decellularization techniques to create a new nerve allograft: an in vitro study using rodent nerve segments. *Neurosurg Focus.* 2017;42(3):E4.
14. Saffari TM, Bishop AT, Shin AY. The Superficial Inferior Epigastric Artery Fascia Flap in Rats. *Journal of Reconstructive Microsurgery Open* 2020; 05(01): e7-e14

15. Gordon T. The role of neurotrophic factors in nerve regeneration. *Neurosurg Focus.* 2009;26(2):E3.
16. Chernousov MA, Carey DJ. Schwann cell extracellular matrix molecules and their receptors. *Histol Histopathol.* 2000;15(2):593-601.
17. Rbia N, Bulstra LF, Lewallen EA, Hovius SER, van Wijnen AJ, Shin AY. Seeding decellularized nerve allografts with adipose-derived mesenchymal stromal cells: An in vitro analysis of the gene expression and growth factors produced. *J Plast Reconstr Aesthet Surg.* 2019;72(8):1316-1325.
18. Sikand K, Singh J, Ebron JS, Shukla GC. Housekeeping gene selection advisory: glyceraldehyde-3-phosphate dehydrogenase (GAPDH) and beta-actin are targets of miR-644a. *PLoS One.* 2012;7(10):e47510.
19. Dudakovic A, Camilleri E, Riester SM, et al. High-resolution molecular validation of self-renewal and spontaneous differentiation in clinical-grade adipose-tissue derived human mesenchymal stem cells. *J Cell Biochem.* 2014;115(10):1816-1828.
20. Livak KJ, Schmittgen TD. Analysis of relative gene expression data using real-time quantitative PCR and the 2(-Delta Delta C(T)) Method. *Methods.* 2001;25(4):402-408.
21. Sun Y, Zhu L, Huang X, Zhou C, Zhang X. Immunohistochemical localization of nerve fibers in the pseudocapsule of fibroids. *Eur J Histochem.* 2014;58(2):2249.
22. Fina L, Molgaard HV, Robertson D, et al. Expression of the CD34 gene in vascular endothelial cells. *Blood.* 1990;75(12):2417-2426.
23. Ferretti A, Boschi E, Stefani A, et al. Angiogenesis and nerve regeneration in a model of human skin equivalent transplant. *Life Sci.* 2003;73(15):1985-1994.
24. Yao D, Li M, Shen D, et al. Gene expression profiling of the rat sciatic nerve in early Wallerian degeneration after injury. *Neural Regen Res.* 2012;7(17):1285-1292.
25. Saffari TM, Bedar M, Zuidam JM, et al. Exploring the neuroregenerative potential of tacrolimus. *Expert Rev Clin Pharmacol.* 2019.
26. Navarro X, Vivo M, Valero-Cabre A. Neural plasticity after peripheral nerve injury and regeneration. *Prog Neurobiol.* 2007;82(4):163-201.
27. Guaiquil VH, Pan Z, Karagianni N, Fukuoka S, Alegre G, Rosenblatt MI. VEGF-B selectively regenerates injured peripheral neurons and restores sensory and trophic functions. *Proc Natl Acad Sci U S A.* 2014;111(48):17272-17277.
28. Hercher D, Kerbl M, Schuh C, et al. Spatiotemporal Differences in Gene Expression Between Motor and Sensory Autografts and Their Effect on Femoral Nerve Regeneration in the Rat. *Front Cell Neurosci.* 2019;13:182.
29. Caseiro AR, Pereira T, Ivanova G, Luis AL, Mauricio AC. Neuromuscular Regeneration: Perspective on the Application of Mesenchymal Stem Cells and Their Secretion Products. *Stem Cells Int.* 2016;2016:9756973.
30. Woodfin A, Voisin MB, Nourshargh S. PECAM-1: a multi-functional molecule in inflammation and vascular biology. *Arterioscler Thromb Vasc Biol.* 2007;27(12):2514-2523.
31. Koopmans G, Hasse B, Sinis N. Chapter 19: The role of collagen in peripheral nerve repair. *Int Rev Neurobiol.* 2009;87:363-379.

32. Hubert T, Grimal S, Carroll P, Fichard-Carroll A. Collagens in the developing and diseased nervous system. *Cell Mol Life Sci.* 2009;66(7):1223-1238.
33. Hoke A, Redett R, Hameed H, et al. Schwann cells express motor and sensory phenotypes that regulate axon regeneration. *J Neurosci.* 2006;26(38):9646-9655.
34. Mills CD, Allchorne AJ, Griffin RS, Woolf CJ, Costigan M. GDNF selectively promotes regeneration of injury-primed sensory neurons in the lesioned spinal cord. *Mol Cell Neurosci.* 2007;36(2):185-194.
35. Ansselin AD, Pollard JD. Immunopathological factors in peripheral nerve allograft rejection: quantification of lymphocyte invasion and major histocompatibility complex expression. *J Neurol Sci.* 1990;96(1):75-88.
36. Walsh PT, Strom TB, Turka LA. Routes to transplant tolerance versus rejection; the role of cytokines. *Immunity.* 2004;20(2):121-131.
37. Clore JN, Cohen IK, Diegelmann RF. Quantitation of collagen types I and III during wound healing in rat skin. *Proc Soc Exp Biol Med.* 1979;161(3):337-340.

APPENDIX

Table 1. mRNA primer sequences per gene

Gene Symbol	Sequence
Gapdh	Fwd: 5′ AGTGCCAGCCTCGTCTCATA 3′ Rev: 3′ GATGGTGATGGGTTTCCCGT 5′
Actb	Fwd: 5′ CAGCCTTCCTTCCTGGGTATG 3′ Rev: 3′ AGGGTGTAAAACGCAGCTCA 5′
Neurotrophic markers	
Gdnf	Fwd: 5′CTGACCAGTGACTCCAATATGC 3′ Rev: 3′ TTAAGACGCACCCCCGATTT 5′
Ngf	Fwd: 5′ CACTCTGAGGTGCATAGCGT 3′ Rev: 3′ CTATTGGTTCAGCAGGGGCA 5′
Pmp22	Fwd: 5′ GTCTGGTCTGCTGTGAGCAT 3′ Rev: 3′ GCCATTGGCTGACGATGGTG 5′
Ptn	Fwd: 5′ GCCGAGTGCAAACAAACCAT 3′ Rev: 3′ TGATTCCGCTTGAGGCTTGG 5′
Angiogenic markers	
Vegfa	Fwd: 5′: AGAAAGCCCATGAAGTGGTGA 3′ Rev: 3′: GCTGGCTTTGGTGAGGTTTG 5′
Pecam1/Cd31	Fwd: 5′ TTGTGACCAGTCTCCGAAGC 3′ Rev: 3′ TGGCTGTTGGTTTCCACACT 5′
Mmp2	Fwd: 5′ AGAGGATACCCCAAGCCACT 3′ Rev: 3′ ATAGCTGTGACCACCACCCT 5′
Cd34	Fwd: 5′ AGTACCCACACGGATGGAGTG 3′ Rev: 3′ CTCGAGAACAGCCAGGTACA 5′
Immunogenic markers	
Cd4	Fwd: 5′ AAGGACTGGCCAGAGACTCA 3′ Rev: 3′ TTTCTTGTTCTCCAGCTCGCA 5′
Cd8	Fwd: 5′ CTCATCTGCTGCCACAGGAA 3′ Rev: 3′ GCCCGGTCTCTTGTGAGAAA 5′
Tnf	Fwd: 5′ CTGTGCCTCAGCCTCTTCTC 3′ Rev: 3′ GCTTGGTGGTTTGCTACGAC 5′
Extracellular matrix (ECM) markers	
Col3A1	Fwd: 5′ CCCGGCAACAATGGTAATCC 3′ Rev: 3′ GACCTCGTGCTCCAGTTAGC 5′
Col1A1	Fwd: 5′ TGACTGGAAGAGCGGAGAGT 3′ Rev: 3′ GATAGCGACATCGGCAGGAT 5′
Fbln1	Fwd: 5′ TGAGAACTATCGCCGCTCTG 3′ Rev: 3′ GGGTGAACTCTCGGAAGGTG 5′
Lamb2	Fwd: 5′ AGTACCCACACGGATGGAGTG 3′ Rev: 3′ CTCGAGAACAGCCAGGTACA 5′

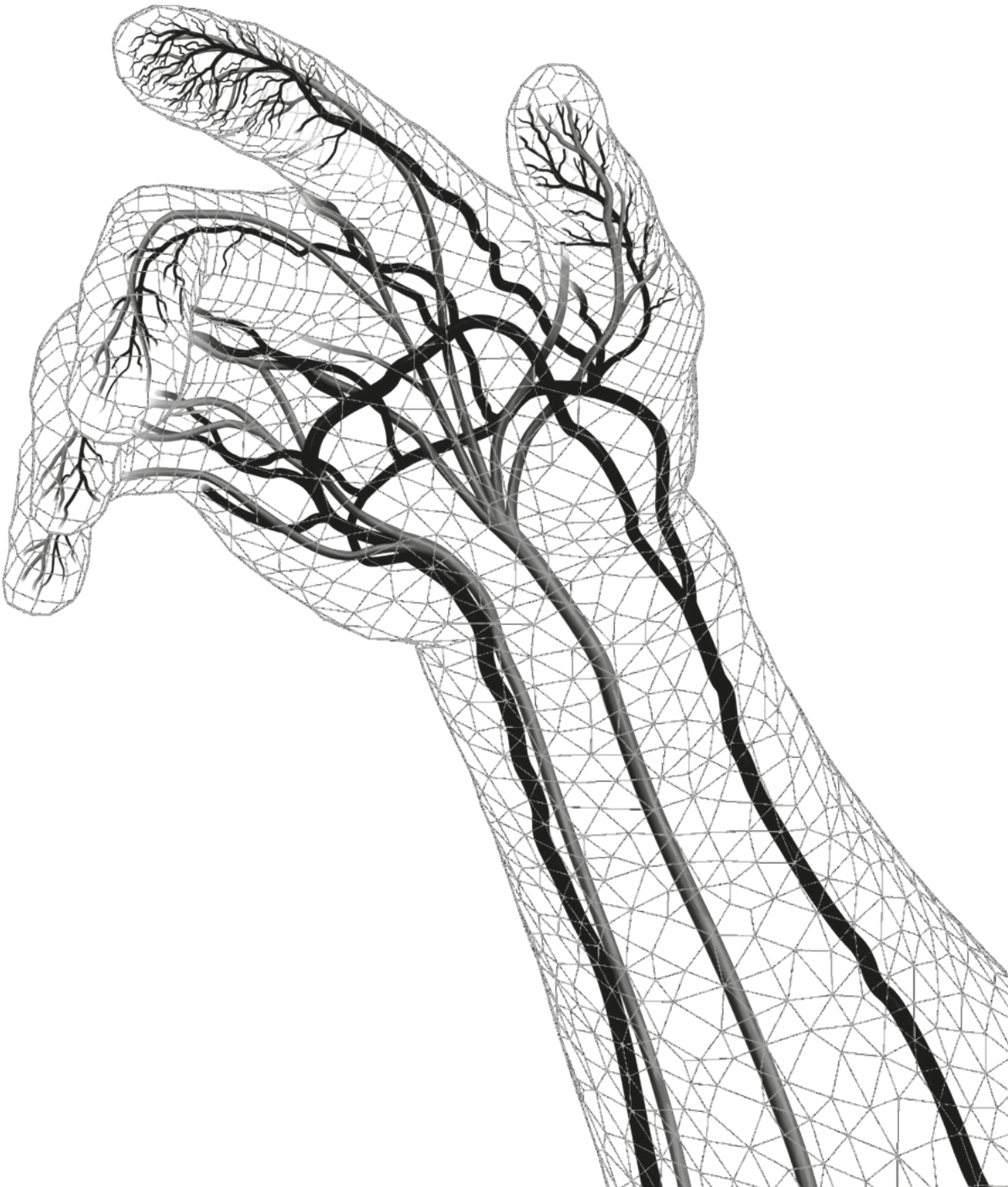

CHAPTER

SEVEN

Surgical Angiogenesis of Decellularized Nerve Allografts Improves Early Functional Recovery in a Rat Sciatic Nerve Defect Model

Tiam M. Saffari[1,2]
Femke Mathot[1,2]
Patricia F. Friedrich[1]
Allen T. Bishop[1]
Alexander Y. Shin[1]

Affiliations

[1]Department of Orthopedic Surgery, Mayo Clinic, Rochester, MN, USA
[2]Department of Plastic-, Reconstructive- and Hand Surgery, Radboud University, Nijmegen, the Netherlands

Plastic and Reconstructive Surgery. 2021.
Accepted to be published in the September 2021 issue.

ABSTRACT

Background

Surgical angiogenesis applied to nerve grafts has been suggested to enhance nerve regeneration after nerve injury. We hypothesized that surgical angiogenesis to decellularized nerve allografts would improve functional recovery in a rat sciatic nerve defect model.

Materials and Methods

Sixty Lewis rats were divided in three groups of 20 animals each. Unilateral sciatic nerve defects were repaired with (i) autografts, (ii) decellularized allografts and (iii) decellularized allografts wrapped with a superficial inferior epigastric fascial (SIEF) flap to add surgical angiogenesis. Twelve and 16 weeks after surgery, nerve regeneration was assessed using functional, electrophysiological, histological and immunofluorescence analyses. Ultrasonography was used during the survival period to noninvasively evaluate muscle atrophy and reinnervation by measuring cross-sectional muscle area.

Results

Surgical angiogenesis of allografts demonstrated significantly improved isometric tetanic force recovery at 12 weeks, compared to allograft alone, which normalized between groups at 16 weeks. Cross-sectional muscle areas showed no differences between groups. Electrophysiology showed superiority of autografts at both time points. No differences were found in histological analysis, besides a significantly inferior N-ratio in allografts at 12 weeks. Immunofluorescent expression of CD34, indicating vascularity, was significantly enhanced in the SIEF group compared to allografts at 12 weeks, with highest expression at 16 weeks compared to all groups.

Conclusions

Surgical angiogenesis with an adipofascial flap to the nerve allograft increases vascularity in the nerve graft, with subsequent improvement of early muscle force recovery, comparable to autografts.

INTRODUCTION

Traumatic nerve injuries are a common cause of severe disability and result in loss of sensory- and motor function [1]. The gold standard remains end-to-end tension-free neurorrhaphy [2,3]. When this is not possible, autograft interposition is needed, requiring harvest of a functional autologous nerve with the associated donor site morbidity [4]. Experimental models have investigated allogenic nerves, processed allografts, conduits and vein grafts for the reconstruction of peripheral nerve injuries [5-7]. While these substitutes have demonstrated successful recovery, outcomes have yet to exceed the results of autografts. It is widely accepted that functional results are poor when nerve grafts are transplanted into scarred recipient beds [8], and that independent blood supply of nerve grafts could improve outcomes [9,10].

Processed nerve allografts are devoid of cellular materials, have no vascular supply and undergo revascularization from the surrounding tissue bed via centripetal revascularization [11]. Surgical addition of vascularization (surgical angiogenesis) has the advantage of ensured blood supply, potentially minimizing the period of ischemia and diminishing fibrosis and central necrosis. Immediate revascularization promotes axonal regeneration [12] and faster reinnervation, which could reduce denervation-induced muscle atrophy [13]. Furthermore, the addition of cellular-based therapy such as adipose-derived mesenchymal stem cells (MSC), could influence vascularization [13]. Adipose tissue itself is a rich source of MSCs, with proven beneficial effects on nerve regeneration [13-18]. The superficial inferior epigastric artery fascial (SIEF) flap is an easily harvested flap that provides surgical angiogenesis while improving nutrition and circulating pluripotent cells to the wound site, as well as a layer of adipose tissue to the nerve injury bed, a potential source of stem cells [19]. Application of either vascularized nerve grafts (VNG) or vascularized flaps around nerve grafts has been suggested to improve outcomes, however, there are conflicting clinical and basic science reports on its efficacy [15,20-23]. In the present study, we investigated the effect of surgical angiogenesis of decellularized nerve allografts on functional motor recovery after segmental nerve repair in rats by comparing allografts placed in a vascularized bed to allografts alone and autografts.

MATERIALS AND METHODS

Animal experiments were approved by the Institutional Animal Care and Use Committee (IACUC A3348-18). A total of 60 male Lewis rats, weighing 200-300 grams (Envigo, USA), were randomly divided into three groups. All rats underwent excision of a 10-mm portion of the sciatic nerve. In group I (nerve autograft, gold standard), this nerve defect was repaired with an ipsilateral reversed autologous graft. In group II, the same gap was reconstructed with a 10-mm processed nerve allograft. In group III, the allograft was wrapped with a SIEF flap [19]. All groups had survival periods of 12 and 16 weeks (N=10 per time point/group) for evaluation of outcomes. Time points were chosen based on previous research and the neuroregenerative capacity of rats [5]. Muscle atrophy and reinnervation was noninvasively measured over time using ultrasonography.

Nerve allograft harvest and processing

Twenty male Sprague-Dawley rats, weighing 250-300 grams, (Envigo, USA) served as donors for harvesting 15-mm segments of the sciatic nerve bilaterally. This species of rats were specifically chosen to create a histocompatibility mismatch to the Lewis rats [24,25]. The sciatic nerves were cleaned from external debris and processed into acellular allografts using a nerve decellularization protocol [26]. Nerves were harvested under sterile conditions and underwent a series of washing steps, were sterilized using g-irradiation and stored at 4°C until use [26].

Surgical procedure

Rats were anesthetized in an isoflurane chamber, shaved and positioned in the nose cone to maintain anesthesia throughout the procedure. Preoperatively Enrofloxacin (Infection prophylaxis, Baytril, Germany, 10mg/kg), 5 mL of NaCl 0.9%, and buprenorphine SR (pain control, Buprenorphine SR-LAB, ZooPharm pharmacy, 0.6mg/kg) were injected subcutaneously. Body temperature was maintained at 37°C with a heating pad.

The sciatic nerve was fully exposed proximally from the inferior margin of the piriformis muscle to approximately 5-mm distal to the bifurcation, under an operating microscope (Zeiss OpMi 6, Carl Zeiss Surgica, Oberkochen, Germany). A 10-mm segment

of the sciatic nerve was excised by sharp transection with microsurgical scissors. In group I, the nerve segment was reversed and placed as an interposition autograft with six 10-0 nylon (10-0 Ethilon, Ethicon Inc., NJ, USA) epineural interrupted sutures. In group II, the nerve gap was bridged with a 10-mm nerve allograft using a similar surgical technique and in group III this nerve allograft was wrapped with a pedicled SIEF flap as previously described [19]. In short, the femoral artery was identified in the groin and the superficial inferior epigastric (SIE) vessels were exposed. The SIEF flap was tunneled subcutaneously toward the nerve reconstruction and wrapped around the nerve to surround both nerve anastomoses (Figure 1).

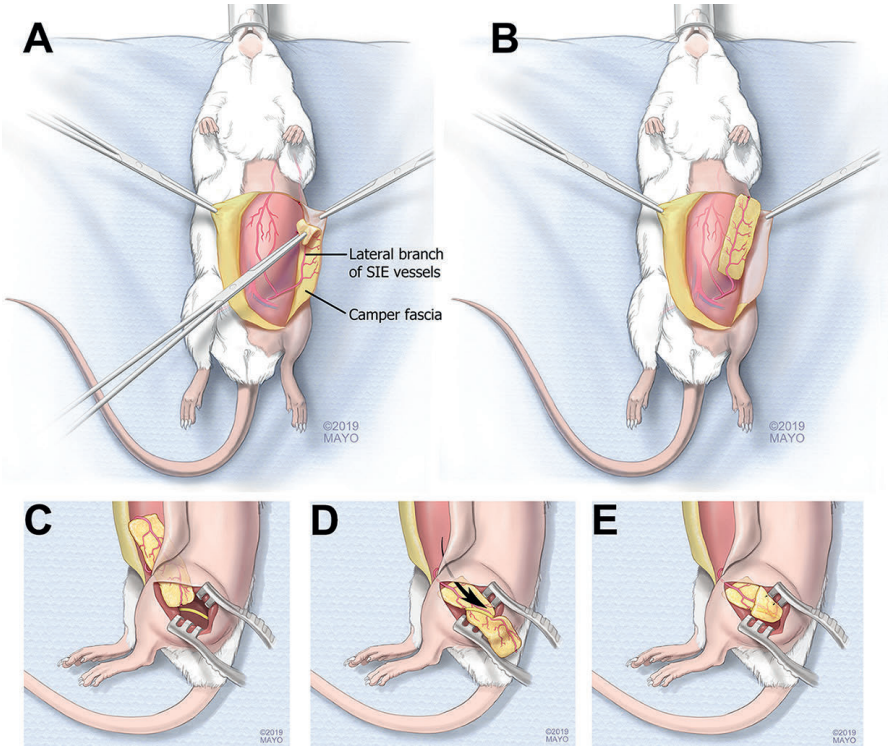

Figure 1. Schematic drawing of the superficial inferior epigastric fascia (SIEF) flap harvest. Depicted is the elevation of the flap from distal to proximal (A), providing a 4 x 3 cm adipofascial flap (B) based on the lateral branch of the superficial inferior (SIE) vessels. The SIEF flap was tunneled subcutaneously toward the nerve without vascular twisting of the epigastric trunk (C) and wrapped around the nerve graft reaching both anastomoses (D). The flap edges were trimmed if needed and two 10-0 nylon sutures were placed to secure the position of the SIEF flap (E). *With permission of the Mayo Foundation 2019 for Medical Education and Research. All rights reserved.*

Wounds were closed in layers, approximating muscle with two 5-0 absorbable interrupted sutures (5-0 Vicryl Rapide, Ethicon Inc., NJ, USA) and the skin was closed subcutaneously. After surgery, all animals were individually housed with *ad libitum* access to food and water.

Survival period evaluation

During the survival period, ultrasonography was used to measure cross-sectional scans of the tibial anterior muscle in the 16-week survival group and these were compared to the contralateral side, as previously described [27].

Non-survival evaluation

At 12 and 16 weeks, the rats underwent a non-survival surgical procedure. Anesthesia was induced by an intraperitoneal injection of ketamine (Ketaset, 80 mg/kg; Fort Dodge Animal Health, Iowa, USA) and xylazine (10mg/kg) and maintained by ketamine (40mg/kg) throughout the procedure. Rats were kept warm at 37°C on the heating pad during this experiment.

Ankle contracture angle - The ankle contracture angle was determined by measuring the angle between the anterior side of the tibia and the dorsal aspect of the paw with the ankle in maximal passive plantar flexion [5,28].

Electrophysiology (compound muscle action potential, CMAP) - The main sciatic nerve proximal to the graft was exposed and CMAP was measured using a miniature bipolar electrode connected to VikingQuest portable electromyelogram (Nicolet Biomedical, Madison, WI). A non-recurrent single stimulation was used with duration of 0.02milliseconds at an intensity level of 2.7mA. The maximal amplitude of the depolarization curve was recorded [5].

Maximum isometric tetanic force (ITF) - Maximum ITF measurements were performed as previously described [29]. Quantification of the ITF provides reproducible evaluation of functional recovery.

After rats were euthanized with Pentobarbital Sodium (Fatal Plus, 390 mg/mL, Vortech, MI, USA), tissues were collected. Tibial muscles were carefully dissected and weighed to evaluate muscle mass. Sciatic nerves and peroneal branches were harvested bilaterally and immediately stored in fixative.

Histology - Peroneal nerve samples were processed and subsequently infiltrated in 50%, 75% and finally 100% epoxy resin and polymerized at 65°C for 12-18 hours to allow cutting 1-µm transverse sections. Samples were stained on a warming plate with toluidine blue (Fisher Scientific, Pennsylvania, USA) for 2-2.5 minutes to evaluate histological outcomes. Nerve area, myelin thickness, axon count, total axon area were determined using NIS-Elements software (NIS-Elements BR 4.51.01), and the N-ratio (ratio between the myelinated fiber area and tissue cable area), indicating the number of axonal sprouting and maturation of the regenerating nerve [30-32], was calculated.

Immunofluorescence - Sciatic nerves were embedded in paraffin, sectioned transversely to a thickness of 5-µm and reacted with immunofluorescent markers CD34, staining vascular endothelial cells and extensively expressed on blood vessels [33], and protein gene product 9.5 (PGP 9.5), a pan-neuronal marker, staining both myelinated and unmyelinated nerve fibers [34], to quantify vascularity and axons, respectively. The CD34 primary antibody (1:2000, rabbit monoclonal, Abcam, UK) was diluted in background reducing diluent (Dako, Agilent Technologies Inc., CA, USA) and incubated for 60 minutes. PGP9.5-Alexa 568 conjugate (1:50, rabbit polyclonal, Dako), using the Zenon-Alexa 568-Rabbit IgG kit (Fisher Scientific) was incubated for 60 minutes, prior to staining with the appropriate secondary antibody (Alexa Goat-Anti-Rabbit 488, 1:200, Fisher Scientific). Counterstain was performed using Hoechst 33342 (Fisher Scientific) for 10 minutes, to stain cell nuclei. Slides were cover slipped and images were obtained using confocal microscope (Zeiss LSM 780, Carl Zeiss Surgical GmbH, Oberkochen, Germany). The total nerve area was defined by the combined area of tissues positively stained for any of PGP 9.5, CD34 and Hoechst. Density of axons and vascularity were normalized to the total nerve area and expressed in percentages.

A detailed description of evaluation measurements is provided (See Appendix).

Statistical analysis

Testing was performed on both the experimental left side and on the contralateral right side, and results were expressed as a percentage of the values of the left to the right side (L/R ratio in %), to diminish the effect of normal biologic variability between animals. Two-way analysis of variance (two-way ANOVA) for ultrasonography analysis and one-way ANOVA for all other outcomes, corrected by Bonferroni post-hoc testing was used for statistical investigation. Sample size (N=10) was calculated by our statistician based on power analysis to find significant differences in functional recovery between groups. All results were reported as the mean and standard error of the mean (SEM), with level of significance set at $\alpha \leq 0.05$.

RESULTS

Animal weight

Differences in sacrifice weight among groups at 12 weeks (P=0.33) and 16 weeks (P=0.23) were not significant.

SIEF group

All arteries were patent at both sacrifice time points and the flap was actively bleeding during dissection.

Wet muscle mass

At 12 weeks, the autograft muscle mass (66.6 ± 2.1% of the contralateral tibial muscle) was superior in comparison to allografts (57.6 ± 2.5%, P=0.01) and the SIEF group (56.0 ± 1.4%, P<0.01). At 16 weeks, autografts measured 70.8 ± 1.8%, allografts 65.9 ± 3.4% and SIEF 61.8 ± 1.5%. The autograft was only significantly superior to the SIEF group (P<0.05) (Figure 2).

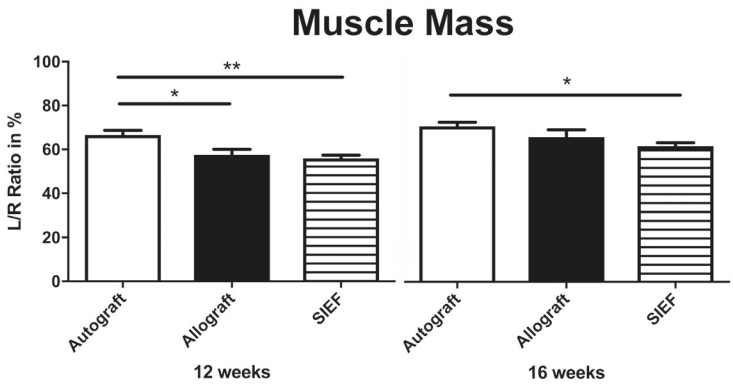

Figure 2. Wet muscle mass of the tibial anterior muscle at 12 and 16 weeks for the autograft, allograft and the allograft wrapped with a superficial inferior epigastric artery fascial (SIEF) flap. Results are expressed as a percentage of the experimental left side to the unoperated right side (L/R Ratio) and are given as the mean ± SEM. *Indicates significance at P<0.05, ** P<0.01). N=10 per group. SEM: Standard error of the mean.

Ankle contracture angle

At 12 weeks, the ankle contracture angle measured 81.6 ± 3.1% in the autograft group, 72.7 ± 1.2% in allografts and 75.8 ± 2.1% in SIEF. Autografts had a significant larger angle compared to allografts (P<0.05). At 16 weeks, all groups normalized to similar results with around 80% recovery.

Electrophysiology

Recovery of the CMAP at 12 weeks showed that autograft (57.2 ± 2.9%) was superior to allograft (35.9 ± 3.6%, P<0.001) and SIEF (46.5 ± 2.6%, P<0.05). This same pattern was seen at 16 weeks; the autograft (66.0 ± 3.3%) was superior to the allograft (45.9 ± 4.8%, P<0.01) and the SIEF (53.1 ± 3.1%, P=0.03, Figure 3).

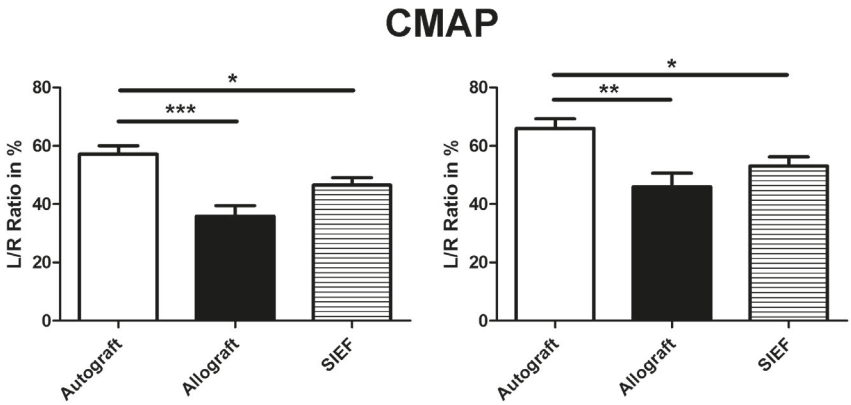

Figure 3. Compound muscle action potential (CMAP) at 12 and 16 weeks for the autograft, allograft and the allograft wrapped with a superficial inferior epigastric artery fascial (SIEF) flap. Results are expressed as a percentage of the experimental left side to the unoperated right side (L/R Ratio) and are given as the mean ± SEM. *Indicates significance at P<0.05, ** P<0.01, ***P<0.001). N=10 per group. SEM: Standard error of the mean.

Isometric tetanic force

At 12 weeks, the recovery of the tibial muscle ITF measurements was 54.7 ± 4.7% for the autograft, 33.3 ± 2.7% for allografts, and 52.4 ± 4.9% for SIEF (Figure 4). In both autografts and the SIEF group, ITF recovered significantly better compared to allografts alone (P<0.01 and P=0.01 respectively). SIEF and autograft ITF outcomes were not different (P=0.58). At 16 weeks, no significant differences were found between groups (autograft 77.3 ± 7.1%, allograft 74.0 ± 5.5%, SIEF 70.2 ± 3.5%, P=0.64).

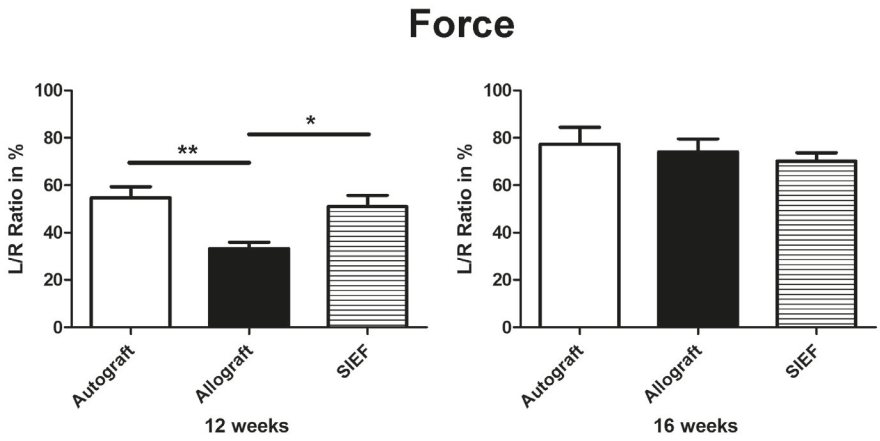

Figure 4. Isometric tetanic force testing (ITF) at 12 and 16 weeks for the autograft, allograft and the allograft wrapped with a superficial inferior epigastric artery fascial (SIEF) flap. Results are expressed as a percentage of the experimental left side to the unoperated right side (L/R Ratio) and are given as the mean ± SEM. *Indicates significance at P<0.05, ** P<0.01). N=10 per group. SEM: Standard error of the mean.

Muscle atrophy over time

A marked loss of tibial muscle cross-sectional area of 60% was found in week four in all groups, followed by an increase up to 16 weeks. At 16 weeks, recovery muscle loss was averaged at 64.8 ± 5.3% for autograft, 66.4 ± 7.3% for allograft and 72.0 ± 4.9% for SIEF (Figure 5). No significant differences were found among groups at the different time points.

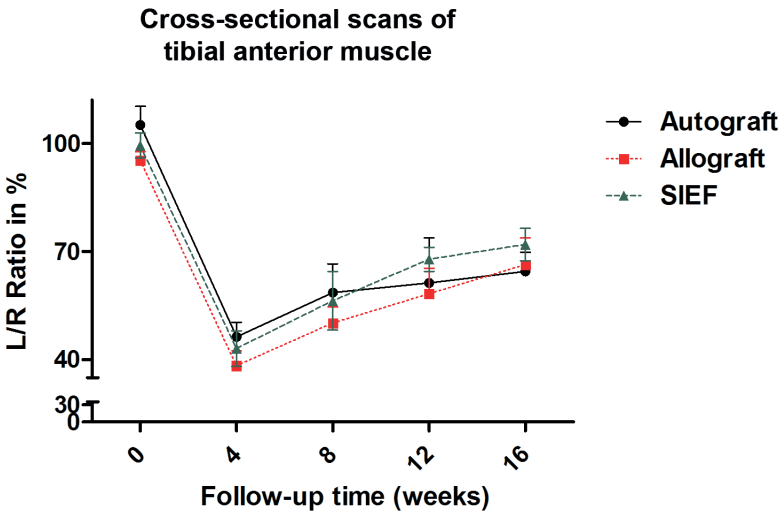

Figure 5. Cross-sectional scans of tibial anterior muscle determined by ultrasonography. Nerve defects repaired with autograft, allograft and the allograft wrapped with a superficial inferior epigastric fascial (SIEF) flap are followed up in time until sacrifice. Results are expressed as a percentage of the experimental left side to the unoperated right side (L/R Ratio) and are given as the mean ± SEM. N=10 per group.

Histological outcomes

No significant differences between groups were found with regard to axon area, axon count and myelin area. The nerve surface area was comparable between groups at 12 weeks. At 16 weeks, nerve area was significantly larger in autografts compared to allografts ($P<0.01$) and SIEF ($P<0.001$). Also, nerve area in allograft was larger compared to SIEF ($P<0.05$). At 12 weeks, the N-ratio showed inferiority of the allograft compared to the autograft and the SIEF group ($P<0.05$). At 16 weeks, no significant

differences were found between groups (Figure 6). An overview of representative nerve sections of the different groups has been provided (Figure 7).

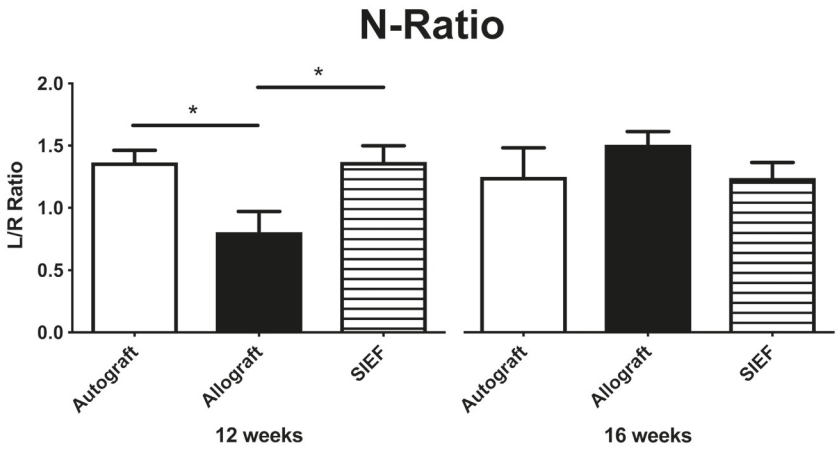

Figure 6. N-Ratio at 12 and 16 weeks for the autograft, allograft and the allograft wrapped with a superficial inferior epigastric artery fascial (SIEF) flap. The N-ratio at 12 weeks showed allograft to be inferior to autograft and allograft wrapped with the SIEF flap. At 16 weeks no differences were found between groups. Results are given as the mean ± SEM. *Indicates significance at P<0.05). N=10 per group. SEM: Standard error of the mean.

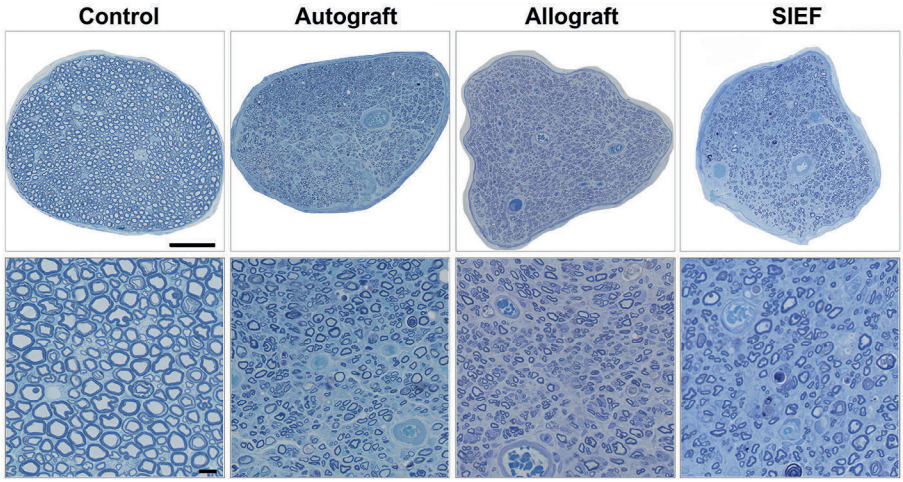

Figure 7. Micrographs of toluidine blue staining of control, autograft, allograft and the allograft wrapped with a superficial inferior epigastric artery fascial (SIEF) flap. Black scale bar is set at 100 nm for upper level photographs. The lower level photographs are taken at a higher magnification; this scale is set at 10 nm.

Evidence of nerve tissue and vascularity

Representative mid-distal graft nerve sections of the experimental groups including control are shown in Figure 8A-D. PGP.9.5 expression showed a consistent distribution throughout the nerve tissue in all groups, as seen in the micrographs. Quantification measured a similar expression between groups for both time points (Figure 8E). Vascularity, determined by CD34 staining, showed consistent distribution throughout the nerve tissue in control and autograft (Figure 8A,B). In allografts, CD34 was mostly expressed in the outer surface of the nerve sample and only little present in the core of the nerve. Wrapping with the SIEF flap resulted in an increased expression in the core of the allograft with consistent distribution throughout the nerve tissue (Figure 8C,D). Quantification measured significant inferiority in allograft compared to other groups at 12 weeks (8F, P<0.001). At 16 weeks, vascularity was significantly higher in the SIEF group compared to other groups (P<0.01 compared to control, P<0.05 compared to autograft, P<0.001 compared to allograft only).

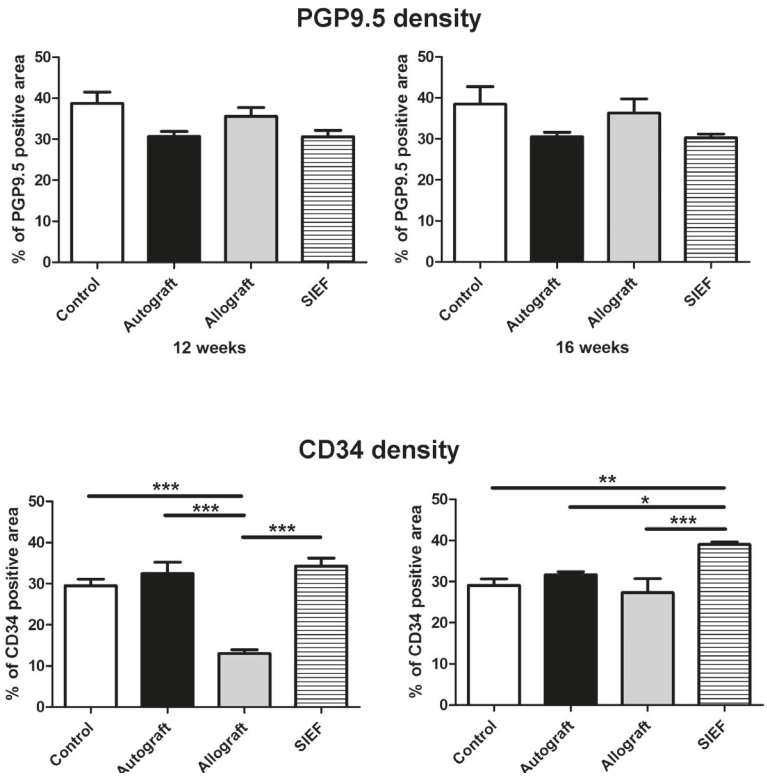

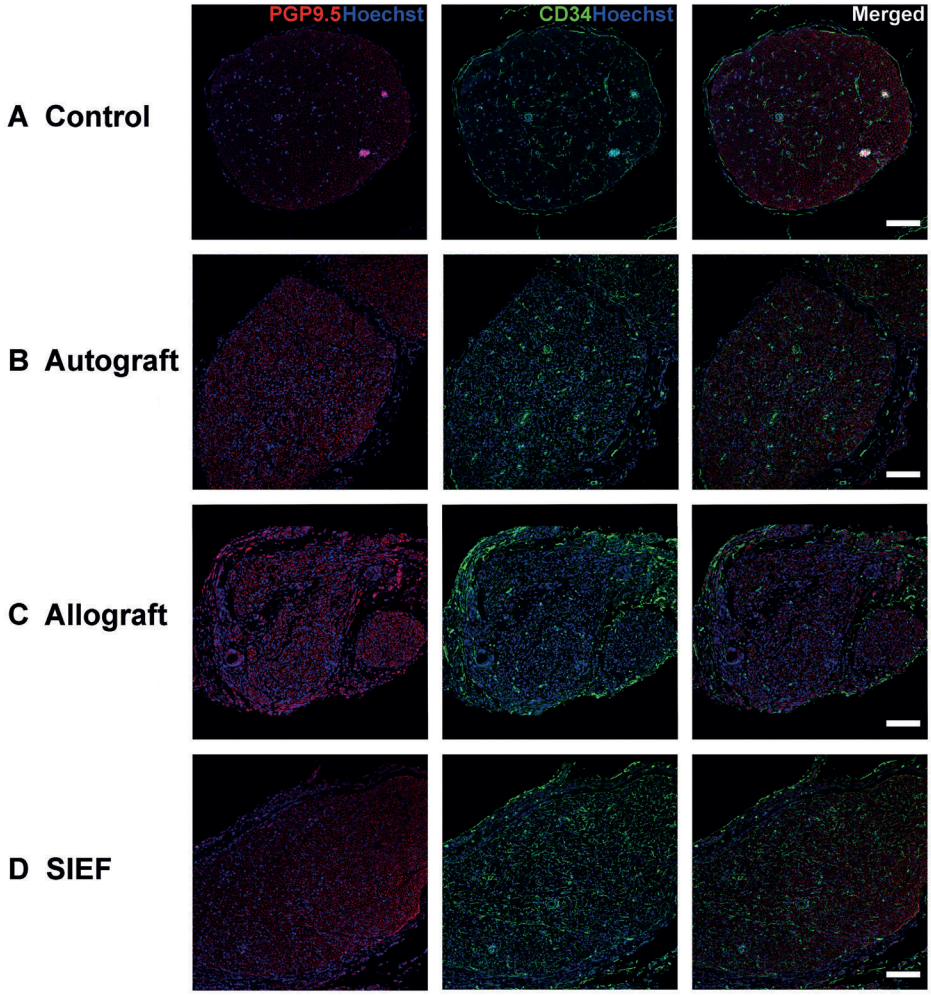

Figure 8. Evidence of nerve tissue and vascularity, determined by immunofluorescent staining of protein gene product 9.5 (PGP9.5) and CD34, respectively. Micrographs showing density in mid-distal graft sections from control nerve samples (A), autograft (B), allograft (C) and allograft wrapped with a superficial inferior epigastric artery fascial flap (SIEF, D) at 12 weeks. PGP.9.5 expression, staining both myelinated and unmyelinated nerve fibers showed a consistent distribution throughout the nerve tissue in all groups. Vascularity, determined by CD34 staining, showed consistent distribution throughout the nerve tissue in control and autograft (A,B). In allografts, CD34 was mostly expressed in the outer surface of the nerve sample and only little present in the core of the nerve. Wrapping with the SIEF flap resulted in an increased expression in the core of the allograft with consistent distribution throughout the nerve tissue (C,D). Density of axons and vascularity (normalized to the combined area of tissues positively stained for any of PGP9.5, CD34 and Hoechst) is shown on the left page, respectively, expressed in percentages. Error bars denote mean ± SEM. *Indicates significance at P<0.05, ** P<0.01, *** P<0.001). Scale bars are set at 100 μm. SEM: Standard error of the mean.

DISCUSSION

Interest in the role of vascularity in nerve regeneration has been longstanding [35]. In the past, experimental animal models have investigated the effects of vascular growth factors such as vascular endothelial growth factor (VEGF) [36], or sought to measure the effect of microsurgical repair of nerve graft with vascular pedicles (e.g. VNG) on nerve regeneration [20,22,23,37,38]. VEGF contributes to angiogenesis via several mechanisms and has also been suggested to influence nerve regeneration [36,39] by stimulating outgrowth of Schwann cells, the original facilitators of nerve regeneration [40,41]. These cited studies have reported conflicting results and are difficult to compare. One previous study evaluated functional recovery in rats and found improved sciatic functional index in VNGs at eight and 12 weeks [20]. This is in line with our study, which showed increased muscle force when allografts were wrapped within an adipofascial flap when compared to allografts alone at 12 weeks. Because of its reproducibility, ITF has become a widely used standardized technique to assess mechanical function and the contractile properties of muscles [42,43]. This study and others have demonstrated that ITF is a reliable technique in determining the degree of functional recovery of a reinnervated muscle as a direct measure of reinnervation [5,44-46].

Electrophysiological outcomes trended to be superior in the allograft wrapped within the SIEF, compared to nerve allograft alone. As CMAP is greatly affected by factors such as changes in temperature and electrode location, there is greater variability than ITF data [31]. Although others have reported VNGs to have significantly higher nerve conduction velocity than non-VNGs [20], this could not be corroborated in our study.

Denervated tibial muscles were characterized by differences in muscle mass and ultrasound measurements. Serial cross-sectional muscle scans *in vivo* provided insights into muscle atrophy and reinnervation over time, but was not sufficiently sensitive enough to determine small differences between groups in our rat model. Although our results did not show a significant difference in muscle mass between allograft and SIEF group, wrapping with the SIEF flap provided a significant, large improvement in muscle force at 12 weeks. Muscle mass includes enlarging but non-contractile muscle fibers, resulting in possible indistinguishable differences in innervated and non-innervated muscles [32,47,48]. It is easy to interpret, however, doubtful to be useful as an evaluation

tool of functional recovery. Muscle force may therefore be a parameter that expresses functional recovery better than muscle mass or cross-sectional area [32].

Histological parameters did not result in differences between groups with respect to axon count, axon area and myelin area. A low N-ratio, seen in allografts at 12 weeks, could be indicative of a relatively larger amount of fibrous tissue [49], compared to SIEF and autografts. This indicates that provision of vascularization to nerve allograft wound bed may decrease fibrosis of the nerve. This is clearly visualized with the expression of CD34 that indicated vascularity in allografts predominantly in the outer layer, while the SIEF flap enhanced vascularity with abundant distribution throughout the nerve graft, reaching the core of the nerve. As few experimental studies have evaluated VNGs or addition of adipofascial flaps [15,20], it remains difficult to compare findings. A previous study has found that at three weeks post-operatively, fat graft wrapping around the nerve coaptation increased lymphocyte infiltration rates and macrophage migration; processes that are involved in the early neural regeneration period [15]. This previous study did not find improved neovascularization after fat graft wrapping [15], possibly due to the chosen end-point and limitations in evaluating vascularity. Despite this study, little has been reported on the effect of adipose tissue placed around nerve reconstructions.

It is assumed that a pedicled adipofascial flap containing adipose tissue and a vascular bundle improves revascularization of the nerve allografts through excreted angiogenic factors and nutrition, provided by the vascular bundle and stem cells in the adipose tissue, while preventing fibrosis and core necrosis [10,50,51]. Blood vessels have been found to precede neural regeneration and stimulate injured axons and non-neuronal cells to produce a supportive microenvironment after nerve injury [35,52,53]. Moreover, capillary changes as well as Schwann cell migration suggest axon growth [54], explaining improved early functional recovery. Although surgical angiogenesis to the allograft continued increasing vascularity in the graft at 16 weeks, functional outcomes did not improve at this time point. This raises the possibility of a ceiling effect of vascularity on nerve regeneration. Addition of other factors combined with surgical angiogenesis, such as stem cells, may be another potential strategy to further improve regeneration. The importance of stem cells relies on their ability to secrete various growth factors, such as neurotrophic factors to stimulate myelin formation, and its potency is emphasized to be influenced by its microenvironment (i.e. paracrine properties) [55]. Adipose tissue,

rich in growth factors and stem cells, may be combined with stem cells delivered to the nerve allograft to achieve a higher state of therapeutic potential[56,57], potentially resulting in synergistic mechanisms to enhance nerve regeneration.

In this study, surgical angiogenesis to nerve allograft produced statistical improvement in a number of measured variables at 12 weeks. These differences were less apparent at 16 weeks, consistent with the well-known superlative nerve regenerative capacity of the rat. It could be speculated that earlier time points prior to 12 weeks, would be ideal in future studies as interventions that result in improved and more rapid nerve regeneration in the logistical growth phase are potentially clinically relevant. This can be ascertained from the recent study by Tang and colleagues, whose ITF outcomes at 16 weeks are in line with the results of this study for all groups [46]. The effect of surgical angiogenesis to nerve allograft could be evaluated at earlier time points or in a larger nerve gap model to overcome these limitations [58]. Additionally, future research may further investigate the impact of fibrosis in the nerve graft to elucidate the suppression of fibrosis during axonal regeneration or the combined effect of surgical angiogenesis and stem cells to improve regeneration.

CONCLUSIONS

Wrapping of processed nerve allografts with a pedicled adipofascial flap to provide surgical angiogenesis increases vascularity of the allograft, as well as improves early muscle force recovery when compared to allografts alone. Although we still do not have a nerve graft substitute that performs as well as autograft nerve, these data support the use of surgical angiogenesis as part of the equation required to improve processed nerve allograft outcomes.

Disclosure

The authors have no financial interests to disclose.

Acknowledgments

We would like to thank Jim Postier for the artwork of Figure 1.

REFERENCES

1. Ciaramitaro P, Mondelli M, Logullo F, et al. Traumatic peripheral nerve injuries: epidemiological findings, neuropathic pain and quality of life in 158 patients. *J Peripher Nerv Syst.* 2010;15(2):120-127.
2. Millesi H. Forty-two years of peripheral nerve surgery. *Microsurgery.* 1993;14(4):228-233.
3. Terzis J, Faibisoff B, Williams B. The nerve gap: suture under tension vs. graft. *Plast Reconstr Surg.* 1975;56(2):166-170.
4. Sunderland S. Factors influencing the course of regeneration and the quality of the recovery after nerve suture. *Brain.* 1952;75(1):19-54.
5. Giusti G, Willems WF, Kremer T, Friedrich PF, Bishop AT, Shin AY. Return of motor function after segmental nerve loss in a rat model: comparison of autogenous nerve graft, collagen conduit, and processed allograft (AxoGen). *J Bone Joint Surg Am.* 2012;94(5):410-417.
6. Mackinnon SE, Hudson AR, Falk RE, Hunter DA. The nerve allograft response--an experimental model in the rat. *Ann Plast Surg.* 1985;14(4):334-339.
7. Millesi H. Progress in peripheral nerve reconstruction. *World J Surg.* 1990;14(6):733-747.
8. Platt H. On the results of bridging gaps in injured nerve trunks by autogenous fascial tubulization and autogenous nerve grafts. . *Br J Surg.* 1919;7:384.
9. D'Arpa S. Vascularized nerve "grafts": just a graft or a worthwhile procedure? *Plast Aesthet Res.* 2016;2(4):183-192.
10. Tarlov IM EJ. Nerve grafts: The importance of an adequate blood supply. *J Neurosurg.* 1945;2:49-71.
11. Chalfoun C, Scholz T, Cole MD, Steward E, Vanderkam V, Evans GR. Primary nerve grafting: A study of revascularization. *Microsurgery.* 2003;23(1):60-65.
12. Terzis JaS, KL. Structure, function, and reconstruction. Hampton Press, Norfolk, VA; 1990: 137–139.
13. Walocko FM, Khouri RK, Jr., Urbanchek MG, Levi B, Cederna PS. The potential roles for adipose tissue in peripheral nerve regeneration. *Microsurgery.* 2016;36(1):81-88.
14. Daly W, Yao L, Zeugolis D, Windebank A, Pandit A. A biomaterials approach to peripheral nerve regeneration: bridging the peripheral nerve gap and enhancing functional recovery. *J R Soc Interface.* 2012;9(67):202-221.
15. Ersen B, Kahveci, R. The Effect of Fat Graft Wrapping on Nerve Regeneration in Early Nerve Regeneration An Experimental Study. *Turkiye Klinikleri Journal of Medical Sciences.* 2018;38(4):303-308.
16. Kolar MK, Kingham PJ. Regenerative effects of adipose-tissue-derived stem cells for treatment of peripheral nerve injuries. *Biochem Soc Trans.* 2014;42(3):697-701.
17. Lin CS, Xin ZC, Deng CH, Ning H, Lin G, Lue TF. Defining adipose tissue-derived stem cells in tissue and in culture. *Histol Histopathol.* 2010;25(6):807-815.
18. Zuk PA. The adipose-derived stem cell: looking back and looking ahead. *Mol Biol Cell.* 2010;21(11):1783-1787.

19. Saffari TM, Bishop AT, Shin AY. The Superficial Inferior Epigastric Artery Fascia Flap in Rats. *J Reconstr Microsurg Open.* 2020;5:e7-e14.
20. Kanaya F, Firrell J, Tsai TM, Breidenbach WC. Functional results of vascularized versus nonvascularized nerve grafting. *Plast Reconstr Surg.* 1992;89(5):924-930.
21. Karcher H, Kleinert R. Regeneration in vascularized and free nerve grafts. A comparative morphological study in rats. *J Maxillofac Surg.* 1986;14(6):341-343.
22. Restrepo Y, Merle M, Michon J, Folliguet B, Barrat E. Free vascularized nerve grafts: an experimental study in the rabbit. *Microsurgery.* 1985;6(2):78-84.
23. Shibata M, Tsai TM, Firrell J, Breidenbach WC. Experimental comparison of vascularized and nonvascularized nerve grafting. *J Hand Surg Am.* 1988;13(3):358-365.
24. Hudson TW, Liu SY, Schmidt CE. Engineering an improved acellular nerve graft via optimized chemical processing. *Tissue Eng.* 2004;10(9-10):1346-1358.
25. Kumta S, Yip K, Roy N, Lee SK, Leung PC. Revascularisation of bone allografts following vascular bundle implantation: an experimental study in rats. *Arch Orthop Trauma Surg.* 1996;115(3-4):206-210.
26. Hundepool CA, Nijhuis TH, Kotsougiani D, Friedrich PF, Bishop AT, Shin AY. Optimizing decellularization techniques to create a new nerve allograft: an in vitro study using rodent nerve segments. *Neurosurg Focus.* 2017;42(3):E4.
27. Hundepool CA, Nijhuis TH, Rbia N, Bulstra LF, Selles RW, Hovius SE. Noninvasive Ultrasound of the Tibial Muscle for Longitudinal Analysis of Nerve Regeneration in Rats. *Plast Reconstr Surg.* 2015;136(5):633e-639e.
28. Lin FM, Pan YC, Hom C, Sabbahi M, Shenaq S. Ankle stance angle: a functional index for the evaluation of sciatic nerve recovery after complete transection. *J Reconstr Microsurg.* 1996;12(3):173-177.
29. Shin RH, Vathana T, Giessler GA, Friedrich PF, Bishop AT, Shin AY. Isometric tetanic force measurement method of the tibialis anterior in the rat. *Microsurgery.* 2008;28(6):452-457.
30. Itoh S, Takakuda K, Ichinose S, Kikuchi M, Schinomiya K. A study of induction of nerve regeneration using bioabsorbable tubes. *J Reconstr Microsurg.* 2001;17(2):115-123.
31. S. Saffari TMS, A.M. Moore, A.Y. Shin. Peripheral Nerve Basic Science Research – What is important for hand surgeons to know? *J Hand Surg Am.* 2021.
32. Vleggeert-Lankamp CL. The role of evaluation methods in the assessment of peripheral nerve regeneration through synthetic conduits: a systematic review. Laboratory investigation. *J Neurosurg.* 2007;107(6):1168-1189.
33. Fina L, Molgaard HV, Robertson D, et al. Expression of the CD34 gene in vascular endothelial cells. *Blood.* 1990;75(12):2417-2426.
34. Sun Y, Zhu L, Huang X, Zhou C, Zhang X. Immunohistochemical localization of nerve fibers in the pseudocapsule of fibroids. *Eur J Histochem.* 2014;58(2):2249.
35. Saffari TM, Bedar M, Hundepool CA, Bishop AT, Shin AY. The role of vascularization in nerve regeneration of nerve graft. *Neural Regen Res.* 2020;15(9):1573-1579.

36. Lee JY, Giusti G, Friedrich PF, Bishop AT, Shin AY. Effect of Vascular Endothelial Growth Factor Administration on Nerve Regeneration after Autologous Nerve Grafting. *J Reconstr Microsurg.* 2016;32(3):183-188.
37. McCullough CJ, Gagey O, Higginson DW, Sandin BM, Crow JC, Sebille A. Axon regeneration and vascularisation of nerve grafts. An experimental study. *J Hand Surg Br.* 1984;9(3):323-327.
38. Seckel BR, Ryan SE, Simons JE, Gagne RG, Watkins E, Jr. Vascularized versus nonvascularized nerve grafts: an experimental structural comparison. *Plast Reconstr Surg.* 1986;78(2):211-220.
39. Dvorak HF, Brown LF, Detmar M, Dvorak AM. Vascular permeability factor/vascular endothelial growth factor, microvascular hyperpermeability, and angiogenesis. *Am J Pathol.* 1995;146(5):1029-1039.
40. Sondell M, Lundborg G, Kanje M. Vascular endothelial growth factor stimulates Schwann cell invasion and neovascularization of acellular nerve grafts. *Brain Res.* 1999;846(2):219-228.
41. Webber CA, Christie KJ, Cheng C, et al. Schwann cells direct peripheral nerve regeneration through the Netrin-1 receptors, DCC and Unc5H2. *Glia.* 2011;59(10):1503-1517.
42. Swanson AN, Wolfe SW, Khazzam M, Feinberg J, Ehteshami J, Doty S. Comparison of neurotization versus nerve repair in an animal model of chronically denervated muscle. *J Hand Surg Am.* 2008;33(7):1093-1099.
43. Yoshimura K, Asato H, Jejurikar SS, Cederna PS, Urbanchek MG, Kuzon WM, Jr. The effect of two episodes of denervation and reinnervation on skeletal muscle contractile function. *Plast Reconstr Surg.* 2002;109(1):212-219.
44. Hundepool CA, Bulstra LF, Kotsougiani D, et al. Comparable functional motor outcomes after repair of peripheral nerve injury with an elastase-processed allograft in a rat sciatic nerve model. *Microsurgery.* 2018;38(7):772-779.
45. Sobotka S, Mu L. Characteristics of tetanic force produced by the sternomastoid muscle of the rat. *J Biomed Biotechnol.* 2010;2010:194984.
46. Tang P, Whiteman DR, Voigt C, Miller MC, Kim H. No Difference in Outcomes Detected Between Decellular Nerve Allograft and Cable Autograft in Rat Sciatic Nerve Defects. *J Bone Joint Surg Am.* 2019;101(10):e42.
47. Buffelli M, Pasino E, Cangiano A. Paralysis of rat skeletal muscle equally affects contractile properties as does permanent denervation. *J Muscle Res Cell Motil.* 1997;18(6):683-695.
48. Dow DE, Cederna PS, Hassett CA, Kostrominova TY, Faulkner JA, Dennis RG. Number of contractions to maintain mass and force of a denervated rat muscle. *Muscle Nerve.* 2004;30(1):77-86.
49. den Dunnen WF, van der Lei B, Schakenraad JM, et al. Poly(DL-lactide-epsilon-caprolactone) nerve guides perform better than autologous nerve grafts. *Microsurgery.* 1996;17(7):348-357.
50. Hobson MI, Brown R, Green CJ, Terenghi G. Inter-relationships between angiogenesis and nerve regeneration: a histochemical study. *Br J Plast Surg.* 1997;50(2):125-131.
51. Saffari TM, Mathot F, Friedrich PF, Bishop AT, Shin AY. Revascularization patterns of nerve allografts in a rat sciatic nerve defect model. *J Plast Reconstr Aesthet Surg.* 2020;73(3):460-468.
52. Caillaud M, Richard L, Vallat JM, Desmouliere A, Billet F. Peripheral nerve regeneration and intraneural revascularization. *Neural Regen Res.* 2019;14(1):24-33.

53. Hobson MI, Green CJ, Terenghi G. VEGF enhances intraneural angiogenesis and improves nerve regeneration after axotomy. *J Anat.* 2000;197 Pt 4:591-605.
54. Muangsanit P, Shipley RJ, Phillips JB. Vascularization Strategies for Peripheral Nerve Tissue Engineering. *Anat Rec (Hoboken).* 2018;301(10):1657-1667.
55. Jiang L, Jones S, Jia X. Stem Cell Transplantation for Peripheral Nerve Regeneration: Current Options and Opportunities. *Int J Mol Sci.* 2017;18(1).
56. Kamat P, Frueh FS, McLuckie M, et al. Adipose tissue and the vascularization of biomaterials: stem cells, microvascular fragments and nanofat-a review. *Cytotherapy.* 2020.
57. Mathot F, Shin AY, Van Wijnen AJ. Targeted stimulation of MSCs in peripheral nerve repair. *Gene.* 2019;710:17-23.
58. Myckatyn TM, Mackinnon SE. A review of research endeavors to optimize peripheral nerve reconstruction. *Neurol Res.* 2004;26(2):124-138.

APPENDIX - MATERIALS AND METHODS

All outcomes were performed bilaterally and compared to the non-operated, contralateral side.

Ultrasonography - was performed using a GE Vivid 7 Ultrasound system (General Electric, Fairfield, CT, USA) and the cross-sectional area (X-C area) was determined bilaterally using Adobe Photoshop CC 2018 (Adobe Systems Incorporated, San Jose, CA, USA) [1].

Maximum ITF measurements - were performed bilaterally as previously described with optimization of preload [2]. In short, the tendon of the tibial anterior muscle was exposed via a second skin incision and incised at the insertion. The leg was fixed to a platform with two Kirschner wires and the tendon was attached to the force transducer. A bipolar stimulator was used to generate the stimulus to the peroneal nerve branch and acquire a signal which was processed using LabVIEW (National Instruments, Austin, Texas). The muscle was kept hydrated with warm 0.9% NaCl during the experiment.

Histological outcomes - A 3-mm segment of both peroneal nerves of all rats (N=10/group/time point), 5-mm distal to the graft, was harvested and immediately stored in Trumps solution. Samples were processed with 0.1M Phosphate Buffer, 1% Osmium tetroxide in buffer, graded series of alcohols and acetone. Samples were subsequently infiltrated in a 50%, 75% and finally 100% epoxy resin and polymerized at 65°C for 12-18 hours. Samples were cut into 1-µm sections, placed on slides, stained with toluidine blue (Fisher Scientific, Pittsburgh, Pennsylvania, USA) for 2-2.5 minutes and coverslipped.

Immunofluorescent outcomes - Sciatic nerve graft samples and the contralateral sciatic nerves were harvested, fixed in 10% formalin for 48 hours and stored in 70% ethanol, until embedding in paraffin. Samples were sectioned transversely to a thickness of 5-µm and retrieved for 20 minutes using Epitope Retrieval2 (EDTA based; Leica). Samples were incubated in 10% Normal Goat Block (Fisher Scientific, Pittsburgh, Pennsylvania, USA) for 30 minutes and reacted with immunofluorescent markers CD34 [3] and protein gene product 9.5 (PGP 9.5) [4], to quantify vascularity and nerve fibers, respectively. The CD34 primary antibody (rabbit monoclonal; Abcam, UK) was diluted

to 1:2000 in Background Reducing Diluent (BRD, Dako, CA, USA) and incubated for 60 minutes. Secondary antibody used for CD34 visualization was Alexa Goat-Anti-Rabbit 488 (Fisher Scientific), diluted at 1:200 in BRD; slides were incubated for 60 minutes.

This was followed by PGP9.5-Alexa 568 conjugate diluted in BRD at 1:50, incubated for 60 minutes. PGP9.5 primary antibody (rabbit polyclonal; Dako) was conjugated to Alexa 568 using the Zenon-Alexa 568-Rabbit IgG kit (Fisher Scientific) 15 minutes prior to incubation. Counterstain was performed using Hoechst 33342 (Fisher Scientific) for 10 minutes, to stain cell nuclei. Slides were coverslipped with an aqueous based ProLong Gold antifade mounting media (Fisher Scientific).

Images of the stained slides were obtained using a fluorescence laser confocal microscope (Zeiss LSM 780, Carl Zeiss Surgical GmbH, Oberkochen, Germany). The total nerve area was calculated by the total combined area of tissues positively stained for any of PGP 9.5, CD34 and Hoechst (staining cell nuclei) per nerve section. Images (N=8/group/time point) were analyzed using ImageJ software.

REFERENCES

1. Hundepool CA, Nijhuis TH, Rbia N, Bulstra LF, Selles RW, Hovius SE. Noninvasive Ultrasound of the Tibial Muscle for Longitudinal Analysis of Nerve Regeneration in Rats. *Plast Reconstr Surg.* 2015;136(5):633e-639e.
2. Shin RH, Vathana T, Giessler GA, Friedrich PF, Bishop AT, Shin AY. Isometric tetanic force measurement method of the tibialis anterior in the rat. *Microsurgery.* 2008;28(6):452-457.
3. Fina L, Molgaard HV, Robertson D, et al. Expression of the CD34 gene in vascular endothelial cells. *Blood.* 1990;75(12):2417-2426.
4. Sun Y, Zhu L, Huang X, Zhou C, Zhang X. Immunohistochemical localization of nerve fibers in the pseudocapsule of fibroids. *Eur J Histochem.* 2014;58(2):2249.

PART II

The Contribution of Angiogenesis and Stem Cells in Nerve Regeneration

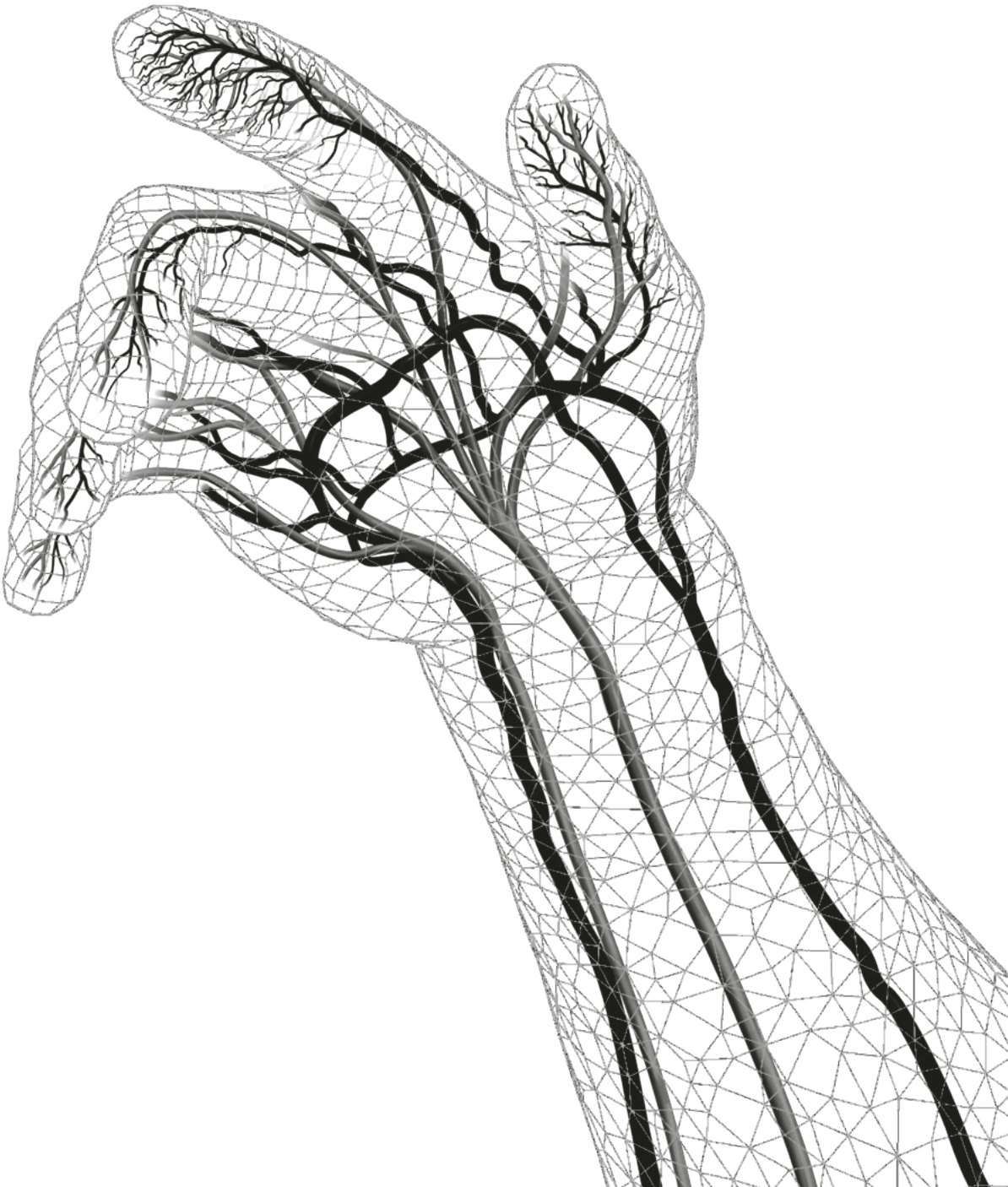

CHAPTER **EIGHT**

The Interaction of Stem Cells and Vascularity in Peripheral Nerve Regeneration

Sara Saffari[1,2]
Tiam M. Saffari[1,2]
Dietmar J.O. Ulrich[2]
Steven E.R. Hovius[2]
Alexander Y. Shin[1]

Affiliations

[1]Division of Hand and Microvascular Surgery, Department of Orthopedic Surgery, Mayo Clinic, Rochester, MN, USA

[2]Department of Plastic and Reconstructive Surgery, Radboud University Medical Center, Nijmegen, the Netherlands

Neural Regeneration Research. 2021;16(8):1510-1517.

ABSTRACT

The degree of nerve regeneration after peripheral nerve injury can be altered by the microenvironment at the site of injury. Stem cells and vascularity are postulated to be a part of a complex pathway that enhances peripheral nerve regeneration, however, their interaction remains unexplored. This review aims to summarize current knowledge on this interaction, including various mechanisms through which trophic factors are promoted by stem cells and angiogenesis. Angiogenesis after nerve injury is stimulated by hypoxia, mediated by vascular endothelial growth factor, resulting in the growth of pre-existing vessels into new areas. Modulation of distinct signaling pathways in stem cells can promote angiogenesis by the secretion of various angiogenic factors. Simultaneously, the importance of stem cells in peripheral nerve regeneration relies on their ability to promote myelin formation and their capacity to be influenced by the microenvironment to differentiate into Schwann-like cells. Stem cells can be acquired through various sources that correlate to their differentiation potential, including embryonic stem cells, neural stem cells, and mesenchymal stem cells. Each source of stem cells serves its particular differentiation potential and properties associated with the promotion of revascularization and nerve regeneration. Exosomes are a subtype of extracellular vesicles released from cell types and play an important role in cell-to-cell communication. Exosomes hold promise for future transplantation applications, as these vesicles contain fewer membrane-bound proteins, resulting in lower immunogenicity. This review presents pre-clinical and clinical studies that focus on selecting the ideal type of stem cell and optimizing stem cell delivery methods for potential translation to clinical practice. Future studies integrating stem cell-based therapies with the promotion of angiogenesis may elucidate the synergistic pathways and ultimately enhance nerve regeneration.

INTRODUCTION

Patients with peripheral nerve injuries (PNI) can face severe disability resulting in sensory loss, motor deficits, and neuropathic pain. These deficits may result in a devastating impact on a patient's quality of life [1]. Despite advancements in microsurgical techniques and basic and translational research, surgical reconstruction of PNIs continues to have unsatisfactory clinical outcomes, particularly for reconstructions of major mixed motor and sensory nerves [2,3]. When end-to-end tension-free neurorrhaphy is not possible, the current gold standard remains reconstruction with autologous cabled nerve graft interposition after excision of the injured nerve stumps. Harvest of autologous nerves faces associated drawbacks, such as permanent donor site morbidity with loss of sensation in the distribution of the harvested nerve [4-7]. Attempts to create a commercially available nerve graft substitute have resulted in a variety of bioabsorbable synthetic conduits or decellularized human allograft nerves. Their clinical efficacy has yet to equal or surpass autologous nerve grafts, especially for defects greater than three centimeters [8].

Engineering of a synthetic substrate for nerve regeneration to mimic the ultrastructure of autologous nerve has been extremely challenging. The use of human allograft fresh nerves for reconstruction requires systemic immunosuppression to prevent graft rejection and is associated with side effects, such as severe opportunistic infections [9,10]. An alternative to fresh human allograft nerves or to engineering a nerve graft is to decellularize and process human allograft nerve. Decellularized allografts serve as a temporary scaffold for regenerating nerve fibers and do not require systemic immunosuppression due to diminished graft rejection potential. Decellularized allografts provide the essential ultrastructural elements and may be pretreated with irradiation, cold preservation, trophic factors, or seeded with Schwann cells or stem cells, to advance outcomes after peripheral nerve reconstruction [4,11]. Stem cell-based therapy may offer a suitable treatment with several regenerative benefits to restore neuronal function, including supporting remyelination and revascularization of the affected organ [12]. Specifically, stem cells that have been differentiated into Schwann-like cells, mimicking the function of the original facilitators of axonal regeneration, may enhance neuron survival to improve functional outcomes [4,13]. Growth factors secreted by stem cells may enhance angiogenesis, the sprouting of new capillaries from preexisting ones, to promote revascularization [14-17].

The exact interaction between stem cell and vascularity remains unexplored and is postulated to be part of a complex pathway that enhances peripheral nerve regeneration. This review will provide an in-depth perspective of currently available stem cell-based therapy applications in PNIs and discusses the interaction between stem cells and vascularity in peripheral nerve regeneration. Furthermore, sources of stem cells, methods of delivery to the injury site, relevant pre-clinical studies and clinical trials, and future applications will be reviewed.

Search strategy and selection criteria

Literature research was performed using PubMed, Web of Science, MEDLINE and Google Scholar databases, using the following search terms: angiogenesis, vascularity, nerve regeneration, nerve transplantation, nerve graft, neural stem cells, mesenchymal stem cells, exosomes and various combinations of the above terms. Available English studies discussing stem cells and vascularity in peripheral nerve injuries in both animals and humans were included until July 2020.

Interaction of stem cells, vascularity and nerve regeneration

The interaction of stem cells, vascularity, and axon regeneration is complex (Figure 1). The paracrine property of stem cells is much broader than previously was appreciated. When stimulated by surrounding tissues, stem cells have the ability to affect vascularity via cell-to-cell communication, differentiation, and release of angiogenic factors, such as vascular endothelial growth factor (VEGF) [18-20]. On the other hand, stem cells demonstrate the capacity to stimulate the upregulation of neurotrophic factors to enhance nerve regeneration as a response to nerve injury [17,19,21,22]. After nerve injury, angiogenesis is stimulated by hypoxia, usually mediated by VEGF, resulting in the growth of pre-existing vessels into new areas. It is postulated that these newly modeled vessel tracks precede the repair of damaged nerves [14,16,23,24]. The therapeutic potency of stem cells in nerve regeneration and vascularity is influenced by its microenvironment. The interaction of the environment, stem cells, and vascularity with respect to peripheral nerve regeneration will be discussed per causal order below.

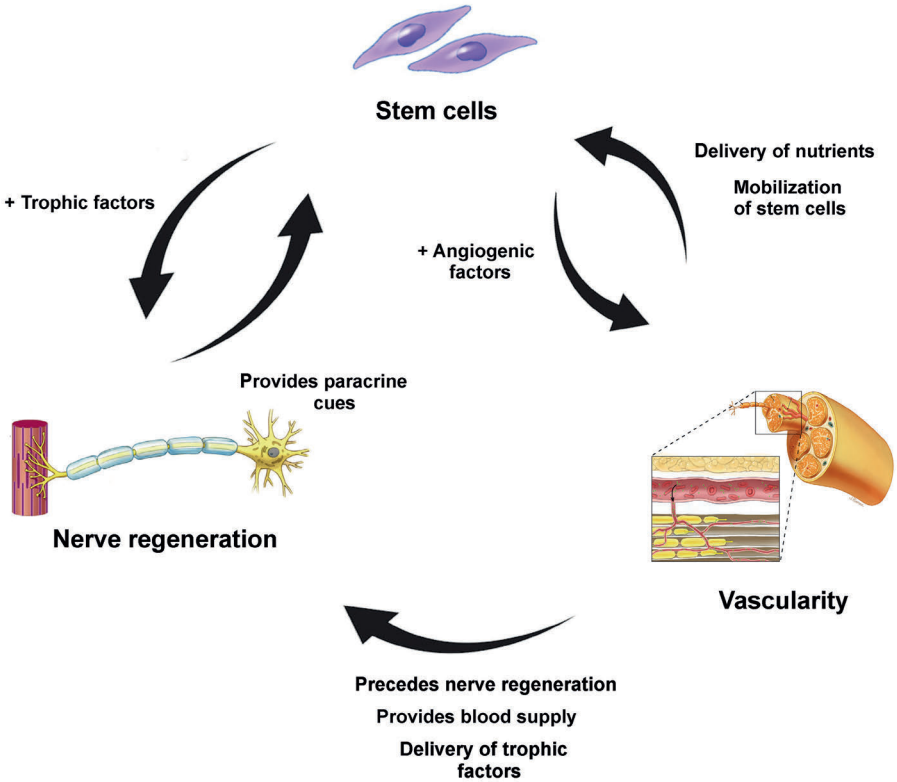

Figure 1. Schematic drawing of interaction between stem cells, vascularity, and nerve regeneration. After a nerve injury, paracrine cues are provided to stem cells to produce trophic and angiogenic factors that enhance nerve regeneration and angiogenesis, respectively. Blood supply mobilizes stem cells and delivers nutrients and trophic factors to the site of injury to improve nerve regeneration. Blood supply is not only important for the survivability of stem cells but also precedes nerve regeneration after nerve trauma. *Copyrighted and used with permission of the Mayo Foundation for Medical Education and Research; all rights reserved.*

Stem cells and revascularization of nerve

Blood vessels have been postulated to be a systemic source of stem cells in regenerating hematopoietic cells secondary to their vascular origin. Embryologically, hematopoietic stem cells emerge closely in the vicinity of vascular endothelial cells [25,26]. The subendothelial zone, located in the tunica intima of blood vessels, has been specifically implicated as a source of endothelial progenitor cells (EPC) [27]. Evidence has demonstrated that other structural layers also serve as niches for stem cells that are

mostly quiescent and are activated in response to injury [28]. The close vicinity of these progenitor cells to the circulation allows for their mobilization to the region of interest to facilitate a number of processes including tissue regeneration [29]. Differentiation of mesenchymal stem cells (MSC) into Schwann-like cells enhances the secretion of various angiogenic factors, including angiopoietin-1 and VEGF-A, resulting in enhanced angiogenic potency and neurite outgrowth [17,30]. MSCs differentiated into Schwann-like cells specifically, have been shown to increase revascularization of nerve allografts after *in vivo* reconstruction of sciatic nerve defects in rats [31].

Revascularization of nerve and neural regeneration

Following PNI, axons and myelin degenerate distally to the injury site by interactions of Schwann cells and macrophages in a process known as Wallerian degeneration [32,33]. During regeneration, blood vessels precede axonal extension and serve as tracks for Schwann cells to migrate and guide axonal growth, suggesting an interdependence between neurite outgrowth and vascularity [34,35]. VEGF is central to the control of angiogenesis and critical in the process of maturation and stabilization of vessels [36,37]. In addition to stimulating the outgrowth of Schwann cells and blood vessels, VEGF also enhances axonal outgrowth from dorsal root ganglia [38]. It has been proposed that VEGF improves hematopoietic stem cell survival by an internal autocrine loop mechanism [38,39]. This mechanism implies that it is not accessible for extracellular inhibitors, such as antibodies, to block this loop and proposes that the VEGF-dependent loop is solely generated in stem cells and not in endothelial cells [39].

VEGF had become the focus of numerous basic science studies and was used to augment nerve grafts. However, it was found that the angiogenic effect of VEGF did not translate into enhanced motor recovery [40], suggesting that the role of vascularity in nerve regeneration does not depend on one element solely, but is broader and more complex [24]. Recent research investigated the effect of an adipofascial vascularized flap on nerve revascularization in nerve allografts using novel microcomputed imaging. These results suggest that revascularization patterns follow longitudinal inosculation, the growth of host vessels from nerve coaptation ends, occurring primarily from proximal, rather than from both nerve ends, as previously believed [41,42]. Organized longitudinally running vessels provide modeled vessel tracks to precede the repair of damaged nerves [14,16,23,24].

Stem cells and nerve regeneration

The importance of stem cells in peripheral nerve regeneration relies on their ability to enhance neurotrophic factors, promote myelin formation, and their capacity to be influenced by the microenvironment to differentiate into Schwann-like cells [12]. Schwann cells are essential within the context of peripheral nerve regeneration after trauma and are crucial during Wallerian degeneration, however, difficult to transplant [4,43]. The acquisition of autologous Schwann cells requires the harvest of large segments of healthy nerve tissue, resulting in donor site morbidities. Additionally, proliferation of Schwann cells *in vitro* is associated with an extensive culturing and expansion time period. As a result of these limitations, research has been directed towards the use of MSCs, which are easily accessible, and can be differentiated into Schwann-like cells [4]. Schwann-like cells are found to express neurotrophic factors and to interact through multiple pathways to support the repair of injured nerves [17,44]. These factors and pathways include nerve growth factor (NGF), brain-derived neurotrophic factor (BDNF), and myelin related growth factors. BDNF is upregulated in motor neurons and increases myelin thickness in regenerating nerves while promoting remyelination and axonal sprouting [4,45]. In myelin sheath formation, a number of myelin proteins are induced such as myelin basic protein (MBP), peripheral myelin protein-22 (PMP22), and pleiotrophin (PTN). PTN is involved in myelinated axon regeneration specifically and is increasingly expressed in differentiated MSCs in comparison to undifferentiated MSCs [46,47]. The level of growth factors in the microenvironment influences the sequential growth factor production by the transplanted stem cells, emphasizing their paracrine feedback properties.

Only 5% of all types of stem cells can spontaneously differentiate into Schwann cells, however, pre-differentiation towards the desired phenotype *in vitro* via chemical induction or transfection with growth factors has been shown to be a more effective method to increase the number of Schwann-like cells. [12,48,49]. Drawbacks of pre-differentiation include the need for additional preparation time and higher costs, making this process less favorable for clinical translation [17]. More investigation is needed to confirm the optimal dosage of transplanted stem cells, delivery methods, *in vivo* survivability, and interaction mechanisms with their environment prior to conducting clinical studies.

STEM CELL SOURCES

Stem cells can be categorized as embryonic stem cells or adult stem cells according to their development stage, which relates to their differentiation potential.

Embryonic stem cells

In 1998, Thomson et al. described the isolation of pluripotent cell lines from the inner cell mass of human blastocyst-stage embryos [50]. Following this discovery, stem cells have been harvested from several fetal as well as adult tissues (Figure 2). Embryonic stem cells (ESC) are undifferentiated cells, capable of self-renewal and have superior differentiation potential and long-term proliferation capacity compared to adult stem cells. ESCs have the ability of *in vivo* myelination since they can differentiate into neurons and glial cells of the central and peripheral nervous system. In humans, the use of ESCs in neural tissue engineering is primarily inhibited by the ethical controversy of the use and destruction of a human embryo. Additional limitations include ESC's immunogenicity and carcinogenic potential including teratoma formation which limits clinical translation. Differentiation of ESCs into specialized neural cell lines remains challenging and protocols have only been established for a few cell lines [4,51-54].

Neural stem cells

Neural stem cells (NSCs) are naturally capable of differentiating into neurons or glial cells and play a role during neurogenesis in the development of the brain and spinal cord, which almost exclusively occurs during embryogenesis. In human adults, NSCs are located in the subventricular zone and hippocampus and have a limited role in the regeneration of central nervous system injuries [53,55,56]. While several basic science studies suggest enhancement of nerve regeneration following NSC administration to the injury site after both acute and chronic PNI [53,57,58], commercially available NSCs have been reported to be associated with the formation of neuroblastoma after implantation [59]. Additional limitations to application in humans include the technical difficulties associated with cell harvest and the need to direct differentiation of specialized neural cell lines. The application of NSCs could greatly benefit clinical practice if these limitations can be overcome [58].

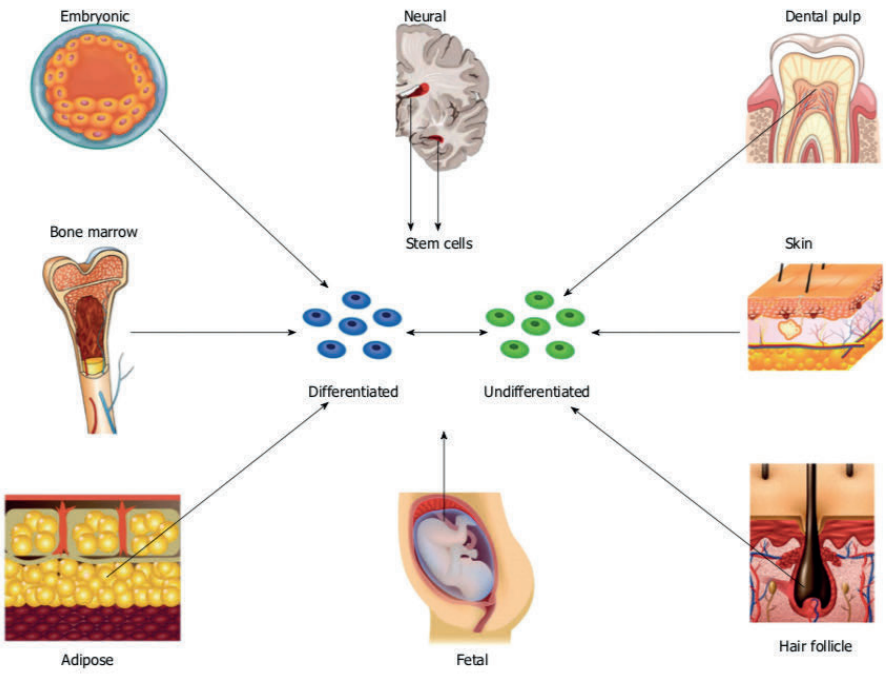

Figure 2. Schematic overview of different sources of stem cells. Embryonic stem cells are obtained from the inner cell mass of the blastocyst and therefore require destruction of the embryo. Nerve stem cells are harvested from the subventricular layer of the lateral ventricle and the subgranular layer of the hippocampus. Bone marrow-derived stem cells are harvested from the marrow cavity of long bones. Adipose-derived stem cells are derived from subcutaneous fat and are abundantly available following commonly performed procedures such as liposuction. Skin derived precursors are harvested from the dermis and represent a related population of cells harvested from hair follicles. Fetal tissue provides populations of cells from amniotic membrane, amniotic fluid, umbilical cord blood, umbilical cord tissue, and Wharton's jelly. Dental pulp stem cells can be harvested from deciduous teeth. *Copyrighted and used with permission of the World Journal of Stem Cells; all rights reserved.* Directly cited from [53] - Augmenting peripheral nerve regeneration using stem cells- A review of current opinion.

Mesenchymal stem cells

The multipotent MSCs can be derived from the bone marrow and a wide range of non-marrow sources, including adipose tissue, peripheral blood, amniotic fluid, umbilical cord, tendon and ligaments, hair follicle, synovial membranes, olfactory mucosa, dental pulp and fetal tissue [60]. Their potential for differentiation, ease of isolation, and immunomodulation have contributed to their considerable application in tissue regeneration. MSCs have the ability to differentiate into all mesoderm lineages: adipose

tissue, bone, muscle, and cartilage [61] and serve as targets for genetic modification. Depending on the appropriate stimuli and environmental conditions, MSCs have shown to express plasticity and transdifferentiation and can be differentiated into non-mesenchymal lineages, such as neurons, astrocytes, Schwann-cell like cells and myelinating cells of the peripheral nervous system to enhance nerve regeneration [4,12,53,62]. Bone marrow-derived and adipose-derived MSCs are the most commonly used stem cells for PNI.

Bone marrow-derived mesenchymal stem cells

Bone marrow-derived mesenchymal stem cells (BMSCs) can differentiate into non-mesodermal lineages such as neurons, astrocytes, and Schwann-like cells under appropriate environmental conditions [62]. Consequently, BMSCs may enhance neurite outgrowth and express neurotrophic factors (NGF, BDNF, glial cell line-derived neurotrophic factor (GDNF), and ciliary neurotrophic factor) as well as extracellular matrix components including collagen, fibronectin, and laminin. Administration of BMSCs to nerves contributes to enhanced angiogenesis [52,63-66]. A number of studies in rodent models have found that BMSC application to conduits and acellular nerve grafts resulted in superior functional outcomes in nerve regeneration compared to untreated grafts [51,53]. BMSCs demonstrated dose-dependent enhancement of the extent of myelination, thickness of myelin sheath, and axonal thickness in a rat sciatic nerve model [67]. When cultured, BMSCs lack immune recognition and have immunosuppressive action, which may overcome induced immune rejection after allogenic transplantation [52,68]. Although BMSCs are more easily harvested than ESCs and NSCs and have minimal ethical use issues, BMSCs have inferior proliferation capacity and differentiation potential. The harvesting procedure is invasive and painful for donors and the quantity of stem cells obtained is lower compared to other sources [12,53].

Adipose-derived mesenchymal stem cells

Adipose-derived mesenchymal stem cells (ADSCs) can easily be harvested from abundant adipose tissue with minimally invasive procedures such as liposuction. Compared to BMSCs, ADSCs show superior stem cell fraction, proliferation, and differentiation potential. ADSCs can be differentiated into a Schwann cell-like phenotype, sharing functional and morphological characteristics, and similar effectivity levels as autologous Schwann cells. It is postulated that ADSCs facilitate endogenous Schwann cell recruitment by expressing growth factors such as NGF, VEGF,

and BDNF leading to a long-lasting therapeutic effect promoting nerve regeneration and protection, which outlasts the life span of ADSC [53,69,70]. Interestingly, ADSCs are reported to support angiogenesis by direct differentiation into vascular endothelium, as well as by associated paracrine effects [71,72]. Difficulties include the unfavorable differentiation potential towards adipocytes [73]. Nonetheless, ADSCs are currently the most practical source of stem cells to obtain and have been and continue to be translated to clinical use [53].

Other types of MSCs including fetal derived stem cells, skin-derived precursors, muscle-derived stem/progenitor cells, hair follicle stem cells and dental pulp stem cells, as well as induced pluripotential stem cells are detailed in Table 1 [12,53]. Currently, inherent disadvantages associated with MSC-based therapy still exist: instability of the cellular phenotype, high cost, ethical issues, and difficulties of cellular origin [74]. These difficulties may be overcome by the application of exosomes.

Exosomes

Recent research has proven that the therapeutic effect of MSCs is highly likely to be accredited to the indirect regeneration of endogenous Schwann cells through cellular paracrine mechanisms, which are partially thought to be mediated by MSC exosomes [75]. MSC exosomes are a subtype of extracellular vesicles released from all cell types, but particularly from stem cells. MSC exosomes located in nearly all biological body fluids including blood, urine, breast milk, ascites, and saliva [76]. These particles maintain cell-to-cell communication by delivering proteins, lipids, DNA, mRNA, and micro ribonucleic acids miRNAs (miRNA), and other subtypes of RNA, which regulate cell biological behavior and can be used to mediate intercellular communication [77-80]. MSC exosomes are found to increase axonal regeneration and promote local angiogenesis by transmitting a number of genetic materials, neurotrophic factors and proteins to axons and thereby restoring the homeostasis of the microenvironment [74]. Furthermore, MSC exosomes have been proven to promote the proliferation of Schwann cells and reduce their apoptosis rate by upregulating the pro-apoptotic Bax mRNA expression resulting in increased regeneration [81]. It is postulated that MSC exosomes are mediators of communication with vascular endothelial cells resulting in enhancement of the plasticity of blood vessels following PNI [82]. MSC exosome-based therapy provides many benefits including the decrease of associated risks with transplantation as exosomes

Table 1 – Overview of sources of stem cells, showing its origin, location of harvest, properties, and mechanisms. The advantages and disadvantages of each mentioned stem cell source are mentioned in the last two columns [12,29,53,74].

Source	Origin	Location of harvest	Properties/ Mechanism	Advantage	Disadvantage
Embryonic stem cell (ESC)	Pluripotent stem cells	Blastocyst-stage embryo	Stimulate myelination, exert neurotrophic factors	- Unlimited source of cells - Superior differentiation potential - Homogenous - Long-term proliferation capacity	- Ethical dilemma - Immunogenicity - Carcinogenic potential (e.g. teratoma) - Differentiation to specialized cell lines remains challenging
Neural stem cell (NSC)	Multipotent stem cells	Sub-ventricular zone, hippocampus	Replace Schwann cells	- Highly migratory cells that give rise to neurons, astrocytes, and oligodendrocytes - Contributing extensively to remyelination	- Difficulty harvesting - Evokes neural-immune reactions after transplantation - Neuroblastoma formation, - Directed differentiation to specialized cell lines remains challenging
Mesenchymal stem cells (MSC)	Multipotent stem cells	Bone marrow, adipose tissue, peripheral blood, amniotic fluid, umbilical cord, tendon and ligaments, hair follicle, synovial membranes, olfactory mucosa, dental pulp and fetal tissue	Stimulate myelination, exert neurotrophic factors	- Dependent on sub-type	- Dependent on sub-type
Bone marrow-derived stem cells (BMSC)	Multipotent stem cells	Bone marrow	Stimulate myelination, exert neurotrophic factors	- Not restricted by ethical concerns - Lack of immune recognition and have immunosuppressive action, resulting in allogenic transplantation without induced immune rejection	- Painful procurement procedure necessitating anesthesia - Inferior proliferation capacity and differentiation potential - Low fraction of stem cells available for use

Table 1 – (Continued)

Source	Origin	Location of harvest	Properties/ Mechanism	Advantage	Disadvantage
Adipose-derived stem cells (ADSC)	Multipotent stem cells	Adipose tissue	Stimulate myelination, exert neurotrophic factors, reduce inflammation	- Minimally invasive harvesting - A higher proportion, superior proliferation, stem cell fraction and differentiation potential compared to BMSCs - Valid Schwann cell alternative, one of the optimal choices for pre-clinical studies, aid angiogenesis	- Differentiation potential exists towards adipocytes
Fetal derived stem cells (FSC)	Multipotent stem cells	Amniotic membrane, amniotic fluid, umbilical cord cells, umbilical cord blood, and Wharton's jelly.	Augmented blood perfusion, enhanced intraneural vascularity	- Easily obtained - Less immunoreactivity	- Require storage of autologous cells after harvest
Skin derived precursors (SKP-SC)	Multipotent cells	Dermis	Replace Schwann cell myelination	- Easy to harvest - Accessible - Highly similar to neural crest cells - Durable proliferative ability	- Prolonged periods of cell expansion
Muscle-derived stem/ progenitor cells (MDSPC)	Progenitor cells	Skeletal muscle	Exert neurotrophic factors	- Highly accessible - Long-term proliferation - Multipotent differentiation	- Limited scientific support
Hair follicle stem cells (HFSC)	Multipotent stem cells	Hair follicle	Replace Schwann cell myelination, exert neurotrophic factors	- Abundant and accessible source, multipotent differentiation - Differentiation into pure human Schwann cell population	- Cannot be stored for long periods, difficult to isolate - Prolonged periods of cell expansion

Table 1 – (Continued)

Source	Origin	Location of harvest	Properties/ Mechanism	Advantage	Disadvantage
Dental pulp stem cells (DPSC)	Multipotent stem cells	Exfoliated deciduous teeth	Replace Schwann cell myelination, exert neurotrophic factors	- Stronger proliferation, greater clonogenicity, and larger population compared to BMSCs - Most convenient source of multipotent stem cells	- Require controlled storage of autologous cells after harvest - Limited scientific support
Induced pluripotent stem cells (iPSC)	Pluripotent stem cells	Dermis, blood	Replace Schwann cell myelination, exert neurotrophic factors	- No ethical and immunosuppressive restrictions - Inducible from easily obtainable somatic cells	- Differentiation occurs with reduced efficiency and increased variability - Higher risk at tumorigenicity - Chromosomal aberrations - Epigenetic memory from original somatic cells
Exosomes	Membrane nanovesicles	In almost all biological body fluids including blood, urine, breast milk, ascites, and saliva	Transmit genetic material, neurotrophic factors, and proteins	- Could eliminate the risks associated to MSC transplantation - Lower immunogenicity - Cross biological barriers - Easier stored and available in the long term while maintaining quality	- No standardized techniques for isolation, quantification, and purification - No ethical safety assessment or guidance. - Limited scientific support.

contain fewer membrane-bound proteins. These characteristics present MSC exosomes with lower immunogenicity, the ability to cross biological barriers, and to be more stable over time [74,83]. The primary limitation of exosomes application is the limited scientific support and lack of standardized techniques for its isolation, quantification and purification. The efficacy of injected MSC exosomes and the effect of MSC exosomes travelling through the body remains unknown and to be explored [84].

Additionally, no guidelines for ethical safety assessment exists yet. MSC exosomes have great potential to be utilized for future therapeutic strategies in clinical practice following PNI if these challenges can be addressed [74].

Mode of stem cell delivery

Stem cells can be delivered to the nerve reconstruction site by a variety of methods (Table 2). The selection of the delivery method depends on the intended mechanism of action of the stem cells. The process of microinjection (either intra-neural, around the nerve, intramuscular or intravenous) decreases the viability of stem cells due to the traumatic damage secondary to the pressure build-up in the syringe and flow through the needle during injection. Furthermore, intra-neural microinjection of stem cells is associated with damage of the nerve ultrastructure with unpredictable cell distributions, obstruction of axonal ingrowth, and leakage of cells [12,17,53,85,86]. Dynamic seeding has been a successful technique in delivering stem cells and results in an efficient and uniform distribution of stem cells. When cells are dynamically seeded on the surface of a decellularized nerve allograft, these cells remain viable on the nerve surface allowing for interaction with the nerve ultrastructure and resulting in the upregulation of neurotrophic factors [17,22]. According to Mathot et al., an efficiency of at least 1 x 10^6 MSCs on a 10-mm nerve graft is needed to generate noticeable outcomes. Induced differentiation of MSCs may have an effect on the final efficiency, as delivery methods have only been tested on undifferentiated MSCs, however, its effect remains unknown [17]. Controversy remains on the optimal method of delivery and requires further evaluation.

Table 2 – Overview of delivery methods of stem cells, showing its efficiency, advantages, and disadvantages. [17,51,53]

Methods	Efficiency	Advantage	Limitations
Intravenous injection	100%	- Does not induce nerve damage and cell-leakage - Focusses on the trophic function of stem cells	- Entrapment stem cells in capillaries - The desired amount at the recipient site may not suffice - Reduction stem cell viability after needle passage due to pressure build-up
Intramuscular injection	100%	- Does not induce nerve damage and cell-leakage - Significantly improves functional recovery and neuro-conduction velocity compared to intravenous injection - Enhances nerve regeneration	- Reduction stem cell viability after needle passage due to pressure build-up, low number of stem cells at nerve regeneration site
Dynamic seeding on nerve grafts or conduits	89.2%	- Does not harm stem cells or nerve infrastructure - More successful than static seeding, uniform distribution of adhered stem cells - Upregulation neurotrophic factors - Very promising method	- Stem cells do not migrate from the delivery site - Can only be used when the nerve gap is bridged with a nerve graft or conduit
Intra-neural microinjection	10-40%	- Delivers a high quantity of cells directly to the site of the inner and middle nerve zones	- Traumatic to stem cells as well as intra-neural architecture - Unpredictable cell distribution, reduction stem cell viability after needle passage due to pressure build-up - Leakage cells - May obstruct axonal ingrowth
Microinjection around nerve	10-40%	- Does not induce nerve damage and cell-leakage - Outcomes comparable to intra-neural microinjection	- Reduction stem cell viability after needle passage due to pressure build-up
Cell encapsulation	Unknown	- Overcomes side effects of transplantation (e.g. teratoma formation, tumors) - Prevents in vivo migration of cells - Enhances the formation of multicellular aggregates	- A high volume of micro-particles needed to reach a beneficial number of cell release
Hydrogel	Unknown	- Similarity to extracellular matrix - Can be processed under mild conditions - Minimally invasive delivery - Degradation can be designed to coincide with angiogenesis and revascularization - Potentially clinical translatable	- Research is still in the early stage - Degradation hydrogel may affect stem cell survivability
3-D printing	Unknown	- Includes the personalized complex features of the nerve structures	- Research is still in the early stages - Technical challenges to realize the formation of the desired nerve structure

The regenerative potential of cell-based therapy

The regenerative potential of cell-based therapy following nerve injury is particularly relevant for large diameter and long nerve defects [87]. In rodent models, extensive research using stem cells in peripheral nerve repair suggests that the application of stem cells enhances functional motor outcomes. It has been shown that stem cells elevate expression of neurotrophic factors, angiogenic growth factors and contribute to angiogenesis [46,52,63,88]. The exact survivability of stem cells *in vivo,* however, is difficult to investigate and remains largely unknown. When MSCs were dynamically seeded on nerve allografts, *in vivo* survivability up to 29 days was found using luciferase-based bioluminescence imaging [89]. This suggests that survivability of stem cells may be hampered by rejection, inflammation, or migration. Larger animal models are also investigating augmentation of nerve repair outcomes by the provision of BMSCs to nerve grafts [90,91]. Tissue-engineered nerve grafts enhanced with autologous BMSCs have been used to repair 50 mm-long median nerve defects in rhesus monkeys. After one year, histological and morphometric analyses of regenerative nerves found results comparable to autograft repair. Blood samples and histopathological examination of nerve found no immune rejection, confirming that tissue-engineered nerve grafts augmented with BMSCs were safe to use in monkeys [92]. Extensive investigations of safety in preceding pre-clinical trials have provided the data necessary to proceeding evaluation of MSCs in clinical trials [93].

Clinical stem cell application is novel and has been applied to several fields including treatment for cardiovascular diseases with promising results [19]. Several clinical trials investigating central nervous system diseases, including spinal cord injury and traumatic brain injury, have proven the safety of MSC application. Ongoing trials suggest that MSCs prepare the environment of injury for axonal ingrowth and stimulate angiogenesis. While this is promising, more studies are needed to assess the time and route of administration to obtain more consistent data [94]. In the field of PNI, most clinical trials related to stem cell treatment focus on hemifacial spasm, burn wound healing and diabetic peripheral neuropathy [4] and are still in the early phases. Although the application of Schwann cells is not desired due to the aforementioned limitations, the first FDA-regulated dose phase I trial on human Schwann cell transplantation in spinal cord injuries has found promising results with no adverse effects [95]. Currently, little pre-clinical or clinical research has addressed the interaction of stem cells and

vascularity in nerve regeneration, which creates an opportunity for elucidating its synergistic pathways in future research.

Future applications

Future applications integrating stem cell-based therapies with the promotion of angiogenesis are needed to enhance nerve regeneration through multiple pathways. Feasibility with respect to cost and time efficiency is needed for translation to clinical practice. Current research developing future applications includes prevascularized stem cell nerve conduits, three-dimensional printing, and hydrogel scaffolding [29,96,97].

Fan et al. have developed a novel prevascularized nerve conduit based on a MSC sheet for treating spinal cord injuries, resulting in enhanced nerve regeneration and revascularization [96]. Other novel research has focused on three-dimensional printing in order to fabricate a nerve guidance conduit with stem cells that reproduces the complex nerve features of a patient's long nerve defect, such as branching nerve networks and intrinsic chemical mechanisms that steer regenerating motor and sensory axons along correct anatomical pathways. Three-dimensional printing may provide the desired personalized dimensions and structures for nerve regeneration and cell organization [97].

Another novel future application focusses on promising stem cell delivery methods, which are still in early stages of research, such as stem cell encapsulation delivered in a hydrogel scaffold [29,98]. Hydrogels constructed of natural biomaterials, including collagen and fibrin, as well as synthetic biomaterials such as poly(lactic-co-glycolic acid) (PLGA) and polyethylene glycol (PEG), may act as carriers for delivery of stem cells or growth factors. The use of hydrogel as a scaffold is attractive due to its high water content mimicking an extracellular matrix as well as its ease of delivery. Hydrogel degradation can be designed to respond to tissue proteases and to deliver stem cells or other growth factors in a timely manner to coincide with the processes of angiogenesis. In vascular tissue engineering, PLGA hydrogels have been designed to ensure a controlled release of angiogenic factors such as VEGF for an extended release time. Basic criteria for the use of hydrogel include effective cell adhesion to the gel matrix, sufficient stem cell survival in the hydrogel, safety for the micro-environment, and mechanical stability [29,99]. The use of prefabricated conduits or encapsulated cells

locally delivered in a hydrogel is feasible, has strong potential to enhance survival of transplanted cells and may be less immunogenic when combined with exosomes.

As tissues consist of multiple cell types, potential synergistic therapeutic benefit may occur when multiple stem cell types are administered simultaneously. By combining the properties and secretion of a mixture of neuroregenerative as well as vascular growth factors, cytokines and miRNA, regenerative capacities may be enhanced. Currently, limited data supporting combined cell type administration exist, however, may be promising for future applications [100,101]. The ideal type of stem cell for translation needs to be easily accessible and harvested, proliferate rapidly without carcinogenic consequences, and immune-compatible. Locally delivered cell-based therapy is expected to increasingly take part in enhancing outcomes after nerve reconstruction in the next decades.

CONCLUSIONS

Improved understanding of the interaction of stem cells and vascularity will provide therapeutic targets to improve outcomes after peripheral nerve reconstruction. The degree of nerve regeneration after PNI is particularly dependent on the local environment of injury and may be altered to promote functional recovery. The microenvironment may be modulated by stem cells and angiogenesis. This topic of interest is complex and involves the secretion of trophic factors that enhance regeneration and revascularization. Revascularization of nerve is suggested to enhance nerve regeneration by organized longitudinally running vessels that provide modeled vessel tracks to precede the repair of damaged nerves. The effect of stem cells, on the other hand, is dependent on their differentiation potential and stimulation by paracrine cues, which are provided by the environment during nerve regeneration. This review discusses the synergistic pathways of stem cells and vascularity and their interaction with nerve following PNI. Despite advancements in well-designed pre-clinical studies, translation of stem cells to clinical practice is currently impeded by ethical issues, risk of tumorigenesis, unknown side-effects and technical challenges. Future research may be shifted towards the use of exosomes, to overcome difficulties associated with the harvest and culture of stem cells. Local modulation of nerve environment is still evolving, and the importance of stem cell and vascularity-based therapies is expected to take a larger part in treatment options of PNIs.

Disclosure

The authors have no financial interests to disclose.

Conflict of interest

The authors have no conflict of interest to disclose.

Acknowledgments

We would like to thank Dr. Fairbairn and colleagues, and the World Journal of Stem Cells for granting us the permission to reprint Figure 2.

REFERENCES

1. Sullivan R, Dailey T, Duncan K, Abel N, Borlongan CV. Peripheral Nerve Injury: Stem Cell Therapy and Peripheral Nerve Transfer. *Int J Mol Sci.* 2016;17(12).
2. Lundborg G. A 25-year perspective of peripheral nerve surgery: evolving neuroscientific concepts and clinical significance. *J Hand Surg Am.* 2000;25(3):391-414.
3. Khalifian S, Sarhane KA, Tammia M, et al. Stem cell-based approaches to improve nerve regeneration: potential implications for reconstructive transplantation? *Arch Immunol Ther Exp (Warsz).* 2015;63(1):15-30.
4. De la Rosa MB, Kozik EM, Sakaguchi DS. Adult Stem Cell-Based Strategies for Peripheral Nerve Regeneration. *Adv Exp Med Biol.* 2018;1119:41-71.
5. Sunderland S. Factors influencing the course of regeneration and the quality of the recovery after nerve suture. *Brain.* 1952;75(1):19-54.
6. Terzis J, Faibisoff B, Williams B. The nerve gap: suture under tension vs. graft. *Plast Reconstr Surg.* 1975;56(2):166-170.
7. Ray WZ, Mackinnon SE. Management of nerve gaps: autografts, allografts, nerve transfers, and end-to-side neurorrhaphy. *Exp Neurol.* 2010;223(1):77-85.
8. Kornfeld T, Vogt PM, Radtke C. Nerve grafting for peripheral nerve injuries with extended defect sizes. *Wien Med Wochenschr.* 2019;169(9-10):240-251.
9. Saffari T, Bedar M, Zuidam J, et al. Exploring the neuroregenerative potential of tacrolimus. *Expert Review of Clinical Pharmacology.* 2019;12(11):1047-1057.
10. Bulatova N, Yousef AM, Al-Khayyat G, Qosa H. Adverse effects of tacrolimus in renal transplant patients from living donors. *Curr Drug Saf.* 2011;6(1):3-11.
11. Patel NP, Lyon KA, Huang JH. An update-tissue engineered nerve grafts for the repair of peripheral nerve injuries. *Neural Regen Res.* 2018;13(5):764-774.
12. Jiang L, Jones S, Jia X. Stem Cell Transplantation for Peripheral Nerve Regeneration: Current Options and Opportunities. *Int J Mol Sci.* 2017;18(1).
13. Keilhoff G, Goihl A, Langnase K, Fansa H, Wolf G. Transdifferentiation of mesenchymal stem cells into Schwann cell-like myelinating cells. *Eur J Cell Biol.* 2006;85(1):11-24.
14. Rissanen TT, Rutanen J, Yla-Herttuala S. Gene transfer for therapeutic vascular growth in myocardial and peripheral ischemia. *Adv Genet.* 2004;52:117-164.
15. Caplan AI. Adult Mesenchymal Stem Cells: When, Where, and How. *Stem Cells Int.* 2015;2015:628767.
16. Risau W. Mechanisms of angiogenesis. *Nature.* 1997;386(6626):671-674.
17. Mathot F, Shin AY, Van Wijnen AJ. Targeted stimulation of MSCs in peripheral nerve repair. *Gene.* 2019.
18. Watt SM, Gullo F, van der Garde M, et al. The angiogenic properties of mesenchymal stem/stromal cells and their therapeutic potential. *Br Med Bull.* 2013;108:25-53.
19. Hong SJ, Traktuev DO, March KL. Therapeutic potential of adipose-derived stem cells in vascular growth and tissue repair. *Curr Opin Organ Transplant.* 2010;15(1):86-91.

20. Rehman J, Traktuev D, Li J, et al. Secretion of angiogenic and antiapoptotic factors by human adipose stromal cells. *Circulation.* 2004;109(10):1292-1298.
21. Kondo K, Shintani S, Shibata R, et al. Implantation of adipose-derived regenerative cells enhances ischemia-induced angiogenesis. *Arterioscler Thromb Vasc Biol.* 2009;29(1):61-66.
22. Rbia N, Bulstra LF, Bishop AT, van Wijnen AJ, Shin AY. A simple dynamic strategy to deliver stem cells to decellularized nerve allografts. *Plastic and reconstructive surgery.* 2018;142(2):402.
23. Carmeliet P, Ferreira V, Breier G, et al. Abnormal blood vessel development and lethality in embryos lacking a single VEGF allele. *Nature.* 1996;380(6573):435-439.
24. Saffari TM, Bedar M, Hundepool CA, Bishop AT, Shin AY. The role of vascularization in nerve regeneration of nerve graft. *Neural Regeneration Research.* 2020;15(9):1573.
25. Chen CW, Corselli M, Peault B, Huard J. Human blood-vessel-derived stem cells for tissue repair and regeneration. *J Biomed Biotechnol.* 2012;2012:597439.
26. Tavian M, Zheng B, Oberlin E, et al. The vascular wall as a source of stem cells. *Annals of the New York Academy of Sciences.* 2005;1044(1):41-50.
27. Zengin E, Chalajour F, Gehling UM, et al. Vascular wall resident progenitor cells: a source for postnatal vasculogenesis. *Development.* 2006;133(8):1543-1551.
28. Zhang L, Issa Bhaloo S, Chen T, Zhou B, Xu Q. Role of Resident Stem Cells in Vessel Formation and Arteriosclerosis. *Circ Res.* 2018;122(11):1608-1624.
29. Fakoya AO. New Delivery Systems of Stem Cells for Vascular Regeneration in Ischemia. *Front Cardiovasc Med.* 2017;4:7.
30. Kingham PJ, Kolar MK, Novikova LN, Novikov LN, Wiberg M. Stimulating the neurotrophic and angiogenic properties of human adipose-derived stem cells enhances nerve repair. *Stem Cells Dev.* 2014;23(7):741-754.
31. Mathot F, Rbia N, Bishop AT, Hovius SE, Shin AY. Adipose derived mesenchymal stem cells seeded onto a decellularized nerve allograft enhances angiogenesis in a rat sciatic nerve defect model. *Microsurgery.* 2020.
32. Waller A. Experiments on the Section of the Glosso-Pharyngeal and Hypoglossal Nerves of the Frog, and Observations of the Alterations Produced Thereby in the Structure of Their Primitive Fibres. *Edinb Med Surg J.* 1851;76(189):369-376.
33. Cheng Q, Wang Y-x, Yu J, Yi S. Critical signaling pathways during Wallerian degeneration of peripheral nerve. *Neural regeneration research.* 2017;12(6):995.
34. Hobson MI, Brown R, Green CJ, Terenghi G. Inter-relationships between angiogenesis and nerve regeneration: a histochemical study. *Br J Plast Surg.* 1997;50(2):125-131.
35. Hobson MI, Green CJ, Terenghi G. VEGF enhances intraneural angiogenesis and improves nerve regeneration after axotomy. *J Anat.* 2000;197 Pt 4:591-605.
36. Akhavani MA, Sivakumar B, Paleolog EM, Kang N. Angiogenesis and plastic surgery. *J Plast Reconstr Aesthet Surg.* 2008;61(12):1425-1437.
37. Connolly DT, Heuvelman DM, Nelson R, et al. Tumor vascular permeability factor stimulates endothelial cell growth and angiogenesis. *J Clin Invest.* 1989;84(5):1470-1478.
38. Sondell M, Lundborg G, Kanje M. Vascular endothelial growth factor stimulates Schwann cell invasion and neovascularization of acellular nerve grafts. *Brain Res.* 1999;846(2):219-228.

39. Gerber HP, Malik AK, Solar GP, et al. VEGF regulates haematopoietic stem cell survival by an internal autocrine loop mechanism. *Nature.* 2002;417(6892):954-958.
40. Lee J-Y, Giusti G, Friedrich PF, Bishop AT, Shin AY. Effect of vascular endothelial growth factor administration on nerve regeneration after autologous nerve grafting. *Journal of reconstructive microsurgery.* 2016;32(03):183-188.
41. Saffari TM, Mathot F, Friedrich PF, Bishop AT, Shin AY. Revascularization patterns of nerve allografts in a rat sciatic nerve defect model. *Journal of Plastic, Reconstructive & Aesthetic Surgery.* 2020;73(3):460-468.
42. Chalfoun C, Scholz T, Cole MD, Steward E, Vanderkam V, Evans GR. Primary nerve grafting: A study of revascularization. *Microsurgery.* 2003;23(1):60-65.
43. Salzer JL, Bunge RP. Studies of Schwann cell proliferation. I. An analysis in tissue culture of proliferation during development, Wallerian degeneration, and direct injury. *J Cell Biol.* 1980;84(3):739-752.
44. Tomita K, Madura T, Sakai Y, Yano K, Terenghi G, Hosokawa K. Glial differentiation of human adipose-derived stem cells: implications for cell-based transplantation therapy. *Neuroscience.* 2013;236:55-65.
45. Gordon T. The role of neurotrophic factors in nerve regeneration. *Neurosurg Focus.* 2009;26(2):E3.
46. Mathot F, Rbia N, Thaler R, Bishop AT, Van Wijnen AJ, Shin AY. Gene expression profiles of differentiated and undifferentiated adipose derived mesenchymal stem cells dynamically seeded onto a processed nerve allograft. *Gene.* 2020;724:144151.
47. Mi R, Chen W, Hoke A. Pleiotrophin is a neurotrophic factor for spinal motor neurons. *Proc Natl Acad Sci U S A.* 2007;104(11):4664-4669.
48. Cuevas P, Carceller F, Dujovny M, et al. Peripheral nerve regeneration by bone marrow stromal cells. *Neurol Res.* 2002;24(7):634-638.
49. Dore JJ, DeWitt JC, Setty N, et al. Multiple signaling pathways converge to regulate bone-morphogenetic-protein-dependent glial gene expression. *Dev Neurosci.* 2009;31(6):473-486.
50. Thomson JA, Itskovitz-Eldor J, Shapiro SS, et al. Embryonic stem cell lines derived from human blastocysts. *science.* 1998;282(5391):1145-1147.
51. Cui L, Jiang J, Wei L, et al. Transplantation of embryonic stem cells improves nerve repair and functional recovery after severe sciatic nerve axotomy in rats. *Stem cells.* 2008;26(5):1356-1365.
52. Yi S, Zhang Y, Gu X, et al. Application of stem cells in peripheral nerve regeneration. *Burns Trauma.* 2020;8:tkaa002.
53. Fairbairn NG, Meppelink AM, Ng-Glazier J, Randolph MA, Winograd JM. Augmenting peripheral nerve regeneration using stem cells: A review of current opinion. *World journal of stem cells.* 2015;7(1):11.
54. Jones I, Novikova LN, Novikov LN, et al. Regenerative effects of human embryonic stem cell-derived neural crest cells for treatment of peripheral nerve injury. *Journal of tissue engineering and regenerative medicine.* 2018;12(4):e2099-e2109.
55. Paspala SAB, Murthy TK, Mahaboob V, Habeeb M. Pluripotent stem cells-a review of the current status in neural regeneration. *Neurology India.* 2011;59(4):558.

56. Matarredona ER, Pastor AM. Neural Stem Cells of the Subventricular Zone as the Origin of Human Glioblastoma Stem Cells. Therapeutic Implications. *Frontiers in Oncology.* 2019;9:779.
57. Heine W, Conant K, Griffin JW, Höke A. Transplanted neural stem cells promote axonal regeneration through chronically denervated peripheral nerves. *Experimental neurology.* 2004;189(2):231-240.
58. Wang C, Lu C-f, Peng J, Hu C-d, Wang Y. Roles of neural stem cells in the repair of peripheral nerve injury. *Neural regeneration research.* 2017;12(12):2106.
59. Johnson TS, O'Neill AC, Motarjem PM, Nazzal J, Randolph M, Winograd JM. Tumor formation following murine neural precursor cell transplantation in a rat peripheral nerve injury model. *Journal of reconstructive microsurgery.* 2008;24(08):545-550.
60. Maltman DJ, Hardy SA, Przyborski SA. Role of mesenchymal stem cells in neurogenesis and nervous system repair. *Neurochemistry international.* 2011;59(3):347-356.
61. Pittenger MF, Mackay AM, Beck SC, et al. Multilineage potential of adult human mesenchymal stem cells. *science.* 1999;284(5411):143-147.
62. Tohill M, Mantovani C, Wiberg M, Terenghi G. Rat bone marrow mesenchymal stem cells express glial markers and stimulate nerve regeneration. *Neuroscience letters.* 2004;362(3):200-203.
63. Fan L, Yu Z, Li J, Dang X, Wang K. Schwann-like cells seeded in acellular nerve grafts improve nerve regeneration. *BMC Musculoskelet Disord.* 2014;15:165.
64. Wei L, Fraser JL, Lu Z-Y, Hu X, Yu SP. Transplantation of hypoxia preconditioned bone marrow mesenchymal stem cells enhances angiogenesis and neurogenesis after cerebral ischemia in rats. *Neurobiology of disease.* 2012;46(3):635-645.
65. Yang Y, Yuan X, Ding F, et al. Repair of rat sciatic nerve gap by a silk fibroin-based scaffold added with bone marrow mesenchymal stem cells. *Tissue Engineering Part A.* 2011;17(17-18):2231-2244.
66. Chen C-J, Ou Y-C, Liao S-L, et al. Transplantation of bone marrow stromal cells for peripheral nerve repair. *Experimental neurology.* 2007;204(1):443-453.
67. Raheja A, Suri V, Suri A, et al. Dose-dependent facilitation of peripheral nerve regeneration by bone marrow–derived mononuclear cells: a randomized controlled study. *Journal of neurosurgery.* 2012;117(6):1170-1181.
68. Aggarwal S, Pittenger MF. Human mesenchymal stem cells modulate allogeneic immune cell responses. *Blood.* 2005;105(4):1815-1822.
69. Erba P, Mantovani C, Kalbermatten DF, Pierer G, Terenghi G, Kingham PJ. Regeneration potential and survival of transplanted undifferentiated adipose tissue-derived stem cells in peripheral nerve conduits. *Journal of Plastic, Reconstructive & Aesthetic Surgery.* 2010;63(12):e811-e817.
70. Kingham PJ, Kalbermatten DF, Mahay D, Armstrong SJ, Wiberg M, Terenghi G. Adipose-derived stem cells differentiate into a Schwann cell phenotype and promote neurite outgrowth in vitro. *Experimental neurology.* 2007;207(2):267-274.
71. Nie C, Yang D, Xu J, Si Z, Jin X, Zhang J. Locally administered adipose-derived stem cells accelerate wound healing through differentiation and vasculogenesis. *Cell transplantation.* 2011;20(2):205-216.

72. Chen Y-T, Sun C-K, Lin Y-C, et al. Adipose-derived mesenchymal stem cell protects kidneys against ischemia-reperfusion injury through suppressing oxidative stress and inflammatory reaction. *Journal of translational medicine.* 2011;9(1):51.
73. Faroni A, Smith RJ, Lu L, Reid AJ. Human Schwann-like cells derived from adipose-derived mesenchymal stem cells rapidly de-differentiate in the absence of stimulating medium. *European Journal of Neuroscience.* 2016;43(3):417-430.
74. Dong R, Liu Y, Yang Y, Wang H, Xu Y, Zhang Z. MSC-Derived Exosomes-Based Therapy for Peripheral Nerve Injury: A Novel Therapeutic Strategy. *BioMed research international.* 2019;2019.
75. Sowa Y, Kishida T, Imura T, et al. Adipose-derived stem cells promote peripheral nerve regeneration in vivo without differentiation into Schwann-like lineage. *Plastic and reconstructive surgery.* 2016;137(2):318e-330e.
76. Kourembanas S. Exosomes: vehicles of intercellular signaling, biomarkers, and vectors of cell therapy. *Annual review of physiology.* 2015;77:13-27.
77. Corrado C, Raimondo S, Chiesi A, Ciccia F, De Leo G, Alessandro R. Exosomes as intercellular signaling organelles involved in health and disease: basic science and clinical applications. *Int J Mol Sci.* 2013;14(3):5338-5366.
78. Rezaie J, Ajezi S, Avci CB, et al. Exosomes and their Application in Biomedical Field: Difficulties and Advantages. *Mol Neurobiol.* 2018;55(4):3372-3393.
79. Blanc L, Vidal M. New insights into the function of Rab GTPases in the context of exosomal secretion. *Small GTPases.* 2018;9(1-2):95-106.
80. Li P, Kaslan M, Lee SH, Yao J, Gao Z. Progress in exosome isolation techniques. *Theranostics.* 2017;7(3):789.
81. Liu CY, Yin G, Sun YD, et al. Effect of exosomes from adipose-derived stem cells on the apoptosis of Schwann cells in peripheral nerve injury. *CNS Neuroscience & Therapeutics.* 2020;26(2):189-196.
82. Gong M, Yu B, Wang J, et al. Mesenchymal stem cells release exosomes that transfer miRNAs to endothelial cells and promote angiogenesis. *Oncotarget.* 2017;8(28):45200.
83. Qing L, Chen H, Tang J, Jia X. Exosomes and their MicroRNA cargo: new players in peripheral nerve regeneration. *Neurorehabilitation and neural repair.* 2018;32(9):765-776.
84. Qi J, Liu Q, Reisdorf RL, et al. Characterization of a purified exosome product and its effects on canine flexor tenocyte biology. *Journal of Orthopaedic Research®.* 2020.
85. Wang Y, Li Z-w, Luo M, Li Y-j, Zhang K-q. Biological conduits combining bone marrow mesenchymal stem cells and extracellular matrix to treat long-segment sciatic nerve defects. *Neural regeneration research.* 2015;10(6):965.
86. F Lévesque M, Neuman T, Rezak M. Therapeutic microinjection of autologous adult human neural stem cells and differentiated neurons for Parkinson's disease: five-year post-operative outcome. *The Open Stem Cell Journal.* 2009;1(1).
87. Faroni A, Mobasseri SA, Kingham PJ, Reid AJ. Peripheral nerve regeneration: experimental strategies and future perspectives. *Adv Drug Deliv Rev.* 2015;82-83:160-167.
88. Zhao Z, Wang Y, Peng J, et al. Repair of nerve defect with acellular nerve graft supplemented by bone marrow stromal cells in mice. *Microsurgery.* 2011;31(5):388-394.

89. Rbia N, Bulstra LF, Thaler R, Hovius SER, van Wijnen AJ, Shin AY. In Vivo Survival of Mesenchymal Stromal Cell-Enhanced Decellularized Nerve Grafts for Segmental Peripheral Nerve Reconstruction. *J Hand Surg Am.* 2019;44(6):514 e511-514 e511.
90. Ding F, Wu J, Yang Y, et al. Use of tissue-engineered nerve grafts consisting of a chitosan/poly(lactic-co-glycolic acid)-based scaffold included with bone marrow mesenchymal cells for bridging 50-mm dog sciatic nerve gaps. *Tissue Eng Part A.* 2010;16(12):3779-3790.
91. Muheremu A, Chen L, Wang X, Wei Y, Gong K, Ao Q. Chitosan nerve conduits seeded with autologous bone marrow mononuclear cells for 30 mm goat peroneal nerve defect. *Sci Rep.* 2017;7:44002.
92. Hu N, Wu H, Xue C, et al. Long-term outcome of the repair of 50 mm long median nerve defects in rhesus monkeys with marrow mesenchymal stem cells-containing, chitosan-based tissue engineered nerve grafts. *Biomaterials.* 2013;34(1):100-111.
93. Pal R, Venkataramana NK, Bansal A, et al. Ex vivo-expanded autologous bone marrow-derived mesenchymal stromal cells in human spinal cord injury/paraplegia: a pilot clinical study. *Cytotherapy.* 2009;11(7):897-911.
94. Badyra B, Sulkowski M, Milczarek O, Majka M. Mesenchymal stem cells as a multimodal treatment for nervous system diseases. *Stem Cells Transl Med.* 2020.
95. Anderson KD, Guest JD, Dietrich WD, et al. Safety of Autologous Human Schwann Cell Transplantation in Subacute Thoracic Spinal Cord Injury. *J Neurotrauma.* 2017;34(21):2950-2963.
96. Fan Z, Liao X, Tian Y, Nie Y. A prevascularized nerve conduit based on a stem cell sheet effectively promotes the repair of transected spinal cord injury. *Acta biomaterialia.* 2020;101:304-313.
97. Du J, Jia X. Engineering nerve guidance conduits with three-dimenisonal bioprinting technology for long gap peripheral nerve regeneration. *Neural Regeneration Research.* 2019;14(12):2073.
98. Allbright KO, Bliley JM, Havis E, et al. Delivery of adipose-derived stem cells in poloxamer hydrogel improves peripheral nerve regeneration. *Muscle & nerve.* 2018;58(2):251-260.
99. Maiti B, Díaz Díaz D. 3D printed polymeric hydrogels for nerve regeneration. *Polymers.* 2018;10(9):1041.
100. Williams AR, Hatzistergos KE, Addicott B, et al. Enhanced effect of combining human cardiac stem cells and bone marrow mesenchymal stem cells to reduce infarct size and to restore cardiac function after myocardial infarction. *Circulation.* 2013;127(2):213-223.
101. Avolio E, Meloni M, Spencer HL, et al. Combined intramyocardial delivery of human pericytes and cardiac stem cells additively improves the healing of mouse infarcted hearts through stimulation of vascular and muscular repair. *Circulation research.* 2015;116(10):e81-e94.

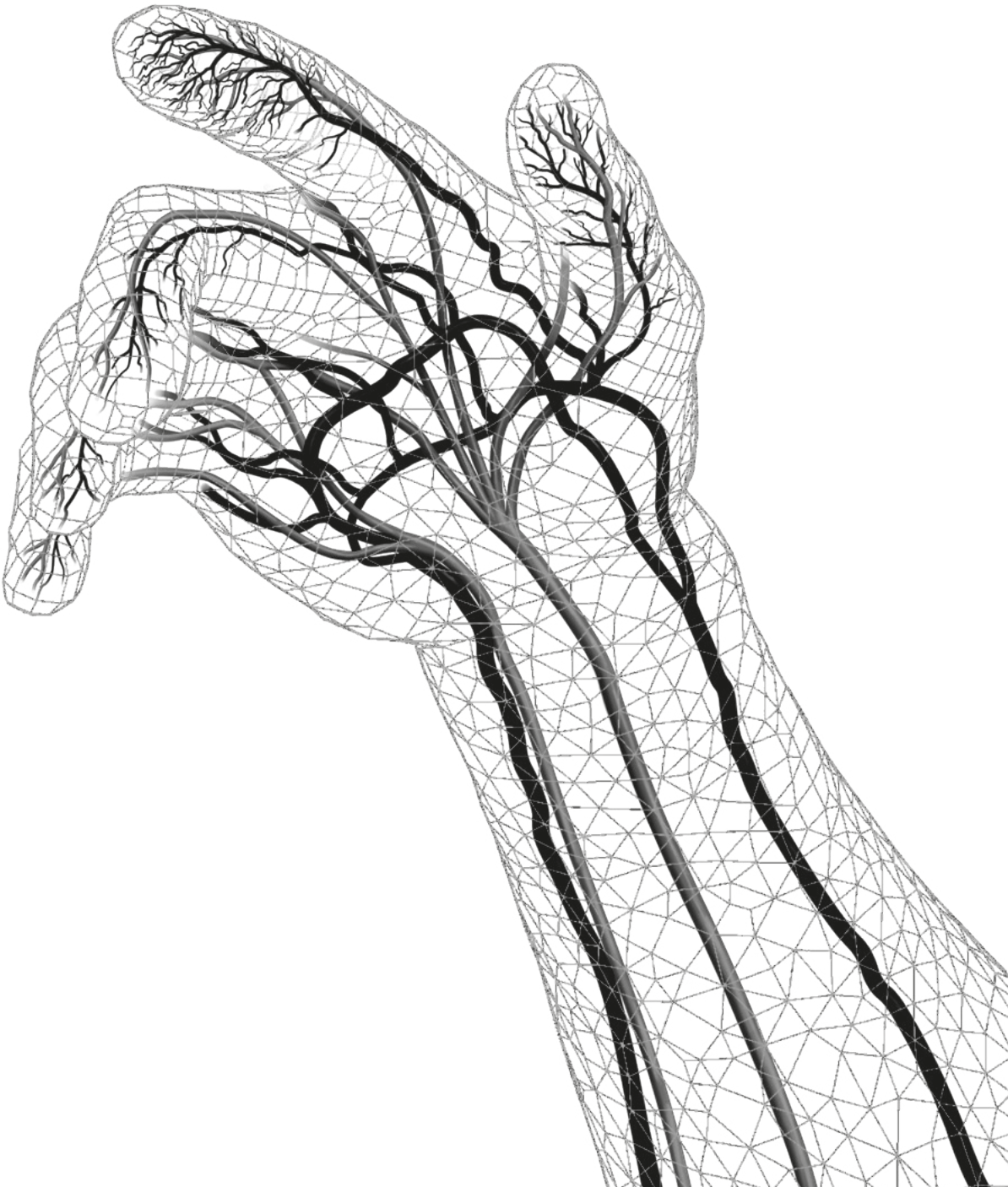

CHAPTER

NINE

Functional Outcomes of Nerve Allografts Seeded with Undifferentiated and Differentiated Mesenchymal Stem Cells in a Rat Sciatic Nerve Defect Model

Femke Mathot[1,2]
Tiam M. Saffari[1,2]
Nadia Rbia[1,3]
Tim H.J. Nijhuis[3]
Allen T. Bishop[1]
Steven E.R. Hovius[2]
Alexander Y. Shin[1]

Affiliations

[1]Department of Orthopedic Surgery, Mayo Clinic, Rochester, MN, USA

[2]Department of Plastic, Reconstructive and Hand Surgery, Radboud University Medical Center, Nijmegen, The Netherlands

[3]Department of Plastic, Reconstructive and Hand Surgery, Erasmus Medical Center, Rotterdam, The Netherlands

Plastic and Reconstructive Surgery. June 21, 2021.

ABSTRACT

Background

Mesenchymal stem cells (MSCs) have the potential to produce neurotrophic growth factors and establish a supportive micro-environment for neural regeneration. The purpose of this study was to determine the effect of undifferentiated and differentiated MSCs dynamically seeded onto decellularized nerve allografts on functional outcomes when used in peripheral nerve repair.

Materials and Methods

In 80 Lewis rats a ten millimeter sciatic nerve defect was reconstructed with (i) autograft, (ii) decellularized allograft (iii) decellularized allograft seeded with undifferentiated MSCs, or (iv) decellularized allograft seeded with MSCs differentiated into Schwann cell-like cells. Nerve regeneration was evaluated over time by cross sectional tibial muscle ultrasound measurements, and at 12 and 16 weeks by isometric tetanic force measurements (ITF), compound muscle action potentials (CMAP), muscle mass, histology and immunofluorescence analyses.

Results

At 12 weeks, undifferentiated MSCs significantly improved ITF and CMAP outcomes compared to decellularized allograft alone, while differentiated MSCs significantly improved CMAP outcomes. The autografts outperformed both stem-cell groups histologically at 12 weeks. At 16 weeks, functional outcomes normalized between groups. At both time points, the effect of undifferentiated versus differentiated MSCs was not significantly different.

Conclusions

Undifferentiated and differentiated MSCs significantly improved functional outcomes of decellularized allografts at 12 weeks and were similar to autograft results in the majority of measurements. At 16 weeks, outcomes normalized as expected. Although differences between both cell-types were not statistically significant, undifferentiated MSCs improved functional outcomes of decellularized nerve allografts to a greater extent and have practical benefits for clinical translation by limiting preparation time and costs.

INTRODUCTION

Peripheral nerve defects not amendable to direct end-to-end neurorrhaphy require reconstruction with interposition nerve graft which could be accomplished with autograft, allograft or synthetic bioabsorbable conduits, each with their benefits and controversies [1-3]. Decellularized nerve allografts have been proposed as an ideal alternative to overcome donor site morbidity and limited supply of autografts [1,4-7]. Improvement of outcomes of decellularized allografts by addition of host derived mesenchymal stem cells (MSCs) has been proposed to overcome the limitations of decellularized allograft nerves by producing trophic factors resulting in a favorable micro-environment for tissue regeneration [8-14]. MSCs are hypothesized to not only stimulate tissue regeneration, but potentially form extracellular matrix components, enhance angiogenesis, inhibit scar formation and control immune responses [15]. Adipose derived MSCs are easily accessible and proliferate faster than bone marrow derived MSCs, while having a similar effect on nerve regeneration and are thus ideal for translation to clinical use [16-18].

In comparison to undifferentiated MSCs, MSCs differentiated into Schwann cell-like cells express neurotrophic and angiogenic genes to a greater extent than undifferentiated MSCs *in vitro* [16,19-21]. Several *in vivo* studies using different MSC-delivery strategies did not demonstrate clear differences between the outcomes of undifferentiated and differentiated MSCs [22,23]. Others reported that differentiated MSCs led to longer regenerating axon distance *in vivo* [19,21,24,25], without resulting in improved functional outcomes [21]. The differentiation process of MSCs requires additional preparation time and expensive differentiation factors, which should be considered in translating bench work to clinical application [16].

Recent studies have reported a non-traumatic strategy to adhere undifferentiated and differentiated MSCs to the surface of decellularized allografts, leading to a 29-day *in vivo* survival of seeded MSCs [26-28]. The adherence of MSCs to the decellularized allograft has demonstrated an interaction between MSCs and the extracellularly matrix leading to enhanced expression of neurotrophic, angiogenic, extracellular matrix and regulatory cell cycle genes in the first three (differentiated MSCs) to seven (undifferentiated MSCs) days after seeding *in vitro*, implying a direct effect of

differentiated MSCs after implementation while undifferentiated MSCs require time to interact with the environment [14].

A comparative study focusing on functional outcomes can elucidate the effect of different cells and their different effective phases on motor nerve regeneration. The purpose of this study was to determine the effect of dynamically seeding undifferentiated and differentiated MSCs onto decellularized nerve allografts[7] with respect to functional and histologic outcomes in a rat sciatic defect model.

MATERIALS AND METHODS

Experimental design

After IACUC institutional review committee and our Institutional Review Board approval (IACUC protocol A2464-00), a 10 mm segmental defect of the sciatic nerve of 80 male Lewis rats weighing 250-300 grams (Envigo, Madison, WI, USA) was repaired with a 10 mm (i) reversed autograft, (ii) decellularized allograft (iii) decellularized allograft seeded with undifferentiated MSCs, or (iv) decellularized allograft seeded with differentiated MSCs. The decellularized allografts originated from Sprague-Dawley rats and were specifically chosen for their histocompatibility mismatch to Lewis rats [29,30]. This simulates the clinical setting where an allogenic processed nerve graft is seeded with autologous MSCs. After 12 and 16 weeks, functional, histological and immunofluorescence outcomes were evaluated.

Nerve allograft collection, processing and seeding

Sixty sciatic nerve segments from 30 Sprague-Dawley rats (Envigo, Madison, WI, USA) weighing 250-350 grams served as nerve allografts. After anesthesia with isoflurane, rats were euthanized, shaved and sterilely prepped. The sciatic nerve was exposed, removed under an operating microscope (Zeiss OpMi6, Carl Zeiss Surgical GmbH, Oberkochen, Germany) and processed according to a previously published protocol [7]. After sterilization with g-irradiation, nerves were stored at 4°C in Phosphate Buffered Saline (PBS) until surgery.

Stem cell preparation and differentiation

MSCs were derived from the inguinal fat pad of inbred Lewis rats according to protocol [16]. Cells were previously characterized by plastic adherence, pluripotency towards mesodermal lineages, the expression of mesenchymal stem cell markers CD29 (88.2%) and CD90 (88.3%) and the absence of hematopoetic cell markers CD34 (91.1% absent) and CD45 (86.0% absent) [26-28].

Both cell-types were cultured in an incubator at 37°C (5% CO_2) and the growth medium was changed every 72 hours. Passage six MSCs were used in this experiment for both differentiated and undifferentiated MSCs.

MSC culture

The stromal cell pellet was re-suspended in normal growth medium consisting of a-MEM (Advanced MEM (1x); Life Technologies Corporation, NY, USA), 5% platelet lysate (PLTMax®; Mill Creek Life Sciences, MN, USA), 1% Penicillin/Streptomycin (Penicillin-Streptomycin (10.000 U/mL; Life Technologies Corporation), 1% GlutaMAX (GlutaMAX Supplement 100X; Life Technologies Corporation) and 0.2% Heparin (Heparin Sodium Injection, USP, 1.000 USP units per mL; Fresenius Kabi, IL, USA).

MSC differentiation

MSCs were differentiated into Schwann cell-like cells using a differentiation cocktail containing 0.14% Forskolin (Sigma-Aldrich corp., MO, USA), 0.01% basis fibroblast growth factor (bFGF; PeproTech, NJ, USA), 0.005% platelet-derived growth factor (PDGF-AA; PeproTech) and 0.02% Neuregulin-1 ß1 (NRG1-b1; R&D systems Inc, MN, USA) [16]. Differentiation was assessed by immunocytochemistry for the expression of S100 (S100; ThermoFisher Scientific, MA, USA), Glial fibrillary acidic protein (GFAP, mouse anti-GFAP; ThermoFisher Scientific) and neurotrophin receptor p75 (p75 NTR, rabbit anti-p75 NTR; ThermoFisher Scientific). Goat anti-rabbit fluorescein isothiocyanate (FITC) and goat anti-mouse cyanine 3 (CY3, both ThermoFisher Scientific) were used as secondary antibodies. Cell nuclei were labeled with 4′,6-diamidino-2-phenylindole (DAPI).

Seeding protocol for allograft nerves

To attach the undifferentiated and differentiated MSCs to the decellularized nerve allografts they were dynamically seeded according to a previously described protocol [28]. Either 1x10^6 undifferentiated MSCs or 1x10^6 differentiated MSCs in 10mL growth medium were placed in a conical tube containing a decellularized nerve allograft. The conical tube was then placed on a bioreactor that was positioned in an incubator at 37°C (5% CO_2). After the bioreactor had rotated for 12 hours, the nerve grafts with the attached MSCs were taken out of the tubes and directly implemented in the Lewis rats. The dynamic seeding strategy previously resulted in 80% and 95% adherence of cells on the surface of the processed allografts for undifferentiated and differentiated MSCs, respectively [27,28].

Surgical procedure of the recipient animals

Under isoflurane anesthesia the right sciatic nerve of the Lewis rat was exposed. A 10 mm segment of the sciatic nerve was excised and reconstructed with a 10 mm graft under an operating microscope (Zeiss OpMi6, Carl Zeiss Surgical GmbH, Oberkochen, Germany). The epineurium was sutured with six 10-0 sutures (10-0 Ethilon, Ethicon Inc., USA), the muscle was approximated (6-0 Vicryl Rapide, Ethicon Inc.) and the skin was closed with a continuous subcutaneous suture (5-0 Vicryl Rapide, Ethicon Inc.). All rats received 5mL of 0.9% saline solution, 0.6mg/kg Buprenorphine and one dose of 30mg/kg diluted trimethoprim/sulfadiazine subcutaneously (Tribissen, Five Star Compounding Pharmacy, Clive, IA). Postoperatively, the rats were individually housed and provided with food and water *ad libitum* with a 12-hour light-dark cycle.

Ultrasound measurements

The cross-sectional tibial muscle area of six randomly selected rats per group was evaluated with ultrasound measurements of both sides at baseline and at two, four, eight, twelve and sixteen weeks after surgery as previously described using a GE Vivid 7 Ultrasound system (General Electric, Fairfield, CT, USA) [31,32]. Cross-sectional area was calculated with Adobe Photoshop CC 2018 (Adobe Systems Incorporated, San Jose, CA, USA).

Nonsurvival procedure

At 12 and 16 weeks, ten rats of each group underwent a non-survival procedure. Anesthesia was induced by isoflurane, followed by intraperitoneal injection of Ketamine (80mg/kg) and Xylazine (10mg/kg) and maintained by additional doses of Ketamine (40mg/kg).

Compound Muscle Action Potentials (CMAP) - A miniature bipolar electrode was clamped around the sciatic nerve proximal to the nerve graft. One ground electrode was placed in surrounding musculature and two recording electrodes were superficially placed in the anterior tibial muscle. The CMAP was measured using a VikingQuest portable electromyelogram (Nicolet Biomedical, Madison, WI). A non-recurrent single stimulation with a duration of 0.02ms at an intensity level of 2.7mA was applied. Maximal amplitude measurements were obtained bilaterally [33,34].

Isometric Tetanic Force (ITF) - The ITF was measured bilaterally per the protocol of Shin and colleagues [35]. The peroneal nerve and tibial muscle were exposed and the hind limb was secured to a testing platform with K-wires through the femur and ankle. The tibial tendon was secured to a clamp in anatomical position and attached to a force transducer (MDB-50; Transducer Techniques, Temecula, CA, USA) whose signals were processed using LabView (National instruments, Austin, Texas). A miniature electrode (Harvard Apparatus, Holliston, MA, USA), stimulated by a bipolar stimulator (Medtronic, Minneapolis, MN, USA) was clamped around the peroneal nerve branch of the sciatic nerve. The muscle tension and the stimulator frequency were optimized after which the maximal ITF was obtained. The tibial muscle was kept moist with warm saline.

Wet tibial muscle mass - Rats were euthanized with an overdose of pentobarbital (Fatal Plus, 390 mg/mL, Vortech, Dearborn, MI, USA) intraperitoneally. Tibial muscles were harvested bilaterally and wet muscle mass was determined after removing the tendon.

Histology **-** A three millimeter segment of both peroneal nerves of all rats were collected and placed into Trumps solution. Specimens were processed with 0.1M Phosphate Buffer, 1% Osmium tetroxide in buffer, graded series of alcohol and acetone. The samples were infiltrated in a 50%, 75% and finally 100% epoxy resin and polymerized

at 65°C for 12-18 hours. Samples were cut in sections at 0.6 microns, placed on slides and stained on a warming plate with Toluidine blue for 2-2.5 minutes. The total tissue cable area (nerve area), axon area, axon count and myelin area were obtained using a Nikon Eclipse 50i microscope and Image Pro Plus Software. The N-ratio was calculated by dividing the myelinated fiber area (axon area and myelin area) by the tissue cable area [36].

Immunofluorescence - Both sciatic nerves of five randomly selected rats per group were dissected and fixed in 10% formalin for 48 hours. Nerves samples were vertically embedded in paraffin and sections from the exact middle were stained for Schwann cell marker S100 and protein gene product 9.5 (PGP9.5), a pan neuronal marker. Immunohistochemical staining was performed at the Pathology Research Core (Mayo Clinic, Rochester, MN, USA) using the Leica Bond RX stainer (Leica, Buffalo Grove, IL, USA). The S100 (rabbit polyclonal; Dako, Agilent Technologies Inc., Carpinteria, CA, USA) and PGP9.5 primary antibody (rabbit polyclonal; Dako, Agilent Technologies Inc.) were diluted to 1:5000 in Background Reducing Diluent (Dako, Agilent Technologies Inc.) and incubated for 60 minutes with the samples, prior to staining with the appropriate secondary antibody (Alexa Goat-Anti-Rabbit 488, 1:300, for S100 and Alexa Goat-Anti-Rabbit 568, 1:200 for PGP9.5) and counterstained with Hoechst 33342 (all ThermoFisher Scientific, MA, USA). Images of the stained slides were obtained with a fluorescence laser confocal microscope (Zeiss LSM 780, Carl Zeiss Surgical GmbH, Oberkochen, Germany). The mean fluorescent density of both stains was measured using ImageJ software.

Statistical analysis

All obtained images were blinded and all outcomes were expressed as a percentage of the contralateral side to correct for biological variability between rats. Non-physiologic outcomes were excluded from analysis after review by a statistician and an independent researcher. Two-way analysis of variance (ANOVA) was used for the cross-sectional tibial area measurements. One-way ANOVA was used to compare all other outcome measures between groups. Post-hoc Bonferroni was used to correct for multiple comparisons. Outcomes were expressed as the mean and the standard error of the mean (SEM). Outcomes of cross-sectional tibial muscle area were expressed as mean difference and the standard error of the mean difference. The level of significance was set at $\alpha \leq 0.05$.

RESULTS

MSC differentiation

Differentiated MSCs showed immunofluorescence for the markers S100, GFAP and p75 NTR, corresponding to Schwann cells that served as positive controls. Undifferentiated MSCs did not show expression of these markers (Figure 1).

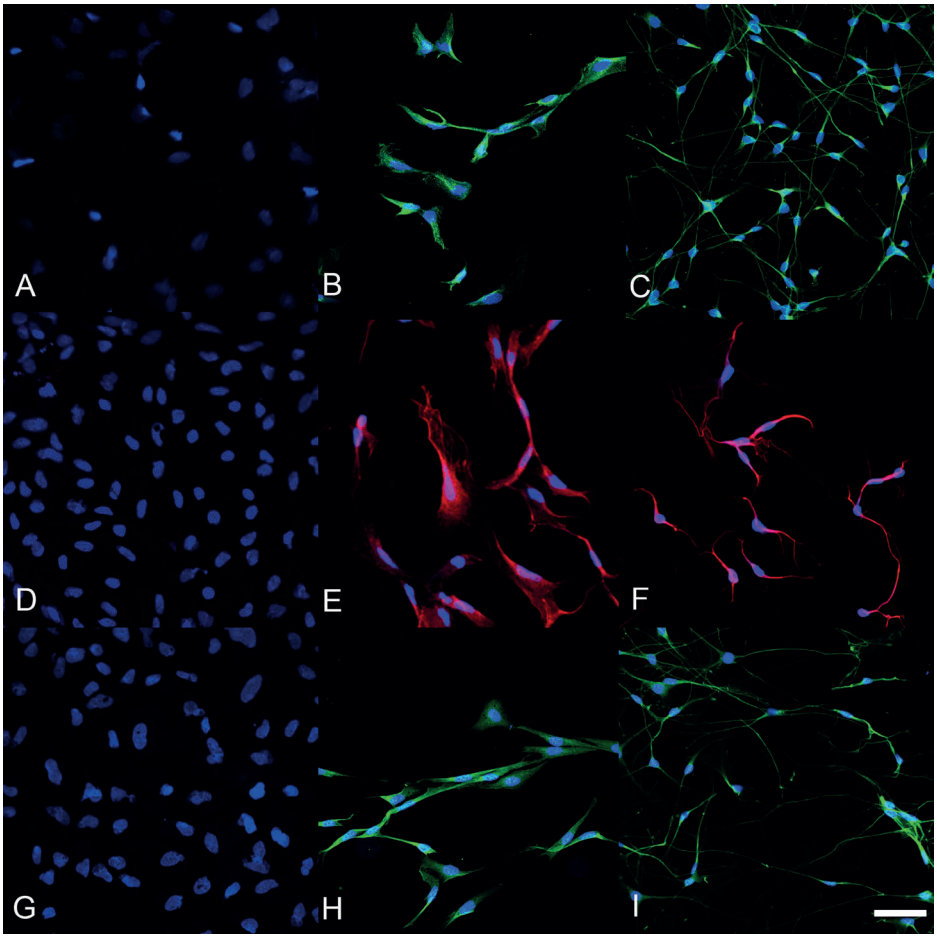

Figure 1. Differentiation of MSCs into Schwann-like cells. Comparison of immunocytochemistry between undifferentiated MSCs (A-D-G), differentiated MSCs (B-E-H) and Schwann cells (C-F-I). Cells are tested for the presence of Schwann cell marker S100 (green, A-B-C), glial cell marker GFAP (red, D-E-F) and neurotrophin Receptor p75 (green, G-H-I). Cell nuclei are DAPI-stained (blue). 40X magnificantion, white scale bar = 40mm.

Functional outcome measurements

Cross-sectional tibial muscle area

No significant differences between the groups were found (Figure 2). Within group comparisons only showed significant differences between the consecutive time points zero and two weeks after surgery for autografts, allografts and allografts seeded with differentiated MSCs. The lowest tibial muscle area in all groups was reached at two weeks (40-60% of the unoperated side) and improved upto 16 weeks, with a cross-sectional tibial muscle area ratio of approximately 75%.

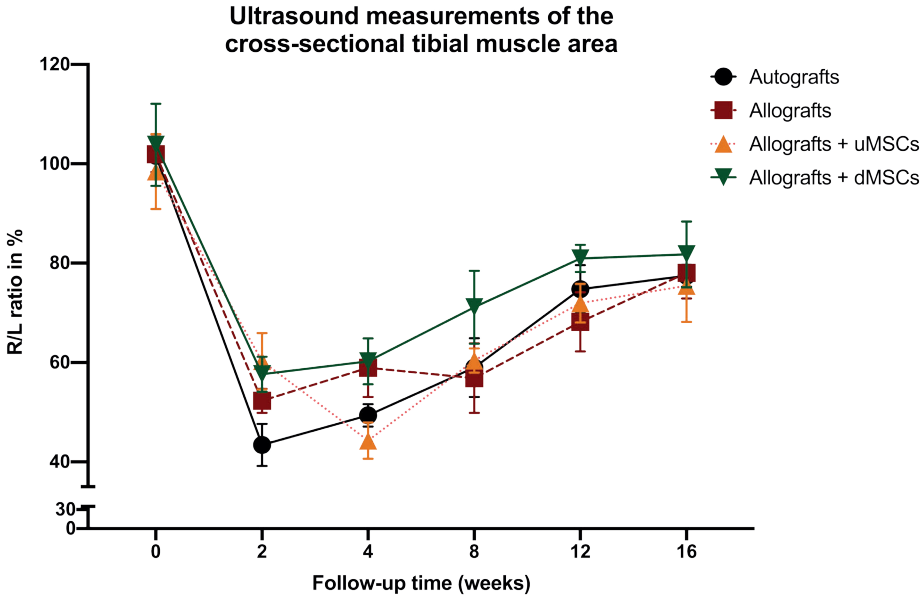

Figure 2. Cross-sectional tibial muscle area ratios (R/L) over time. No significant differences were found between groups. Autografts (+15.77 ±6.56%) and unseeded allografts (+11.33 ±9.22%) had the strongest increase in muscle area between 8 and 12 weeks, while allografts seeded with undifferentiated MSCs (+16.13 ±3.83%) and differentiated MSCs (+10.87 ±9.29%) experienced their strongest increase between 4 and 8 weeks after surgery. uMSCs: undifferentiated MSCs, dMSCs: differentiated MSCs, error bars: Standard error of the mean.

Compound Muscle Action Potential (CMAP)

At 12 weeks, CMAP ratio of unseeded allografts (13.48 ±5.00%) was significantly inferior to autografts (53.78 ±5.82%) (P<0.001), allografts seeded with undifferentiated MSCs (44.32 ±7.20%) (P=0.004) and differentiated MSCs (48.89 ±5.37%) (P<0.001, Figure 3). At 16 weeks, CMAP ratio was normalized between all groups, with 57.51 ±7.54% for autografts, 52.26 ±5.80% for allografts, 66.04 ±7.28% for allografts with undifferentiated MSCs and 61.49±8.16% for allografts with differentiated MSCs.

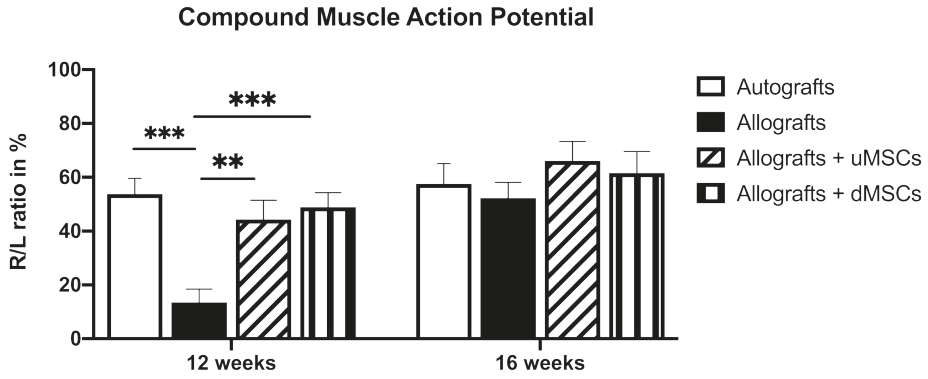

Figure 3. Compound muscle action potential ratios (CMAP, R/L) at 12 and 16 weeks. CMAP recovery of unseeded allografts was significantly inferior compared to all other groups at 12 weeks. uMSCs: undifferentiated MSCs, dMSCs: differentiated MSCs, * indicated P<0.05, ** indicated P<0.01, *** indicated P<0.001, error bars: Standard error of the mean.

Isometric Tetanic Force (ITF)

The ITF ratio of allografts seeded with undifferentiated MSCs (49.74 ±6.80%) was significantly higher compared to unseeded allografts (26.32 ±4.36%) (P=0.017) at 12 weeks (Figure 4). The ratio in autografts (44.16 ±3.32%) and allografts seeded with differentiated MSCs (43.10 ±4.59%) did not demonstrate significant differences with any of the other groups. At 16 weeks, the ITF ratio of autografts (51.11 ±4.98%), allografts (56.22 ±4.44%), allografts with undifferentiated MSCs (56.12 ±6.51%) and allografts with differentiated MSCs (53.86 ±4.47%) did not significantly differ.

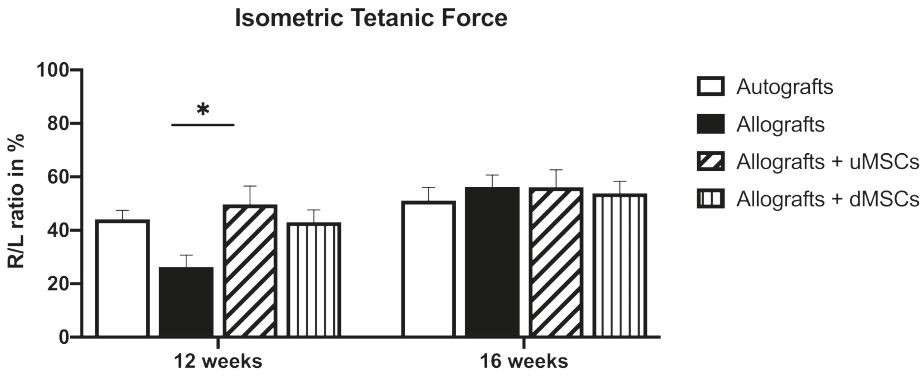

Figure 4. Isometric Tetanic Force ratios (R/L) at 12 and 16 weeks. ITF recovery of unseeded allografts were significantly inferior compared to allografts seeded with undifferentiated MSCs at 12 weeks. uMSCs: undifferentiated MSCs, dMSCs: differentiated MSCs, * indicated P<0.05, ** indicated P<0.01, *** indicated P<0.001, error bars: Standard error of the mean.

Muscle mass

At 12 weeks, unseeded allografts measured a significantly lower tibial muscle mass ratio (49.54 ±2.30%) compared to autografts (59.84 ±1.64%) (P=0.021, Figure 5). Allografts with undifferentiated and differentiated MSCs measured a muscle mass ratio of 57.68 ±2.87% and 55.21 ±2.36% respectively. At 16 weeks, the muscle mass ratio of allografts seeded with undifferentiated MSCs was 59.96 ±3.79%, which significantly differed from autografts (74.13 ±1.90%) (P=0.002). Unseeded allografts and allografts seeded with differentiated MSCs had a muscle mass ratio of 69.09 ±1.54% and 70.09 ±2.60% respectively.

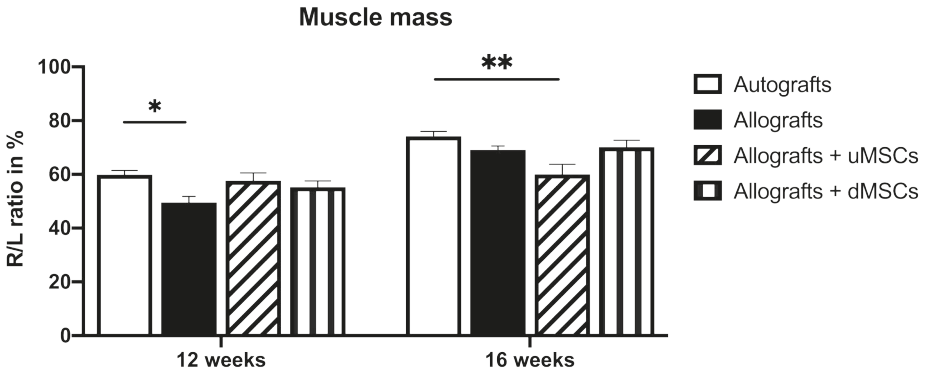

Figure 5. Wet tibial muscle mass ratios (R/L) at 12 and 16 weeks. Autografts showed a significantly higher muscle mass recovery compared to unseeded allografts at 12 weeks, and allografts seeded with undifferentiated MSCs at 16 weeks. uMSCs: undifferentiated MSCs, dMSCs: differentiated MSCs, * indicated P<0.05, ** indicated P<0.01, *** indicated P<0.001, error bars: Standard error of the mean.

Histology

All obtained histology and immunofluorescence values are displayed in table 1. Figure 6 provides representative nerve sections of the different groups. At 12 weeks, autografts had a significant larger axon area ratio compared to unseeded allografts (P<0.001), allografts seeded with undifferentiated MSCs (P<0.001) and allografts seeded with differentiated MSCs (P=0.004). At 16 weeks, no significant differences in axon area ratio between groups were found. The axon count, myelin area and nerve area measures did not demonstrate any significant differences between groups at any of the time points. Autografts had a significant higher N-ratio compared to unseeded allografts (P=0.023) and allografts seeded with undifferentiated MSCs (P=0.040) at 12 weeks. At 16 weeks, autografts had a significantly better N-ratio compared to unseeded allografts (P=0.003), allografts with undifferentiated MSCs (P=0.025) and allografts with differentiated MSCs (P=0.002) (Figure 7).

Table 1. Histology and immunofluorescence outcomes obtained at 12 and 16 weeks for all groups. Outcomes are displayed as the mean and the standard error of the mean (SEM).

	Autografts	Allografts	Allografts + undifferentiated MSCs	Allografts + differentiated MSCs
Axon area				
12 weeks	27.58 ±2.93%	10.14 ±1.89%	11.76 ±1.62%	15.48 ±2.27%
16 weeks	35.95 ±4.63%	21.90 ±3.41%	20.07 ±3.18%	20.84 ±5.65%
Axon count				
12 weeks	56.87 ±7.47%	32.42 ±5.38%	39.61 ±5.11%	47.39 ±5.55%
16 weeks	50.93 ±7.20%	38.94 ±2.67%	42.04 ±6.91%	43.37 ±13.49%
Myelin area				
12 weeks	57.12 ±4.77%	38.43 ±7.18%	40.11 ±3.58%	46.86 ±4.06%
16 weeks	69.63 ±8.12%	57.53 ±6.25%	50.69 ±5.72%	41.93 ±7.33%
Nerve area				
12 weeks	77.97 ±7.58%	63.77 ±5.74%	61.58 ±3.53%	71.09 ±6.23%
16 weeks	77.37 ±8.55%	79.18 ±8.09%	66.27 ±7.40%	60.74 ±8.77%
N-ratio				
12 weeks	59.06 ±2.48%	42.62 ±5.89%	46.58 ±3.59%	46.58 ±3.59%
16 weeks	72.22 ±2.93%	53.57 ±3.04%	57.53 ±2.74%	51.71 ±5.34%
S100 density				
12 weeks	96.48 ±1.16%	97.84 ±1.65%	92.85 ±3.17%	94.88 ±3.11%
16 weeks	102.37 ±6.94%	93.54 ±2.38%	94.61 ±3.86%	95.92 ±5.90%
PGP9.5 density				
12 weeks	106.95 ±16.30%	105.26 ±4.88%	101.13 ±9.55%	98.62 ±7.97%
16 weeks	92.81 ±5.15%	101.89 ±12.22%	98.13 ±13.88%	76.68 ±6.25%

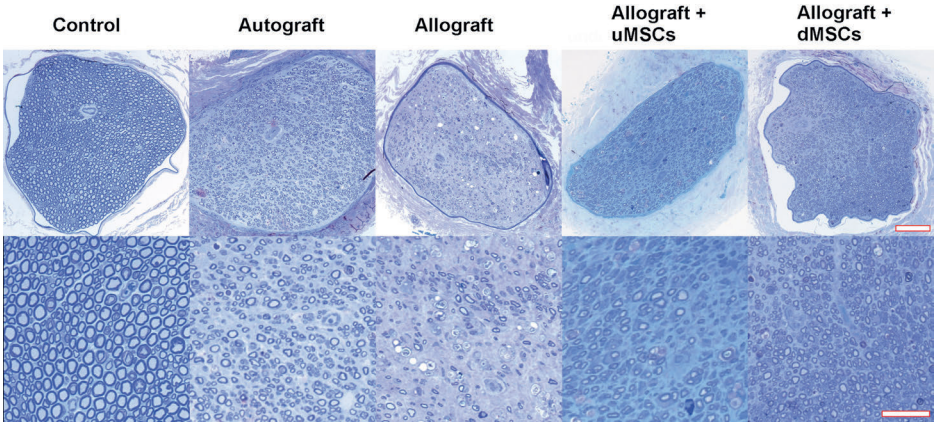

Figure 6. Examples of obtained images of peroneal nerve sections stained with toluidine blue at 12 weeks of follow-up. Scale bar upper images = 1mm, lower images = 0.5mm.

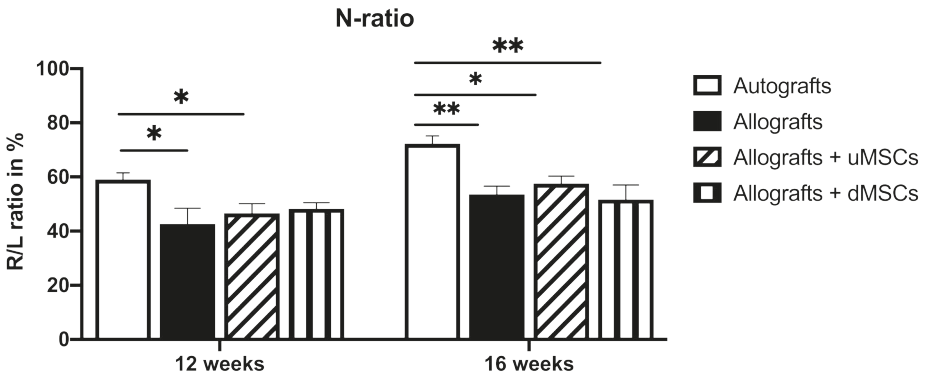

Figure 7. N-ratios (R/L) at 12 and 16 weeks. Autografts had a significant better N-ratio than unseeded allografts and allografts seeded with undifferentiated MSCs at 12 weeks and compared to other groups at 16 weeks. uMSCs: undifferentiated MSCs, dMSCs: differentiated MSCs, * indicated P<0.05, ** indicated P<0.01, *** indicated P<0.001, error bars: Standard error of the mean.

Immunofluorescence

S100 and PGP9.5 density outcomes are displayed in table 1. Examples of obtained immunofluorescence images are displayed in Figure 8. Between group comparisons showed no significant differences in S100 and PGP9.5 density ratio at both time points (Figure 9).

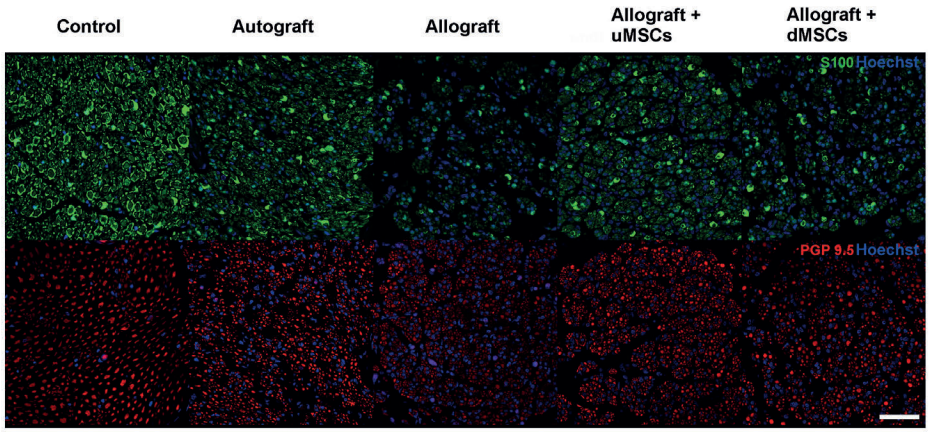

Figure 8. An overview of immunofluorescent staining of S100 (Schwann cells, green) and protein gene product 9.5 (PGP9.5, red), respectively. Micrographs showing density in mid-distal graft sections from control nerve samples, autograft, allograft, allografts seeded with undifferentiated mesenchymal stem cells (uMSC) and mesenchymal stem cells differentiated into Schwann cell-like cells (dMSC) at 12 weeks. Cell nuclei are stained with Hoechst (blue) and obtained with 20X magnification. The white scale bar is set at 0.2 mm.

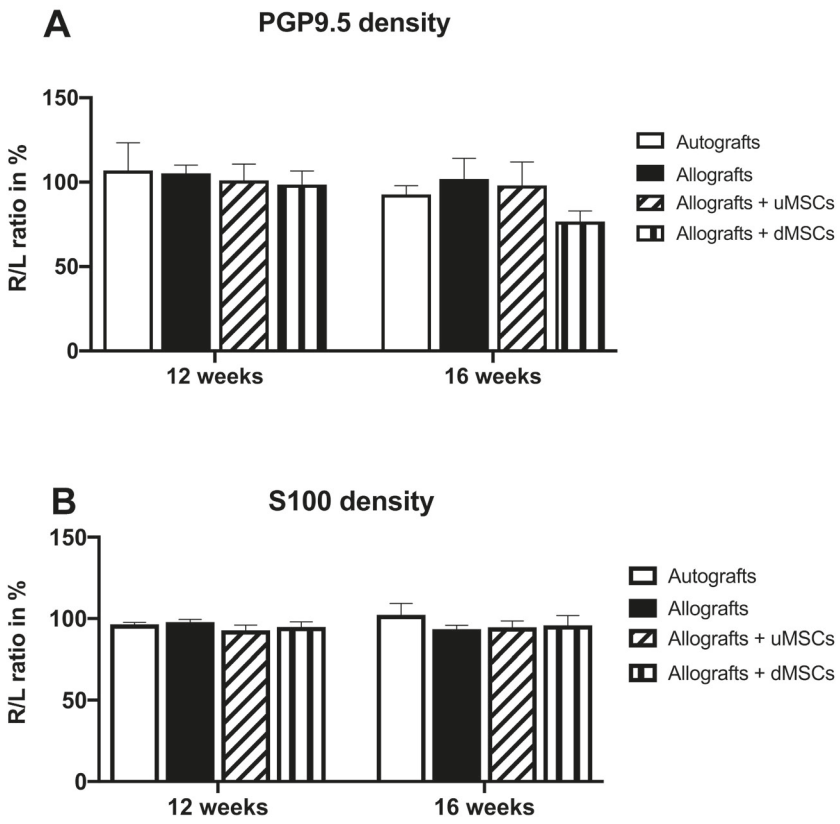

Figure 9. Immunofluorescent staining of protein gene product 9.5 (PGP9.5) and S100 at 12 and 16 weeks. Density of axons (normalized to the combined area of tissues positively stained for any of PGP9.5, S100 and Hoechst) is shown in A and B, respectively, expressed in percentages. No differences were found between groups or time points for either PGP 9.5 or S100. uMSCs = undifferentiated MSCs, dMSCs = differentiated MSCs. error bars Standard error of the mean.

DISCUSSION

Despite advances in decellularization techniques for allograft nerves, nerve autograft remain the gold standard for segmental defect reconstruction of critical motor or sensory nerves [1,6]. To overcome the limitations of decellularized allograft nerves, MSCs have been hypothesized to improve outcomes of decellularized allograft nerves [7] by producing proteins and cytokines that establish a micro-environment favorable for neural regeneration [8,12-14,37]. Differentiated MSCs have been demonstrated to exert their neurotrophic effect immediately after implementation by expressing increased levels of neurotrophic genes, while undifferentiated MSCs require additional time to interact with the surrounding tissue prior to expressing neurotrophic genes [14]. The purpose of this study was to determine the effect of dynamically seeding undifferentiated and differentiated MSCs onto decellularized nerve allografts [7] with respect to functional and histologic outcomes in a rat sciatic defect model, in order to determine which cell-type has greatest clinical potential.

In this study, MSCs were successfully differentiated into Schwann cell-like cells [16] and dynamically seeded onto decellularized nerve allografts [27]. Compared to unseeded allografts, undifferentiated MSCs led to significant improvement of both ITF and CMAP (P=0.017 and P=0.004) outcomes at 12 weeks, while differentiated MSCs only led to significant improved CMAP outcomes (P<0.001). These findings correspond to the study of Hou and colleagues whom observed that (differentiated) MSC-seeded grafts recovered earlier than acellular grafts when measuring electrophysiology, with significant results at 12 weeks [38]. Differences between groups normalized at 16 weeks which is consistent with the study of Tang and colleagues, demonstrating normalizing ITF measurements at 16 weeks of follow-up [39]. Functional assessment did not result in any significant differences between both cell-types for all functional outcome measures at 12 and 16 weeks, which is in line with published studies of Orbay and Watanabe [22,23]. The hypothesized consequences of different effective phases of both cell-types could not be confirmed in this study.

At 16 weeks, no significant differences in functional outcomes between groups were found, except for muscle mass recovery that was significantly better in autografts than in allografts seeded with differentiated MSCs (P=0.002). Although muscle mass is easily obtainable, it is an indirect measurement of motor outcome as enlarged muscle

fibers do not neccesarily feature improved contractility [36]. ITF has been described to objectively quantify contractility of muscle fibers and is easily reproducible [36]. The vulnerability of CMAP measurements, which is affected by the placement of all individual electrodes, may explain why the CMAP outcomes are greater than the ITF measures [40].

Histologically, the autografts had significantly better N-ratios in the peroneal nerves at both time points compared to all other groups. Although not examined, this could be explained by less formation of fibrosis in autografts [41]. Due to small groups and insufficient sensitivity of density measures, the histology outcomes could not be significantly confirmed by immunofluorescence outcomes, but unseeded nerve allografts subjectively seem to contain less Schwann cells and axons compared to all other groups.

Autografts were used as control group to test whether MSCs could improve outcomes of decellularized allografts up to a level equal to that of autografts. While an additional control group in which sham surgery is performed would also be interesting to include, it would require the undesirable and precious use of additional animals. Alternatively, outcomes of the operated side were normalized to the unoperated control side in order to relate the test-outcomes to normal nerve and muscle function (providing a R/L ratio).

The significant differences between groups presented at 12 weeks and normalized after 16 weeks, insinuates that nerve regeneration in motor nerves in rats will occur after 12 weeks, independently from the type of nerve repair. This finding may be correlated to the demonstrated finite survival of MSCs up to 29 days *in vivo*. It is suggested that MSCs significantly enhance nerve regeneration up to 12 weeks after which the superlative neuroregenerative capacity of rats takes over, due to the apoptosis of the MSCs [42]. The superlative neuroregenerative capacity of rats is a commonly described explanation and can be mitigated in a larger animal model [26,39]. Absent significant differences when comparing cross-sectional tibial muscle areas is also a likely consequence of using a small animal model with small cross-sectional nerve areas, relatively leading to larger standard errors and less significant differences between groups [31,32]. Future research should be performed on multiple time points in larger animal models with larger nerve gaps to potentially translate outcomes to humans.

Considering the overall goal to improve outcomes of decellularized nerve allografts in clinical practice, clinical applicability should be considered when interpretating results. The use of autologous differentiated MSCs requires approximately 4-5 weeks of preparation time, compared to 2-3 weeks for undifferentiated MSCs [16]. Moreover, the costs of the differentiation cocktail required to differentiate MSCs into Schwann cell-like cells are high and add to the costs of extended cell culture. Differences between undifferentiated an differentiated MSCs were not statistically significant in light of the analyzed factors, but undifferentiated MSCs improved functional outcomes of decellularized nerve allografts to a greater extent than differentiated MSCs. Taking all of these factors into consideration, undifferentiated MSCs have the greatest potential for bench-to-bedside application. Hypothetically, at the day of presentation in a clinical setting, adipose tissue can be obtained using minimally invasive techniques from the patient with nerve injury, MSCs can then be derived from this tissue and cultured for approximately two weeks after which the MSCs can be dynamically seeded onto an off-the-shelf commercially available nerve allografts, 12 hours in advance of the nerve repair. Translation to a larger animal model to ensure the enhanced functional outcomes, study of the capacity of human MSCs to be seeded on clinically available nerve allografts and FDA approval are potential hurdles that need to be addressed prior to application of the presented strategy in clinical practice.

CONCLUSIONS

Undifferentiated and differentiated MSCs significantly improved functional outcomes of decellularized allografts at 12 weeks in motor nerves and equaled the autograft results in the majority of outcome measurements. At 16 weeks, outcome measures normalized as expected. Considering clinical applicability, undifferentiated MSCs are more attractive as outcomes did not significantly differ between both cell-types, and differentiation requires increased time and cost.

Acknowledgements

We thank Roman Thaler, PhD, for assisting with cell culture and differentiation of the mesenchymal stem cells. We thank Patricia F. Friedrich for assistance with the preparations of the experiments.

REFERENCES

1. Giusti G, Willems WF, Kremer T, Friedrich PF, Bishop AT, Shin AY. Return of motor function after segmental nerve loss in a rat model: comparison of autogenous nerve graft, collagen conduit, and processed allograft (AxoGen). *The Journal of bone and joint surgery American volume.* 2012;94(5):410-417.
2. Millesi H. Progress in peripheral nerve reconstruction. *World J Surg.* 1990;14(6):733-747.
3. Mackinnon SE, Hudson AR, Falk RE, Hunter DA. The nerve allograft response--an experimental model in the rat. *Ann Plast Surg.* 1985;14(4):334-339.
4. Whitlock EL, Tuffaha SH, Luciano JP, et al. Processed allografts and type I collagen conduits for repair of peripheral nerve gaps. *Muscle & nerve.* 2009;39(6):787-799.
5. Cho MS, Rinker BD, Weber RV, et al. Functional outcome following nerve repair in the upper extremity using processed nerve allograft. *The Journal of hand surgery.* 2012;37(11):2340-2349.
6. Rbia N, Shin AY. The Role of Nerve Graft Substitutes in Motor and Mixed Motor/Sensory Peripheral Nerve Injuries. *The Journal of hand surgery.* 2017;42(5):367-377.
7. Hundepool CA, Nijhuis TH, Kotsougiani D, Friedrich PF, Bishop AT, Shin AY. Optimizing decellularization techniques to create a new nerve allograft: an in vitro study using rodent nerve segments. *Neurosurgical focus.* 2017;42(3).
8. Caplan AI. Adult Mesenchymal Stem Cells: When, Where, and How. *Stem cells international.* 2015;2015:628767.
9. Mushtaq M, DiFede DL, Golpanian S, et al. Rationale and design of the Percutaneous Stem Cell Injection Delivery Effects on Neomyogenesis in Dilated Cardiomyopathy (the POSEIDON-DCM study): a phase I/II, randomized pilot study of the comparative safety and efficacy of transendocardial injection of autologous mesenchymal stem cell vs. allogeneic mesenchymal stem cells in patients with non-ischemic dilated cardiomyopathy. *Journal of cardiovascular translational research.* 2014;7(9):769-780.
10. Shen H, Wang Y, Zhang Z, Yang J, Hu S, Shen Z. Mesenchymal Stem Cells for Cardiac Regenerative Therapy: Optimization of Cell Differentiation Strategy. *Stem cells international.* 2015;2015:524756.
11. Nam HY, Karunanithi P, Loo WC, et al. The effects of staged intra-articular injection of cultured autologous mesenchymal stromal cells on the repair of damaged cartilage: a pilot study in caprine model. *Arthritis research & therapy.* 2013;15(5):R129.
12. Castro-Manrreza ME, Montesinos JJ. Immunoregulation by mesenchymal stem cells: biological aspects and clinical applications. *Journal of immunology research.* 2015;2015:394917.
13. Rbia N, Bulstra LF, Saffari TM, Hovius SER, Shin AY. Collagen Nerve Conduits and Processed Nerve Allografts for the Reconstruction of Digital Nerve Gaps: A Single-Institution Case Series and Review of the Literature. *World neurosurgery.* 2019;127:e1176-e1184.
14. Mathot F, Rbia N, Thaler R, Bishop AT, Van Wijnen AJ, Shin AY. Gene expression profiles of differentiated and undifferentiated adipose derived mesenchymal stem cells dynamically seeded onto a processed nerve allograft. *Gene.* 2020;724:144151.

15. Mathot F, Shin AY, Van Wijnen AJ. Targeted stimulation of MSCs in peripheral nerve repair. *Gene.* 2019.
16. Kingham PJ, Kalbermatten DF, Mahay D, Armstrong SJ, Wiberg M, Terenghi G. Adipose-derived stem cells differentiate into a Schwann cell phenotype and promote neurite outgrowth in vitro. *Experimental neurology.* 2007;207(2):267-274.
17. Yoshimura H, Muneta T, Nimura A, Yokoyama A, Koga H, Sekiya I. Comparison of rat mesenchymal stem cells derived from bone marrow, synovium, periosteum, adipose tissue, and muscle. *Cell and tissue research.* 2007;327(3):449-462.
18. di Summa PG, Kingham PJ, Raffoul W, Wiberg M, Terenghi G, Kalbermatten DF. Adipose-derived stem cells enhance peripheral nerve regeneration. *Journal of plastic, reconstructive & aesthetic surgery : JPRAS.* 2010;63(9):1544-1552.
19. Kingham PJ, Kolar MK, Novikova LN, Novikov LN, Wiberg M. Stimulating the neurotrophic and angiogenic properties of human adipose-derived stem cells enhances nerve repair. *Stem cells and development.* 2014;23(7):741-754.
20. Tomita K, Madura T, Sakai Y, Yano K, Terenghi G, Hosokawa K. Glial differentiation of human adipose-derived stem cells: implications for cell-based transplantation therapy. *Neuroscience.* 2013;236:55-65.
21. Ladak A, Olson J, Tredget EE, Gordon T. Differentiation of mesenchymal stem cells to support peripheral nerve regeneration in a rat model. *Experimental neurology.* 2011;228(2):242-252.
22. Orbay H, Uysal AC, Hyakusoku H, Mizuno H. Differentiated and undifferentiated adipose-derived stem cells improve function in rats with peripheral nerve gaps. *Journal of plastic, reconstructive & aesthetic surgery : JPRAS.* 2012;65(5):657-664.
23. Watanabe Y, Sasaki R, Matsumine H, Yamato M, Okano T. Undifferentiated and differentiated adipose-derived stem cells improve nerve regeneration in a rat model of facial nerve defect. *Journal of tissue engineering and regenerative medicine.* 2017;11(2):362-374.
24. Keilhoff G, Goihl A, Stang F, Wolf G, Fansa H. Peripheral nerve tissue engineering: autologous Schwann cells vs. transdifferentiated mesenchymal stem cells. *Tissue engineering.* 2006;12(6):1451-1465.
25. Kappos EA, Engels PE, Tremp M, et al. Peripheral Nerve Repair: Multimodal Comparison of the Long-Term Regenerative Potential of Adipose Tissue-Derived Cells in a Biodegradable Conduit. *Stem cells and development.* 2015;24(18):2127-2141.
26. Rbia N, Bulstra LF, Thaler R, Hovius SER, van Wijnen AJ, Shin AY. In Vivo Survival of Mesenchymal Stromal Cell-Enhanced Decellularized Nerve Grafts for Segmental Peripheral Nerve Reconstruction. *The Journal of hand surgery.* 2018.
27. Mathot F, Rbia N, Bishop AT, Hovius SER, Van Wijnen AJ, Shin AY. Adhesion, distribution, and migration of differentiated and undifferentiated mesenchymal stem cells (MSCs) seeded on nerve allografts. *Journal of plastic, reconstructive & aesthetic surgery : JPRAS.* 2019.
28. Rbia N, Bulstra LF, Bishop AT, van Wijnen AJ, Shin AY. A simple dynamic strategy to deliver stem cells to decellularized nerve allografts. *Plastic and reconstructive surgery.* 2018.
29. Hudson TW, Zawko S, Deister C, et al. Optimized acellular nerve graft is immunologically tolerated and supports regeneration. *Tissue engineering.* 2004;10(11-12):1641-1651.

30. Kumta S, Yip K, Roy N, Lee SK, Leung PC. Revascularisation of bone allografts following vascular bundle implantation: an experimental study in rats. *Arch Orthop Trauma Surg.* 1996;115(3-4):206-210.
31. Hundepool CA, Nijhuis TH, Rbia N, Bulstra LF, Selles RW, Hovius SE. Noninvasive Ultrasound of the Tibial Muscle for Longitudinal Analysis of Nerve Regeneration in Rats. *Plastic and reconstructive surgery.* 2015;136(5):633e-639e.
32. Bulstra LF, Hundepool CA, Friedrich PF, Nijhuis TH, Bishop AT, Shin AY. Motor Nerve Recovery in a Rabbit Model: Description and Validation of a Noninvasive Ultrasound Technique. *The Journal of hand surgery.* 2016;41(1):27-33.
33. Hundepool CA, Bulstra LF, Kotsougiani D, et al. Comparable functional motor outcomes after repair of peripheral nerve injury with an elastase-processed allograft in a rat sciatic nerve model. *Microsurgery.* 2018;38(7):772-779.
34. Giusti G, Lee JY, Kremer T, Friedrich P, Bishop AT, Shin AY. The influence of vascularization of transplanted processed allograft nerve on return of motor function in rats. *Microsurgery.* 2016;36(2):134-143.
35. Shin RH, Vathana T, Giessler GA, Friedrich PF, Bishop AT, Shin AY. Isometric tetanic force measurement method of the tibialis anterior in the rat. *Microsurgery.* 2008;28(6):452-457.
36. Vleggeert-Lankamp CL. The role of evaluation methods in the assessment of peripheral nerve regeneration through synthetic conduits: a systematic review. Laboratory investigation. *J Neurosurg.* 2007;107(6):1168-1189.
37. Ma S, Xie N, Li W, Yuan B, Shi Y, Wang Y. Immunobiology of mesenchymal stem cells. *Cell death and differentiation.* 2014;21(2):216-225.
38. Hou SY, Zhang HY, Quan DP, Liu XL, Zhu JK. Tissue-engineered peripheral nerve grafting by differentiated bone marrow stromal cells. *Neuroscience.* 2006;140(1):101-110.
39. Tang P, Whiteman DR, Voigt C, Miller MC, Kim H. No Difference in Outcomes Detected Between Decellular Nerve Allograft and Cable Autograft in Rat Sciatic Nerve Defects. *J Bone Joint Surg Am.* 2019;101(10):e42.
40. S. Saffari TMS, A.M. Moore, A.Y. Shin. Peripheral Nerve Basic Science Research – What is important for hand surgeons to know? *J Hand Surg Am.* 2021.
41. den Dunnen WF, van der Lei B, Schakenraad JM, et al. Poly(DL-lactide-epsilon-caprolactone) nerve guides perform better than autologous nerve grafts. *Microsurgery.* 1996;17(7):348-357.
42. Rbia N, Bulstra LF, Thaler R, Hovius SER, van Wijnen AJ, Shin AY. In Vivo Survival of Mesenchymal Stromal Cell-Enhanced Decellularized Nerve Grafts for Segmental Peripheral Nerve Reconstruction. *The Journal of hand surgery.* 2019;44(6):514.e511-514.e511.

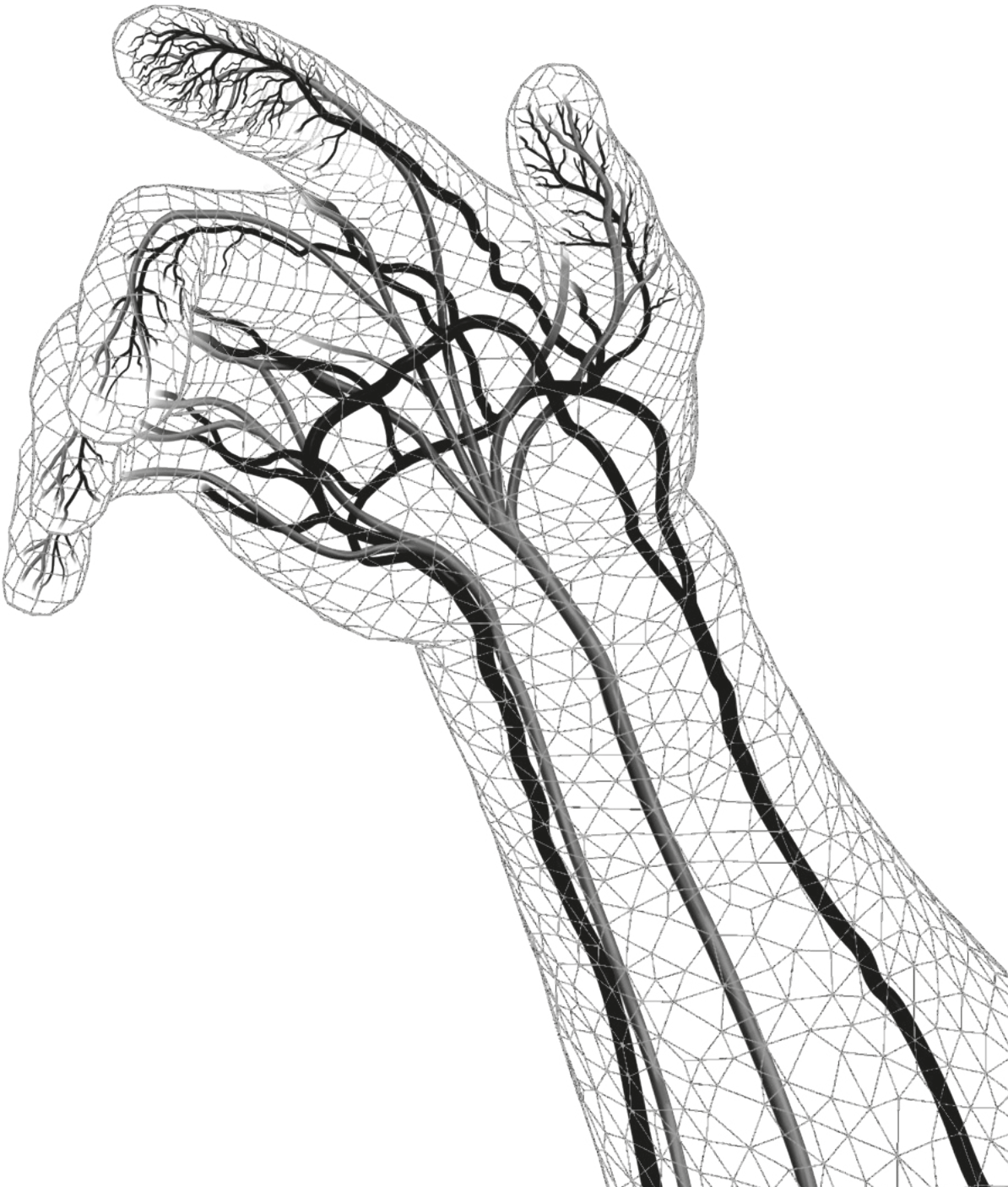

CHAPTER

TEN

Microcomputed Analysis of Nerve Angioarchitecture after Combined Stem Cell Delivery and Surgical Angiogenesis to Nerve Allograft

Tiam M. Saffari[1,2]
Femke Mathot[1,2]
Roman Thaler[1]
Andre J. van Wijnen[1,3]
Allen T. Bishop[1]
Alexander Y. Shin[1]

Affiliations

[1]Department of Orthopedic Surgery, Mayo Clinic, Rochester, MN, USA
[2]Department of Plastic-, Reconstructive- and Hand Surgery, Radboud University, Nijmegen, the Netherlands
[3]Department of Biochemistry and Molecular Biology, Mayo Clinic, Rochester, MN, USA

Journal of Plastic, Reconstructive & Aesthetic Surgery. 2020 Dec 24.

ABSTRACT

Introduction

Detailed three-dimensional (3D) evaluation of microvasculature is evolving to be a powerful tool, providing mechanistic understanding of angiomodulating strategies. The aim of this study was to evaluate the microvascular architecture of nerve allografts after combined stem cell delivery and surgical angiogenesis in a rat sciatic nerve defect model.

Materials and Methods

In 25 Lewis rats, sciatic nerve gaps were repaired with (i) autografts, (ii) allografts, (iii) allografts wrapped in a pedicled superficial inferior epigastric artery fascia (SIEF) flap to provide surgical angiogenesis, combined with (iv) undifferentiated mesenchymal stem cells (MSC) and (v) MSCs differentiated into Schwann cell-like cells. At two weeks, vascular volume was measured using microcomputed tomography, and percentage and volume of vessels at different diameters were evaluated and compared to controls.

Results

The vascular volume was significantly greatest in allografts treated with undifferentiated MSCs and surgical angiogenesis combined, compared to all experimental groups ($P<0.01$ compared to autografts, $P<0.0001$ to allografts, $P<0.05$ to SIEF and SIEF combined with differentiated MSCs, respectively). Volume and diameters of vessel segments in nerve allografts were enhanced by surgical angiogenesis. These distributions were further improved when surgical angiogenesis was combined with stem cells, with greatest increase found when combined with undifferentiated MSCs.

Conclusions

The interaction between vascularity and stem cells remains complex, however, this study provides some insight into its synergistic mechanisms. The combination of surgical angiogenesis with undifferentiated MSCs specifically, results in the greatest increase of revascularization, size of vessels, and stimulation of vessels to reach the middle longitudinal third of the nerve allograft.

INTRODUCTION

The outcome of tissue transplantation critically depends on tissue revascularization [1]. Nerve trauma is often associated with extensive soft tissue damage, enhancing disability and impeding restoration of limb function [2]. In adult traumatic brachial plexus injuries, concomitant vascular injury portends a worse functional outcome following reconstruction [3], emphasizing the role of vascularization in nerve reconstruction and subsequently nerve regeneration. A few studies suggest that revascularization patterns of allograft nerves after reconstruction is via proximal inosculation, a process of revascularization occurring primarily from proximal to distal [4,5]. Diminishing fibrosis and central necrosis in nerve grafts by early revascularization of the graft may enhance axonal regeneration, especially in larger diameter nerve grafts [4]. Surgical angiogenesis by a pedicled adipofascial flap is a potential strategy to improve the microcirculation and thus revascularization [6-8].

Stem cells offer several regenerative benefits to peripheral nerve regeneration, including secretion of trophic factors that promote angiogenesis, remyelination and a supportive microenvironment [9]. Adipose-derived mesenchymal stem cells (MSC) specifically are relatively easy to be isolated and are capable of differentiating into mesoderm lineages [9,10].

The combination of surgical angiogenesis and MSCs to allograft nerves may further improve neovascularization in allografts. Detailed three-dimensional (3D) evaluation of microvasculature is becoming a powerful tool to provide mechanistic understanding of angiomodulating strategies and could be applied to investigate this interaction in nerve allografts [11]. The purpose of this study was to evaluate the early microvascular architecture of nerve allografts enhanced with stem cell delivery and surgical angiogenesis in a rat sciatic nerve defect model.

MATERIALS AND METHODS

Animal experiments were approved by the Mayo Clinic Institutional Animal Care and Use Committee (IACUC A3348-18).

Experimental design

Twenty-five male Lewis rats, weighing between 250-300 grams (Envigo, USA), were randomly divided into five groups to reconstruct unilateral sciatic nerve gaps, depicted in Table 1. In group I, a unilateral 10-mm sciatic nerve gap was repaired with an ipsilateral reversed autologous graft to create a mismatch in the alignment of nerve fibers (gold standard). For group II-V, decellularized allograft nerves were used to reconstruct the nerve gap. In group II, a 10-mm allograft was used to reconstruct the nerve gap. In group III-V, these nerve allografts were placed in a vascularized bed using a pedicled superficial inferior epigastric artery fascia (SIEF) flap to provide surgical angiogenesis [6]. Prior to surgery of group IV and V, allografts were dynamically seeded with undifferentiated MSCs and MSCs differentiated into Schwann cell-like cells, respectively, combining stem cells and surgical angiogenesis. After survival of two weeks, Microfil® was injected to preserve vasculature and microcomputed tomography (micro CT) analysis of blood vessel morphology and distribution was performed [12]. Results were compared to non-operated sciatic nerve (control) samples (N=10).

Table 1. Experimental design. dMSC: differentiated mesenchymal stem cells, SIEF: superficial inferior epigastric artery fascial (SIEF) flap, uMSC: undifferentiated mesenchymal stem cells.

Groups		Description	Survival time 2 weeks (N)	Outcome measurements
I	Autograft	Autograft	5	Micro computed analysis • Vascular volume • Volume of vessels (mm^3) • Percentage of vessels (%)
II	Allograft	Decellularized allograft	5	
III	SIEF	Decellularized allograft + SIEF flap	5	
IV	uMSCs + SIEF	Decellularized allograft + undifferentiated MSCs + SIEF flap	5	
V	dMSCs + SIEF	Decellularized allograft + differentiated MSCs + SIEF flap	5	

Nerve allograft harvest and processing

Ten male Sprague-Dawley rats (Envigo, Madison, WI, USA), weighing 250-300 grams, served as donors for harvesting a 15-mm segment of the sciatic nerve bilaterally. Sprague-Dawley rats were used to obtain a major histocompatibility complex mismatch with the recipient Lewis rats [13,14]. After rats were anesthetized in an isoflurane inducted chamber and euthanized with an overdose of Pentobarbital Sodium (Fatal Plus, 390 mg/mL, Vortech, Dearborn, MI, USA), sciatic nerves were collected, cleaned from external debris and processed using a five-day decellularization protocol utilizing elastase and chondroitinase to become acellular allografts [15]. After processing, the nerves were sterilized using g-irradiation and stored in phosphate buffer saline at 4°C. All steps were carried out at room temperature with agitation under sterile conditions and in a laminar flow hood.

Mesenchymal stem cell preparation and culture

Rat MSCs from a previously characterized lineage were used for experiments [16]. These MSCs were derived from the inguinal fat pad of inbred Lewis rats [17], characterized by plastic adherence, pluripotency towards mesodermal lineages, the expression of MSC surface markers CD29 and CD90, and absence of hematopoietic cell surface markers CD34 and CD45 [18]. The stromal cell pellet was re-suspended in growth medium consisting of advanced Minimum Essential Medium (a-MEM (1x); Life Technologies Corporation (LTC)), 5% platelet lysate (PLTMax®; Mill Creek Life Sciences, MN, USA), 1% Penicillin/Streptomycin (Penicillin-Streptomycin (10.000 U/mL; LTC), 1% GlutaMAX (GlutaMAX Supplement 100X; LTC) and 0.2% Heparin (Heparin Sodium Injection, USP, 1.000 USP units per mL; Fresenius Kabi, IL, USA).

Mesenchymal stem cell differentiation

MSCs were differentiated into Schwann cell-like cells according to protocol [17]. This protocol has shown to morphologically change 81.5% of the MSCs exposed to the differentiation medium into a typical spindle-like shape [17]. Cells were treated with ß-mercaptoethanol (Sigma-Aldrich, MO, USA) and all-trans-retinoic acid (1:1000 of

stock dilution, 35 mg/mL diluted in dimethyl sulfoxide (DMSO); Sigma-Aldrich), prior to introducing a differentiation solution to the growth medium containing 0.14% Forskolin (10 mM dissolved in DMSO, Sigma-Aldrich), 0.01% basis fibroblast growth factor (bFGF; 100 mg/mL dissolved in 5 mM Tris Hydrochloride buffer, PeproTech, NJ, USA), 0.005% platelet-derived growth factor (PDGF-AA; 100 mg/mL dissolved in 10 mM acetic acid, PeproTech) and 0.02% Neuregulin-1 ß1 (NRG1-b1; 100 µg/mL reconstituted in phosphate buffered saline (PBS), R&D systems Inc, MN, USA). Successful differentiation was previously assessed by immunohistochemistry [18].

All MSC cultures were maintained at subconfluent levels in a 37 °C incubator with 5% CO2 and passaged with TrypLE (Invitrogen, UK). Growth medium was changed every 72 hours. In this experiment, passage five cells were used to seed allografts.

Seeding allograft nerves with mesenchymal stem cells

For group IV and V, ten allografts were dynamically seeded for 12-24 hours with 1x10^6 undifferentiated MSCs (N=5) and 1x10^6 differentiated MSCs (N=5), respectively [16]. Briefly, decellularized nerve allografts were sterilely combined with 1x10^6 cells in a TubeSpin® Bioreactor tube (Midwest Scientific, MO, USA) containing cell culture medium (Figure 1A). Tubes were placed on a bioreactor with a fixed speed of 18 RPM in the incubator for 12-24 hours until surgery. Seeding efficiency using this dynamic seeding strategy has been previously validated [16,18].

Surgical procedure

Rats were anesthetized in an isoflurane chamber, shaved, prepped and positioned in the nosecone to maintain anesthesia throughout the procedure. Preoperatively, the following were administered subcutaneously: 5 mL of NaCl 0.9% solution (to prevent dehydration), Enrofloxacin (Baytril, Bayer, Germany, 10mg/kg, providing infection prophylaxis) and Buprenorphine SR (Buprenorphine SR-LAB, ZooPharm pharmacy, 0.6mg/kg, pain control). Body temperature during surgery was maintained at 37°C with a heating pad.

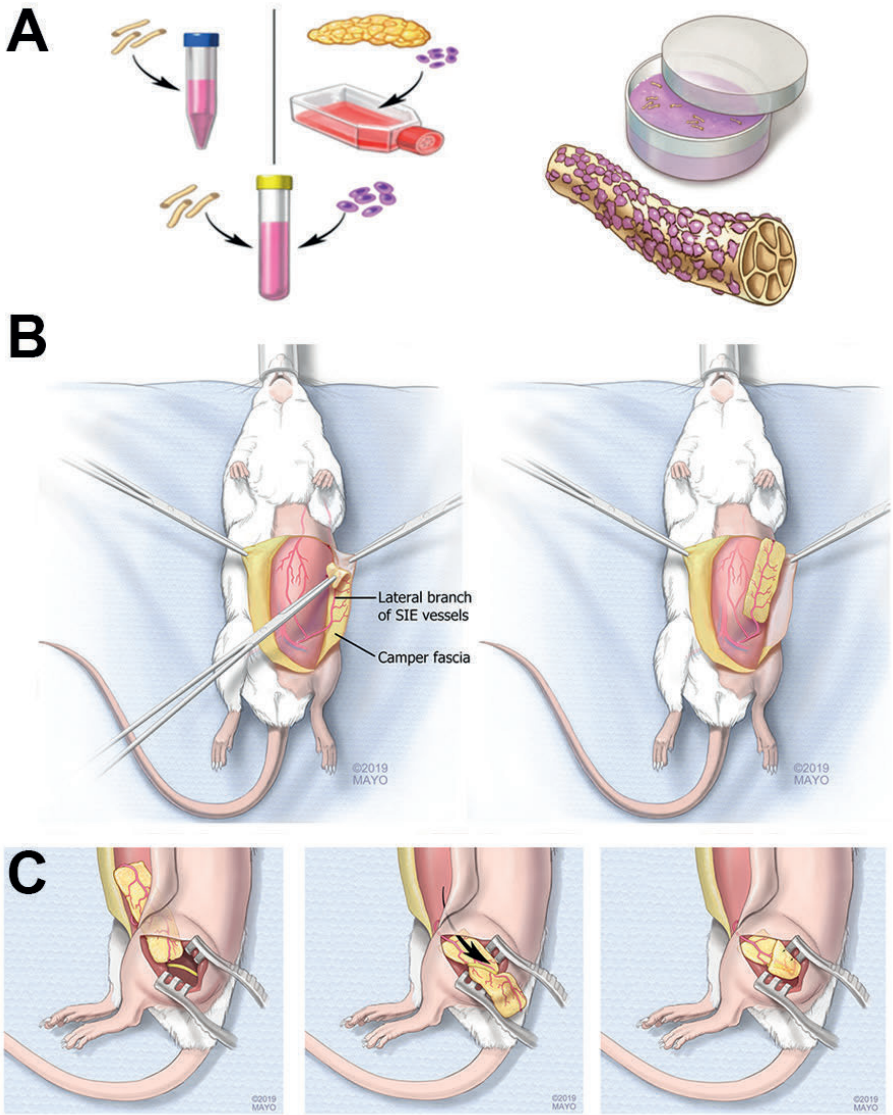

Figure 1. Nerve graft seeding technique and schematic drawing of the superficial inferior epigastric fascia (SIEF) flap harvest. Depicted is the stem cell isolation from adipose tissue and dynamic seeding of nerve allografts (A). The elevation of the flap from distal to proximal is depicted in B, providing a 4 x 3 cm adipofascial flap based on the lateral branch of the superficial inferior (SIE) vessels. The SIEF flap was tunneled subcutaneously toward the nerve without vascular twisting of the epigastric trunk and wrapped around the nerve allograft reaching both anastomoses (C). Flap edges were trimmed and two 10-0 nylon sutures were placed to secure the position of the SIEF flap. *With permission of the Mayo Foundation, Copyright Mayo Foundation 2020. All rights reserved.*

The left sciatic nerve of each rat was fully exposed proximally from the inferior margin of the piriformis muscle to approximately 5 mm distal to the bifurcation, under an operating microscope (Zeiss OpMi 6, Carl Zeiss Surgica, Oberkochen, Germany). A 10-mm segment of the sciatic nerve was excised by sharp transection with microsurgical scissors. In group I, the nerve segment was reversed and placed as an interposition autograft with six 10-0 nylon (10-0 Ethilon, Ethicon Inc., Sommerville, NJ, USA), epineural interrupted sutures on either side of the repair. In group II, the nerve gap was bridged with a 10-mm decellularized allograft with use of a similar surgical technique. In group III-V, surgical angiogenesis was provided to the allograft (group III), combined with undifferentiated MSCs (group IV) and differentiated MSCs (group V), respectively. In detail, the nerve gap was repaired with an allograft which was consecutively wrapped in the pedicled SIEF flap [6]. Briefly, the femoral artery was identified in the groin on the ipsilateral side of the nerve reconstruction, whereafter the superficial inferior epigastric (SIE) vessels were exposed. The 4 x 3 cm SIEF flap containing subcutaneous fat, inguinal fat, the femoral vasculature and SIE vessels, was tunneled subcutaneously toward the nerve reconstruction and wrapped around the nerve, covering both the proximal and distal nerve repair, providing surgical angiogenesis to the entire nerve allograft (Figure 1B).

In all groups, wounds were closed in layers, approximating muscle with two 5-0 absorbable interrupted sutures (5-0 Vicryl Rapide, Ethicon Inc.). The skin was closed subcutaneously, using the same suture. Postoperatively, the rats were individually housed and provided with food and water *ad libitum* with a 12-hour light-dark cycle.

Nonsurvival procedure

Two weeks after surgery, rats were anesthetized and euthanized with 1mL intraperitoneal injection of Pentobarbital Sodium. After preserving nerve vasculature by injection of yellow Microfil® compound (MV 8mL, diluent 15mL, and curing agent 1.2mL, Flow Tech, Inc., Carver, MA, USA) in the descending aorta according to protocol, nerve samples were harvested bilaterally and cleared using graded series of ethanol [12].

Outcome measurements

Preserved vasculature in the nerve segments was quantified using a SkyScan 1276 micro CT (Bruker Corporation, Billerica, MA, USA) at 40kV voltage, 200 µA current and 10 µm resolution, as previously described [12]. Three-dimensional images of the samples were reconstructed using Hierarchical InstaRecon software (NRecon, 1.7.4.2., InstaRecon, 2.0.4.0. InstaRecon) and AnalyzePro software (AnalyzeDirect, Inc.,Overland Park, KS) was used to segment blood vessels. The volume of the vasculature was expressed as a percentage of the total nerve volume (vessel%).

Evaluation of blood vessel morphology

For all transplanted nerve groups and controls, a vasculature tree skeleton was generated using an ERODE/DILATE program (written by the Department of Physiology and Biomedical Engineering at Mayo Clinic, Rochester, MN) [19]. This program allowed for optimal morphological information of the entire vasculature network including measurement of the following morphological parameters; volume and percentage of vessels at different diameters. Using this program, the volume of vessels within a selected lumen diameter range was estimated. Specifically, the distance between the two most distant lying voxels within these vessels was determined to describe vessel thicknesses. The average of the local voxel thicknesses within the structure yields the vessel thickness (lumen diameter in µm). As the cubic voxel side dimension was 10 µm, the nerve microvessels were always derived in 20 µm increments. Due to a finite imaging field, some vessels could not be visually connected and were excluded from the data. The volume (in mm^3) and percentage (in %) of the averaged vessel counts were calculated for each group to depict the vascular distribution.

Analysis

Vascular volume results were analyzed and compared to ten non-operated sciatic nerve (control) samples, randomly selected from two rats of each experimental group. The nerve samples were included in the study if they underwent successful preservation of vasculature, defined by observation of yellow nailbeds on either paw. Investigators could not be blinded to the experimental groups during perfusion of Microfil®, but the micro CT was performed by an independent technician to provide

unbiased data. Analysis of variance (ANOVA) with Bonferroni post-hoc tests were used for comparisons between groups. Spatial distribution analysis was performed using the ERODE/DILATE program [19]. Diameter groups with a minimum of two values per diameter range were included for analysis. Results were reported as the mean and standard error of the mean (SEM), and the level of significance was set at $\alpha \leq 0.05$.

RESULTS

During follow-up, no SIEF flap necrosis occurred and no infections were seen (groups III-V). At sacrifice, all SIEF flaps were well vascularized and demonstrated active bleeding at its margins. Successful preservation of vasculature was achieved in all nerve graft samples (total of N=25) and unoperated control nerve samples (N=10).

Macroscopic appearance of the vessels in the nerve samples

Nerve samples were imaged using the micro CT for 3D visualization of the vessels, depicted in Figure 2. Revascularization consisting of a mesh network occurred from both host stumps in nerve allograft samples, leaving the middle longitudinal third (referred to as mid-section) of the nerve avascular (2C). Surgical angiogenesis enhanced the mesh network of microvessels sprouting into the nerve towards the mid-section (2D). When surgical angiogenesis was combined with undifferentiated MSCs, revascularization reached the mid-section of the graft, showing microvessels along the entire length of the nerve graft (2E). This increase was less evident when surgical angiogenesis was combined with differentiated MSCs (2F). In nerve autografts, thicker longitudinally running vessels were recognized along the entire length of the nerve (2B), comparable to unoperated control (2A).

Vascular volume

Vascular volume outcomes of all groups are described in Table 2 and results are depicted in Figure 3. The vascular volume in allografts was found to be lowest compared to all groups and significantly inferior to control ($P<0.0001$) and SIEF combined with undifferentiated MSCs ($P<0.0001$). SIEF combined with undifferentiated MSCs was significantly superior compared to all experimental groups ($P<0.01$ compared to

autograft, P<0.0001 to allograft, P<0.05 to SIEF only and P<0.05 to SIEF combined with differentiated MSCs, respectively), and comparable to control (P=0.15).

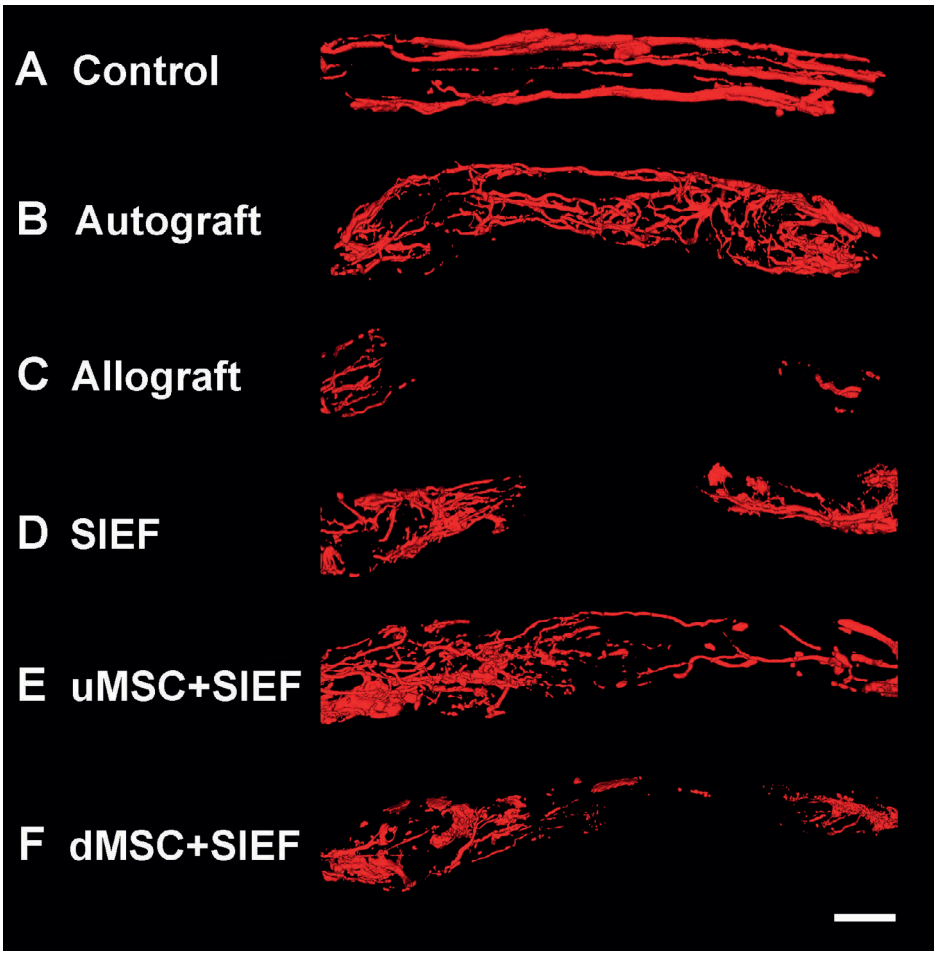

Figure 2. Micro computed tomography (micro CT) images of nerve samples. Micro CT images of unoperated control nerve (A), autograft (B), allograft (C), and allograft wrapped in a pedicled superficial inferior epigastric artery fascial (SIEF) flap (D), combined with undifferentiated mesenchymal stem cells (uMSC, E) or mesenchymal stem cells differentiated into Schwann cell-like cells (dMSC, F). Images were obtained at two weeks. Nerve samples were positioned from proximal to distal (left to right, respectively). Scale bar is set at 1 mm. In the supplementary data, videos of these nerve samples are provided to give a 3D representation of the micro CT.

Table 2. Outcomes of vascular volume. Results were expressed as mean% vessel ± SEM, SEM: Standard error of the mean. dMSC: differentiated mesenchymal stem cells, SIEF: superficial inferior epigastric artery fascial (SIEF) flap, uMSC: undifferentiated mesenchymal stem cells.

Groups	Vascular volume
Control	4.52 ± 0.33
Autograft	2.51 ± 0.26
Allograft	1.35 ± 0.41
SIEF	3.38 ± 0.56
uMSCs + SIEF	5.57 ± 0.72
dMSCs + SIEF	3.16 ± 0.18

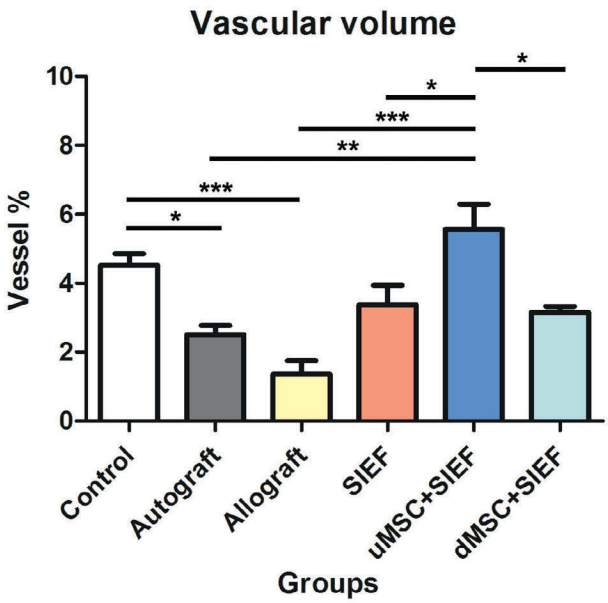

Figure 3. Vascular volume of nerve groups at 2 weeks using micro computed tomography (micro CT). Results of control nerve, autograft, allograft, and allograft wrapped in a pedicled superficial inferior epigastric artery fascial (SIEF) flap, combined with undifferentiated mesenchymal stem cells (uMSC+SIEF) or mesenchymal stem cells differentiated into Schwann cell-like cells (dMSC+SIEF). Results were expressed as a percentage (vessel%) of the total nerve area and given as the mean ± SEM. *Indicates significance at $P < 0.05$, **$P < 0.01$, ***$P < 0.0001$. SEM: Standard error of the mean.

Blood vessel morphology

Evaluation of the nerve angioarchitecture allowed for determination of the distribution of blood vessels in nerve sample groups. Diameters of blood vessels found in autograft nerves ranged from 0-220 µm, 0-200 µm in allografts and 0-200 µm in control nerves

(Figure 4). For the SIEF group this was found to be ranging from 0-240 μm, 0-340 μm when combined with undifferentiated MSCs and 0-300 μm when combined with differentiated MSCs, respectively (Figure 5).

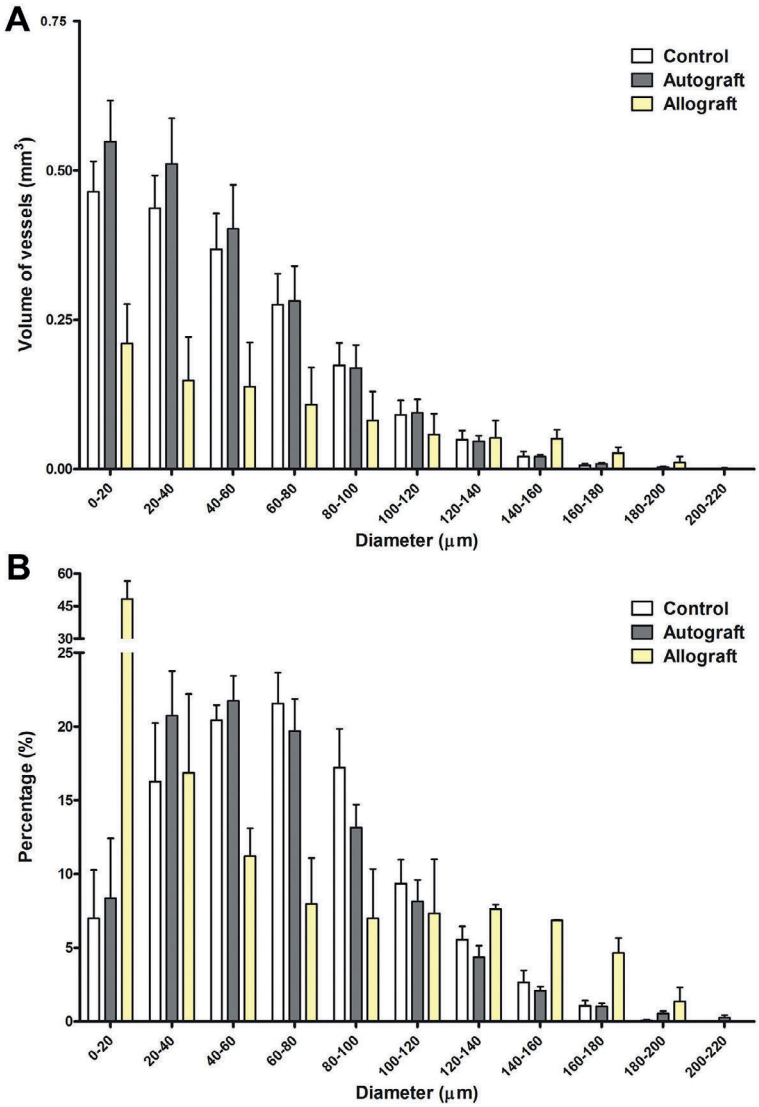

Figure 4. Spatial vessel distribution of control, autograft and allograft groups, based on volume and percentage of vessel segments. Histograms presenting the relative proportion of a given diameter distribution of blood vessels in control, autograft and allograft nerve groups. Results were analyzed based on volume (A) and percentage (B), and presented as the mean ± SEM. Vessel diameters were given in 20 μm increments and were ranging from 0-220 μm. SEM: Standard error of the mean.

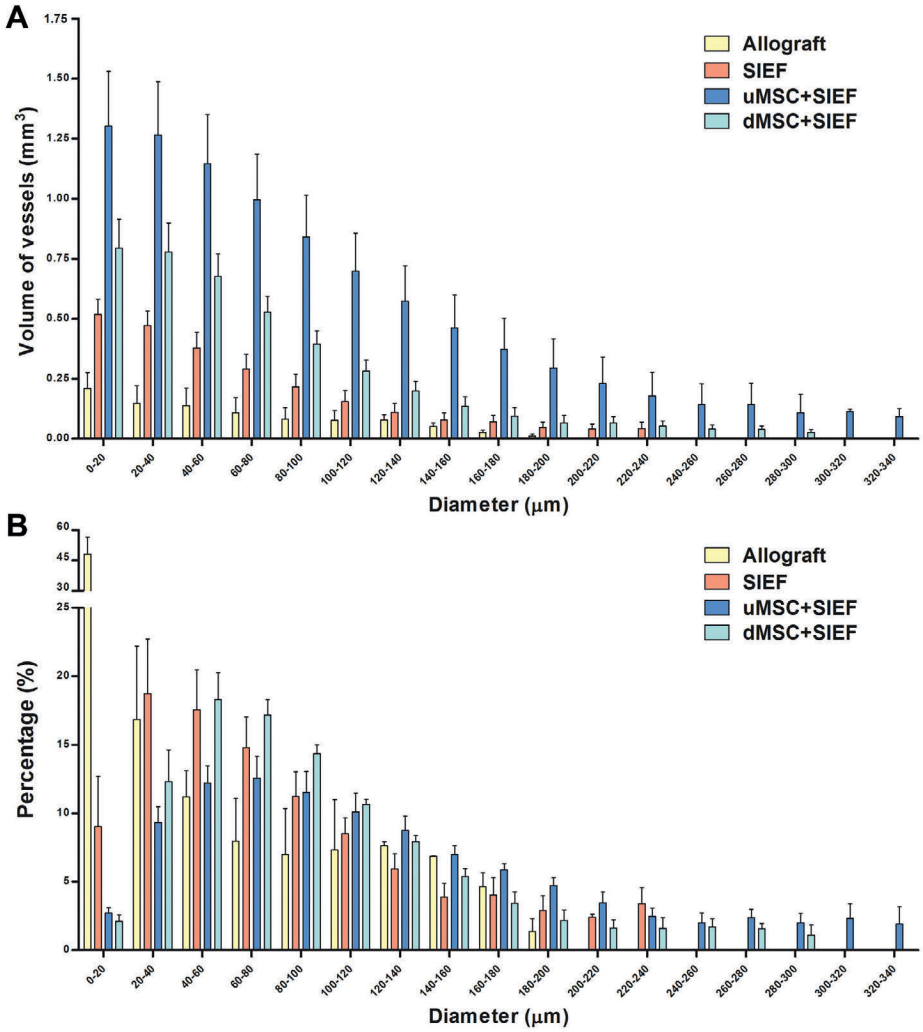

Figure 5. Spatial vessel distribution of allograft groups combined with surgical angiogenesis and stem cell delivery, based on volume and percentage of vessel segments. Histograms presenting the relative proportion of a given diameter distribution of blood vessels in allograft, allograft wrapped in a pedicled superficial inferior epigastric fascial (SIEF) flap, combined with undifferentiated mesenchymal stem cells (uMSC+SIEF) or mesenchymal stem cells differentiated into Schwann cell-like cells (dMSC+SIEF) groups. Results were analyzed based on volume (A) and percentage (B) and presented as the mean ± SEM. Vessel diameters were given in 20 μm increments and were ranging from 0-340 μm. SEM = Standard error of the mean.

Spatial distribution of blood vessels

Control, autograft and allograft nerves

The vessels were distributed per volume, to describe a vessel segment volume prior to sprouting into a new segment and per percentage to denote the lumen diameter distribution, respectively. The relation of the volume to the diameter within blood vessels was distributed in a linear matter (Figure 4A). The greatest volume measured 0.55±0.07mm^3 for autografts, 0.21±0.07 mm^3 for allografts and 0.46±0.05 mm^3 for controls, respectively (4A). For allografts, most of these vessels were 0-20 µm (48%) and these vessel counts decreased as diameters increased. For autografts, the majority of vessels were between 20-80 µm (21% for 20-40 µm, 22% for 40-60 µm and 20% for 60-80 µm). A similar bell-shaped pattern was observed in controls, where most vessels were distributed between 20-100 µm (16% for 20-40 µm, 20% for 40-60 µm, 22% for 60-80 µm and 17% for 80-100 µm) (Figure 4B).

Allograft, SIEF and SIEF nerves combined with stem cells

The volume of vessels was largely increased when allografts were wrapped within a SIEF flap and further increased when combined with stem cells. Largest volume of vessels and diameter were found when SIEF was combined with undifferentiated MSCs (1.30±0.23 mm^3, Figure 5A). The greatest measured volume for SIEF combined with differentiated MSCs was 0.79±0.12 mm^3 and 0.52±0.06 mm^3 for SIEF, respectively (Figure 5A). Addition of the SIEF flap resulted in an increased vessel diameter compared to allograft only, resulting in 18% of vessels being between 20-40 µm and the vessels to be more uniformly distributed with regard to diameter (Figure 5B). This increase in vessel diameter was more prominently visible in nerve allografts that received both surgical angiogenesis and stem cell delivery; resulting in the distribution to be skewed to the right (i.e. larger vessels). Blood vessels in the differentiated MSCs and SIEF group combined, showed little percentage of small vessels (2% for 0-20 µm) with a peak of 18% for 40-60 µm and broad distribution towards 300 µm. When undifferentiated MSCs were combined with the SIEF flap, it resulted in the broadest distribution of vessels compared to all other groups, with majority of vessels to be distributed between 0-140 µm (5B).

Overview of volume distribution

To give an overview of all groups, volumes of vessels with corresponding diameters were presented as means and combined in one figure (Figure 6). The control and autograft showed a similar distribution of vessels, with a large overlap. Allografts showed the lowest volume of vessels and this pattern was increased when wrapping within a SIEF flap, with regard to both volume and diameter distribution. The addition of stem cell seeding further improved these distributions, with greatest increase found when combined with undifferentiated MSCs.

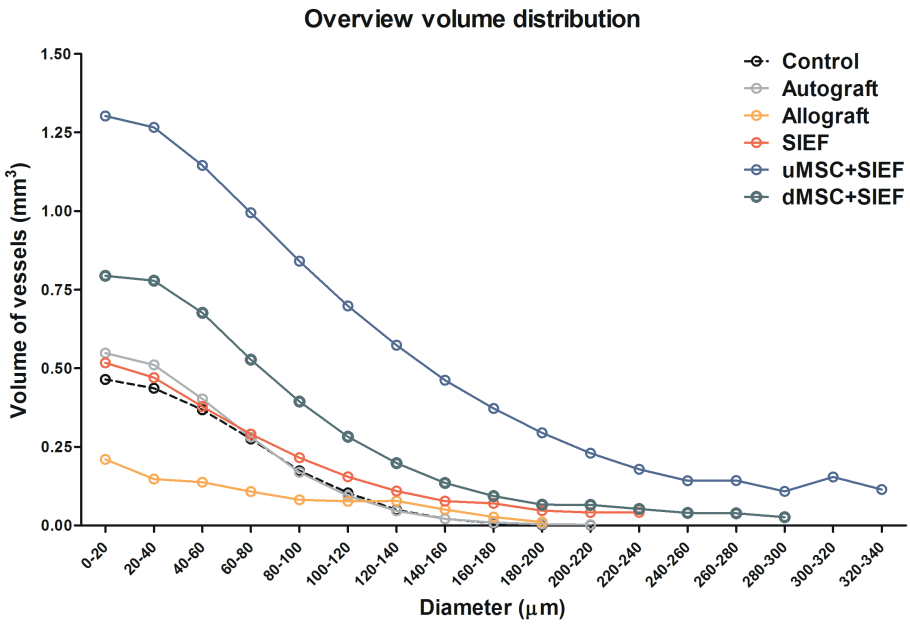

Figure 6. Overview of blood vessel diameter distribution based on volume after three-dimensional reconstruction using micro computed tomography (micro CT). Diameter distribution of blood vessels of control, autograft, allograft, allograft wrapped in a pedicled superficial inferior epigastric fascial (SIEF) flap, combined with undifferentiated mesenchymal stem cells (uMSC+SIEF) or mesenchymal stem cells differentiated into Schwann cell-like cells (dMSC+SIEF). Groups were ranked based on volume and presented as the mean to give an overview of all groups.

DISCUSSION

Nerves are vascularized through two systems: the extrinsic and intrinsic blood supply. Both systems serve as a nutrient system and are responsible for the cellular metabolism of the nerve [20]. After injury, blood flow is increased to help prevent the nerve from ischemia [21], resulting in a cascade of biological processes over time including activation of angiogenesis, sprouting of vascular endothelial cells and remodeling of blood vessels [22]. In vascularized nerve grafts, blood flow was found to be increased compared to non-vascularized nerve grafts, starting from the first postoperative day [23]. This finding is in line with our study, which demonstrated enhanced vascularity in nerve grafts to which surgical angiogenesis via a SIEF flap was applied. The combination of surgical angiogenesis and stem cells, in particular undifferentiated MSCs, resulted in further enhancement of vascularity and has not been previously described. Stem cells are known for their paracrine properties and exert different functions when influenced by their environment [24]. Differentiation of MSCs in Schwann cell-like cells results in specific gene expression profiles and are found to express high gene-levels in the first 72 hours after seeding on nerve samples *in vitro*, while undifferentiated MSCs are characterized by enhanced gene-levels after one week [25]. Specifically, vascular endothelial growth factor (VEGF) was expressed in higher levels by undifferentiated MSCs compared to differentiated MSCs [25], potentially explaining the findings in this study. Undifferentiated MSCs combined with the SIEF flap not only increased vascularity, but also resulted in revascularization of the mid-section of the graft at two weeks (Figure 2E), emphasizing that stimulation of centripetal revascularization is determined by the surrounding tissue [4,26].

Previous studies have reported increased vascularity in decellularized allografts treated with differentiated MSCs versus undifferentiated MSCs at 16 weeks [27]. Vascularity was measured using a two-dimensional method, which lacks details of nerve angioarchitecture compared to a 3D method. Additionally, this study did not evaluate the provision of surgical angiogenesis. With different experimental designs, it is difficult to compare our results at two weeks to their 16 week outcomes [27]. The synergistic effect of stem cells and surgical angiogenesis is hypothesized to be due to the adipofascial flap providing vascular delivery of trophic factors, sufficient nutrients and oxygen, resulting in less hypoxia vital to sustaining survivability of stem cells [28,29]. Stem cells have a neuroprotective and immunomodulatory effect causing less fibrosis

and scarring, subsequently resulting in improved diffusion to meet the demands of cellular metabolism [24,30,31]. The interaction between stem cells and vascularity remains complex and has not been thoroughly investigated.

The organization of vessels in reconstructed nerves has been of interest. Only few studies have explored the 3D microvasculature of peripheral nerves [27,32-35], emphasizing the necessity for imaging of nerve revascularization in conjunction with nerve reconstruction after trauma. It has been suggested that the amount of revascularization is enhanced at the sites of nerve coaptation in response to the acute hypoxia during nerve trauma [35,36]. Macrophages play an important role as sensors of hypoxia to induce angiogenesis during this process [37]. In addition, vessels away from the coaptation sites were found to be more organized and less frequently branched [35]. This is in line with our results, specifically in the nerve allografts that have been wrapped with a SIEF flap that was combined with undifferentiated MSCs. Blood vessels are found to provide directionality to Schwann cell movement and may therefore play a guidance role to neuronal precursors to enhance nerve regeneration [37,38].

Detailed evaluation of nerve angioarchitecture to the capillary level using 3D-skeletonization and its further analysis provided in this paper contributes to understanding of vessel organization. Although the interpretation of the macroscopic images suggests that larger diameter longitudinally running vessels are seen in autografts and controls (Figure 2), the vessel distribution analysis states differently and shows that nerve graft groups wrapped within the pedicled SIEF flap result in larger diameters of vessels (Figure 5). This incongruence may be reconciled in a few ways. First, the macroscopic images are depicted longitudinally, not providing visual insight into the lumen diameters of the vessels. Second, the volume of vessels (Figures 4A and 5A) depict the volume of vessel segments prior to its sprouting into a new segment. Although the measured volume segments of groups receiving surgical angiogenesis are comparable to or higher than controls and autografts, these account for a smaller portion in terms of percentage. Third, the vessel distribution analysis solely analyzes the provided 3D-skeleton without correcting for the total quantified vascular volume. This suggests that the evaluated spatial distributions need to be interpreted independently from the total volume to overcome a distorted picture of data.

Other limitations include the effective voxel size (10 mm). As such, the smallest branches are not visible, resulting in some arterial and venous trees not to be connected in the macroscopic figures. Furthermore, the use of Microfil® is limited to *ex vivo* analysis of specimens, hampering longitudinal studies in one animal [39]. Although these limitations exist, visualization of vessels after Microfil® preservation remains a highly advanced yet relatively simple technique with a broad application range to evaluate vessel volume and distributions in any organ or animal model [12].

Future studies are needed to explore the role of surgical angiogenesis and stem cell delivery on nerve allografts on the long-term in rats and in larger animal models (e.g. rabbits) to provide evidence needed for clinical translation in the future. As limited studies are available that discuss their role on the immunogenicity of nerve allografts [25,40], increased understanding of the alteration of the micro-environment of nerve and its effect on immune tolerance will contribute to improve reconstructive options for peripheral nerve injuries.

CONCLUSIONS

Accurate interpretation of 3D angioarchitecture provides insight into hierarchical assembly and changes in vascular patterns, thus understanding of the interaction between vascularity and stem cells. Based on this study, we can conclude that surgical angiogenesis contributes to revascularization of nerve allografts. The combination of surgical angiogenesis with undifferentiated MSCs specifically, results in the greatest increase of revascularization, size of vessels, and stimulation of vessels to reach the mid-section of the nerve allograft.

Acknowledgements

The authors would like to thank Jim Postier (Rochester, MN) for the artwork of Figure 1 and Andrew J. Vercnocke for his help with the ERODE/DILATE program. This work was supported in part by the Mayo Clinic X-ray Imaging Core.

Conflicts of interest

None declared.

Supplemental Video 1: Videos of the micro CT imaged nerves in Figure 2.

Scan the QR code to view the videos of Chapter 10.

REFERENCES

1. Hobson MI, Brown R, Green CJ, Terenghi G. Inter-relationships between angiogenesis and nerve regeneration: a histochemical study. *Br J Plast Surg.* 1997;50(2):125-131.
2. Nichols JS, Lillehei KO. Nerve injury associated with acute vascular trauma. *Surg Clin North Am.* 1988;68(4):837-852.
3. Huang AE, Noland SS, Spinner RJ, Bishop AT, Shin AY. Outcomes of Reconstructive Surgery in Traumatic Brachial Plexus Injury with Concomitant Vascular Injury. *World Neurosurg.* 2019.
4. Saffari TM, Mathot F, Friedrich PF, Bishop AT, Shin AY. Revascularization patterns of nerve allografts in a rat sciatic nerve defect model. *J Plast Reconstr Aesthet Surg.* 2020;73(3):460-468.
5. Chalfoun C, Scholz T, Cole MD, Steward E, Vanderkam V, Evans GR. Primary nerve grafting: A study of revascularization. *Microsurgery.* 2003;23(1):60-65.
6. Saffari TM, Bishop AT, Shin AY. The Superficial Inferior Epigastric Artery Fascia Flap in Rats. Journal of Reconstructive Microsurgery Open 2020; 05(01): e7-e14
7. Giessler GA, Friedrich PF, Shin RH, Bishop AT. The superficial inferior epigastric artery fascia flap in the rabbit. *Microsurgery.* 2007;27(6):560-564.
8. Foo A, Martin-Playa P, Sebastin Muttath SJ. Arterialized Posterior Interosseous Nerve Graft for Digital Neuroma. *Tech Hand Up Extrem Surg.* 2019;23(4):152-154.
9. Jiang L, Jones S, Jia X. Stem Cell Transplantation for Peripheral Nerve Regeneration: Current Options and Opportunities. *Int J Mol Sci.* 2017;18(1).
10. Pittenger MF, Mackay AM, Beck SC, et al. Multilineage potential of adult human mesenchymal stem cells. *Science.* 1999;284(5411):143-147.
11. Luzhansky ID, Sudlow LC, Brogan DM, Wood MD, Berezin MY. Imaging in the repair of peripheral nerve injury. *Nanomedicine (Lond).* 2019;14(20):2659-2677.
12. Saffari TM, Mathot F, Bishop AT, Shin AY. New methods for objective angiogenesis evaluation of rat nerves using microcomputed tomography scanning and conventional photography. *Microsurgery.* 2019.
13. Hudson TW, Liu SY, Schmidt CE. Engineering an improved acellular nerve graft via optimized chemical processing. *Tissue Eng.* 2004;10(9-10):1346-1358.
14. Kumta S, Yip K, Roy N, Lee SK, Leung PC. Revascularisation of bone allografts following vascular bundle implantation: an experimental study in rats. *Arch Orthop Trauma Surg.* 1996;115(3-4):206-210.
15. Hundepool CA, Nijhuis TH, Kotsougiani D, Friedrich PF, Bishop AT, Shin AY. Optimizing decellularization techniques to create a new nerve allograft: an in vitro study using rodent nerve segments. *Neurosurg Focus.* 2017;42(3):E4.
16. Rbia N, Bulstra LF, Bishop AT, van Wijnen AJ, Shin AY. A simple dynamic strategy to deliver stem cells to decellularized nerve allografts. *Plast Reconstr Surg.* 2018.
17. Kingham PJ, Kalbermatten DF, Mahay D, Armstrong SJ, Wiberg M, Terenghi G. Adipose-derived stem cells differentiate into a Schwann cell phenotype and promote neurite outgrowth in vitro. *Exp Neurol.* 2007;207(2):267-274.

18. Mathot F, Rbia N, Bishop AT, Hovius SER, Van Wijnen AJ, Shin AY. Adhesion, distribution, and migration of differentiated and undifferentiated mesenchymal stem cells (MSCs) seeded on nerve allografts. *J Plast Reconstr Aesthet Surg.* 2019.
19. Sangaralingham SJ, Ritman EL, McKie PM, et al. Cardiac micro-computed tomography imaging of the aging coronary vasculature. *Circ Cardiovasc Imaging.* 2012;5(4):518-524.
20. Terzis JK, Skoulis TG, Soucacos PN. Vascularized nerve grafts. A review. *Int Angiol.* 1995;14(3):264-277.
21. Lundborg G. Ischemic nerve injury. Experimental studies on intraneural microvascular pathophysiology and nerve function in a limb subjected to temporary circulatory arrest. *Scand J Plast Reconstr Surg Suppl.* 1970;6:3-113.
22. Wang H, Zhu H, Guo Q, et al. Overlapping Mechanisms of Peripheral Nerve Regeneration and Angiogenesis Following Sciatic Nerve Transection. *Front Cell Neurosci.* 2017;11:323.
23. Kanaya F, Firrell J, Breidenbach WC. Blood flow of segmentally divided and folded nerve. *J Reconstr Microsurg.* 1993;9(6):429-433.
24. Mathot F, Shin AY, Van Wijnen AJ. Targeted stimulation of MSCs in peripheral nerve repair. *Gene.* 2019;710:17-23.
25. Mathot F, Rbia N, Thaler R, Bishop AT, Van Wijnen AJ, Shin AY. Gene expression profiles of differentiated and undifferentiated adipose derived mesenchymal stem cells dynamically seeded onto a processed nerve allograft. *Gene.* 2020;724:144151.
26. Tarlov I. The importance of an adequate blood supply. *J Neurosurg.* 1945;2:49-71.
27. Mathot F RN, Bishop AT, Hovius SER, Shin AY. Adipose derived mesenchymal stem cells seeded onto a decellularized nerve allograft enhances angiogenesis in a rat sciatic nerve defect model *accepted at Microsurgery.* 2020.
28. Zhang W, Wray LS, Rnjak-Kovacina J, et al. Vascularization of hollow channel-modified porous silk scaffolds with endothelial cells for tissue regeneration. *Biomaterials.* 2015;56:68-77.
29. Fan Z, Liao X, Tian Y, Xuzhuzi X, Nie Y. A prevascularized nerve conduit based on a stem cell sheet effectively promotes the repair of transected spinal cord injury. *Acta Biomater.* 2020;101:304-313.
30. Jain RK, Au P, Tam J, Duda DG, Fukumura D. Engineering vascularized tissue. *Nat Biotechnol.* 2005;23(7):821-823.
31. Reid AJ, Sun M, Wiberg M, Downes S, Terenghi G, Kingham PJ. Nerve repair with adipose-derived stem cells protects dorsal root ganglia neurons from apoptosis. *Neuroscience.* 2011;199:515-522.
32. Bikis C, Thalmann P, Degrugillier L, et al. Three-dimensional and non-destructive characterization of nerves inside conduits using laboratory-based micro computed tomography. *J Neurosci Methods.* 2018;294:59-66.
33. Zamir M, Twynstra J, Vercnocke AJ, et al. Intrinsic microvasculature of the sciatic nerve in the rat. *J Peripher Nerv Syst.* 2012;17(4):377-384.
34. Wang HK, Wang YX, Xue CB, et al. Angiogenesis in tissue-engineered nerves evaluated objectively using MICROFIL perfusion and micro-CT scanning. *Neural Regen Res.* 2016;11(1):168-173.
35. Bikis C, Degrugillier L, Thalmann P, et al. Three-dimensional imaging and analysis of entire peripheral nerves after repair and reconstruction. *J Neurosci Methods.* 2018;295:37-44.

36. Kingham PJ, Kolar MK, Novikova LN, Novikov LN, Wiberg M. Stimulating the neurotrophic and angiogenic properties of human adipose-derived stem cells enhances nerve repair. *Stem Cells Dev.* 2014;23(7):741-754.
37. Cattin AL, Burden JJ, Van Emmenis L, et al. Macrophage-Induced Blood Vessels Guide Schwann Cell-Mediated Regeneration of Peripheral Nerves. *Cell.* 2015;162(5):1127-1139.
38. Saffari TM, Bedar M, Hundepool CA, Bishop AT, Shin AY. The role of vascularization in nerve regeneration of nerve graft. *Neural Regen Res.* 2020;15(9):1573-1579.
39. Hlushchuk R, Haberthur D, Djonov V. Ex vivo microangioCT: Advances in microvascular imaging. *Vascul Pharmacol.* 2019;112:2-7.
40. Saffari TM, Badreldin A, Mathot F, et al. Surgical angiogenesis modifies the cellular environment of nerve allografts in a rat sciatic nerve defect model. *Gene.* 2020;751:144711.

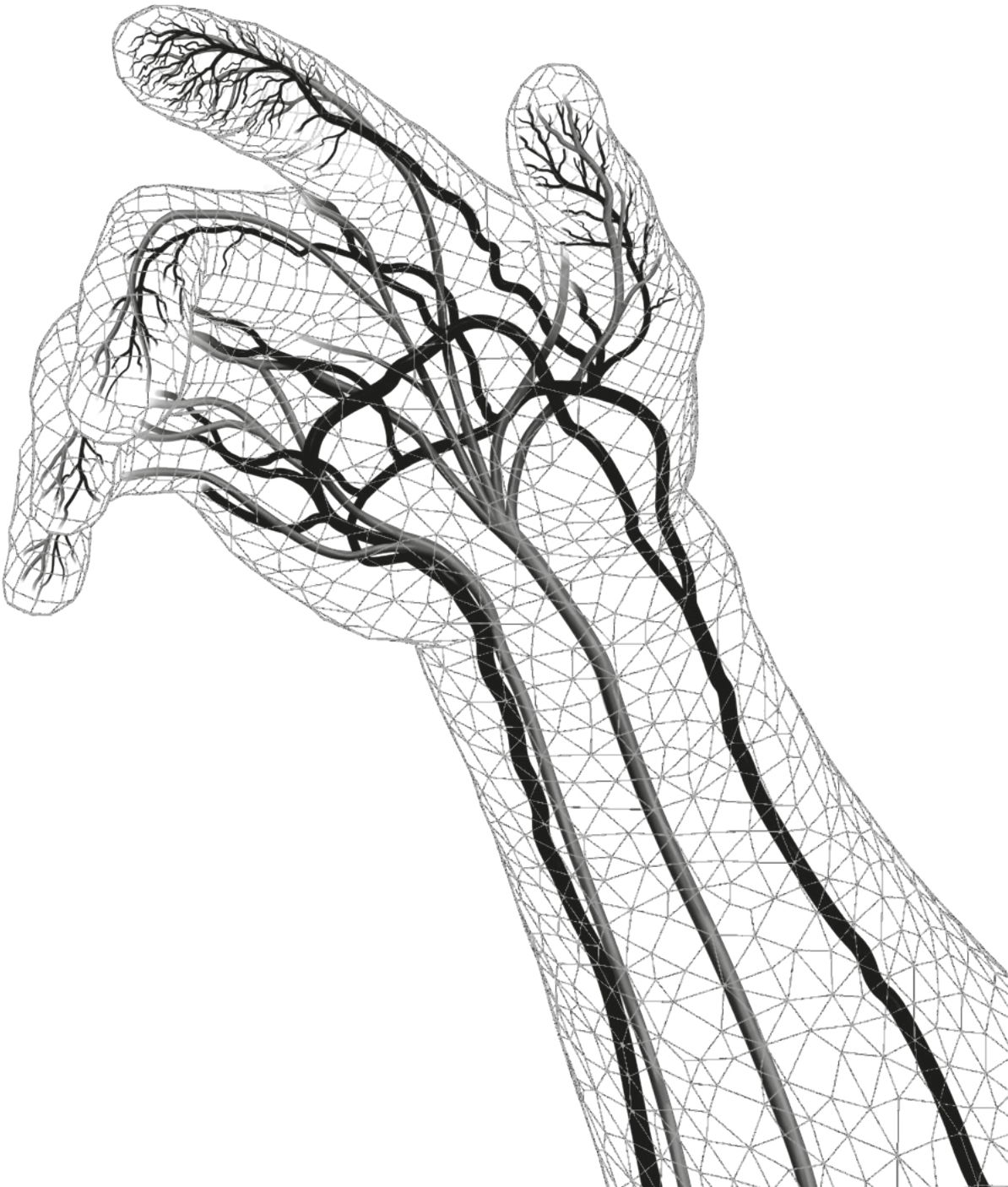

CHAPTER ELEVEN

General Discussion

GENERAL DISCUSSION

The study of peripheral nerve regeneration potential dates back to ancient times, with the first descriptions found in Galen's writings in the second century A.D. [1]. Despite advancements in research and microsurgical techniques, complete motor recovery from peripheral nerve injuries and reconstruction is still rarely achieved. With regeneration proceeding at a rate of 1 mm per day, reinnervation of target neuromuscular junctions may take months and a prolonged delay may result in irreversible changes in the target muscle resulting in detrimental functional recovery [2-4]. Providing reconstruction options to meet the critical window of time, therefore, has remained a focus of research in 2021 and has led to the research question of this thesis: *Does augmentation of nerve allografts with angiogenesis and stem cells improve revascularization and subsequently nerve regeneration?*

The discussion is divided in two parts: the role of angiogenesis (Part I) and the combined effect of angiogenesis and stem cells (Part II). Furthermore, future perspectives and research needed to translate these findings from bench to bedside are explored.

PART I: THE ROLE OF ANGIOGENESIS IN NERVE REGENERATION

In the 1980's, several experimental and clinical studies investigated the effectiveness of adding vascularization to a nerve graft. Sensory and functional motor recovery results were conflicting when comparing vascularized nerve grafts (VNG) to non-vascularized nerve grafts (NVNG) [5-11]. To this end, the addition of vascular endothelial growth factor (VEGF) to nerve allografts was investigated in a rat sciatic nerve defect model. Unfortunately, VNGs face many technical obstacles and are indicated in large nerve defects to improve outcomes in complex and unique cases [12,13]. With no direct comparison to NVNGs, conclusions on the superiority of VNGs is only speculated and not proven. The overarching faced problem is that only case studies are available and no controlled studies exist that evaluate the provision of vascularization to the nerve bed. Transplantation of a nerve graft based on its arterial pedicle (VNG) is technically challenging and does not alter the tissue bed. The aim of **Chapter 3** was to validate a surgical technique that provides angiogenesis to the nerve bed. The pedicled superficial inferior epigastric artery fascial (SIEF) flap in the rat was

validated to provide vascularity to the sciatic nerve area. This flap was raised from the abdomen, rotated and subcutaneously tunneled towards the sciatic nerve. The pedicled SIEF flap was wrapped around the nerve graft, covering the entire nerve and both reconstruction sites. This technique was proven reliable, demonstrated a total success rate of flap viability without necrosis at 12 and 16 weeks, did not require microsurgical repair of blood vessels and therefore decreased the risk of complications. This method was used in the subsequent studies of this thesis to evaluate the role of vascularization on nerve allografts.

To understand the effect of the SIEF flap on nerve grafts and the mechanisms of vascularization, I aimed to evaluate the amount of (neo)angiogenesis. Previous studies have focused on immunohistochemical staining, which lacks the three-dimensional (3D) interconnectivity of the vasculature in serial histological sections [14,15]. Therefore, conventional photography and microcomputed tomography (micro CT) were investigated to objectively quantify vascular surface area and vascular volume, respectively, as measurements of angiogenesis in the nerve. These novel techniques were validated in **Chapter 4** and objectively provided detailed two-dimensional (2D) and 3D information. The ultimate goal is to describe neoangiogenesis -the formation of new blood vessels- [16] in nerve. This would allow us to evaluate and compare neoangiogenic effects of various treatments. However, the distinction between pre-existing and newly formed vessels is technically difficult. The decellularized nerve allograft is per definition acellular and undergoes revascularization *in vivo* after implementation. Measuring angiogenesis in decellularized nerve allografts over time gives an estimation of the newly formed vessels and could be compared to allografts augmented with a adipofascial flap to evaluate the effect of vascularization.

By combining the described techniques in Chapters 3 and 4, **Chapter 5** investigated *how augmentation of nerve allografts with angiogenesis affects revascularization patterns* over time. The findings provided evidence for answering two important questions. First, it was shown that augmentation of nerve allografts with angiogenesis increases revascularization. While this finding does not come unexpected, it strongly supports the vascular contribution of the surrounding bed. Revascularization of nerve is postulated to occur from (i) extraneural vascular contribution from surrounding beds (centripetal revascularization) and (ii) longitudinal bidirectional inosculation from the proximal and distal ends of the graft [17-19]. One may argue that the muscular

bed in this experimental design was not poorly vascularized, questioning the relevance of adding an adipofascial flap. Nevertheless, it seemed that the vascular bundle being in close vicinity and traveling parallel with the nerve over an adequate distance in the adipofascial bed was a contributing factor to revascularization [20,21]. In contrast, the revascularization of nerve allografts that were not wrapped in a vascularized adipofascial flap remained poor. The second finding suggests that an improved vascularized bed promotes longitudinal inosculation, in particular proximal inosculation, and confirms the theory of centripetal revascularization. There has been controversy regarding the mechanism of revascularization and studies have investigated this topic using various approaches to assess angiogenesis including histology [22,23], angiography [19,24,25] and evaluation of blood flow [5,18,26-28]. While previous studies support bidirectional longitudinal inosculation from the proximal and distal ends of the nerve graft [17-19,24], a more recent study by Chalfoun and colleagues is in line with our findings and also favored proximal vascular inosculation [26]. Advanced technology, such as micro CT, used in this study, provides the ability to identify 3D interconnectivity of the vasculature and may be used to describe spatial differences in revascularization in more detail [29].

What effect does angiogenesis have on nerve allografts at a cellular level?

Theoretically, a well vascularized bed enhances the local cellular environment near the nerve repair site -the paracrine environment- to support tissue healing after injury and subsequently diminish fibrosis [30]. The hallmark of fibrosis is the chronic accumulation of myofibroblasts, which are the primary extracellular matrix (ECM)-secreting cells. Depending on the ECM composition, this could lead to either physiological or pathological tissue repair [31]. Myofibroblasts in fibrotic diseases originate from several sources, including from phenotypic differentiation of fibrocytes and transition of endothelial cells, often regulated by transforming growth factor (TGF)-β [32,33]. While chronic hypoxia stimulates this differentiation, it has been suggested that acute hypoxia induces angiogenesis which subsequently decreases the conversion of fibroblasts into pro-fibrotic myofibroblasts [34,35] (Figure 1). Furthermore, angiogenesis is critical for ECM synthesis that is needed for remodeling successful tissue repair [36,37].

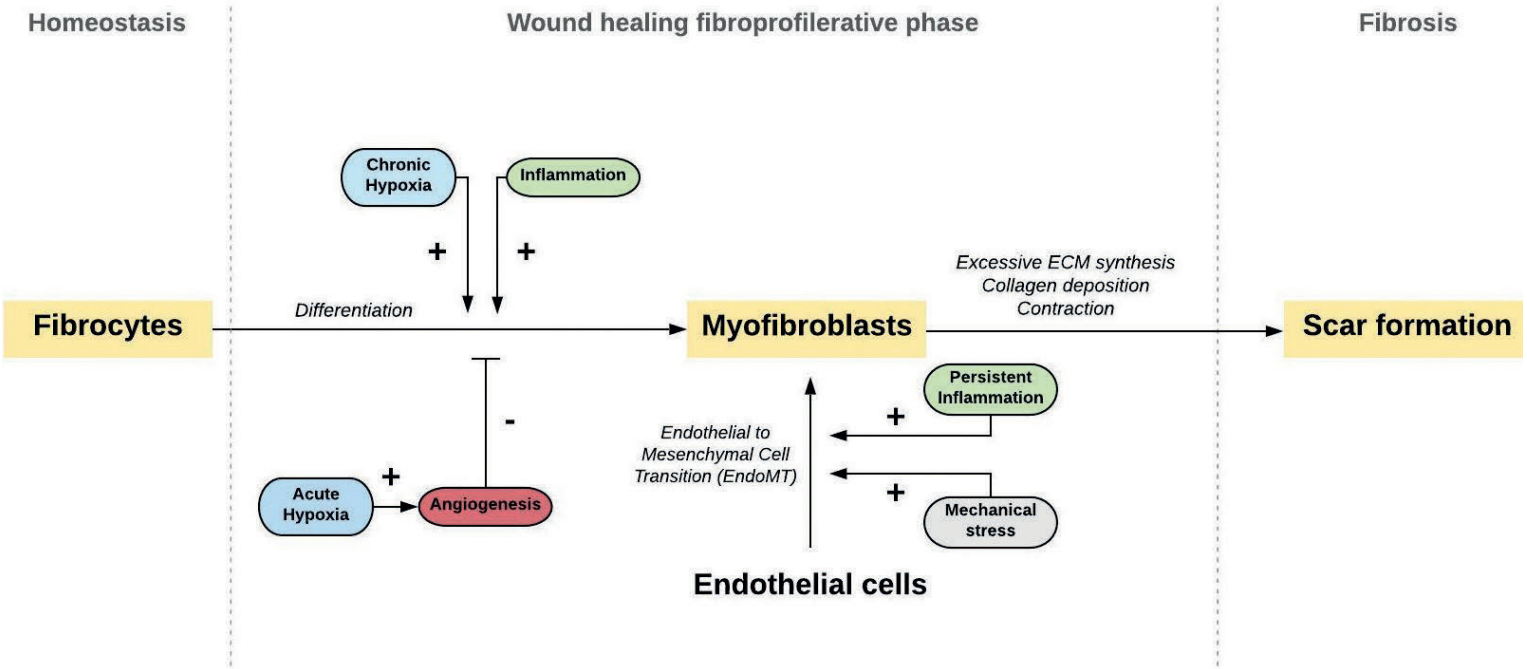

Figure 1. Hypothetical mechanisms that drive fibrocyte and endothelial cell activation towards myofibroblasts. Activated myofibroblasts are important mediators of wound healing. During tissue injury, fibroblasts can differentiate into myofibroblasts. This process is mainly driven by hypoxia and could be decreased by angiogenesis. In specific conditions, myofibroblasts can also arise from endothelial cells via endothelial to mesenchymal transition (EndoMT). Myofibroblasts can follow several different cell fates and can participate in tissue remodeling beyond repair, leading to scar formation. Scar formation, or fibrosis, is characterized by excessive extracellular matrix (ECM) synthesis, collagen deposition and contraction.

Collagens are abundantly present in the ECM of peripheral nerves. Of the 29 collagen types, type I and III, specifically, are believed to provide mechanical support for axonal growth and regeneration after peripheral nerve injury [38,39]. In this chapter, a significant increase was found in gene expression profiles of collagen type I and III in nerve allografts wrapped around with the SIEF flap. These SIEF samples also confirmed increased angiogenesis, using various angiogenic markers i.e. Cd34, Pecam1/Cd31, Vegfa and Mmp2. Furthermore, using flowcytometry, peripheral T cells were evaluated in the blood samples of rats. At one week postoperatively, T helper population (CD4) was significantly increased in SIEF rats, compared to baseline, untreated rats. These data support the hypothesis that an adipofascial flap plays a role in suppressing nerve fibrosis after injury, by providing both an immune tolerant paracrine environment and increasing angiogenesis to the nerve allograft. Achieving a reduction of fibrotic tissue formation is a desired aim and hallmark of improved nerve regeneration.

The *in vivo* setting of **Chapter 6** brings along both advantages as disadvantages that need to be addressed. First, this study lacks gene expression profile evaluation over time. Gene expression varies significantly over time and following these profiles over a time course may provide more information. Due to experimental logistics, costs of surgery and animal maintenance, obtaining longitudinal gene expression values remains more feasible *in vitro* [40,41]. Second, data on baseline expression in healthy peripheral nerves is scarce, making it difficult to understand causal relationships in gene regulation pathways. On the other hand, the *in vivo* setting allowed for environmental cues, such as growth factors and supporting cells, reflecting changes in the context of the ECM environment. These cues influence the proliferation and differentiation of immune cells and stem cells, reflecting a physiologically realistic context [42].

In **Chapter 7**, the aim was to investigate the impact of angiogenesis on motor recovery. While various outcome measurements are available to assess motor recovery, isometric tetanic force (ITF) has remained a reliable technique in determining the degree of motor recovery of a reinnervated muscle as a direct measure of reinnervation [43]. In this chapter, it was found that augmentation of decellularized nerve allografts with angiogenesis resulted in enhanced early motor recovery, comparable to autografts. The contributing factors hypothesized to be leading to this result are twofold and answer

the main objective for Part I: *Does augmentation of nerve allografts with angiogenesis improve revascularization and subsequently nerve regeneration?*

First, the SIEF flap increases vascularity which precedes nerve regeneration. Enhanced vascularity in the nerve graft was objectively measured using micro CT, photography, gene expression, immunofluorescence, and subjectively scored after immunohistochemical staining. The literature review, presented in **Chapter 2**, suggests that angiogenesis precedes the repair of damaged nerves and is therefore in line with this hypothesis. Second, the SIEF flap diminishes nerve fibrosis, leading to enhanced nerve regeneration. The N-ratio presents the number of axonal sprouting and maturation of the regenerating nerve and a low N-ratio could be indicative of a relatively larger amount of fibrous tissue [44]. A significant lower N-ratio was found in nerve allografts, compared to allografts augmented with angiogenesis and nerve autografts. In **Chapter 2**, it was presented that prolonged denervation time leads to intraneural fibrosis and core necrosis which negatively affects the nerve regeneration process [45]. The SIEF flap is found to not solely improve revascularization, but also to decrease graft ischemic time, subsequently impeding necrosis [46]. Taken together with the gene expression results described in **Chapter 6**, the hypothesis could be made that a well vascularized bed, provided by the SIEF flap, suppresses nerve fibrosis. However, more extensive research is needed to further evaluate perineural scar formation and its effect on nerve regeneration. The future perspectives will be presented later in this chapter.

In conclusion, evidence is provided that decellularized nerve allografts could be augmented with angiogenesis through the adipofascial SIEF flap, which provides a well vascularized bed for the nerve graft. This well vascularized bed stimulates a broad spectrum of paracrine actions, not solely induced by the secretion of VEGF, providing an anti-inflammatory microenvironment. This environment is suggested to enhance revascularization of the nerve graft, diminish nerve fibrosis and subsequently improve nerve regeneration.

PART II: THE CONTRIBUTION OF ANGIOGENESIS AND STEM CELLS IN NERVE REGENERATION

Neural stem cell (NSC) research is not novel. The discovery of adult NSCs and neurogenesis occurred in the 1960s and since then a great amount of research has been focusing on increasing our understanding of NSCs [47-49]. Despite advancements, stem cell transplantation still remains in pre-clinical stages and has to make significant headways into clinical practice. Stem cell-based therapy may offer a suitable treatment with several regenerative benefits to restore neuronal function, including supporting remyelination and revascularization of the affected organ [50]. Specifically, stem cells that have been differentiated into Schwann cell-like cells, mimicking the function of the original facilitators of axonal regeneration, may enhance neuron survival to improve motor outcomes [51,52]. Growth factors secreted by stem cells may enhance angiogenesis, the sprouting of new capillaries from preexisting ones, to promote revascularization [53-56]. On the other hand, vasculature serves as a niche for stem cells that are mostly quiescent and are activated in response to injury [57,58]. The interaction of stem cells with vascularity and its contribution to nerve regeneration remains complex, however, it is postulated to be interconnected and interdependent. To understand the mechanisms of action, studies have been designed to investigate interactions per causal order.

Previous studies have shown that seeding of adipose-derived mesenchymal stem cells (MSC) onto decellularized nerve allografts results in an elevation of neurotrophic and angiogenic factors [40,41]. Using our established techniques to objectively measure angiogenesis, revascularization was found to be increased in nerve allografts that were seeded with MSCs compared to unseeded nerve allografts [59]. These MSCs were dynamically seeded onto nerve allografts, leading to evenly distributed cells on the outer surface of nerve grafts. This technique does not damage the nerve infrastructure nor is harmful to cell viability [60,61]. While many researchers have questioned how the presence of MSCs on the outer surface may elicit therapeutic potential for nerve regeneration, I hypothesize that the stem cell secretome, i.e. the paracrine factors secreted by stem cells and utilized for inter-cell communication, plays a more important role in this process than the location of the MSCs [62]. The stimulated stem cell secretome and the circular coverage of the nerve graft with MSCs have contributed to the centripetal pattern of increased revascularization [59], together leading to enhanced motor outcomes of nerve allografts seeded with undifferentiated and differentiated

MSCs, presented in **Chapter 9**. Undifferentiated MSCs delivered to the nerve allograft specifically, results in a significant increase in isometric tetanic force.

How does the augmentation of nerve allografts with stem cells enhance motor recovery? I could hypothesize that stem cells improve a pro-tolerogenic cellular paracrine environment for nerve allografts, resulting in stimulation of neurotrophic and angiogenic growth factors, ultimately leading to enhanced motor recovery. Undifferentiated and differentiated MSCs each exert different interactions with the surrounding microenvironment leading to their individual stem cell secretome over time *in vitro* [40]. However, it remains unclear how the differences in interactions with the microenvironment may change *in vivo* over a period of months, as the finite survival of MSCs is described up to 29 days in rats [63]. It is believed that the growth factors, secreted by MSCs, stimulate neuroregenerative cascades which consecutively remain active past stem cell survival, resulting in motor outcome changes at 12 weeks. At 16 weeks, outcomes between all groups have been normalized, consistent with the well-known superlative nerve regenerative capacity of the rat [64].

After investigating the independent effects of (i) angiogenesis (Part I of the general discussion) and (ii) stem cells on nerve regeneration, these two have been combined to *evaluate their effect on microvascular architecture of nerve allografts.*

In **Chapter 10**, it was found that the combination of angiogenesis with undifferentiated MSCs resulted in the greatest increase of revascularization of nerve allografts compared to all experimental groups. Not only has this combined treatment led to the increase of quality (i.e. size and distribution) of vessels, but it has also regulated directionality of vessels resulting in reaching the mid-section of the nerve allograft. While angiogenesis combined with differentiated MSCs resulted in a mesh network of non-organized microvessels, longitudinally running vessels along the entire length of the nerve graft were found when undifferentiated MSCs were combined with angiogenesis. Although the interaction of angiogenesis and stem cells has not been investigated previously, these findings provide evidence for a novel interaction that may further enhance nerve regeneration. I hypothesize that the (i) increase in vascularity and (ii) supportive paracrine microenvironment, provided by stem cells and SIEF flap, aid in diminishing fibrosis of the nerve graft, subsequently leading to enhanced nerve regeneration. This may be further supported by (iii) organized

longitudinally running vessels that provide modeled vessel tracks to precede the repair of damaged nerves [53,55,65,66].

Contemplating the above mentioned results, I could argue which subtype of MSCs is most beneficial for nerve regeneration. While differentiated MSCs specifically, have been shown to improve revascularization when seeded onto nerve allografts [59], the effect of undifferentiated MSCs is more evident in enhancing motor recovery. This may put my hypothesis that revascularization leads to improved motor recovery in question. However, no evidence regarding the *in vivo* secretome of undifferentiated MSCs compared to differentiated MSCs seeded onto nerve allografts has been available, making it difficult to understand the interaction of these cells with nerve in the rat model. Second, due to the lack of a high resolution micro CT scanner, these results were found using conventional photography at 16 weeks [59]. This 2D method lacks information regarding the interconnectivity of the vascular tree and solely considers a 16 week time point, limiting our understanding of the vessel organization over time. Third, seeding of nerve allografts with differentiated MSCs led to a mesh network of non-organized microvessels in the nerve [59]. This is in line with results found in Chapter 10. Concluding from prior results presented in this thesis, organized vessels may precede growing axons while non-aligned vessels may lack this guidance function. More research is needed to understand how the augmentation of nerve allograft with stem cells has led to enhanced motor outcomes at 12 weeks and to tie these in with our findings prior to drawing conclusions. In reality, considering the prolonged culture time and higher costs of differentiated MSCs [67,68], the fact that differentiated MSCs are not proven superior to undifferentiated MSCs and that the latter results in an enhanced motor recovery to a greater extent, I believe that undifferentiated MSCs are more desirable for clinical application.

CONCLUSIONS

The results from this thesis have expanded our mechanistic understanding of revascularization of nerve and provide evidence for the use of vascularized adipofascial flaps to enhance nerve allograft outcomes. The ability of vasculature to provide a niche for stem cells, which are activated in response to injury, suggests that blood vessels are more widely involved in tissue regeneration than was previously appreciated. Not solely the amount of vascularity is of importance, but the distribution and direction

of newly formed vessels are equally important to facilitate axonal outgrowth. The use of stem cells in peripheral nerve regeneration holds significant promise as these cells have the ability to respond to appropriate stimuli in their microenvironment, resulting in enhanced motor outcomes. Augmentation of nerve allografts with undifferentiated MSCs results in longitudinally running vessels along the entire length of the nerve graft, providing guidance for axon growth. In contrast, differentiated MSCs lead to a mesh network of non-organized microvessels in the nerve, possibly lacking this guidance. Although current evidence explaining their cellular interaction with nerve and vascularity during regeneration remains insufficient, practical considerations lean towards the use of undifferentiated MSCs. Aforementioned possible pathways for further nerve regeneration research are provided to enhance mechanistic understanding during the process of nerve regeneration and to achieve results with allografts comparable to nerve autografts.

FUTURE PERSPECTIVES AND RESEARCH

Numerous important questions regarding the cellular interactions *in vivo* remain: What is the exact number of stem cells needed to exert a beneficial effect? What is the optimal route of stem cell administration and does the provision of vascularity actually prolong the viability of stem cells? These unanswered questions are contributing to the fact why stem cell nerve research is still ongoing and its application has yet to make headways into clinical practice. Some may have the same arising question: *will this ever happen?* Science is beautifully complex and not all breakthroughs in basic science will eventually be clinically relevant or feasible. However, they do expand our mechanistic understanding of complex biological processes. The key elements of successful nerve regeneration are fibrocytes, Schwann cells and vascularity. Finding these three elements, or their substitution, in a fine balance remains a challenge. I believe that the results provided in this thesis serve as a stepping stone towards new insights. The interaction between stem cells, vascularity and nerve regeneration is depicted in Figure 2 and hypothesizes how these factors interact to eventually lead to enhancing nerve regeneration of nerve allografts. Currently, few studies have addressed the interaction of stem cells and vascularity in nerve regeneration, which creates an opportunity for elucidating its synergistic pathways in future research.

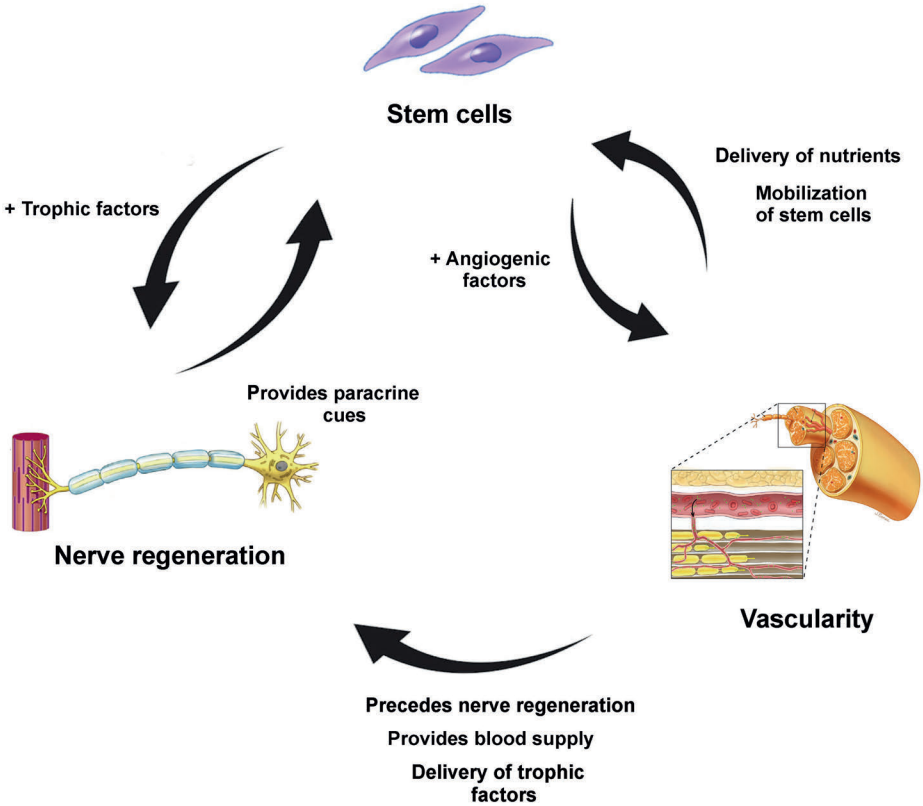

Figure 2. Schematic drawing of interaction between stem cells, vascularity, and nerve regeneration. After a nerve injury, paracrine cues are provided to stem cells to produce trophic and angiogenic factors that enhance nerve regeneration and angiogenesis, respectively. Blood supply mobilizes stem cells and delivers nutrients and trophic factors to the site of injury to improve nerve regeneration. Blood supply is not only important for the survivability of stem cells but also precedes nerve regeneration after nerve trauma. *Copyrighted and used with permission of the Mayo Foundation for Medical Education and Research; all rights reserved.*

- **Planned experiments at Mayo Clinic:** the nerve research line will be advanced towards the investigation of long-term results after combined angiogenesis and stem cell delivery to evaluate motor recovery. To overcome the superlative nerve regenerative capacity of the rat, studies will then be translated to a larger nerve gap model in rabbits. The rabbit model will allow for confirmation of the independent effect of angiogenesis and stem cell delivery found in rats and assess the combined application which will provide stronger evidence for clinical translation.

- **Augmentation of nerve autografts with angiogenesis:** while the goal is to augment off-the-shelf decellularized nerve allografts to meet outcomes of autografts, it would be interesting to investigate the effect of angiogenesis on nerve autograft to enhance nerve regeneration. Future experimental research could compare the autograft wrapped within a pedicled SIEF flap to the autograft alone to assess motor recovery outcomes. This has great potential for clinical translation, as many pedicled adipofascial flap options currently exist that could augment the autologous sural nerve, or any other autologous donor nerve, depending on the location of the injury.

- **The role of adipose tissue in nerve fibrosis:** another interesting future aspect for investigation would be to assess the role of adipose tissue in perineural scar formation. Scar formation after peripheral nerve injury is a significant clinical problem that impedes regeneration [69,70]. Results from this thesis suggest that the adipofascial flap provides a supportive microenvironment that diminishes nerve fibrosis. Further histologic assessment could be performed to evaluate the collagen deposition, and cellular count of fibroblasts and inflammatory cells in nerve tissue [71]. The experimental groups could include (i) nerve graft wrapped within a pedicled adipofascial flap and (ii) autologous fat grafting administered to the nerve graft, compared to the (iii) nerve graft alone. The concept of fat grafting has been longstanding in the field of reconstructive surgery and has become a dynamic modality to improve functional outcomes and aesthetic form in clinical practice [72].

REFERENCES

1. Terzis JK, Sun DD, Thanos PK. Historical and basic science review: past, present, and future of nerve repair. *J Reconstr Microsurg.* 1997;13(3):215-225.
2. Pan YA, Misgeld T, Lichtman JW, Sanes JR. Effects of neurotoxic and neuroprotective agents on peripheral nerve regeneration assayed by time-lapse imaging in vivo. *J Neurosci.* 2003;23(36):11479-11488.
3. Gutmann E, Guttmann L, Medawar P, Young J. The rate of regeneration of nerve. *Journal of Experimental Biology.* 1942;19(1):14-44.
4. Mackinnon SE. Surgical management of the peripheral nerve gap. *Clin Plast Surg.* 1989;16(3):587-603.
5. Daly PJ, Wood MB. Endoneural and epineural blood flow evaluation with free vascularized and conventional nerve grafts in the canine. *J Reconstr Microsurg.* 1985;2(1):45-49.
6. Koshima I, Harii K. Experimental study of vascularized nerve grafts: multifactorial analyses of axonal regeneration of nerves transplanted into an acute burn wound. *J Hand Surg Am.* 1985;10(1):64-72.
7. Pho RW, Lee YS, Rujiwetpongstorn V, Pang M. Histological studies of vascularised nerve graft and conventional nerve graft. *J Hand Surg Br.* 1985;10(1):45-48.
8. Restrepo Y, Merle M, Michon J, Folliguet B, Barrat E. Free vascularized nerve grafts: an experimental study in the rabbit. *Microsurgery.* 1985;6(2):78-84.
9. Doi K, Kuwata N, Sakai K, Tamaru K, Kawai S. A reliable technique of free vascularized sural nerve grafting and preliminary results of clinical applications. *J Hand Surg Am.* 1987;12(5 Pt 1):677-684.
10. Shibata M, Tsai TM, Firrell J, Breidenbach WC. Experimental comparison of vascularized and nonvascularized nerve grafting. *J Hand Surg Am.* 1988;13(3):358-365.
11. Rose EH, Kowalski TA, Norris MS. The reversed venous arterialized nerve graft in digital nerve reconstruction across scarred beds. *Plast Reconstr Surg.* 1989;83(4):593-604.
12. Terzis JK, Kostopoulos VK. Vascularized nerve grafts for lower extremity nerve reconstruction. *Ann Plast Surg.* 2010;64(2):169-176.
13. Terzis JK, Kostopoulos VK. Vascularized nerve grafts and vascularized fascia for upper extremity nerve reconstruction. *Hand (N Y).* 2010;5(1):19-30.
14. Kline TL, Knudsen BE, Anderson JL, Vercnocke AJ, Jorgensen SM, Ritman EL. Anatomy of hepatic arteriolo-portal venular shunts evaluated by 3D micro-CT imaging. *J Anat.* 2014;224(6):724-731.
15. Perrien DS, Saleh MA, Takahashi K, et al. Novel methods for microCT-based analyses of vasculature in the renal cortex reveal a loss of perfusable arterioles and glomeruli in eNOS-/- mice. *BMC Nephrol.* 2016;17:24.
16. Carmeliet P, Collen D. Transgenic mouse models in angiogenesis and cardiovascular disease. *J Pathol.* 2000;190(3):387-405.
17. Tarlov IM EJ. Nerve grafts: The importance of an adequate blood supply. *J Neurosurg.* 1945;2:49-71.
18. Lind R, Wood MB. Comparison of the pattern of early revascularization of conventional versus vascularized nerve grafts in the canine. *J Reconstr Microsurg.* 1986;2(4):229-234.

19. Penkert G, Bini W, Samii M. Revascularization of nerve grafts: an experimental study. *J Reconstr Microsurg.* 1988;4(4):319-325.
20. Terzis JK, Skoulis TG, Soucacos PN. Vascularized nerve grafts. A review. *Int Angiol.* 1995;14(3):264-277.
21. Wongtrakul S, Bishop AT, Friedrich PF. Vascular endothelial growth factor promotion of neoangiogenesis in conventional nerve grafts. *J Hand Surg Am.* 2002;27(2):277-285.
22. Hobson MI, Brown R, Green CJ, Terenghi G. Inter-relationships between angiogenesis and nerve regeneration: a histochemical study. *Br J Plast Surg.* 1997;50(2):125-131.
23. Lee WP, Constantinescu MA, Butler PE. Effect of early mobilization on healing of nerve repair: histologic observations in a canine model. *Plast Reconstr Surg.* 1999;104(6):1718-1725.
24. Mani GV, Shurey C, Green CJ. Is early vascularization of nerve grafts necessary? *J Hand Surg Br.* 1992;17(5):536-543.
25. Lee JY, Giusti G, Friedrich PF, Bishop AT, Shin AY. Effect of Vascular Endothelial Growth Factor Administration on Nerve Regeneration after Autologous Nerve Grafting. *J Reconstr Microsurg.* 2016;32(3):183-188.
26. Chalfoun C, Scholz T, Cole MD, Steward E, Vanderkam V, Evans GR. Primary nerve grafting: A study of revascularization. *Microsurgery.* 2003;23(1):60-65.
27. Prpa B, Huddleston PM, An KN, Wood MB. Revascularization of nerve grafts: a qualitative and quantitative study of the soft-tissue bed contributions to blood flow in canine nerve grafts. *J Hand Surg Am.* 2002;27(6):1041-1047.
28. Best TJ, Mackinnon SE, Midha R, Hunter DA, Evans PJ. Revascularization of peripheral nerve autografts and allografts. *Plast Reconstr Surg.* 1999;104(1):152-160.
29. Ghanavati S, Yu LX, Lerch JP, Sled JG. A perfusion procedure for imaging of the mouse cerebral vasculature by X-ray micro-CT. *J Neurosci Methods.* 2014;221:70-77.
30. Clore JN, Cohen IK, Diegelmann RF. Quantitation of collagen types I and III during wound healing in rat skin. *Proc Soc Exp Biol Med.* 1979;161(3):337-340.
31. Hinz B, Phan SH, Thannickal VJ, et al. Recent developments in myofibroblast biology: paradigms for connective tissue remodeling. *Am J Pathol.* 2012;180(4):1340-1355.
32. Huang C, Ogawa R. The Vascular Involvement in Soft Tissue Fibrosis-Lessons Learned from Pathological Scarring. *Int J Mol Sci.* 2020;21(7).
33. Wang S, Meng XM, Ng YY, et al. TGF-beta/Smad3 signalling regulates the transition of bone marrow-derived macrophages into myofibroblasts during tissue fibrosis. *Oncotarget.* 2016;7(8):8809-8822.
34. Nieves Torres EC, Yang B, Brahmbhatt A, Mukhopadhyay D, Misra S. Blood outgrowth endothelial cells reduce hypoxia-mediated fibroblast to myofibroblast conversion by decreasing proangiogenic cytokines. *J Vasc Res.* 2014;51(6):458-467.
35. Modarressi A, Pietramaggiori G, Godbout C, Vigato E, Pittet B, Hinz B. Hypoxia impairs skin myofibroblast differentiation and function. *J Invest Dermatol.* 2010;130(12):2818-2827.
36. Steinbrech DS, Longaker MT, Mehrara BJ, et al. Fibroblast response to hypoxia: the relationship between angiogenesis and matrix regulation. *J Surg Res.* 1999;84(2):127-133.

37. Schultes G, Gaggl A, Kleinert R, Karcher H. Vascularized versus non-vascularized nerve transfers: histologic study in rats. *J Reconstr Microsurg.* 2001;17(8):637-642.
38. Siironen J, Sandberg M, Vuorinen V, Roytta M. Expression of type I and III collagens and fibronectin after transection of rat sciatic nerve. Reinnervation compared with denervation. *Lab Invest.* 1992;67(1):80-87.
39. Koopmans G, Hasse B, Sinis N. Chapter 19: The role of collagen in peripheral nerve repair. *Int Rev Neurobiol.* 2009;87:363-379.
40. Mathot F, Rbia N, Thaler R, Bishop AT, Van Wijnen AJ, Shin AY. Gene expression profiles of differentiated and undifferentiated adipose derived mesenchymal stem cells dynamically seeded onto a processed nerve allograft. *Gene.* 2020;724:144151.
41. Rbia N, Bulstra LF, Lewallen EA, Hovius SER, van Wijnen AJ, Shin AY. Seeding decellularized nerve allografts with adipose-derived mesenchymal stromal cells: An in vitro analysis of the gene expression and growth factors produced. *J Plast Reconstr Aesthet Surg.* 2019;72(8):1316-1325.
42. Jesuraj NJ, Nguyen PK, Wood MD, et al. Differential gene expression in motor and sensory Schwann cells in the rat femoral nerve. *J Neurosci Res.* 2012;90(1):96-104.
43. Vleggeert-Lankamp CL. The role of evaluation methods in the assessment of peripheral nerve regeneration through synthetic conduits: a systematic review. Laboratory investigation. *J Neurosurg.* 2007;107(6):1168-1189.
44. den Dunnen WF, van der Lei B, Schakenraad JM, et al. Poly(DL-lactide-epsilon-caprolactone) nerve guides perform better than autologous nerve grafts. *Microsurgery.* 1996;17(7):348-357.
45. Bassilios Habre S, Bond G, Jing XL, Kostopoulos E, Wallace RD, Konofaos P. The Surgical Management of Nerve Gaps: Present and Future. *Ann Plast Surg.* 2018;80(3):252-261.
46. McCullough CJ, Gagey O, Higginson DW, Sandin BM, Crow JC, Sebille A. Axon regeneration and vascularisation of nerve grafts. An experimental study. *J Hand Surg Br.* 1984;9(3):323-327.
47. Altman J, Das GD. Autoradiographic and histological studies of postnatal neurogenesis. I. A longitudinal investigation of the kinetics, migration and transformation of cells incorporating tritiated thymidine in neonate rats, with special reference to postnatal neurogenesis in some brain regions. *J Comp Neurol.* 1966;126(3):337-389.
48. Altman J, Das GD. Autoradiographic and histological evidence of postnatal hippocampal neurogenesis in rats. *J Comp Neurol.* 1965;124(3):319-335.
49. Takagi Y. History of Neural Stem Cell Research and Its Clinical Application. *Neurol Med Chir (Tokyo).* 2016;56(3):110-124.
50. Jiang L, Jones S, Jia X. Stem Cell Transplantation for Peripheral Nerve Regeneration: Current Options and Opportunities. *Int J Mol Sci.* 2017;18(1).
51. De la Rosa MB, Kozik EM, Sakaguchi DS. Adult Stem Cell-Based Strategies for Peripheral Nerve Regeneration. *Adv Exp Med Biol.* 2018;1119:41-71.
52. Keilhoff G, Goihl A, Langnase K, Fansa H, Wolf G. Transdifferentiation of mesenchymal stem cells into Schwann cell-like myelinating cells. *Eur J Cell Biol.* 2006;85(1):11-24.
53. Rissanen TT, Rutanen J, Yla-Herttuala S. Gene transfer for therapeutic vascular growth in myocardial and peripheral ischemia. *Adv Genet.* 2004;52:117-164.
54. Caplan AI. Adult Mesenchymal Stem Cells: When, Where, and How. *Stem Cells Int.* 2015;2015:628767.

55. Risau W. Mechanisms of angiogenesis. *Nature.* 1997;386(6626):671-674.
56. Mathot F, Shin AY, Van Wijnen AJ. Targeted stimulation of MSCs in peripheral nerve repair. *Gene.* 2019.
57. Zhang L, Issa Bhaloo S, Chen T, Zhou B, Xu Q. Role of Resident Stem Cells in Vessel Formation and Arteriosclerosis. *Circ Res.* 2018;122(11):1608-1624.
58. Bautch VL. Stem cells and the vasculature. *Nat Med.* 2011;17(11):1437-1443.
59. Mathot F, Rbia N, Bishop AT, Hovius SER, Shin AY. Adipose derived mesenchymal stem cells seeded onto a decellularized nerve allograft enhances angiogenesis in a rat sciatic nerve defect model. *Microsurgery.* 2020.
60. Mathot F, Rbia N, Bishop AT, Hovius SER, Van Wijnen AJ, Shin AY. Adhesion, distribution, and migration of differentiated and undifferentiated mesenchymal stem cells (MSCs) seeded on nerve allografts. *J Plast Reconstr Aesthet Surg.* 2020;73(1):81-89.
61. Rbia N, Bulstra LF, Bishop AT, van Wijnen AJ, Shin AY. A Simple Dynamic Strategy to Deliver Stem Cells to Decellularized Nerve Allografts. *Plast Reconstr Surg.* 2018;142(2):402-413.
62. L PK, Kandoi S, Misra R, S V, K R, Verma RS. The mesenchymal stem cell secretome: A new paradigm towards cell-free therapeutic mode in regenerative medicine. *Cytokine Growth Factor Rev.* 2019;46:1-9.
63. Rbia N, Bulstra LF, Thaler R, Hovius SER, van Wijnen AJ, Shin AY. In Vivo Survival of Mesenchymal Stromal Cell-Enhanced Decellularized Nerve Grafts for Segmental Peripheral Nerve Reconstruction. *J Hand Surg Am.* 2019;44(6):514 e511-514 e511.
64. Tang P, Whiteman DR, Voigt C, Miller MC, Kim H. No Difference in Outcomes Detected Between Decellular Nerve Allograft and Cable Autograft in Rat Sciatic Nerve Defects. *J Bone Joint Surg Am.* 2019;101(10):e42.
65. Carmeliet P, Ferreira V, Breier G, et al. Abnormal blood vessel development and lethality in embryos lacking a single VEGF allele. *Nature.* 1996;380(6573):435-439.
66. Saffari TM, Bedar M, Hundepool CA, Bishop AT, Shin AY. The role of vascularization in nerve regeneration of nerve graft. *Neural Regen Res.* 2020;15(9):1573-1579.
67. Mathot F, Shin AY, Van Wijnen AJ. Targeted stimulation of MSCs in peripheral nerve repair. *Gene.* 2019;710:17-23.
68. Kingham PJ, Kalbermatten DF, Mahay D, Armstrong SJ, Wiberg M, Terenghi G. Adipose-derived stem cells differentiate into a Schwann cell phenotype and promote neurite outgrowth in vitro. *Exp Neurol.* 2007;207(2):267-274.
69. Atkins S, Smith KG, Loescher AR, et al. Scarring impedes regeneration at sites of peripheral nerve repair. *Neuroreport.* 2006;17(12):1245-1249.
70. Sunderland S. The function of nerve fibers whose structure has been disorganized. *Anat Rec.* 1951;109(3):503-513.
71. Mekaj AY, Manxhuka-Kerliu S, Morina AA, Duci SB, Shahini L, Mekaj YH. Effects of hyaluronic acid and tacrolimus on the prevention of perineural scar formation and on nerve regeneration after sciatic nerve repair in a rabbit model. *Eur J Trauma Emerg Surg.* 2017;43(4):497-504.
72. Vyas KS, Vasconez HC, Morrison S, et al. Fat Graft Enrichment Strategies: A Systematic Review. *Plast Reconstr Surg.* 2020;145(3):827-841.

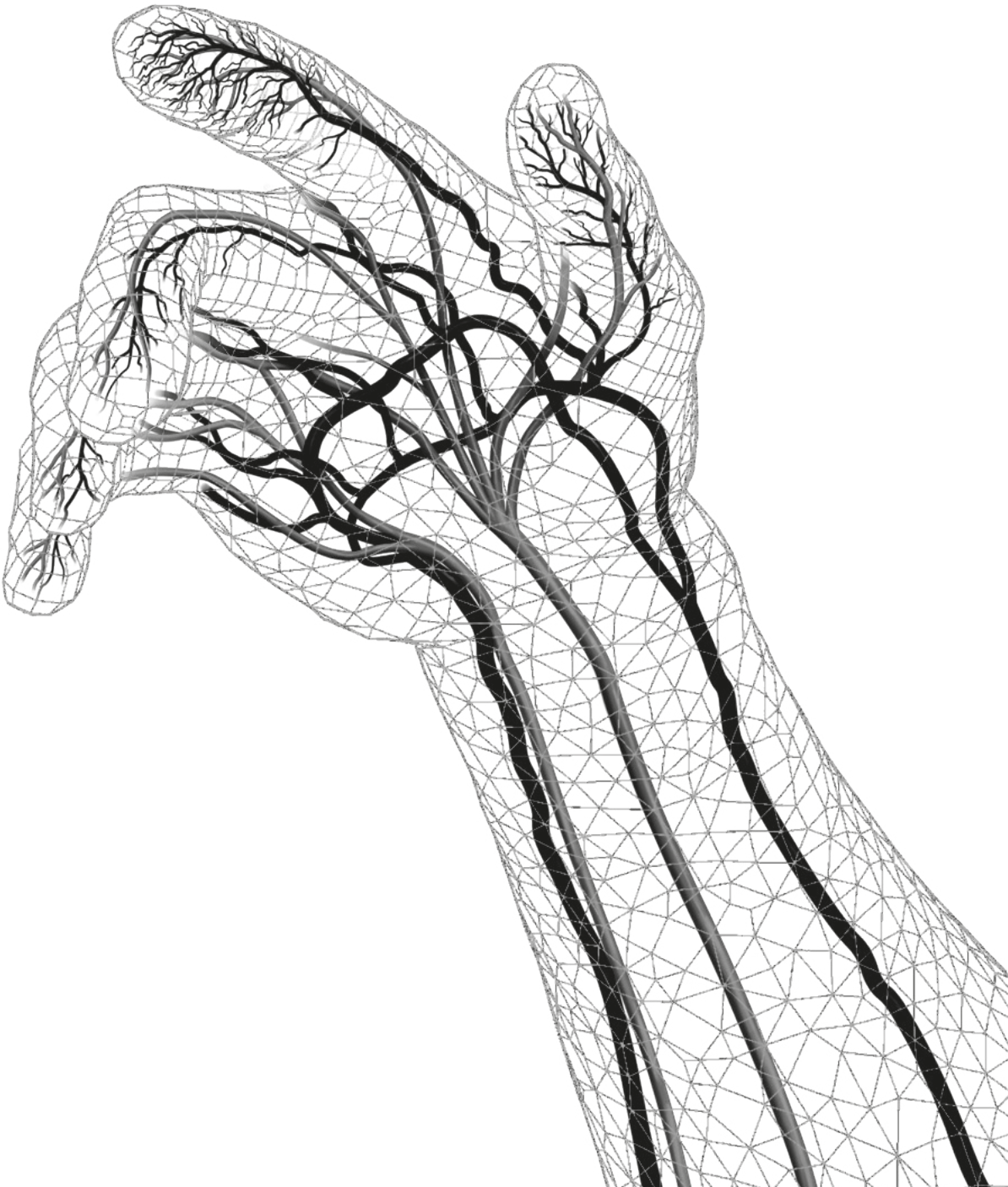

CHAPTER TWELVE

Summary / Samenvatting

SUMMARY

Enhancing decellularized nerve allograft to equal autograft performances has been an ongoing challenge for surgeons and nerve scientists. This thesis is part of a research collaboration with the Mayo Clinic (MN, USA) and builds on the results of previously conducted research, leading to this thesis called *"Augmentation of nerve allografts with angiogenesis and stem cells"*. The hypothesis of this thesis was if augmentation of decellularized nerve allograft environment with angiogenesis and stem cells improves nerve regeneration and revascularization. In **Chapter 1** a general introduction on peripheral nerve injury and reconstruction including a historical background of the research line and an overview of the specific aims of this thesis is provided.

PART I: THE ROLE OF ANGIOGENESIS IN NERVE REGENERATION

In Part I, the role of angiogenesis in nerve regeneration has been investigated, represented by Chapter 2-7. The review in **Chapter 2** details the role of vascularization in nerve regeneration of nerve grafts including all relevant publications until August 2019. The processes underlying the formation of blood vessels are described and an overview of the effect of vascularization on nerve regeneration in basic science and clinical applications is provided. Nerve characteristics such as length of the gap, nature of the nerve (e.g. motor nerves, mixed motor and sensory nerves, or sensory nerves) and the regeneration rate per animal were found to cause difficulty in comparison. In clinical studies, outcomes were strongly correlated with the time course and degree of denervation. Well-designed clinical studies comparing vascularized nerve grafts (VNG) to non-vascularized nerve grafts (NVNG) remain lacking and existing studies are inconclusive. Although VNGs have the potential to improve nerve reconstruction after injury, the surgeries are demanding and require microvascular experience. The conclusions suggest that technical obstacles could be overcome by provision of vascularized flaps that may enhance revascularization of reconstructed peripheral nerve injuries.

In **Chapter 3**, the surgical technique for the superficial inferior epigastric artery fascial (SIEF) flap has been described that provides vascularization to the nerve bed. Outcomes demonstrated a total success rate of SIEF flap viability without necrosis at 12 and 16 weeks, providing evidence that this flap is durable and could be used for future

studies in this thesis. We recommend this simple technique to add vascularization to various tissues in the lower abdomen, genital area, thigh, and upper limb of the rat.

To objectively measure angiogenesis in nerve samples, the use of conventional photography and micro computed tomography (micro CT) was investigated in **Chapter 4**. Vascular volume and vascular surface area, calculated with micro CT and photography respectively, both reflect vessel percentage of the nerve graft and could be used in the same samples. Besides the amount of vascularity, these methods allow for dimensional visualization of vessels to allow for insight in the connectivity of the vascular tree. The micro CT specifically, provides three-dimensional (3D) interconnectivity of the vasculature and contributes to crucial description of neovascularization patterns. Our results indicated a significant correlation ($r = 0.951$, $p = 0.049$) between the vascular volume and the vascular surface area measurements, demonstrating that these methods could be used either complementary or separately, depending on the aims of the study.

In **Chapter 5**, described techniques in Chapter 3 and Chapter 4 were combined to investigate revascularization patterns in a rat sciatic nerve defect model over time. Starting at two weeks, vascularization consisting of a mesh network occurred from both host stumps in decellularized nerve allografts and SIEF nerve samples, leaving the middle part avascularized. Over time, sprouted vessels reached the middle parts of the nerve and this was more evident from the proximal than from the distal end. The SIEF flap significantly improved revascularization of allograft nerve at two, 12 and 16 weeks compared to allograft alone. In nerve autografts, longitudinal running vessels were recognized that ran along the entire length of the nerve. These vessels appeared thicker compared to the newly formed vessels in the allograft and SIEF nerve samples, comparable to unoperated samples (negative control). This study suggests that an improved vascularized bed promotes longitudinal inosculation, in particular proximal inosculation, and confirms the theory of centripetal revascularization.

In **Chapter 6**, the effect of angiogenesis was studied at a cellular level in a rat sciatic nerve defect model to investigate its effect on nerve fibrosis. In this study, we demonstrated that a well vascularized bed (i.e. SIEF flap) enhances the local cellular environment near the nerve repair site, called the paracrine environment, to support tissue healing after injury and subsequently diminish fibrosis. Fibrocytes

and endothelial cells can be activated towards myofibroblasts to participate in the formation of nerve fibrosis. Angiogenesis was recognized in slowing down the differentiation towards pro-fibrotic myofibroblasts. In SIEF rats, an increased T helper population ($CD4^+$ cells) was found after one week postoperatively in peripheral blood, indicating that immune reactive changes could be detected peripherally. The use of flowcytometry to detect peripheral T cells in blood samples is feasible and could be expanded to multiple time points and a larger set of immune cells to provide a broader evaluation of the short-term immune reaction.

The results presented in **Chapter 7** show that augmentation of decellularized nerve allografts with angiogenesis improves early functional recovery in a rat sciatic nerve defect model. The mechanisms directing towards this result are twofold. First, the SIEF flap increases vascularity which precedes nerve regeneration. Enhanced vascularity in the nerve graft was measured using micro CT, photography (Chapter 5), gene expression levels, immunohistochemical staining (Chapter 6) and immunofluorescence (Chapter 7). Second, the SIEF flap diminishes nerve fibrosis, leading to enhanced nerve regeneration. This is supported by analyzed collagen deposition levels (Chapter 6) and the fact that an improved N-ratio was found in SIEF compared to allograft only (Chapter 7). A well vascularized bed, provided by the SIEF flap, not solely improves revascularization, but is also suggested to decrease graft ischemic time, subsequently impeding necrosis.

PART II: THE CONTRIBUTION OF ANGIOGENESIS AND STEM CELLS IN NERVE REGENERATION

In Part II, the contribution of angiogenesis and stem cells in nerve regeneration has been investigated, represented by Chapter 8-10. In **Chapter 8**, a review on the interaction of stem cells and vascularity in peripheral nerve regeneration is provided. Stem cells can be acquired through various sources that correlate to their differentiation potential, including embryonic stem cells, neural stem cells, and mesenchymal stem cells (MSC). Each source of stem cells serves its particular differentiation potential and properties associated with the promotion of revascularization and nerve regeneration. The effect of stem cells is dependent on paracrine cues provided by the environment during nerve regeneration. Despite advancements in pre-clinical studies, translation of stem cells application to clinical practice is currently limited by ethical issues, culture technique

challenges and risk of tumorgenesis. To overcome the difficulties associated with the harvest of stem cells, delay in culture and high costs of stem cells, future research could be directed towards the use of exosomes.

In **Chapter 9**, the outcomes of stem cell seeding onto decellularized nerve allografts in a rat sciatic nerve defect model are provided. The main finding was that seeding of nerve allografts with both undifferentiated MSCs and MSCs differentiated into Schwann cell-like cells resulted in improved functional outcomes. Seeding with undifferentiated MSCs leads to a significant increase in force. It is hypothesized that stem cells promote a tolerogenic cellular paracrine environment for nerve allografts, resulting in the stimulation of neurotrophic and angiogenic growth factors, ultimately leading to enhanced functional recovery. Undifferentiated MSCs and MSCs differentiated into Schwann cell-like cells each exert different interactions with the surrounding microenvironment leading to their individual stem cell secretome over time. When taken preparation time, costs and achieved effect on functional recovery into account, undifferentiated MSCs have more potential for future research in peripheral nerve reconstruction.

In **Chapter 10**, the combined effect of angiogenesis and stem cells on microvascular architecture of decellularized nerve allografts was evaluated in a rat sciatic nerve defect model. Vascular volume was measured using micro CT and spatial distribution analysis was used to evaluate volume and diameter of vessel segments. These distributions were enhanced in nerve allografts augmented with angiogenesis and further improved when angiogenesis was combined with MSCs. The greatest increase of vascular volume, size of vessels and revascularization of the mid-section of the nerve allograft was found when angiogenesis was combined with undifferentiated MSCs. This combination is hypothesized to work synergistically resulting in organized longitudinally running vessels that provide modeled vessel tracks to precede the repair of damaged nerves.

In **Chapter 11**, the results of this thesis are discussed in light of current literature. Furthermore, possible pathways for further nerve regeneration research are provided. After nerve injury, vascular endothelial cells guide the regeneration of peripheral nerve axons by producing vascular endothelial growth factor (VEGF). This process is induced by hypoxia and stimulates a cascade of pathways. A well vascularized bed stimulates a

broad spectrum of paracrine actions, not solely induced by the secretion of VEGF, and provides an anti-inflammatory microenvironment. This environment is suggested to enhance revascularization of the decellularized nerve allograft, diminish nerve fibrosis and subsequently improve nerve regeneration. A pedicled adipofascial flap is a durable and simple technique to provide vascularization to the nerve wound bed and create such an microenvironment. Both the provision of undifferentiated and differentiated MSCs improved functional outcomes of decellularized nerve allografts. The delivery of undifferentiated MSCs is favored considering the shorter culture time and the greater functional recovery that was achieved. The combination of undifferentiated MSCs and angiogenesis specifically, leads to the increase of quality (i.e. size and distribution) of vessels and is postulated to regulate directionality of vessels. The distribution and direction of newly formed vessels are believed to be equally important to facilitate axonal outgrowth.

NEDERLANDSE SAMENVATTING

Sinds de introductie van gedecellulariseerde allogene zenuwtransplantaten (allograft) wordt er gestreefd naar het verbeteren van de uitkomsten om de resultaten van de autogene zenuwtransplantaten (autograft) te behalen. Dit proefschrift getiteld *"De toevoeging van vascularisatie en stamcellen aan allogene zenuwtransplantaten"* is voortgekomen uit een samenwerking met de Mayo Clinic (Verenigde Staten) en gebaseerd op de resultaten van eerder verricht onderzoek. De hypothese van dit proefschrift is dat de toevoeging van vascularisatie en stamcellen leidt tot een verbeterde zenuw regeneratie en revascularisatie van gedecellulariseerde allogene zenuwtransplantaten in de rat. In **Hoofdstuk 1** wordt een algemene inleiding gegeven over perifere zenuwschade en reconstructie. Daarnaast worden de voortgaande resultaten van de onderzoekssamenwerking gepresenteerd en de doelstellingen van dit proefschrift beschreven.

DEEL I: DE ROL VAN ANGIOGENESE IN ZENUWREGENERATIE

In het eerste deel van dit proefschrift is de rol van angiogenese in zenuwregeneratie onderzocht. Dit deel resulteerde in 7 hoofdstukken, waarbij in het **tweede hoofdstuk** een overzicht wordt gegeven van de rol van vascularisatie in zenuwregeneratie in de vorm van een review. In dit literatuuronderzoek zijn alle relevante studies geïncludeerd, welke zijn gepubliceerd tot en met augustus 2019. De embryogenese van bloedvaten wordt besproken en daarnaast wordt een overzicht gegeven van het effect van vascularisatie in zenuwregeneratie in zowel basaal onderzoek als klinische studies. De lengte van het te reconstrueren zenuwdefect, type zenuw (motorische, gemengde of sensorische zenuw) en diermodel verhinderden directe vergelijking van de gevonden resultaten. In klinische studies waren de uitkomsten gecorreleerd met de mate van zenuwschade en het beloop na een letsel. Wegens het tekort aan goed ontworpen klinische studies was er onvoldoende bewijs gevonden voor het gebruik van gevascularisseerde zenuwtransplantaten versus niet-gevascularisseerde zenuwtransplantaten. Alhoewel gevascularisseerde zenuwtransplanten een potentieel herbergen om uitkomsten na zenuwreconstructie te verbeteren, tonen de resultaten dat de operaties vaak complexer zijn en microvasculaire ervaring vereisen. De resultaten van dit artikel indiceren het gebruik van een gevascularisseerde adipofasciale lap om uitkomsten na zenuwreconstructie te verbeteren.

In **Hoofdstuk 3** is een chirurgische techniek beschreven voor de gesteelde adipofasciale lap (SIEF), gevoed door de oppervlakkige epigastrische slagader (SIEA). Deze lap wordt geoogst in het abdomen, geroteerd op de vaatsteel en subcutaan getunneld naar het been. Daar wordt deze lap om de nervus ischiadicus heen gewikkeld om vascularisatie toe te voegen aan het zenuwbed. Na een follow-up van 12 en 16 weken was de lap vitaal in alle gevallen. De resultaten van deze studie valideren de SIEF lap als een betrouwbare techniek om vascularisatie toe te voegen en bieden bewijs om deze lap te gebruiken in de experimenten van dit proefschrift. Wij zouden het gebruik van de SIEF lap aanraden om vascularisatie toe te voegen in het bekken, de genitaal regio en het bovenbeen van de rat.

In **Hoofdstuk 4** onderzochten wij methoden om de vaatstructuur van getransplanteerde zenuwen in de rat dimensionaal te kunnen beschrijven en de angioneogenese objectief te meten. Door middel van conventionele fotografie (tweedimensionaal) werd het vasculaire oppervlak gemeten en met behulp van micro computertomografie (micro CT, driedimensionaal) werd het vasculaire volume in kaart gebracht in dezelfde zenuw. Daarna kon voor elke techniek de bloedvat/zenuw ratio worden berekend welke werd gepresenteerd in percentages (vessel%). Voorts konden deze technieken worden gebruikt om de vasculaire patronen in kaart te brengen om de nieuwvorming van vaten (angioneogenese) te beschrijven. Wegens het driedimensionale beeld van de micro CT, droeg deze techniek hier in het bijzonder aan bij. De correlatie tussen beide methoden was significant ($r = 0.951$, $p = 0.049$) voor beide tijdspunten. Deze resultaten tonen aan dat beide technieken kunnen worden toegepast afhankelijk van het doel van de studie.

Het **vijfde hoofdstuk** combineert de technieken beschreven in Hoofdstuk 3 en 4 om revascularisatie van gedecellulariseerde allogene zenuwtransplantaten ter reconstructie van perifeer zenuwletsel in de rat te beschrijven. Na twee weken begon revascularisatie in de allogene zenuwtransplantaten in combinatie met een SIEF lap vanuit beide zenuwuiteinden op gang te komen bestaande uit dunne, kleine bloedvaatjes. Het middelste deel bleef vooralsnog avasculair. Gedurende de follow-up bleek de groei van de nieuwgevormde vaten evidenter vanuit proximaal dan vanuit distaal. Het toevoegen van de SIEF lap verbetert de revascularisatie van allogene zenuwtransplantaten significant op 2, 12 en 16 weken, vergeleken met alleen het allogene zenuwtransplantaat. In autogene zenuwtransplantaten werden grotere longitudinaal lopende vaten herkend over de gehele lengte van de zenuw, vergelijkbaar

met ongeopereerde controle zenuwen. Deze studie toont aan dat revascularisatie primair van proximaal wordt aangestuurd (proximale inosculatie) en niet van beide uiteinden zoals voorheen werd gedacht. De centripetale revascularisatie theorie wordt bevestigd, welke de mate van revascularisatie aan de mate van bloedtoevoer correleert.

In **Hoofdstuk 6** hebben wij ons gericht op het evalueren van de moleculaire mechanismen die ten grondslag liggen aan het effect van angioneogenese op zenuwregeneratie en zenuwfibrose. De resultaten van deze studie toonden aan dat een goed gevascularisseerd zenuwbed de paracriene signalering stimuleert. Bij paracriene signalering diffuseren de signaalmoleculen (o.a. groeifactoren) lokaal in het omliggende weefsel en grijpen deze aan op dichtbij gelegen cellen om weefselregeneratie na letsels te bevorderen en fibrose te verminderen. Bij fibrose differentiëren fibrocyten en endotheelcellen zich tot myofibroblasten. Wanneer myofibroblasten zijn gevormd, kunnen bindweefselenzymen worden gesecreteerd welke aanleiding geven tot pathologische zenuwfibrose. De resultaten van dit hoofdstuk wijzen aan dat angioneogenese dit proces kan afremmen. Na een week waren CD4 T helper cellen significant verhoogd in het perifere bloed van zenuwen waar een SIEF lap om het allogene zenuwtransplantaat was gewikkeld. Deze bevinding geeft aan dat de lokale veranderingen perifeer gedetecteerd kunnen worden met behulp van flowcytometrie. Deze techniek blijkt betrouwbaar om perifere immuuncellen in het bloed te detecteren en kan worden uitgebreid met het aantal markers en tijdspunten om een beter overzicht te geven van de immuunreactie na zenuwreconstructie.

In **Hoofdstuk 7** hebben wij ons gericht op het evalueren van functieherstel in ratten waarbij een gesteelde lap is toegevoegd aan het allogene zenuwtransplantaat. Er werd gevonden dat de spierkracht, gemeten met de isometrische tetanische krachttest, na 12 weken significant was verbeterd door angioneogenese. Deze bevinding kan als volgt verklaard worden: allereerst zorgt de SIEF lap voor een toename van vascularisatie in de zenuwen. Deze nieuwgevormde bloedvaten vormen routes en zullen de regeneratie van axonen langs dit traject aansturen. De toegenomen vascularisatie is gemeten met behulp van micro CT, conventionele fotografie (Hoofdstuk 5), genexpressie, immuno-histochemie (Hoofdstuk 6) en immuno-fluorescentie (Hoofdstuk 7). Ten tweede reduceert de SIEF lap de vorming van zenuwfibrose in de allogene zenuwtransplantaten. Dit bevordert de zenuwregeneratie, resulterend in een verbeterde spierkracht. Dit

wordt ondersteund door de geanalyseerde collageen deposities (Hoofdstuk 6) en het feit dat een verhoogde N-ratio werd gevonden na toevoeging van de SIEF lap (Hoofdstuk 7). De N-ratio representeert de graad van myelinisatie, waarbij een lagere ratio suggererend is voor fibrose. Een goed gevascularisseerd zenuwbed, verzorgd door de SIEF lap, leidt niet alleen tot een toename in revascularisatie van de zenuwen, maar vermindert de ischemietijd welke necrose tegengaat.

DEEL II: DE CONTRIBUTIE VAN ANGIOGENESE EN STAMCELLEN AAN ZENUWREGENERATIE

In het tweede deel van dit proefschrift is de rol van angioneogenese en stamcellen in zenuwregeneratie onderzocht (Hoofdstuk 8-10). In **Hoofdstuk 8** beschreven wij de interactie van stamcellen, vascularisatie en zenuwregeneratie in een review. Er zijn meerdere bronnen voor pluripotente stamcellen. Afhankelijk van de graad van differentiatie, en dus het differentiatiepotentieel, kunnen verschillende type stamcellen worden onderscheiden waaronder embryonale stamcellen, neurale stamcellen en stamcellen verkregen vanuit vetweefsel (mesenchymale stamcel, MSC). De eigenschappen van een stamcel hebben effect op het uitrijpen tot verschillende soorten gespecialiseerde cellen (differentiatie), welke via paracriene signalering geassocieerd zijn met het bevorderen van revascularisatie en zenuwregeneratie. Ondanks de vooruitgang in stamcelonderzoek, bestaat er een risico van oncogenese en zijn de kweekcondities nog niet optimaal, hetgeen het klinisch gebruik van deze cellen limiteert. Daarnaast zijn er cruciale uitdagingen voor het optimaliseren van de bron en de beschikbaarheid van de stamcellen en de kosten van het differentiatieproces. Om deze redenen kan in de toekomst aangestuurd worden op onderzoek naar nieuwe ontwikkelingen zoals het gebruik van exosomen.

In **Hoofdstuk 9** zijn de functionele uitkomsten van allogene zenuwtransplantaten na toevoeging van ongedifferentieerde en gedifferentieerde MSCs in het ratmodel gepresenteerd. Het toevoegen van zowel ongedifferentieerde als gedifferentieerde MSCs resulteerden in verbeterde functie. Ongedifferentieerde MSCs in het bijzonder, toonden een significante toename in spierkracht, gemeten met de isometrische tetanische krachttest. De hypothese is dat stamcellen de paracriene signalering bevorderen om afstoting van het allogene transplantaat tegen te gaan danwel te verminderen. Dit samenspel van signalen is complex en betreft onder andere een

toename in gesecreteerde angiogene en neurotrofe groeifactoren, welke leidt tot een toename in spierkracht. Wanneer ongedifferentieerde MSCs worden gedifferentieerd tot gespecialiseerde cellen die de functie van Schwanncellen nabootsen, noemen wij ze 'Schwann cell-like' cellen of gedifferentieerde MSCs. Beide typen MSCs stimuleren een individuele secretie van groeifactoren, gemoduleerd door interacties met extrinsieke signalen vanuit de micro-omgeving. Wanneer wij het effect op functioneel herstel en de verschillen in kweekcondities in acht nemen, betogen wij dat ongedifferentieerde MSCs meer potentieel bieden voor therapeutische toepassingen.

Voor een beter begrip van het effect van angioneogenese en stamcellen op revascularisatie, werden deze gecombineerd toegepast in **Hoofdstuk 10** om de microvasculaire architectuur in allogene zenuwtransplantaten in een ratmodel beter te evalueren. Het vasculaire volume werd in kaart gebracht met behulp van micro CT en de distributiepatronen werden geanalyseerd om inzicht te geven in het volume en de diameter van de vaatsegmenten. De resultaten van dit hoofdstuk toonden aan dat deze distributies werden verbeterd na de toevoeging van de SIEF lap. Wanneer aan de allogene zenuwtransplantaten hiernaast ook MSCs werden toegevoegd, namen de vaatsegmenten verder toe in volume en diameter. De combinatie van ongedifferentieerde MSCs en angioneogenese zorgde voor de grootste toename van vascularisatie, vaatgrootte en -volume en een revascularisatie vanuit de zenuwuiteinden tot het midden van het transplantaat. Wij geloven dat de combinatie van een goed gevascularisseerd zenuwbed en stamcellen synergistisch werkt, resulterend in de organisatie van vaatstructuren om zo de zenuwregeneratie in goede banen te leiden.

In **Hoofdstuk 11** zijn de bevindingen uit dit proefschrift bediscussieerd in een breder perspectief en zijn suggesties en aanbevelingen voor toekomstig onderzoek gedaan. Na zenuwletsel spelen vasculaire endotheelcellen een grote rol. Onder hypoxische omstandigheden neemt de productie van vasculaire endotheliale groeifactor (VEGF) toe, welke de endotheelcellen aanzet tot proliferatie. Voorts spelen de nieuwgevormde bloedvaten een rol in het leiden van regenererende perifere axonen. Een goed gevascularisseerd bed stimuleert de paracriene signalering en creëert een anti-inflammatoire micro-omgeving voor het transplantaat, geïnduceerd door een cascade van cytokinen en niet enkel door VEGF. Deze omgeving kan de revascularisatie van gedecellularisseerde allogene zenuwtransplantaten verbeteren, zenuwfibrose

verminderen en hiermee de zenuwregeneratie bevorderen. Het toevoegen van een vaatbed met behulp van een gesteelde adipofasciale lap is een betrouwbare en simpele techniek om deze omgeving te creëren. Zowel de toevoeging van ongedifferentieerde als gedifferentieerde MSCs verbetert functioneel herstel van gedecellulariseerde allogene zenuwtransplantaten. Het gebruik van ongedifferentieerde MSCs heeft de voorkeur gezien de significante toename in kracht en het kortere kweekproces. Wij betogen dat de combinatie van een goed gevascularisseerd zenuwbed en stamcellen synergistisch werkt, resulterend in de organisatie van vaatstructuren om zo de zenuwregeneratie in goede banen te leiden. Voor dit proces spelen zowel de distributie als de richting van de nieuwgevormde bloedvaten een rol in het leiden van regenererende axonen.

APPENDICES

RESEARCH DATA MANAGEMENT

The FAIR data principles are guiding principles on how to make data **Findable**, **Accessible**, **Interoperable** and **Reusable**.

All animal experiments were conducted in accordance with institutional, national and international guidelines for animal care and the federal law concerning animal welfare. The studies were reviewed and approved by the Institutional Animal Care and Use Committee (IACUC).

Data of the experiments is collected using Labview, Analyze Pro and NIS-Elements software (NIS-Elements BR 4.51.01). Data has been transferred and handled using Excel to calculate the operated/nonoperated ratios in %. These numbers could be used to perform statistical analysis. Data is stored and archived as described with the FAIR principles, see below.

Findable

Since this is a collaborative research, with an international and interdisciplinary approach to research, the data is stored at the Mayo Clinic. Regular backups are done to protect against accidental or malicious data loss. Encryption is used for safely storing and sending files.

Accessible

Authentication and authorization is provided once a research fellow is part of the research line and access is granted to the secured folder. Research fellows are in close communication and their fellowships often overlap to provide exchange of knowledge and help to understand and access the data. A group Dropbox is available with progress papers to provide understanding to all research students that are involved in these projects. Each research fellow provides a Dropbox folder with the most recent research knowledge and latest updates that are necessary to conduct and understand the data and projects.

Interoperable

The data is integrated with previous data from the ongoing research line. Applications for processing data are provided on Mayo Clinic computers and data could be analyzed using standard analysis programs such as PRISM or SPSS.

Reusable

The principal investigator (PI) of the Neural Regeneration Research Laboratory, Prof. Alexander Y. Shin, has access to all data and has a clear understanding of all data and research projects that are being conducted. Clear point-by-point protocols have been provided in organized folders that could be used to replicate the experiments and data or combine these in different settings. Data and samples remain accessible by the PI, PhD candidate and laboratory members for 10 years after publication of each study.

LIST OF PUBLICATIONS

Publications included in this thesis

1. **Saffari TM**, Bishop AT, Shin AY. The superficial inferior epigastric artery fascia flap in rats. J Reconstr Microsurg Open 2020;5:e7–e14.
2. **Saffari TM**, Mathot F, Bishop AT, Shin AY. New methods for objective angiogenesis evaluation of rat nerves using microcomputed tomography scanning and conventional photography. Microsurgery. 2020;40(3):370-376.
3. **Saffari TM**, Bedar M, Hundepool CA, Bishop AT, Shin AY. The role of vascularization in nerve regeneration of nerve graft. Sep 2020. Neural Regen Res 15(9).
4. **Saffari TM,** Mathot F, Friedrich PF, Bishop AT, Shin AY. Revascularization patterns of nerve allografts in a rat sciatic nerve defect model. J Plast Reconstr Aesthet Surg. 2020 Mar 73(3).
5. **Saffari TM**, Badreldin A, Mathot F, Bagheri L, Bishop AT, van Wijnen AJ, Shin AY. Surgical angiogenesis modifies the cellular environment of nerve allografts in a rat sciatic nerve defect model. Gene. 2020 Aug 15;751.
6. **Saffari TM**, Mathot F, Thaler R, van Wijnen AJ, Bishop AT, Shin AY. Microcomputed analysis of nerve angioarchitecture after combined stem cell delivery and surgical angiogenesis to nerve allograft. J Plast Reconstr Aesthet Surg. 2020.
7. Saffari S, **Saffari TM**, Ulrich DJO, Hovius SER, Shin AY. The interaction of stem cells and vascularity in peripheral nerve regeneration. Neural Regen Res. 2021;16(8):1510-1517.
8. Mathot F, **Saffari TM**, Rbia N, Nijhuis THJ, Bishop AT, Hovius SER, Shin AY, Functional outcomes of nerve allografts seeded with undifferentiated and differentiated mesenchymal stem cells in a rat sciatic nerve defect model. Plastic and Reconstructive Surgery. 2021 Jun 21.
9. **Saffari TM**, Mathot F, Friedrich PF, Bishop AT, Shin AY, Surgical angiogenesis of decellularized nerve allografts improves early functional recovery in a rat sciatic nerve defect model. Plastic and Reconstructive Surgery. 2021.

Other publications

1. **Saffari TM**, Schüttenhelm BN, van Neck JW, Holstege JC. Nerve reinnervation and itch behavior in a rat burn wound model. Wound Repair Regen. 2018,. Jan;26910:16-26.
2. **Saffari TM***, Bijlard E*, van Bodegraven EAM, Mureau MAM, Hovius SER, Huygen FJPM. Sensory perception and nerve fiber innervation in patients with keloid scars: an investigative study. Eur J Dermatol. 2018 Dec 1;28(6):828-829 * contributed equally.
3. Rbia N, Bulstra LF, **Saffari TM**, Hovius SER, Shin AY. Collagen nerve conduits and processed nerve allografts for the reconstruction of digital nerve gaps: a single-institution case series and review of the literature. World Neurosurg. 2019;127:e1176-e1184.
4. **Saffari TM,** Bedar M, Zuidam JM, Shin AY, Baan CC, Hesselink DA, Hundepool CA. Exploring the neuroregenerative potential of tacrolimus. Expert Rev Clin Pharmacol. 2019 Nov;12(11).
5. Zuo KJ, **Saffari TM**, Chan K, Shin AY, Borschel GH. Systemic and local FK506 (tacrolimus) and its application in peripheral nerve surgery. J Hand Surg Am. 2020 Aug;45(8).
6. **Saffari TM**, Arendt CJ, Bishop AT, Spinner RJ, Shin AY. Role of tacrolimus in return of hand function after lower trunk brachial plexus injury in a lung transplantation patient: a case report. BMJ Case Rep. 2020 May 6;13(5).
7. **Saffari TM**, Chan K, Saffari S, Zuo KJ, Borschel GH, Shin AY, Combined local delivery of tacrolimus and stem cells in fibrin gel is a viable potential treatment for enhancing peripheral nerve regeneration, Biotechnol Bioeng 2021 Jul;118(7):2804-2814.
8. Saffari S, **Saffari TM**, Moore AM, Shin AY. Peripheral Nerve Basic Science Research-What Is Important for Hand Surgeons to Know? J Hand Surg Am. 2021;46(7):608-618.
9. Ikumi A, Gingery A, Toyoshima Y, Zhao C, Moran SL, Livia C, Rolland T, Peterson T, Sabbah MS, Boroumand S, **Saffari TM**, Behfar A, Shin AY, Amadio PC. Administration of purified exosome product in a rat sciatic serve reverse autograft model. Plastic and Reconstructive Surgery. 2021 Jun 21.
10. Bedar M, **Saffari TM**, Friedrich PF, Giusti G, Bishop AT, Shin AY. Maximum isometric tetanic force measurement of the tibialis anterior muscle in the rat. J Vis Exp. 2021(172).

Institute for Health Sciences
Radboudumc

PHD PORTFOLIO

Name PhD Candidate: T.M. Saffari Department: Plastic and Reconstructive Surgery Graduate School: Radboud Institute for Health Sciences Radboudumc	**PhD Period:** ***2018 –2021*** ***Radboudumc Supervisors: Prof. D.J.O. Ulrich and Prof. S.E.R. Hovius*** ***Mayo Clinic Supervisor: Prof. A.Y. Shin***

	Year(s)	ECTS
TRAINING ACTIVITIES		
a) Courses & Workshops		
Mayo Clinic College of Medicine, Rochester, Minnesota, USA		
• Animal Handling Courses of Rat and Pig, Mayo Clinic, MN, USA	2018	1.25
• Human Specimen Course Institutional Review Board (IRB)	2018	1.25
• Microsurgery Course, Mayo Clinic, MN, USA	2018	3.00
• Microsurgery, Erasmus Medical Center, the Netherlands	2018	3.00
• Statistics Course, Mayo Clinic, MN, USA	2018	4.00
• Animal Blood Drawing Course, Mayo Clinic, MN, USA	2019	0.20
• Scientific Writing Course, Mayo Clinic, MN, USA	2019	2.00
Radboud Institute for Health Sciences, Radboudumc, the Netherlands		
• Graduate School Specific Introductory Course	2020	0.75
• Scientific Integrity Course Radboudumc	2020	1.00
b) Seminars & Lectures		
• Trimed Hand Course, San Diego, USA	2018	0.50
• Trimed Cadaver Lab, MN, USA	2019	0.50
• Aptis Cadaver Lab, MN, USA	2019	1.00
• Axogen Cadaver Lab, MN, USA	2020	1.00
c) Conferences & Symposia		
Attendance conferences		
• American Society of Surgeons of the Hand (ASSH), Boston, USA	2018	0.75
• American Society of Peripheral Nerve, Palm Springs (ASPN), USA	2019	1.00
• American Society of Surgeons of the Hand (ASSH), Las Vegas, USA	2019	0.75
• American Society of Peripheral Nerve (ASPN), Palm Springs, USA	2020	0.75
• Plastic Surgery Research Council (PSRC), Online	2020	1.00
• Federation of European Societies for Surgery of the Hand (FESSH), Online	2020	1.25
• American Society of Peripheral Nerve (ASPN), Online	2021	1.00
• Plastic Surgery Research Council (PSRC), Online	2021	1.00
• Federation of European Societies for Surgery of the Hand (FESSH), Online	2021	1.00
• Plastic Surgery The Meeting (PSTM), Atlanta, USA *(November 2021, Registered)*	2021	1.00

Attendance symposia		
• Mayo Clinic Orthopedic Research Council (MRC)	2019, 2020	0.20
• Jenifer Jowsey Research day, Mayo Clinic	2019	0.10
Oral presentations		
• A retrospective comparison of collagen nerve conduits and processed nerve allografts for the reconstruction of digital nerve gaps - ASSH 2018	2018	0.5
• The interaction between mesenchymal stem cells, neoangiogenesis and functional recovery of processed nerve allografts in peripheral nerve repair - ASPN 2019	2019	0.5
• Neoangiogenesis patterns in surgical revascularized nerve allografts in a rat sciatic nerve defect model - ASPN 2020 - MRC 2019 - PSRC 2020 - FESSH 2020	2019, 2020	2.00
• Surgical angiogenesis to nerve allografts improves early functional recovery in a rat sciatic nerve defect model - MRC 2020 - PSRC 2020 - FESSH 2020	2020	1.50
• Combined local delivery of tacrolimus and stem cells in fibrin gel is a viable potential treatment for enhancing peripheral nerve regeneration - PSRC 2020 - ASPN 2021	2020, 2021	0.50
• Microcomputed analysis of nerve angioarchitecture after combined stem cell delivery and surgical angiogenesis to nerve allograft - ASPN 2021 - *High ranked nerve abstracts* - FESSH 2021 - PSRC 2021 - PSTM 2021	2021	2.00
• Surgical angiogenesis modifies the cellular environment of decellularized nerve allografts in a rat sciatic nerve defect model - ASPN 2021 - FESSH 2021	2021	1.00
Posters		
• The effects of surgical angiogenesis on motor recovery in processed nerve allografts in a rat sciatic nerve defect model, ASSH 2019	2019	0.50
• Role of tacrolimus in return of hand function after lower trunk brachial plexus injury in a lung transplantation patient: a case report, ASPN 2020	2020	0.50
• Combined local delivery of tacrolimus and stem cells in fibrin gel is a viable potential treatment for enhancing peripheral nerve regeneration, FESSH 2020	2020	0.50

d) Other		
• Introduction day Mayo Clinic, MN, USA • Introduction day Radboudumc • Hand Surgery meetings and Grand Rounds, Mayo Clinic, MN, USA • Weekly Plastic Surgery Research Meeting Radboudumc • Peer revision of scientific publications for Plastic and Reconstructive Surgery (PRS) and Plastic and Reconstructive Surgery Global Open (PRS GO)	2018 2020 2018, 2019 2020 2019-2021	0.50 0.50 3.00 1.50 1.25
Awards and Grants • Jenifer Jowsey Orthopedic Research Fellow Award, Mayo Clinic, Rochester, USA • Michael van Vloten Foundation, personal funding for Research Fellowship, €10.000 • Catharine van Tussenbroek Foundation, personal funding for Research Fellowship, €1.250 • Obaid vascularized composite tissue grant award, $100.000 *Enhancing the regenerative potential of allograft nerve reconstruction by modulation of local environment. Contributed together with Prof. A.Y. Shin and co-investigators*	2019 2018 2018 2020	
TEACHING ACTIVITIES		
e) Supervision of students		
• Minor Plastic Surgery Erasmus Medical School. "Reconstruction from head to hands". - *The role of vascularization in nerve regeneration* - *The effect of tacrolimus in nerve regeneration* • Neural Regeneration Research Laboratory Mayo Clinic. Supervision of M. Bedar (Research Fellow) and S. Saffari (Research Trainee)	2018 2019-2021	 1.75 1.75 7.00
TOTAL		**56.00**

A

CURRICULUM VITAE

Tiam Mana Saffari was born on May 3rd 1992 in Capelle aan den IJssel, the Netherlands. During high school, she was selected for the Junior Medical School (JMS) program at the Erasmus Medical University. JMS is a scientific pre-university program for ambitious high school students and allows for entering Medical School upon completion. As a 16-year-old student, she observed her first case in the operation room which was a trauma case of the hand from a circular saw table (Dr. E.T. Walbeehm). This case sparked her first interest in peripheral nerve and hand surgery. She completed JMS with a thesis on "Peripheral nerve injury in cold-intolerant rats" (Dr. L. Duraku and Dr. E.T. Walbeehm). After graduating from Erasmiaans Gymnasium (Rotterdam) in 2010, she started Medical School at the Erasmus University in Rotterdam. Her special interest in reconstructive surgery did not fade away and was further fueled during her elective Minor course on "Reconstruction from Head to Hands: A Multidisciplinary View" during her third year. Mana was motivated to apply for a research master and commenced the Neuroscience Master simultaneous to the Master of Medicine. During the Neuroscience Master, she conducted research on "Nerve reinnervation and itch behavior in a rat burn wound model" which resulted in her first scientific paper (Dr. B.N. Schüttenhelm, Dr. J.C. Holstege).

After graduating from Medical School and Neuroscience in 2018, Mana was granted the opportunity to perform research at the Mayo Clinic (Rochester, MN, USA) under supervision of Prof. A.Y. Shin and Prof. A.T. Bishop as part of her PhD. She focused on the role of angiogenesis and adipose-derived mesenchymal stem cells in enhancing nerve allograft outcomes. The Mayo Clinic has awarded her with the Jowsey Research Fellow Award for the research contributions in basic science nerve research, in particular the project on "Revascularization patterns of nerve allografts in a rat sciatic nerve defect model". During her research fellowship, the laboratory also commenced a collaboration with Dr. G.H. Borschel to investigate the combined local delivery of stem cells and tacrolimus (FK506) to nerve. She presented her work at international conferences, supervised several students and is a member of the Plastic and Reconstructive Surgery (PRS) Resident Advisory Board.

Upon completion of her research fellowship, Prof. dr. S.E.R. Hovius and Prof. dr. D.J.O. Ulrich granted her a PhD position at the Radboud University Medical Center (Nijmegen, the Netherlands) through a collaboration between Mayo Clinic and Radboud University Medical Center. Under great mentorship, Mana has developed her passion for (basic science) research, education and nerve surgery. After obtaining her PhD Degree, Mana aspires to become a Plastic Surgeon. She will continue her journey of becoming a surgeon-scientist and hopes to motivate other students and colleagues along the way in pursuing their dreams.

A LETTER TO A YOUNG RESEARCHER

Scientists stand on the shoulders of giants. It is without doubt that the realization of this PhD thesis is a product of great teamwork and is built on research that has been previously conducted. Although my name is written on the cover of this book that you hold in your hands, it would not have been possible to achieve this without the support and collaboration of many researchers and mentors.

The journey of a PhD is not always an easy one. While many see a list of publications as a measure of success, I would like to also show you the *other side*. As a PhD candidate you will meet your own, unique obstacles on your way to graduation. We do not see the number of rejections for every paper, prior to its acceptance. We do not see the long nights and weekends of work. We do not see the failures. If you are struggling to hold on to your intrinsic motivation, *you are not alone*. However, once you have reconnected with your intrinsic motivation, it will be easier to persevere through the hardest parts of your training and to manage the workload. I would like to encourage you to celebrate the victories, but also to embrace the failures because these allow you to grow. As my mentor Dr. Shin said many times "*Fall down seven times, stand up eight*".

In my opinion, building a career is not possible without having great mentors. I have been grateful to learn from and to be supported by wonderful mentors. The true mentors of my life have been my parents. The two most hard-working people that I have ever seen. My parents taught me the value of education, how to be authentic in my actions and most importantly: they taught me about *humanity*.

Dear students and researchers, while you are rising in your journey of becoming a great surgeon, scientist or professor, please do not forget to stay human. Be kind to your colleagues and be patient to the ones you teach. Your impact can be tremendous for the next generation. Stand up for yourself or others in an unpleasant work environment. Speak up for diversity, equity and inclusion. Turn criticism into motivation and fuel to reach your goals.

To the young researchers and medical students, our future leaders, know that you can make a change and make the world turn. Although my PhD journey has nearly come to an end, the road to be(coming) a good mentor and mentee will be ongoing. I have overcome many challenges during this journey and I know you can do that too. And with that, my goal to give back to the next generation becomes my next challenge.

ACKNOWLEDGEMENTS / DANKWOORD

The realization of this PhD thesis has been nothing, but the product of great teamwork. This journey has allowed me to step outside my comfort zone and fly from Rotterdam to Rochester to perform research at the Mayo Clinic. I was privileged to work with knowledgeable colleagues during the past three years. My appreciation for everyone that has contributed to this PhD thesis is tremendous, and I would like to thank you all.

Geachte **prof. dr. Ulrich**, dank voor uw vertrouwen in mij en de kans om mijn PhD thesis af te ronden aan het Radboudumc. Ik ben trots op de samenwerking die deze onderzoekslijn tot stand brengt en hoop dat dit nog vele jaren voortgezet kan worden. Bedankt voor uw kritische blik en feedback om deze PhD thesis te verbeteren.

Geachte **prof. dr. Hovius**, dank voor uw uitzonderlijke begeleiding tijdens het schrijven van mijn PhD thesis. Ik zal ons eerste gesprek in uw huiskamer onder het genot van een kopje koffie (en klassieke muziek) niet vergeten. Zonder uw vertrouwen in mij was deze thesis nooit tot stand gekomen. Wegens COVID-19 waren onze meetings online, maar dit heeft het proces zeker niet in de weg gestaan. Uw kritische blik heeft mij gedreven om dieper te duiken in de materie om al mijn standpunten te kunnen onderbouwen en tot dit resultaat te komen.

Dear **Dr. Shin**, thank you for being my mentor and supporting me throughout all my career dreams. You have introduced me to a new world of research, care for patients and career possibilities. By the end of every lab lunch on Monday, we would have (*at least*) ten new ideas for projects and new tasks that we would text to ourselves so we would not forget. You have given me so many opportunities to investigate new ideas, visit and present at many conferences and provided me the freedom to travel to many places in the United States. I will never forget our trip to Toronto to visit the Borschel laboratory! Our weekly updates continued even after I finished my research fellowship. I believe we make a great team for writing grants and I am glad we can sharpen each other's sword. Thank you for all that you have taught me to become a better scientist, microsurgeon, doctor, writer and friend. Dear **Patti Shin**, thank you for your hospitability and showing me around in Rochester in my first week!

Dear **Dr. Bishop**, thank you for giving me the opportunity to work in the lab. Your critical questions improved our work tremendously and I am grateful to have learned from you. The Christmas tree decorating event at your home during Thanksgiving gave us the ultimate Christmas feeling in Rochester. It is unbelievable how you find time to be a musician, pilot and coffee expert besides being a great surgeon and researcher. I will be the first in line when the orchestra comes to the Netherlands!

Graag wil ik de leden van de leescommissie bedanken voor de interesse in mijn proefschrift. **Prof dr. Bartels**, **Prof. dr. Malessy** en **Dr. Ruigrok**, dank voor het commentaar wat jullie hebben gegeven. **Dr. van Alfen**, **Prof. dr. Ritt** en **Dr. de Ruiter**, hartelijk dank dat u bereid bent zitting te nemen in de promotiecommissie: het is een eer dat jullie onderdeel willen zijn van mijn promotie en ik kijk ernaar uit met u allen van gedachten te mogen wisselen.

Dear **Pat**, thank you for welcoming me in the lab. You have taught me all there is to know about rats. Because of your help I felt comfortable to handle the rats and perform the surgeries. I truly enjoyed our small talk in the lab during and in between work!

I had the pleasure to work with many colleagues of the **van Wijnen laboratory**. Thank you for your valuable time to help me during my research fellowship at Mayo. In particular, I wish to thank **Roman**, **Leila**, **Amr** and **Marina**. Your help and advice was invaluable. Dear **Dr. van Wijnen**, I have benefited from collaboration and many great discussions with you. The stem cell projects were not possible without your lab and your knowledge of gene expression is just incredible. Thank you for your continuous support.

Dear **Bill Anding**, **Eric Sheahan**, **Mayo Clinic X-ray Imaging Core**, **LouAnn Gross**, **Vivian Negron**, **Peggy Gosse Rahnenfuehrer** and the **Pathology Research Core team**, **Abbie Kaehler** and her entire team, thank you for your hard work and contributions to this PhD thesis.

Dear **Jim Postier**, your medical artwork has elevated the papers of this thesis tremendously. After seeing your first images for the SIEF technique, I knew that I wanted to ask your help to design the cover of my thesis. I had the idea of the hand in

my mind since 2018. You were able to put my ideas on paper and with your creativity it turned out even more amazing than I would have imagined. Thank you.

Beste staf, assistenten en onderzoekers van de **afdeling Plastische Chirurgie in het Radboudumc**, dank dat jullie mij warm hebben verwelkomd. Onze interactie was helaas voornamelijk virtueel wegens COVID-19, maar jullie presentaties, vragen en updates tijdens de meetings waren lichtpunten tijdens het vele schrijven thuis. Beste **Pascale Reijers**, dank voor je hulp tijdens de laatste loodjes van mijn promotietraject!

Onderzoekers van de zenuwlijn, **Caroline**, **Liselotte** en **Nadia**, dank voor het werk wat jullie hebben neergezet. Zonder jullie voorafgaand onderzoek en nette protocollen was mijn onderzoek niet mogelijk. Jullie stonden altijd open om mijn vragen te beantwoorden en het werk van de onderzoekslijn kritisch te beoordelen. Het was een eer om met jullie samen te werken. **Femke**, dank dat je naar Mayo bent gevlogen om mij te helpen met de sacrifices! Ons eerste uitje in Boston (ASSH congres) werd snel gevolgd door lange dagen in het lab. Je was altijd beschikbaar aan de telefoon of via email en bracht nieuwe inzichten in het onderzoek. Wat bijzonder dat wij dit avontuur op 10 september samen kunnen afronden!

Lieve **Dolph**, mijn lab maatje! Wat had ik zonder jou moeten doen in Rochester. Onze vele uren in het lab, Steam koffie pauzes, Friday morning hand meetings (om 6:30, waar ik bij was wanneer ik geen operaties had gepland..), house parties en nog veel meer avonturen zal ik nooit vergeten. Je hebt mijn tijd in Rochester een feest gemaakt! Ik ben blij dat wij deze vriendschap hebben voortgezet in Nederland. Een #2 San Diego trip zal toch echt snel moeten volgen. Ik ben zo trots op jou en blij om deze promotieweek met jou te mogen delen.

My Parker family: **Saurabh, Prateek** and **Shu**, my Parker brothers! What started at meeting at the Parker kitchen table, resulted in many brunch dates and Tap House nights. Prateek, let's finish off with your *#anotherroundforthetable* very soon. I am so happy that I have met you guys and hope that we will have a reunion somewhere in the USA soon!

Carla, I am so thankful to have met you! You are a true role model and the summer months we spent together were so much fun. We can talk about everything there is in life and I cannot wait to visit you and your family in Portugal someday soon.

Caro, **Max**, **little Lou**, **Laure**, **Anna**, **Raphael**, **Nick** and **Sarika**, thank you for all the fun moments in Rochester. Your friendship and hospitality truly made Rochester feel like my second home. Who doesn't love a good Moscow Mule?! You are all wonderful people and I am grateful to have met such inspiring, sweet, smart and warm-hearted people that I can call my friends.

Verena, bedankt dat jij en **Raymond** binnen 10 minuten voor mijn deur stonden en mij een fancy cabrio ride naar het ziekenhuis hebben geboden. Dank dat jij uren naast me heb gezeten. Nu kan ik zelf ook beamen dat Mayo het #1 ziekenhuis van de wereld is!

Lieve **Mircea**, mijn liefde voor onderzoek is eigenlijk ontstaan tijdens onze Neuroscience tijd. Sindsdien kunnen we altijd alles bespreken en is geen onderwerp te gek om aan te snijden. Waarschijnlijk is mijn PhD onderzoek het énige onderwerp waar ik meer vanaf weet dat jij (*yes!*). Snel zul ook jij je PhD verdedigen!

Lieve **Nara**, wat hebben wij veel meegemaakt samen. Onze vriendschap betekent zo ongelooflijk veel voor mij. Het maakt niet uit hoeveel tijdverschil of afstand er is, we weten elkaar wel te vinden. Merci voor je support tijdens dit avontuur.

Mijn liefste paranimfen, **Bahar** en **Tara**. Samen opgegroeid, samen geneeskunde doorgelopen, samen het leven geleefd, samen zoveel trips en sleepovers. Ik wist vanaf het allereerste moment al dat ik hier samen met jullie zou staan tijdens mijn verdediging. Ik ben zo dankbaar dat ik het leven mag delen met jullie en weet zeker dat we dit voor altijd zullen doen.
Tara, ik ben zo blij dat ik je naast mijn zus ook mijn collega kan noemen! Ik ben ongelooflijk trots dat je het onderzoek in Mayo hebt overgenomen. Zusjes, friends, roommates, co-auteurs, collega's: ik kan niet in woorden uitdrukken hoe bijzonder ik het vind dat wij alles in het leven delen.

Mijn allerliefste familie: **Amir**, **Tiam**, **Mehri**, **Willem, Mariam**, **Hesam** & de kids **Kian** en **Ryan**, alles is leuker met deze lieve familie. Onze feestjes thuis zijn de allermooiste momenten voor mij en ik waardeer het feit dat wij altijd voor elkaar klaar zullen staan. Merci dat jullie er op deze mooie dag ook bij zijn.
To my extended **family**; aunts, uncles and cousins, thank you for the continuous love and support that you have given me over the years.

Mijn liefste **ouders**, baba va maman joon, zonder jullie steun had ik hier vandaag niet gestaan. Jullie hebben mij laten zien wat hard werken is, maar ook dat je van elk moment in het leven moet genieten. Merci voor jullie onvoorwaardelijke liefde en steun.

My dearest **Utku**, meeting you in Rochester was the most unexpected surprise. Your jokes make me laugh every day and with each other's support, we make the best team. Thank you for supporting me through this process in so many ways: from offering me emotional support during our walks in the forest to providing me professional advice. I cannot wait to see what the future holds for us.

Mana Saffari
Rotterdam, June 2021

A

Institute for Health Sciences
Radboudumc